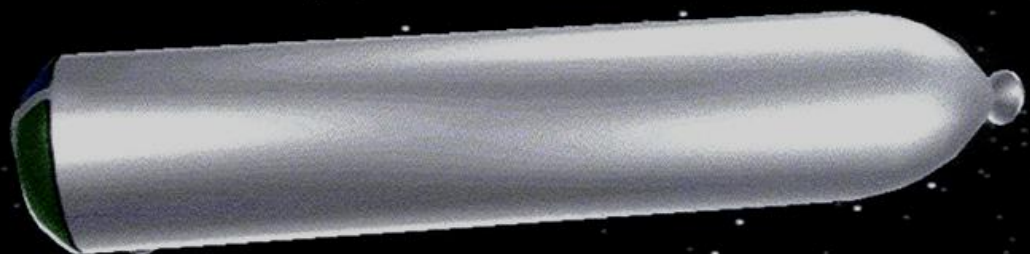




note: contact
paul.kirsch.tothestars@gmail.com
for an updated 2017 book

Quantum Electromagnetic Laser Propulsion



Larry D. Maurer
Director - Engineering

Michael E. Miller
Director - Research

*also from UNI**TEL**:*



"the HOLO-1 Quantum Computer Prototype" book

(release date to-be-announced)



"Quantum Laser Applications in Medicine" book

(release date to-be-announced)



"*Flying Colors*" book

the true-life 1981 Eugene, Oregon UFO sighting (witnessed by hundreds including police) that permitted an up-close demonstration and observation of a "transparent laser"

(release date to-be-announced)



"Macroscopic Quantum Tunneling" interactive computer simulation

(release date to-be-announced)



"Tunnel Time" documentary film available in VHS or DVD formats

(release date to-be-announced)

for additional information, please contact

Larry Maurer
c/o UNI**TEL**, Inc.
P.O. Box 42585
Portland, OR 97245-0585

<http://www.unitelnw.com>

note: contact
paul.kirsch.tothestars@gmail.com for
an updated 2017 book. Mr. Maurer
passed away in 2011.

Quantum Electromagnetic Laser Propulsion

Larry D. Maurer

Michael E. Miller

(edited by Mark McWilliams <http://www.stealthskater.com>)

Limited Promotional Edition
Published by STAR*SHOTS Studio
South Charleston, West Virginia

Quantum Electromagnetic Laser Propulsion
Copyright © 2002
Limited Promotional Edition
First Printing July, 2002

note: contact

**paul.kirsch.tothestars@gmail.com for
an updated 2017 book. Mr. Maurer
passed away in 2011.**

All rights reserved, including the rights to reproduce this book or portions thereof in any form whatsoever. Limited portions can be reproduced for use in trade journals or media review. All other reproduction is prohibited without the written permission from UNITEL, P.O. Box 42585, Portland, OR 97245-0585 .

Quantum Electromagnetic Laser Propulsion
Larry D. Maurer & Michael E. Miller
160 pages, illustrated

Larry Maurer -- Secretary-Treasurer and Director-of-Engineering -- has worked in the structural and mechanical engineering industry in a design capacity since 1978. He was the project manager for many successfully completed projects in a variety of construction technologies. He has also been the technical representative for several engineering firms in Eugene, Oregon.

Mr. Maurer supervised his own engineering department while working with Bonney, Bennett and Peters who were the second largest engineering consultant firm on the West Coast in 1978. Mr. Maurer proved adept at coordinating very complicated construction projects between internal and external electrical, structural, and mechanical divisions.

Michael Miller -- President and Director-of-Research -- is a scientist and inventor with the rare ability to apply recently proven theoretical physics to the development of useful products. Mr. Miller concentrated on developing and refining the application of quantum mechanical theory to the construction of practical devices during the '70's

Mr. Miller has had many successful formal technical meetings with top physicists and engineers including the University of Oregon, Oregon State University, Boeing Aerospace & Electronics, McDonnell-Douglas Aircraft Co. He is recognized as a competent scientist with comprehensive knowledge and innovator regarding quantum physics. (*Dr. Rudolph C. Hwa, Director of the Theoretical Institute of Science, University of Oregon, interviewed Mr. Miller in March, 1983 before Dr. Hwa would commit himself to review **UNITEL**'s aerospace propulsion system. When the 3-hr in-depth discussion of physics concepts concluded, Dr. Hwa congratulated Mr. Miller of being a brilliant physics expert and stated he wished "that there was someone with Mike's vision at the University of Oregon".*)

Both Mr. Miller and Mr. Maurer have proven their skills as top innovators in quantum electronics design by winning patent awards and compiling positive scientific and professional peer evaluation. Together they formed **UNITEL**, Inc. in 1982 for the express purpose of patenting, manufacturing, and marketing **UNITEL** products.

Acknowledgements

Many people have exchanged ideas with us over-the-years to strengthen the basic propositions in the **UNITEL** patents owned by co-inventors Larry Maurer and Michael Miller. And countless others in informal personal and Internet chats have engaged in thought-provoking and constructive debates. Their individual contributions have been incorporated with our own research that is now in its third decade. To all of them we offer our sincere gratitude.

Special thanks is due **Dave Froning** and **Yoshinari Minami** for their many years of encouragement and support. We are also grateful to **Paul Kirsch** for his technical writing and editing assistance. **Tim Ventura** recently contacted us about his "Biefeld-Brown Effect Generator" that partially proved certain portions of our aerospace theories. And **Mark McWilliams** transformed our manuscript into a finished book.

L. D. M. , M. E. M.

Foreword

This book represents the continuation of the study of electromagnetism, lasers, black holes and fiber bundle technology; specifically applied to a feasible aerospace propulsion system with deep-space exploration capabilities.

The words of the late Dr. Werner Von Braun remain strongly embedded in Larry Maurer's memories from the speech he gave on the importance of space exploration at the University of Oregon, MacArthur Court in 1959. It came a few months after the infamous Russian satellite Sputnik passed over the United States earlier that year. Both Maurer and Miller remember standing on their front lawns with their families watching in awe at the Sputnik as a fast-moving blinking white light crossing the summer night sky. They remember how everyone felt sort of "naked", like their privacy was invaded for the first time and there was the helpless feeling that there was nothing anyone could do but watch. That bold maneuver by the Soviets certainly got the attention of every American to the stark reality of the race in technology to explore and conquer space.

It is obvious that if anyone were to traverse the vast distance of outerspace to reach any distant planet or star system to explore, they would certainly have to travel faster than the speed-of-light. To put it simply, nothing else will do ... so why even bother with developing any other type of propulsion designs such as super rockets, antimatter powered craft, solar sails, etc. It is our belief that **Macroscopic Quantum Tunneling (MQT)** is the only realistic way of traveling if one wants to reach any distant point in the Universe.

With the advent of modern technology and the progress of laser technology, **UNITEL**'s advanced and sophisticated spaceship design is right in step. Free-space optics (**FSO**) technology and its industrial applications are close in similarity to the design of **UNITEL**'s projected laser plasma that is the heart of the laser propulsion system design. FSO systems are basically fiber-optics without the fiber. Much information and other characteristics of laser technology can be applied to **UNITEL**'s highly controlled, high-speed computer-modulated projected laser plasma. The highly precise modulation from the onboard computer system will be clocked in **femtoseconds**. This will provide complete control of the velocity and maneuverability similar to a high-speed helicopter that will allow the vehicle to fly from a "hover" mode to exceedingly fast velocity anywhere on the x-, y-, or z-axis in the Earth's atmosphere or outerspace. We expect to break all existing records for speed, distance and duration.

The Principals of **UNITEL** -- Larry Maurer and Michael Miller -- would like to thank the many esteemed researchers that have provided them with the tools of know-how to be able to design a craft such as this. Their work is the culmination of many years of intense research into the works of t'Hooft, Yang, Wheeler, Tesla, Dirac and several other important pioneering scientists.

The design of **UNITEL**'s **High-Speed Mass Transportation** vehicle -- with payload -- employs no moving parts. It is all-electrically powered and requires no bulky fuels or propellants. This **quantum mechanical propulsion system** design is the first of its kind and operates on principles other than the usual action-reaction types of propulsion systems (*that fire a blast of energy out of the back of a vehicle to propel it forward such as rockets or jets*). Simply stated, our vehicle will be pulled along by a strong electromagnetic attraction instilled in the spiraling charged particle beam laser plasma that is focused in front of the vehicle.

Our all-electric vehicle design will be a “High-Speed Mass Transportation Vehicle” and is crudely comparable to the well known “**Mag-Lev**” high speed train that floats on superconducting magnets -- which was originally designed at MIT in 1973 (John Joannopoulos et al) -- has successfully been working for a number of years in Europe and Japan. There have been many advancements and improvements on the original design since then. Our vehicle will require the standard type of superconducting mag-lev tracks for suspension of the vehicle while docking at the station for boarding passengers and loading cargo. However, upon departing the station at point 'A' there will be no need for tracks! The vehicle will literally create and fly through it's own “**flux tube**” that is highly magnetic and is produced out of the projected charged particle beam plasma directed in front of the vehicle. This eliminates the need for the usual superconducting tracks that mag-levs float upon.

The latest Japan Railway (JR) mag-lev design is somewhat comparable to our flight system design. The JR train will travel at 800 kilometers per hour and will “fly” through tunnels in a partial vacuum to reduce air resistance more efficiently. It is well known that a **magnetic attraction** can be instilled on a laser beam. The projected and excited stress energy tensor field in front of the **UNITEL** ship “sweeps” out everything in the projected Meissner-type flux tube plasma and creating a vacuum condition. Our vehicle will fly through the partial vacuum of the projected RF confined flux tube or string-like laser plasma due to adiabatic pressure as if it were an invisible tunnel. This effect can be described as if the vehicle were a ping-pong ball being sucked up a vacuum cleaner tube.

UNITEL’s Type VI **MOSS** (Macroscopically Observable Superconductive State) vehicle will employ the three-part, equal **Red**, **Green** & **Blue** section, laser lens to produce specific quantum effects in order to be used for propulsion. MOSS pertains to a system that is observable on a large-scale, yet bound to the same quantum laws as a subatomic particle. The fact that atoms or particles can exist on a Macroscopic scale was recently proven with the creation of a Bose-Einstein condensate -- a proven MOSS system.

On a subatomic level quantum mechanics describes the light string that is part of a quantum particle system -- such as an electron-positron or electron-hole pair -- where only one end point is required by quantum law to be moving at the speed-of-light. The projected laser plasma directed in front of **UNITEL**’s exteriorly charged vehicle assumes the role of a Macroscopic light string. The projected laser plasma and exterior charged vehicle assumes the character of the basic system found throughout physics and can be described as “two bodies held together by a spring-like structure”. Our vehicle will traverse or commute up the light string like a particle such as an electron or photon. This is considered **electromagnetic propulsion**, and we will utilize a quantum mechanical function intrinsic to monopoles in order to generate a strong magnetic attraction instilled in the projected, pulsed laser plasma to the exterior charged vehicle. There has been a great deal of controversy concerning our application of the **monopole** effect of our propulsion system, mainly because a monopole itself has never been observed. However, Dr.'s **Raymond Chiao** and **Akira Tomita**, at the University of California in Berkley, were able to physically measure quantum monopole-like effects on a Macroscopic scale. They were able to physically apply these effects to optical fibers & RF waveguides.

For traveling vast distances that are normally unattainable with conventional technology, such as from Earth to the nearest solar system, our ship will **quantum tunnel** (elastically). Tunneling is a commonplace phenomenon at sub-nuclear levels and occurs in semiconductors, nuclear fusion, and the tunneling electron microscope. **UNITEL** will use the lens to generate abruptly-opposed electromagnetic bucking waves, denoting a direct interaction with the Zero-Point Energy (**ZPE**). The ZPE is found in the

3°K vacuum of space. It is referred to as "zero point" because the energy is not thermal in nature. The ZPE consists of random quantum fluctuation and is maintained by a flux of electrical energy flowing through four-dimensional spacetime. Acting as a single "giant electron", the **UNITEL** aerospace vehicle will tunnel through the fabric of spacetime to arrive at a calculated destination. In this manner, our vehicle will demonstrate superluminal or faster-than-light capabilities.

Even though monopoles have not yet been observed, there have been successful applications of helically-wound optical fibers and RF waveguides producing monopole effects such as parallel transport on a Macroscopic scale. We will also produce parallel transport -- which is purely a geometrical effect -- with our pulsed, spiraling laser plasma. Centrifugal force is exerted on the projected plasma is directed toward the center of the circular motion of the spiraling plasma, not away from it. This phenomenon is attributed to the massively rotating charged naked singularity at the end point of the projected plasma. This three-phased projected plasma confines the excitonic gasses and provides a path of parallel transport, affine connection, that automatically aligns the trapped charged particles in one direction like the atoms in a magnet. These particles then move without resistance in a superfluidic fashion. **Excitons** perfectly replace the information particles called phonons or **Cooper pairs**. However, excitons can carry the same information in a vacuum as phonons can not operate in a vacuum. The exciton mechanism in a superconductor phonon-mediated electron-electron interaction is replaced by excitons. As in the case of phonons, the excitons cause the electrons to attract, forming bound states known as Cooper pairs.

The cost of building these vehicles and stations would be much less in comparison to the cost of building modern jet aircraft passenger planes, airports and maintenance facilities and personnel. Since tracks aren't required, our system would even rival standard trains in comparing costs for the construction of both.

*Like some of the word-renowned scientists who inspired us, **UNITEL** may be ahead-of-its-time and waiting for present-day technology to catch up to what theory predicts. But the rewards represent the next level of technology for mankind. And -- let's face it --- if this challenging new physics-engineering combination were all that easy, then everyone would be doing it ... and you wouldn't be reading this book right now!*



P.O. Box 42585 Portland, OR 97242-0585
www.unitelnw.com

Larry Maurer

July 10, 2002

| | |
|--|-----|
| Acknowledgements | vii |
| Foreword | ix |
| | |
| Abstract | 1 |
| 1 - Introduction | 9 |
| 2 - the Type VI Vehicle | 29 |
| 3 - Aircraft Frame and Hull Composition | 31 |
| 4 - Exterior Charged "Smart Skin" Hull | 45 |
| 5 - Power Source | 53 |
| 6 - Lens | 55 |
| 7 - Control and Navigation | 73 |
| 8 - the Lamb Shift | 81 |
| 9 - Polarized Beam | 83 |
| 10 - Macroscopic Quantum Tunneling | 97 |
| 11 - Conclusions | 121 |
| 12 - References | 123 |
| 13 - Supplemental Documents | 131 |

Figures

page

- 3 ... Fig. 1 - Field Extension Dynamics
5 ... Fig. 2 - Force Between Quarks
6 ... Fig. 3 - Lens Design
7 ... Fig. 4 - UNITEL's Space Vehicle and projected laser plasma
10 ... Fig. 5 - Docking Tracks from Mag-Lev design
11 ... Fig. 6 - artist's conception of UNITEL's proposed space vehicle (*rear view*)
12 ... Fig. 7 - artist's conception of UNITEL's proposed space vehicle (*front view*)
13 ... Fig. 8 - Geometry of Radiated RF Wave Fronts
13 ... Fig. 9 - scale model of UNITEL 's spaceship (*front view*) with technician model figures
14 ... Fig. 10 - Doped Crystallite
15 ... Fig. 11 - Light Interacting With Matter
16 ... Fig. 12 - Pulsed Laser technique that produces the potential EM Wells that traps excitonic gasses
17 ... Fig. 13 - UNITEL 's laser lens compared to a "radar gun"
18 ... Fig. 14 - Dipole Magnetic Fields created by a Circulating Electric Charge
19 ... Fig. 15 - Magnetic Monopole Geometry
20 ... Fig. 16 - Electric and Magnetic Fields created by Magnetic Monopoles
21 ... Fig. 17 - Time History Paths of an Electrically-Charged Particle moving through the magnetic field produced by a Magnetic Monopole
22 ... Fig. 18 - Symmetry between Magnetic Monopoles and Matter/Anti-Matter
23 ... Fig. 19 - Magnetic Orientation on an Atomic Scale
24 ... Fig. 20 - Dipole Magnetic and Electric Fields
25 ... Fig. 21 - artist's conception of the field topology/dynamics of projected laser plasma
26 ... Fig. 22 - conceptual drawing from UNITEL 's proposed laser Mag-Lev mass transportation design
26 ... Fig. 23 - Main Body Vehicle with multiple "drones"
28 ... Fig. 24 - cut-away drawing of UNITEL 's vehicle frame with smartskin & hull
29 ... Fig. 25 - Geometrical Paths taken by a Charge Particle scattered by a Fixed Monopole
31 ... Fig. 26 - VIPER 3000 Fiber Placement System
34 ... Fig. 27 - Fuselage Mandrels at Cincinnati Machine's plant
34 ... Fig. 28 - scale model of UNITEL 's proposed all-electric laser propulsion space vehicle
35 ... Fig. 29 -a collage of various pictures of the scale model
36 ... Fig. 30 - Crystal Structures in Solid Helium
36 ... Fig. 31 - Fabrication of "Quantum Dots"
37 ... Fig. 32 - Bright Light from Microwave-excitation of Sulfur Atoms
38 ... Fig. 33 - Current Densities of commonly-used Superconducting Materials
38 ... Fig. 34 - an example of Supercooling a Superconductor
39 ... Fig. 35 - Berkeley Lab's Superconducting Magnet Group's Cooling Chamber
40 ... Fig. 36 - Cross-Section of a Laboratory Superconducting Magnet
41 ... Fig. 37 - Sample Composite Superconductors
42 ... Fig. 38 - Focusing Particle Beams with Superconducting Magnets
42 ... Fig. 39 - "Type I" and "Type II" Superconductors
43 ... Fig. 40 - the hull cross-section illustration of the UNITEL craft
45 ... Fig. 41 - Applied Sciences, Inc.'s study of applications of diamond semiconductor technology
46 ... Fig. 42 - Avco, Inc.'s proposal to shield a craft with a close-adhering "cloud of electrons"

- 48 ... Fig. 43 - Berekley Lab's Superconducting Magnet Croup
 49 ... Fig. 44 - Mathematical Model of a Reaction-Diffusion Mechanism
 50 ... Fig. 45 - examples of Acoustic Surface Waves
 51 ... Fig. 46 - rear and side views of the **UNITEL** craft [scale model]
 53 ... Fig. 47 - front views of the **UNITEL** craft [scale model]
 55 ... Fig. 48 - "Doping" Semiconductors to create Junctions
 57 ... Fig. 49 - Zero-Point Motion and Energies of a Particle in a Crystal Lattice
 58 ... Fig. 50 - Wave Functions of Solid Helium Atoms
 58 ... Fig. 51 - Close Hex-Pac of Type II-VI Semiconductor Compound Structure
 59 ... Fig. 52(A) - Beam Structure of Potential EM Wells (Level 1)
 59 ... Fig. 52(B) - Beam Structure of Potential EM Wells (Level 2)
 59 ... Fig. 52(C) - Beam Structure of Potential EM Wells (Level 3)
 59 ... Fig. 52(D) - Beam Structure of Potential EM Wells (Level 4)
 60 ... Fig. 53 - the Charge-Color Placement in the Lens
 61 ... Fig. 54 - Chirped Pulse Amplification
 62 ... Fig. 55 - typical MBE equipment used in the UIC Microphysics Lab
 63 ... Fig. 56 - a Fiber Bundle on a sphere
 64 ... Fig. 57 - Geometrical Paths in a Fiber Bundle
 65 ... Fig. 58 - **UNITEL**'s projected pulsed-chirped spiraling laser plasma
 66 ... Fig. 59 - **UNITEL**'s design uses the General Vector Potential (GVP) -- Part 1
 67 ... Fig. 60 - **UNITEL**'s design uses the General Vector Potential (GVP) -- Part 2
 68 ... Fig. 61 - Rotation of a Projected Plasma Field to produce 'white' color
 71 ... Fig. 62 - Type II "Strong Electric" Superconducting Vacuum
 73 ... Fig. 63 - Quantum ChromoDynamics (QCD) vs. Quantum ElectroDynamics (QED)
 74 ... Fig. 64 - Luminescence Spectrums of a Biexcitonic Gas
 75 ... Fig. 65 - Potential Energy Wells in Excitons, Biexcitons, and Electron-Hole liquids
 76 ... Fig. 66 - Radiating Properties of RGB & Higgs' Field
 77 ... Fig. 67 - a "wormhole" in HyperSpace
 79 ... Fig. 68 - a quark-antiquark "bubble"
 79 ... Fig. 69 - Dependency of "Fine Structure" Constants on inter-particle Separation Distances
 84 ... Fig. 70 - Phonon-Scattering Processes in Solid Helium
 86 ... Fig. 71 - Adiabatic Changes in Quantum Systems
 87 ... Fig. 72 - Changing Circularly-Polarized Light into Linearly-Polarized
 88 ... Fig. 73 - the Quantum Geometric Phase
 89 ... Fig. 74 - Isotopic-Spin Symmetry in another Gauge theory
 90 ... Fig. 75 - a Neutron's Spin Vector in a Magnetic Field
 92 ... Fig. 76 - the electric field produced by Orthogonal 's' and 'p' fields
 93 ... Fig. 77(A) - Electrons confined to a 2-dimensional layer in a strong Magnetic Field -- Part 1
 94 ... Fig. 77(B) - Electrons confined to a 2-dimensional layer in a strong Magnetic Field -- Part 2
 97 ... Fig. 78 - FTL using a "Wormhole"
 98 ... Fig. 79 - John Wheeler's depiction of Quantum Vacuum Fluctuation
 99 ... Fig. 80 - Topology of Space
 102 ... Fig. 81 - Broken and UnBroken Symmetry of the Vector Boson
 103 ... Fig. 82 - the Higgs Boson
 105 ... Fig. 83 - Transitioning from Real-Space to Hyper-Space
 108 ... Fig. 84 - Interstellar Travel by Hyper-Space Navigation
 111 ... Fig. 85 - 'Time' and 'Imaginary-Time' in Real-Space and Hyper-Space
 114 ... Fig. 86 - Polarization Modulation of Ordinary Electromagnetic Radiation

- 115 ... Fig. 87 - Probing Specially-Condition EM Radiation
- 116 ... Fig. 88 - Experiment to Detect Interaction with the ZPE
- 117 ... Fig. 89 - Topology of Vacuum Field Disturbance
- 118 ... Fig. 90 - Special Relativity Solutions that permit FTL Travel
- 120 ... Fig. 91 - Screening of Charge in a Dipolar Medium
- 121 ... Fig. 92 - photo of "Lifter" (Biefeld-Brown effect)

Supplemental Documents

- | <u>page</u> | |
|--|--------|
| 132 ... A - UNITEL 's Type VI MOSS Prototype Vehicle AutoCAD Drawing | 1-of-7 |
| 133 ... B - UNITEL 's Type VI MOSS Prototype Vehicle AutoCAD Drawing | 2-of-7 |
| 134 ... C - UNITEL 's Type VI MOSS Prototype Vehicle AutoCAD Drawing | 3-of-7 |
| 135 ... D - UNITEL 's Type VI MOSS Prototype Vehicle AutoCAD Drawing | 5-of-7 |
| 136 ... E - UNITEL 's Type VI MOSS Prototype Vehicle AutoCAD Drawing | 6-of-7 |
| 137 ... F - UNITEL 's Type VI MOSS Prototype Vehicle AutoCAD Drawing | 7-of-7 |
| 138 ... G - UNITEL 's HOLO-1 Lens Composition AutoCAD Drawing | 3-of-4 |
| 139 ... H - UNITEL 's HOLO-1 Lens Composition AutoCAD Drawing | 4-of-4 |
| 140 ... I - UNITEL 's Space Shuttle Prototype AutoCAD Drawing | 1-of-2 |
| 141 ... J - UNITEL 's Space Shuttle Prototype AutoCAD Drawing | 2-of-2 |
| 142 ... K - the challenging UNITEL Material-Sciences R&D Effort | |
| 143 ... L - comparing the semiconductor properties of Silicon(Si) with HgCdTe | |
| 144 ... M - Facilities Researching Advanced Semiconductor Fabrication Technologies | |
| 145 ... N - the Cover of the Japanese Patent awarded to UNITEL | |
| 146 ... O - January 2000 Space Technology and Applications International Forum | |
| 147 ... P - July 2000 AIAA/ASME/SAE/ASEE Joint Propulsion Conference & Exhibit | |
| 148 ... Q - a letter to UNITEL from Boeing Aerospace and Electronics | |
| 149 ... R - October 1993 Congress of the International Astronautical Federation | |

ABSTRACT

UNITEL's exteriorly charged, specifically-shaped, computer-modulated Type VI vehicle design (**1**) (U.S. patent no. **4,817,102**, Japanese patent no. **1,864,717**) with the forward positioned Acoustically-Activated Semi-conducting Laser (AASL) lens, interacts with the Zero-Point Energy (**ZPE**) field as found in the 3°K vacuum of outer space (**2**). The projected spiraling charged particle beam plasma emitted from the AASL lens is composed of pulsed, coherent photon charged particle beam spin-wave packets (**3**) that are effectively potential color-ElectroMagnetism-squared (EMc^2) wells.

UNITEL's pulsed-chirped laser plasma is similar to the beam produced by the "**Pulsed Table-Top Lasers**" (**99**) that produce more power than "1000 Hoover Dams" (or even all the combined hydroelectric dams on planet Earth). This is due to the acceleration of trapped particles called "Wake Field Effect". The exterior charged vehicle with its niobium-tin-titanium-diamond "**smartskin**" hull (**45**) will interact with the projected laser plasma and be attracted to the projected beam. This high-speed computer-modulated interaction is in the femtosecond range. There is more power produced by the smartskin exterior charge system. Scientists and engineers of **Berkeley Lab's Superconducting Magnet Group** experienced the rush of shattering a world record. The team's newest niobium-tin dipole electromagnet reached an unprecedented field-strength of 14.7 Tesla. This is more than 300,000 times the strength of Earth's magnetic field.

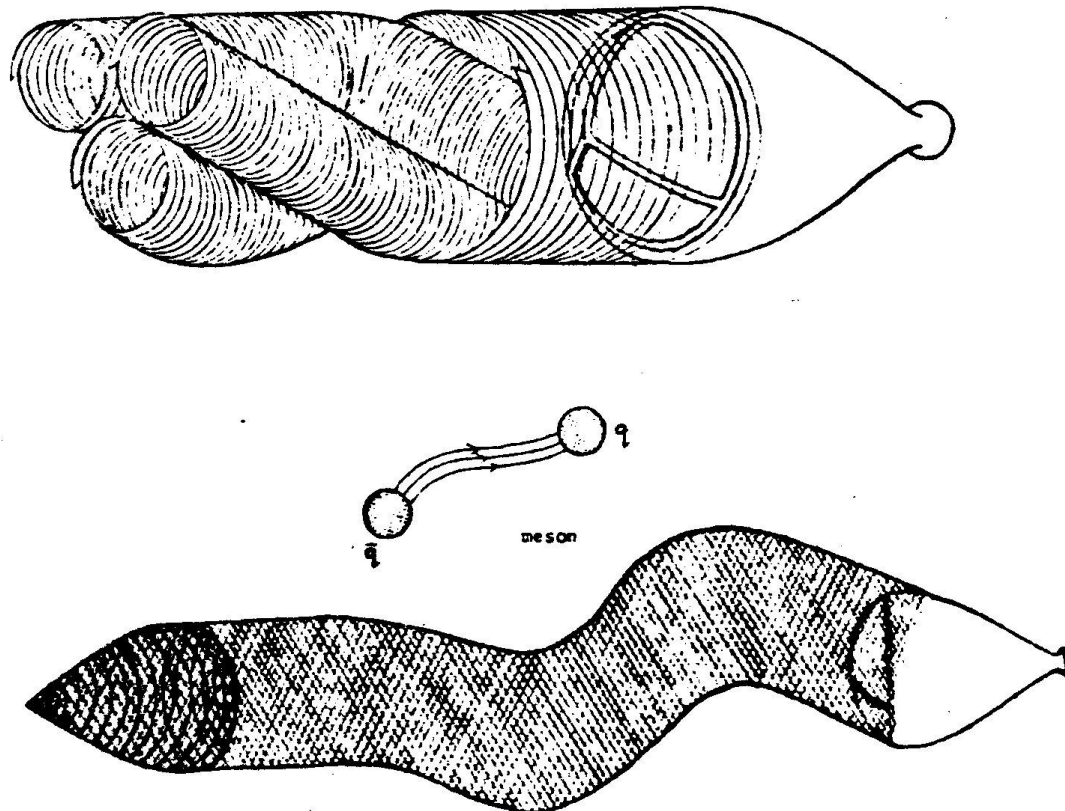
"These forces are enormous, about 3 million pounds or more than the combined thrust of more than a dozen 747 planes," says Gourlay of the Berkeley Lab team. *"To withstand this force, we needed a really good support structure design."* Taking advantage of all this incredible power, UNITEL has designed the system that will be timed so that complicated ordering of the projected beam causes the superconducting quantum particle system that depends on topological and geometrical interactions to take place. The system will produce a force of attraction of 39 orders of magnitude stronger than the force of one G. There is no conventional "action-reaction" propulsion system that can match this strength of attraction. The UNITEL vehicle will be very lightweight with no heavy, cumbersome fuels or propellants.

The design Gourlay and his colleagues employed is centered around a "common-coil racetrack" geometry, whereby a pair of coils shaped like an oval racetrack are shared between two apertures to produce opposing magnetic fields. As Gourlay describes the racetrack design: *"A racetrack coil design offers a flat geometry that can handle the forces and is well suited for use in a particle accelerator"*. UNITEL's composite multi-layered smartskin structured hull will have the ability to store vast amounts of energy in the form of magnetic fields as the wired Berkeley Lab electromagnet. UNITEL's design employs the same "racetrack" principle, only in this case the "tracks" are part of the projected plasma and not an array of coils. The precise curvature of UNITEL's proposed lens is the fiber bundle attachment point of a superconducting string that provides the mean-free path for parallel transport of particles (*i.e.*, excitons, electrons, etc.). This spiraling pathway is much like a ramp for the particles trapped and projected within the laser plasma, which automatically aligns all particles in one direction like the electrons in an ordinary magnet. The trapped particles are accelerated (like the racetrack accelerator at Berkeley Labs) to produce trillions of volts of energy via the Wake-Field effect.

The magnet at Berkeley Labs was chilled to make its coils superconducting, then energized up in field strength until it began warming along some part of the coils causes the magnet to lose its superconductivity. This temporary loss of superconductivity is called "quenching." After quenching occurs, the magnet was re-cooled and training resumed. The process was repeated until the magnet reached the field-strength limit dictated by the properties of its superconductor. It took the Berkeley team 35 quenches to reach 14.7 Tesla at 4° Kelvin (the old record of 13.5 Tesla was achieved at 1.8° Kelvin). **UNITEL**'s high-temperature superconducting smartskin hull is the first of its kind to produce and maintain a superconducting state that does not need to be supercooled. The design of **UNITEL**'s proposed vehicle produces and maintains the superconducting state of the ship and projected laser plasma. This is accomplished with the applied geometry of the vehicle which is the General Vector Potential (GVP) for electricity and magnetism. An important feature to establish and maintain superconductivity and prevent decoherence is the clocking of the entire ship to field system, which is in the femtosecond range. Timing of the ship interactions with the projected pulsed- chirped laser plasma is very important. The extremely high-temperature modulated exterior charge, which is fractional 1/3, on the vehicle with proper frequency and harmonics applied in each 1/3 section, will be the first of its kind: a high-temperature Macroscopically Observable Superconducting State (MOSS).

The design of **UNITEL**'s high-speed Mass Transportation vehicle with payload employs no moving parts; is electrically-powered, and requires no bulky fuels or propellants. This quantum mechanical propulsion system design is the first of its kind and operates on principles other than the usual action-reaction types of propulsion systems that fires a blast of energy out of the back of a vehicle to propel it forward (*i.e.*, rockets or jet). Simply stated, our vehicle will be pulled along by a strong electromagnetic attraction instilled in the spiraling charged particle beam laser plasma that is focused in front of the vehicle. The projected RF (microwave) field lines in the projected charged particle plasma perfectly mimic the field lines in a ferromagnet. One could say that this vehicle design can be thought of as a “front wheel drive” system. The intensity of the magnetic attraction can be compared to an electron seeking a hole. Wherever a hole appears, that is where an electron will go to seek its ground. The same goes for the design of our space ship. In this case, the exteriorly charged vehicle is seeking the endpoint of its projected charged particle laser plasma, which is opposite of charge and polarity.

FIELD EXTENSION DYNAMICS



F - 3

Figure 1 - Field Extension Dynamics

The main goal of the design for this quantum electromagnetic vehicle and projected laser field is to simulate natural quantum-level physical effects so that our ship and projected laser field is one very large quantum particle system, or one gigantic electron-hole (exciton) or electron-positron (4). This is the familiar model of “two spherical bodies connected by a spring-like structure” that is found to be true for describing most quantum particles (5). A quote from Bryce DeWitt: “*When a quantum effect -- such as particle production or vacuum energy -- reacts back on the curvature of spacetime, curvature itself becomes a quantum object*” (6). Classically, the energy of a particle is the sum of its kinetic and a possible potential energy” (*i.e.*, monopole vacuum expectation value). Concerning the projected laser plasma and its massive charged rotating end-point assuming the characteristic of one of the two quantum bodies and spring-like structure is the scientific description of the interaction of a particle with the Higgs’ field in the Zero-Point Energy (ZPE) quantum mechanical vacuum order parameter of spacetime (7). The ZPE is found in the 3°K

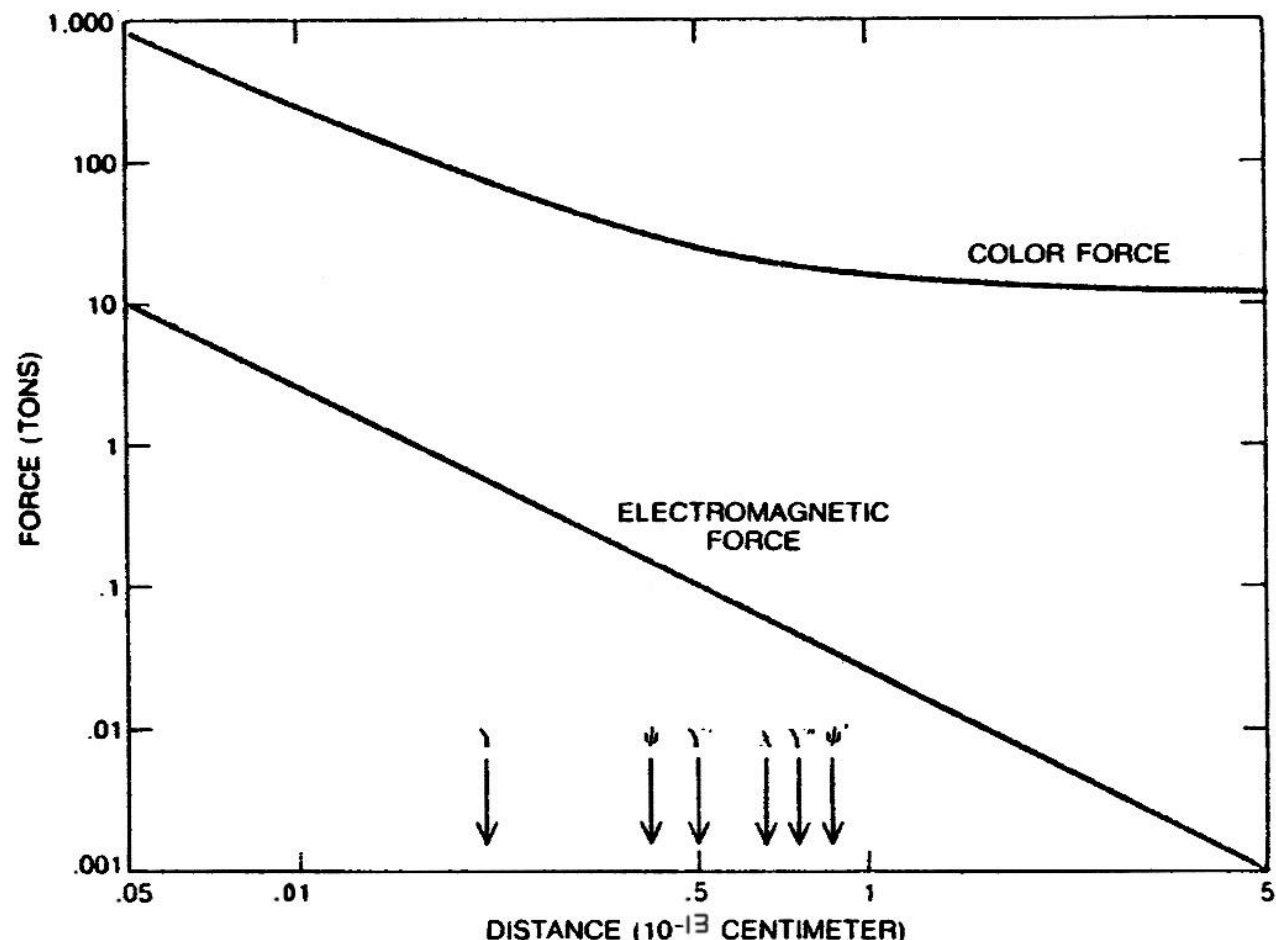
vacuum of space. It is referred to as zero point, because the energy is not thermal in nature. The ZPE consists of random quantum fluctuations and is maintained by a flux of electrical energy flowing through four-dimensional space-time. This contributes to the energy of the particle with respect to the vacuum. That energy is equivalent to a mass (8). In certain theories, impressions of the Higgs' field dynamical internal structure is composed with causally separated domains pointing in different internal group directions causing a monopole to be formed where they meet. The value of the Higgs field goes to zero in the center (9).

UNITEL's patented design utilizes accepted methods of quantum electromagnetic design to potentially allow the vehicle and crew to perform Macroscopic Quantum Tunneling (MQT) to traverse vast distances of outer space in a feasible time frame (10). **UNITEL**'s aerospace vehicle electromagnetic (laser) propulsion design has the potential to travel at near light speed velocities with the ability to utilize higher (5 through 11) dimensions. We shall call these higher dimensions "Hyper-Space".

To provide a realistic way of exploring our Universe to discover new and habitable planets, we would have to send a spaceship to the stellar systems at more than a distance of several hundred light-years away. A spaceship traveling at the velocity of light would obviously present numerous disadvantages for human transport in periods of 200 to 300 years of traveling. This paper describes our propulsion theory that will allow travel to the distant regions of our Universe -- several hundred light-years from planet Earth -- in just a few days!

Assuming that a Hyper-Space has the characterization of Euclidian Space, **Minami** (80) derived the appropriate Lorentz transformations between the two coordinate systems. These will produce the time transformation between Real Space and Hyper-Space by the method of analytic continuation on the elapsed time of the spaceship. For instance, if the spaceship achieves a velocity V_s of $0.999999999c$ ($c=3\times10^8$ m/s) in Real-Space, then **one hour** in Hyper-Space corresponds to **31,622 hours** or 3.6 years in Real-Space. Although 100 hours shown on a clock in the spaceship during Hyper-Space navigation is equal to 70 hours elapsed time on Earth, the spaceship at a quasi-light velocity could travel to stars 253 light-years away in 100 hours.

The coupling strength of these quantum mechanical interactions begins on the order of $1/137$ (12) and proceeds in a largely momentum dependent form to the strength of one and then to $137n$ and beyond to create a Macroscopically Observable Superconductive State (MOSS). The beginning coupling strength can be defined by Quantum ElectroDynamics (QED), which is part of the standard particle physics model that describes the electromagnetic force governing the interaction of electrons and light. On the other hand, $137n$ is defined by Quantum ChromoDynamics (QCD), which is part of the standard model of particle physics that describes strong interactions involving quarks, gluons and the color force (13).

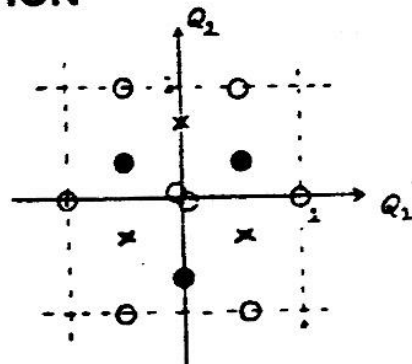
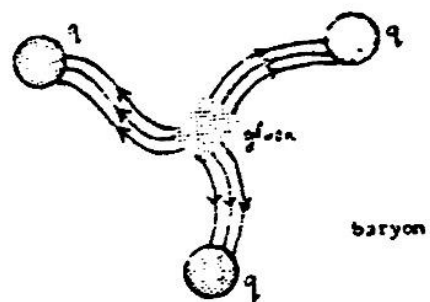


FORCE BETWEEN QUARKS -- called the "color force" -- seems to obey a law significantly different from the one that describes the electromagnetic force. The strength of the electromagnetic force between two particles varies inversely as the square of the distance between them. Such a force law corresponds to a straight, sloping line on this logarithmic graph. At exceedingly short distances, the color force also seems to follow an inverse-square law. But beyond about 10^{-13} centimeters the force may have a constant value independent of the distance. If the long-range force is constant, data from quarkonium suggest its magnitude is about 16 tons. The force law shown is based on a model devised by John Richardson, who was then at SLAC.

Figure 2 - Force Between Quarks Law

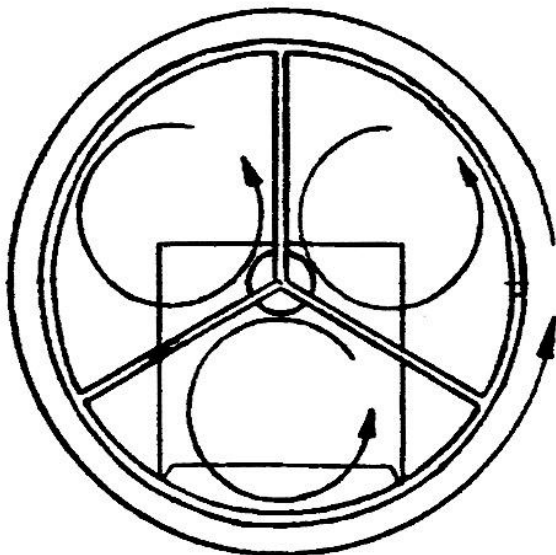
The projected charged particle laser plasma is attached to our vehicle and assumes the character of a flux-tube bond between a microscopic quark/anti-quark bound state (meson) or three-quark state (baryon) (14) system with monopole/anti-monopole interactions (15). All ship-to-field interactions will be controlled completely by an on-board computer and will provide a feasible control system for propelling the vehicle (manned or unmanned) with a payload to travel in outer space or within the Earth's atmosphere in a manner much like a helicopter.

FIELD CROSS-SECTION



○ photon electric charges

- quark electric charges, × anti-quark electric charges.



F - 4

Figure 3 - Lens Design

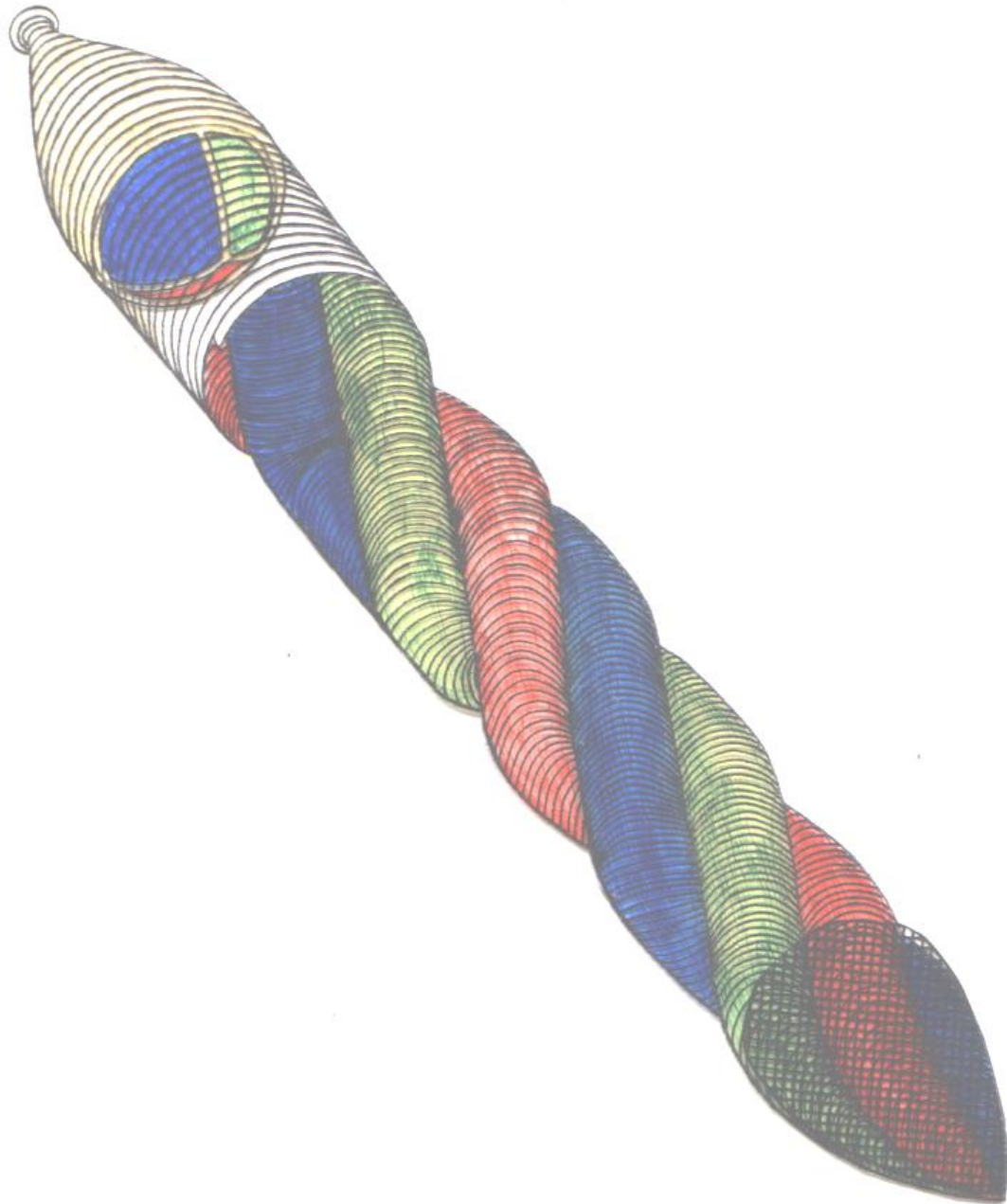
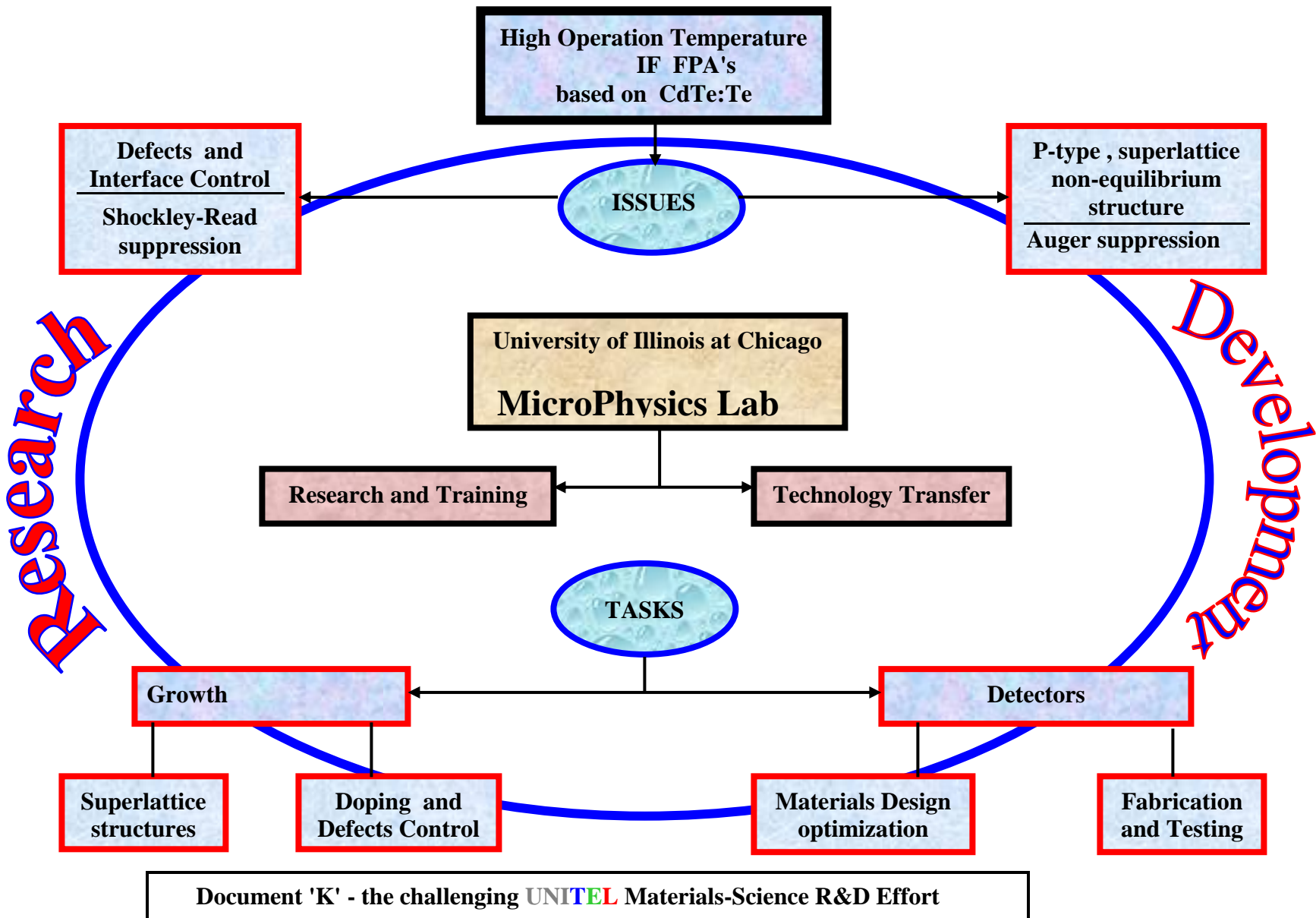


Figure 4 - UNITEL's space vehicle and projected laser plasma



1 - INTRODUCTION

The design of our MOSS aerospace vehicle with payload employs **no moving parts**; it is all electrically powered and requires no bulky fuels or propellants. This quantum mechanical propulsion system design is the first of its kind and operates on principles other than the usual action-reaction types of propulsion systems that fire a blast of energy out of the back of a vehicle to propel it forward (*i.e.*, rockets or jets). The design of **UNITEL**'s computer-modulated (see "**HOLO-1 Quantum Holographic Computer**" December 7, 1998) exteriorly charged craft allows complete control of flight navigation and steering. In fact, the magnitude of controlled performance should be safe enough to be an efficient high-speed public mass transit system (see "**UNITEL's High-Speed Mass Transportation Vehicle**" November 2, 2000).

The design of the aerospace vehicle is somewhat comparable to the familiar Mag-Lev (16) in that our vehicle will require conventional mag-lev tracks for suspension of the vehicle while docking for boarding crew and loading cargo. One of the conditions in the design of this type of exteriorly charged vehicle is that it cannot touch the ground -- or any other surface -- for that matter. There are no protuberances, wings, etc. in the design that is a specific size & shape, that being the "capped cone" or teardrop shape (17). It has been well known since the '40s that the "**teardrop**" shape is the ideal electromagnetic shape. Once ready for flight, the vehicle and crew will require no suspension except from the mag-lev tracks while docking. The cushion of electromagnetism provides no resistance to the vehicle, allowing ideal conditions for the vehicle to be pulled along by the attractive projected charged particle laser beam.

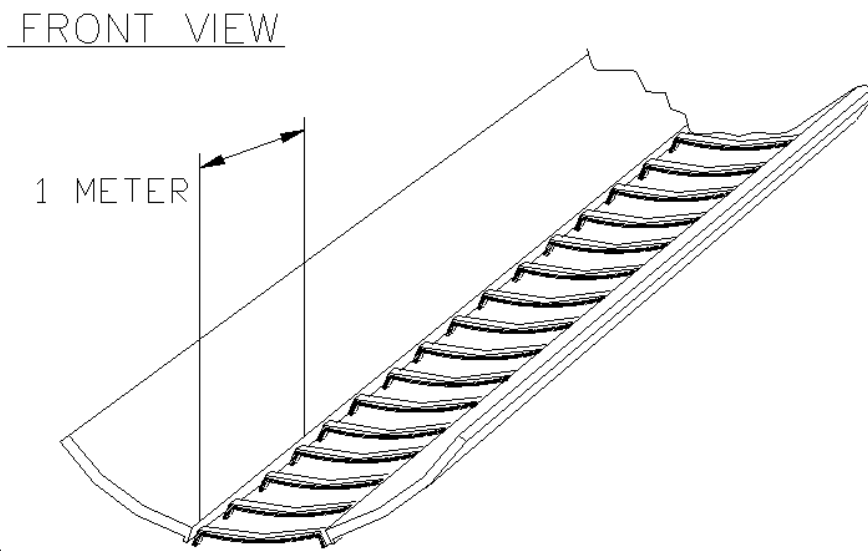
The May '02 issue of ***Scientific American*** contains the earth-shaking article on page 80, entitled "***Extreme Light***" and the Pulsed Table-Top Lasers that produce more power than "1000 Hoover Dams" (99). At **UNITEL**, we have the pulsed table-top lasers that all but prove what we are saying is true: (with a working prototype) our system will do what their Pulsed Table-Top lasers do ... only much more!! From the article: *"These compact lasers can fire a hundred million shots per day and can concentrate their power onto a spot the size of a micron, producing the highest light intensities on earth. Associated with these gargantuan power densities are the largest electric fields ever produced, in the range of a trillion volts per centimeter. Such intense laser light interacting with matter re-creates the extreme physical conditions that can be found only in the cores of stars, or in the vicinity of a black hole: the highest temperatures, 10^{10} Kelvins; the largest magnetic fields, 10^9 Gauss; and the largest acceleration of particles, 10^{25} times the Earth's gravity."*

We "chirp" our laser by chirping the RF-activating wave packets that essentially will produce the same result -- a huge gain in energy in the projected laser field. From the article on page 90: "... electron oscillation velocities near the speed-of-light, it curls the paths of the electrons and gives them tremendous momentum in the direction of the light beam. This effect plays a central role in relativistic optics."

UNITEL's basic laser system is also a pulsed chirped system that will produce the same basic effects that the Pulsed Lap-Top lasers in the article do. It isn't that hard for one to make the comparison and see how our design is essentially the same in that both are pulsed chirped laser systems that accelerate the trapped particles. However **UNITEL**'s laser system is significantly more sophisticated than the standard description of the Pulsed Table-Top Lasers described in the article. One important aspect of **UNITEL**'s design is that it will produce **monopole** effects similar to what **Akira Tomita & Raymond Chiao** did with their monopole applications to RF waveguides and optical fibers. We take advantage of that curl effect

along with timing or clocking the pulsed laser field to instill proper rotation to create Berry's Phase and parallel transport mechanism effects in the beam.

The vehicle will literally fly through it's own "flux tube" by adiabatic pressure that is created by the projected highly magnetic charged particle beam plasma directed in front of the ship. Simply stated, **our vehicle will be pulled along by a strong electromagnetic attraction instilled in the spiraling charged particle beam laser plasma that is focused in front of the vehicle.**



TYPICAL REPULSIVE TRACK
AT DOCKING STRUCTURE

Figure 5 - Docking Tracks from Mag-Lev design

The charged particle beam will be projected from the three equal part **Red, Green & Blue** (tuned electromagnetic frequencies), doped, RF-transparent, Type II-VI semiconducting compound AASL crystallite lens **(18)** that is located in the forward area of the ship.

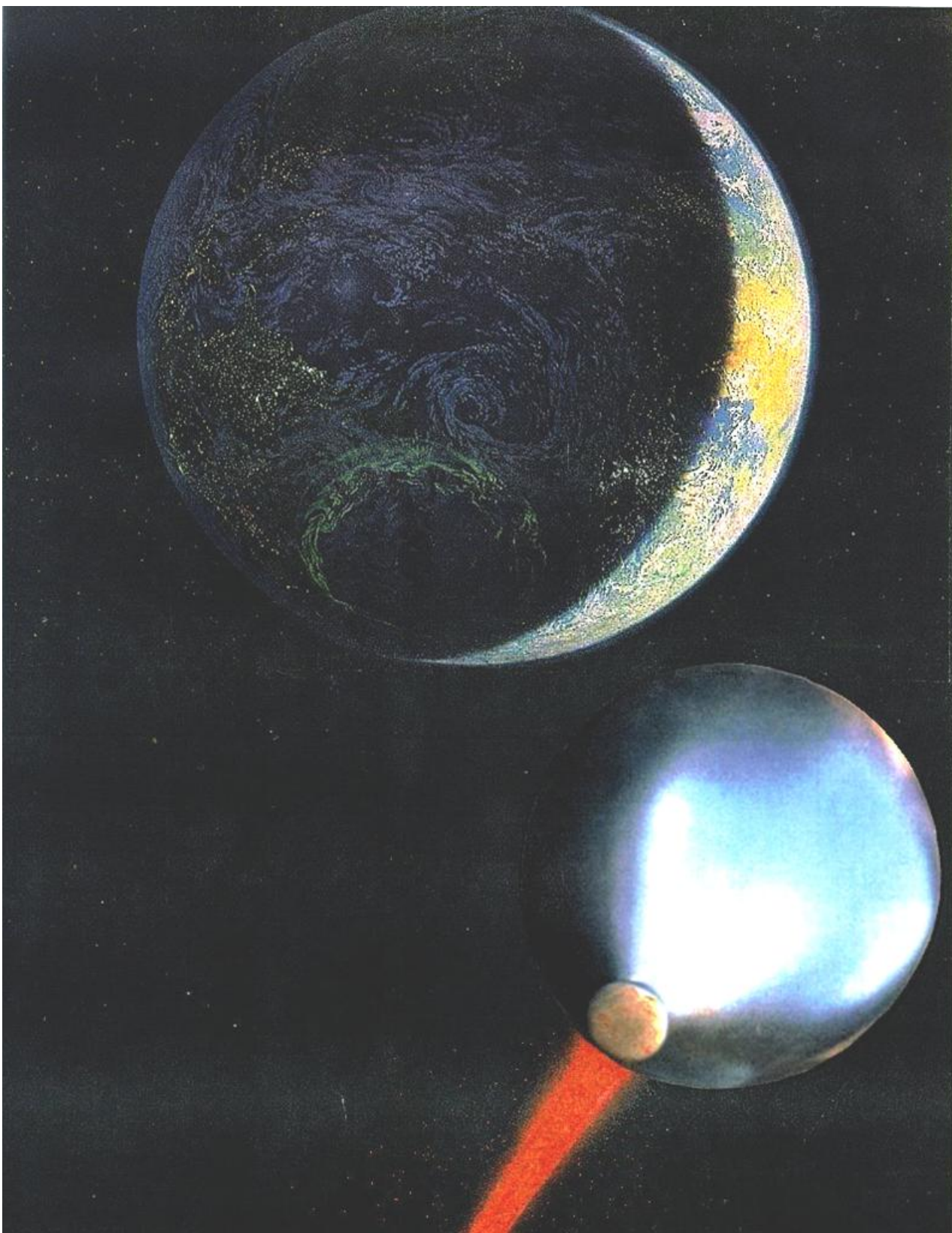


Figure 6 - artist's conception of UNITEL's proposed space vehicle (rear view)

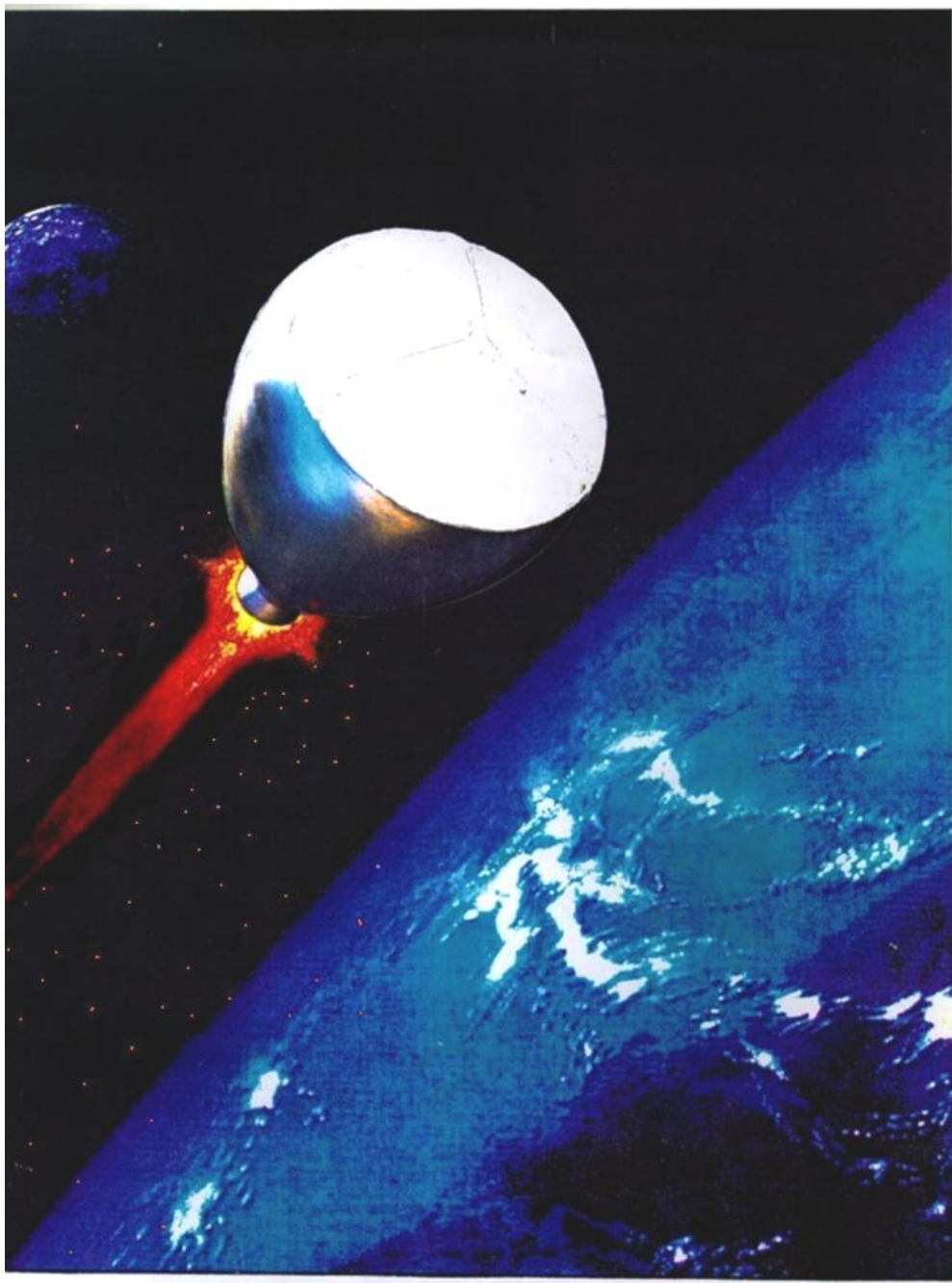
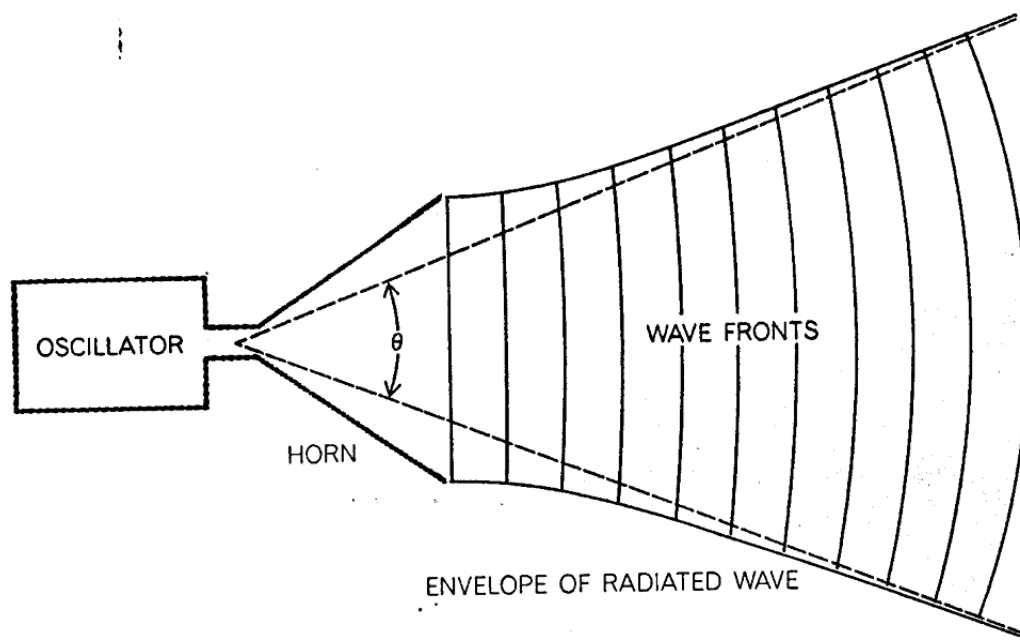


Figure 7 - artist's conception of UNITEL's proposed space vehicle (front view)

The tuned lens with forward bias will allow internally produced waves of **excitons** to couple to the external acoustic shock wave that is focused on the surface of the lens (19).



RADIO WAVES obtained from a radio (oscillator) in the form of a pulsating current can be fed into a suitably designed horn (center), from which they are radiated into space in the form of a beam that spreads at an angle (θ) roughly equal to the wavelength of the radiation divided by the diameter of the horn's aperture. The wave fronts of the beam are essentially plane at the mouth of the horn and assume a spherical shape as the beam progresses away from the horn. The angle θ has been exaggerated here; normally it is less than 10 degrees.

Figure 8 - Geometry of Radiated RF Wave Fronts courtesy *Scientific American*, Jan'66 (41)

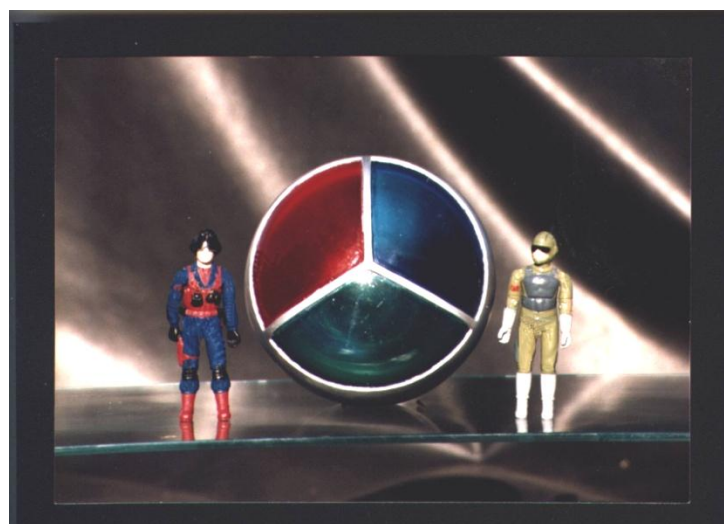
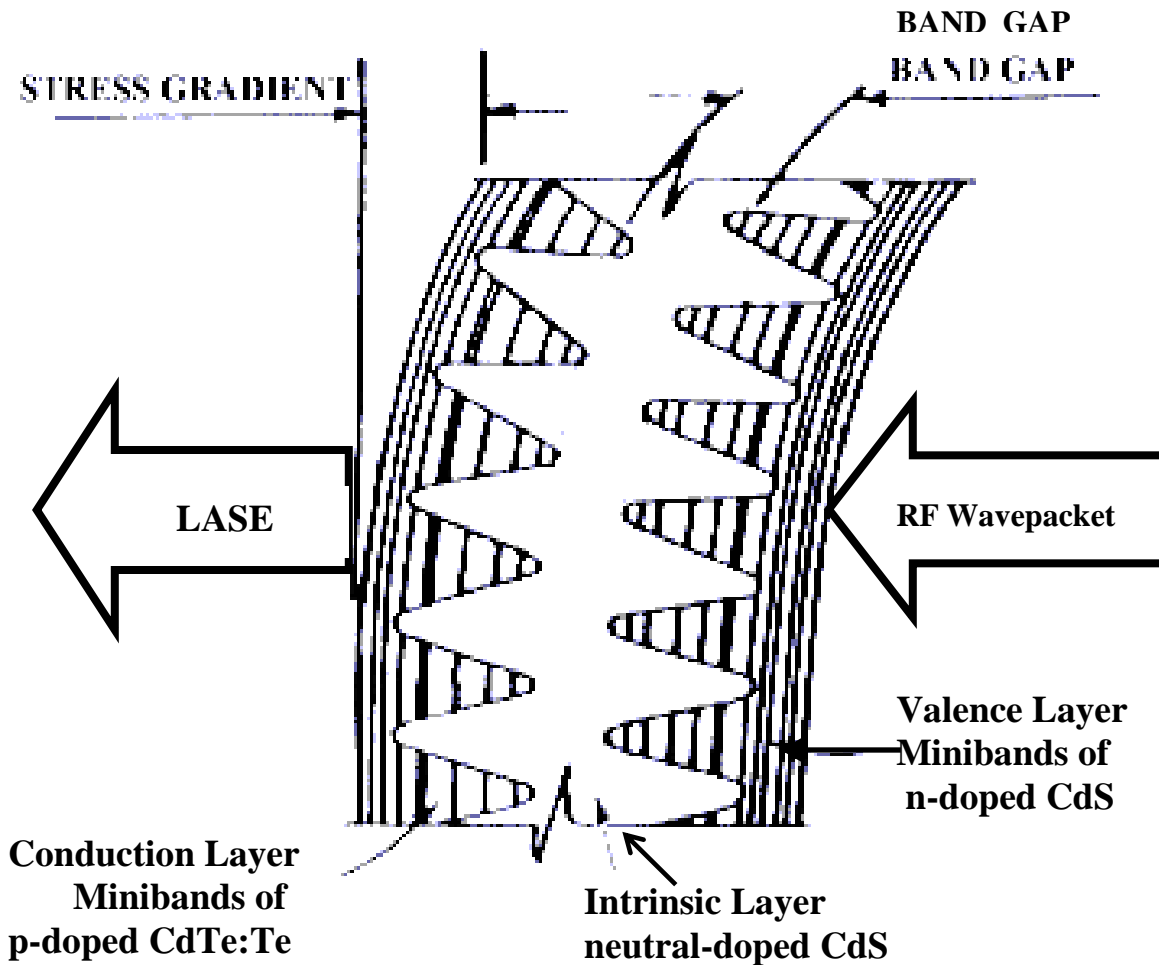


Figure 9 - scale model of UNITEL's aerospace vehicle (front view) with technician model figures

The projected acoustic shock wave (20) produces a "wind" of **phonons** that scatters excitons and tunnels through the lens to combine and lase on the surface where both photons and excitons couple to the acoustic shock wave (21).



"Laser Lens Composition"

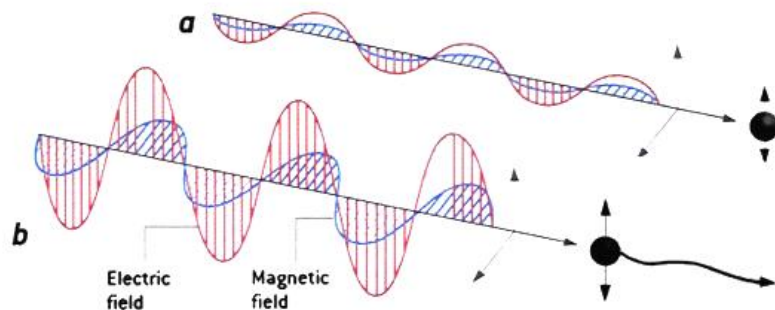
Figure 10 - Doped Crystallite

The acoustic shock wave then "pops out" into a point-like shape due to photon acceleration producing the leading edge. The RF constituents close of the lateral and trailing edge that is produced by pulsing the field. The three separate **Red**, **Green** & **Blue** spiraling beams that are produced by the lens travel at different phase velocities and recombine to give an elliptically polarized beam at one ellipse per cycle (optical electrical field vector).

LIGHT INTERACTING WITH MATTER

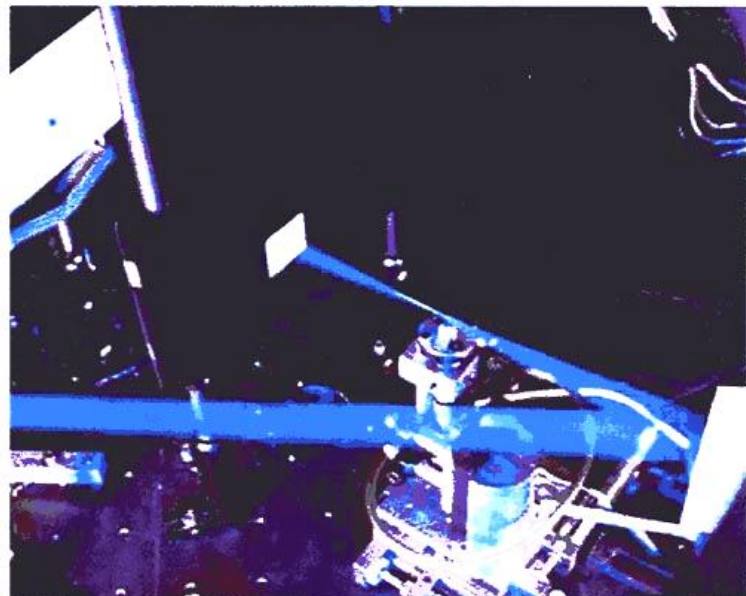
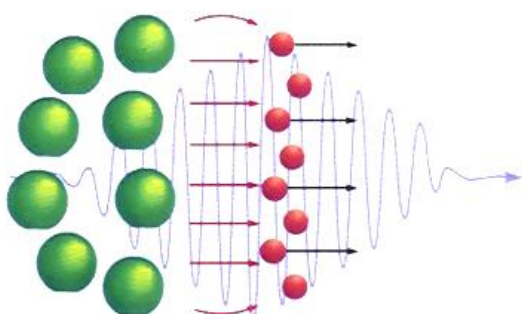
RELATIVISTIC OPTICS

FOR LIGHT of ordinary intensity (*a*), the light's electric field [red waves] makes electrons oscillate at relatively low speeds. At extremely high intensities (*b*), the electrons oscillate at nearly the speed of light, and the light's magnetic field [blue waves] makes them fly forward with very high momentum.



WAKE-FIELD ACCELERATION

HIGH-INTENSITY LIGHT striking a plasma (*below*) pushes the electrons to very high speeds, leaving the heavier positive ions (green) behind and producing a powerful electric field (red lines) between these separated charges. This separation of charges and the associated electric field trails along in the wake of the light and can accelerate other charged particles to very high energy.



ULTRAHIGH-INTENSITY LASER PULSE (added in blue) focused on a jet of helium gas by a parabolic mirror accelerates electrons from the gas to 60 MeV in one millimeter. A fluorescent screen (upper left) detects the high-energy electron beam.

Figure 11 - Light Interacting With Matter (courtesy *Scientific American*, May '02 (99))

The combination of the three separate electromagnetic wavelengths (Red, Green & Blue) is required to form a true electromagnetic wave packet (22). It has been demonstrated that strain confinement in a parabolic potential well is a versatile method for capturing and controlling a gas of excitonic particles. **It is the Wannier-Mott excitons that exhibit the hydrogen-like series that we wish to produce and confine in our projected charged particle beam (23).**

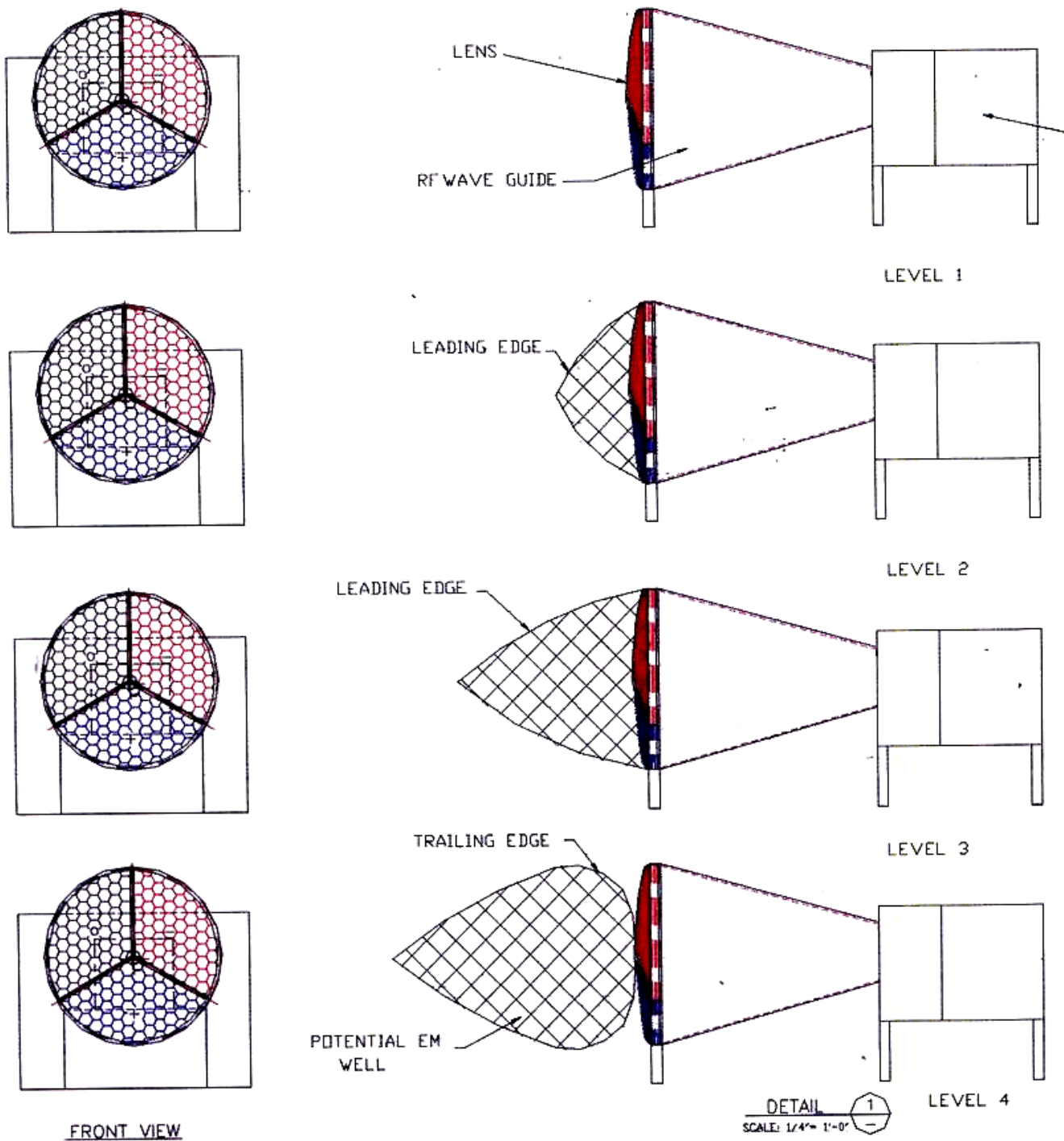


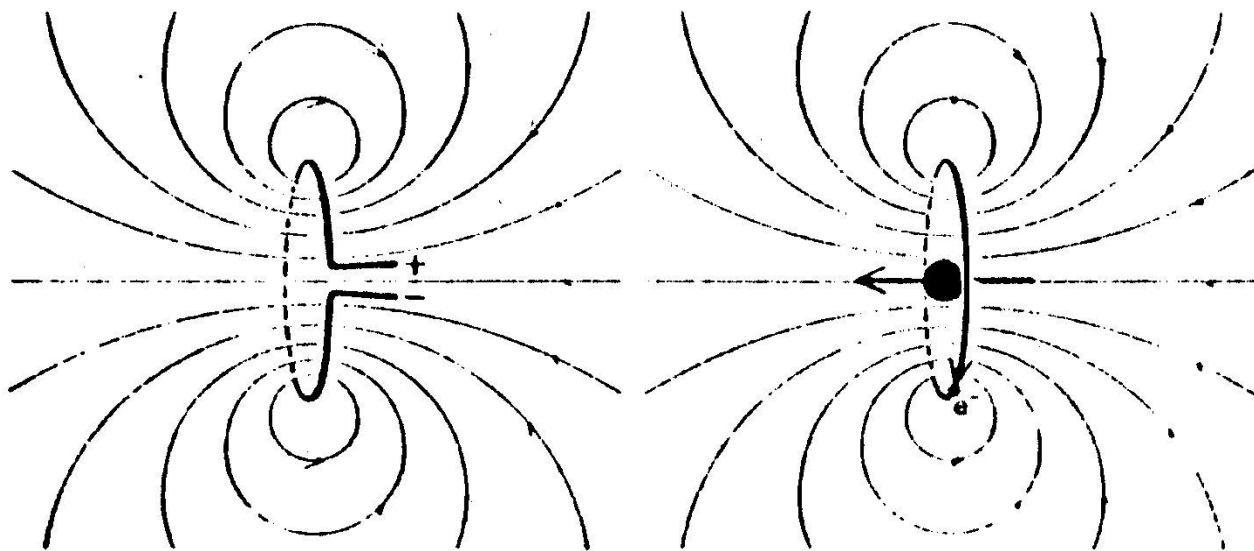
Figure 12 - Pulsed Laser technique that produces the potential EM wells with Leading/Trailing edge dynamics that traps the excitonic gasses and accelerates them to produce the Wake Field Effect.

There is virtually no comparison between any types of explosive propellant that could match the transport capabilities of electromagnetic attraction to our MOSS spaceship. The vehicle will be highly maneuverable -- much like a helicopter with the ability to travel at various rates of velocity -- from a hover mode to near light speed. The flight control system located within the vehicle will include a very high-speed integrated circuit (VHSIC) computer to allow a smooth transition between low to extremely high velocities. Operation and directional control of the vehicle will be accomplished by computer-controlled phase conjugate (radar) steering techniques.



Figure 13 - compares UNITEL's laser lens is compared to a "radar gun" whereby a reference return wave can also be employed in the space vehicle for steering & navigation purposes.

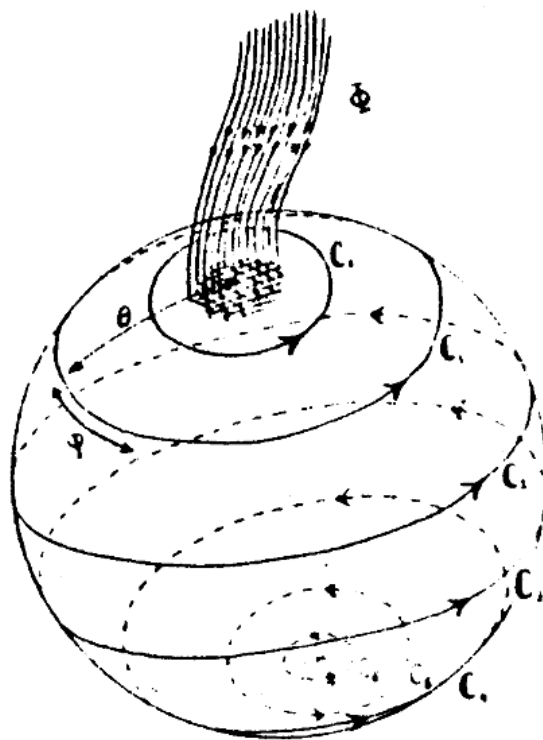
The specifically shaped, exteriorly charged hull of our space vehicle will interact with the ZPE field in the vacuum of outer space through the projected three-phase, charged particle beam that produces the strong electromagnetic attraction to the vehicle.



CIRCULATING ELECTRIC CHARGE in a loop of wire generates a dipole magnetic field with its axis oriented at a right angle to the plane of the loop (*left*) . The movement of bound electrons around the nucleus of an atom constitutes a similar loop of current and endows the atom with a corresponding dipole field (*right*). Only one representative electron is shown.

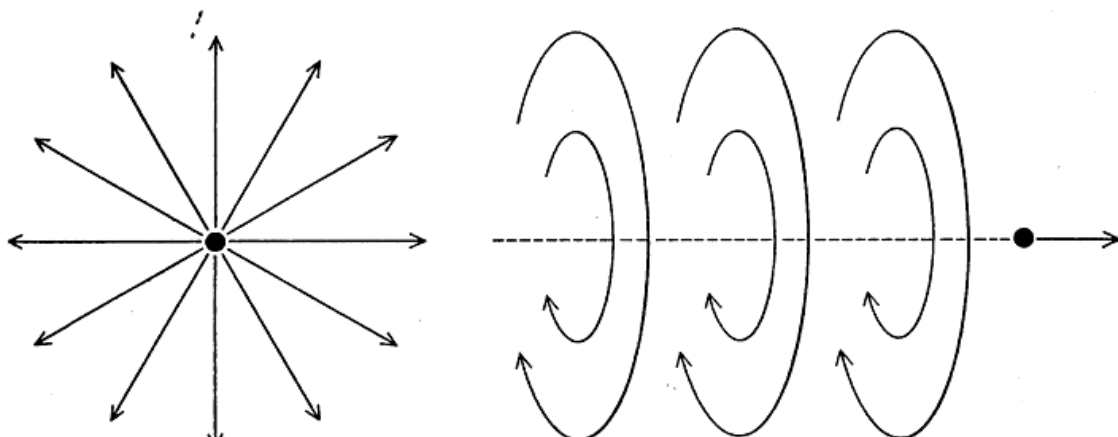
Figure 14 - Dipole Magnetic Fields created by a Circulating Electric Charge
(courtesy Scientific American, June '80 (66))

UNITEL's proposed vehicle will be attracted to the **magnetic monopolar charge** on the projected beaded plasma (24), which is opposite in polarity (North) to the (South) magnetic monopolar topological rotating standing, running or retarded wave charge configuration that is induced by the RF diode system on the vehicle's hull (25). Our MOSS system is designed to polarize and make coherent the random fluctuations in the ZPE field. The "zero point" refers to zero degrees Kelvin and this means the energy fluctuations are not thermal in nature.

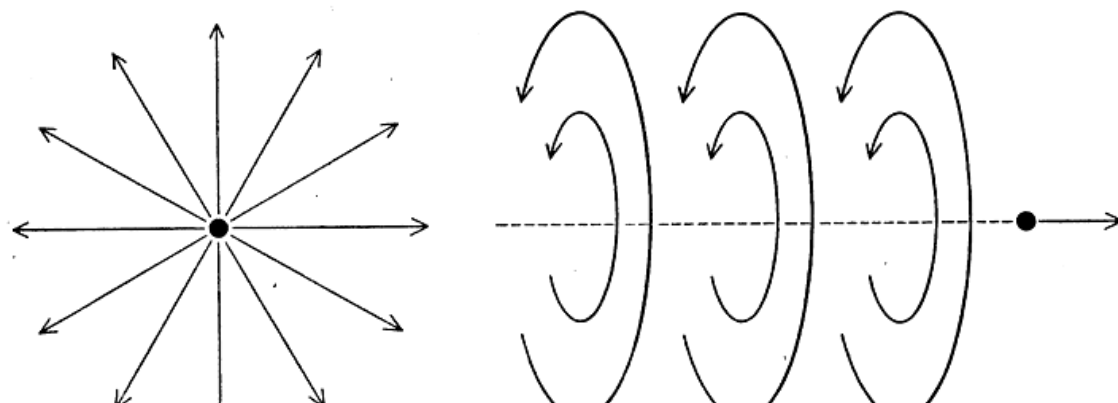


The contour C on the sphere around the monopole. We displace it from C_0 to C_1 , etc., until it shrinks at the bottom of the sphere. We require that there be no singularity at that point.

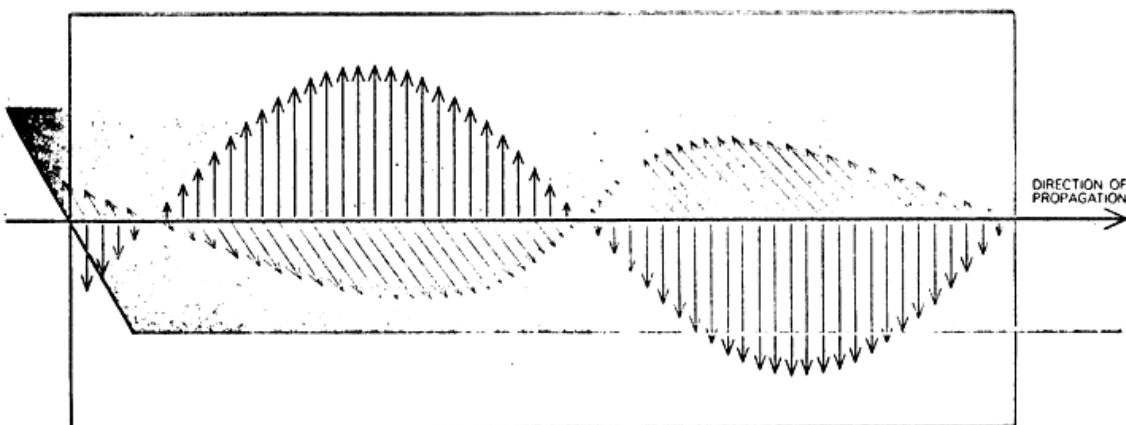
Figure 15 - Magnetic Monopole Geometry (69)



PROTON (black dot) sets up an electric field (black arrows) around itself when standing motionless (left). In motion (right) it creates both an electric field (not shown here) and a magnetic field (arrows). The magnetic field is weaker than the electric field and is oriented differently. In actuality the electric field in the drawing at the left extends in 3 dimensions.

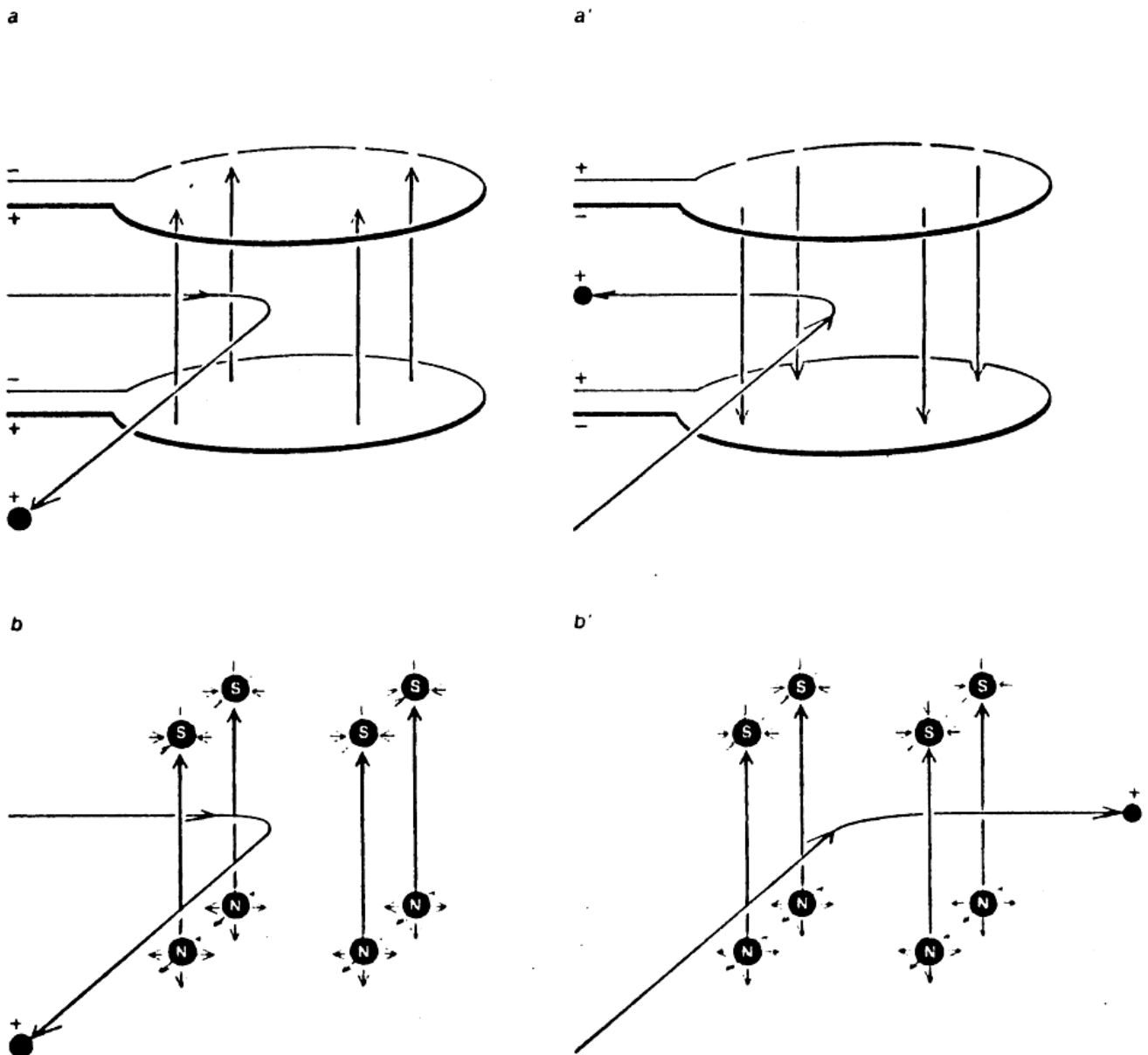


MONOPOLE (black dot) would create a magnetic field around itself when stationary (left) and an electric field when in motion (right). A North monopole is shown here. The electric field around a moving South monopole would be in the opposite direction. For complete electromagnetic symmetry, "magnetically charged" monopoles as well as electrically charged particles



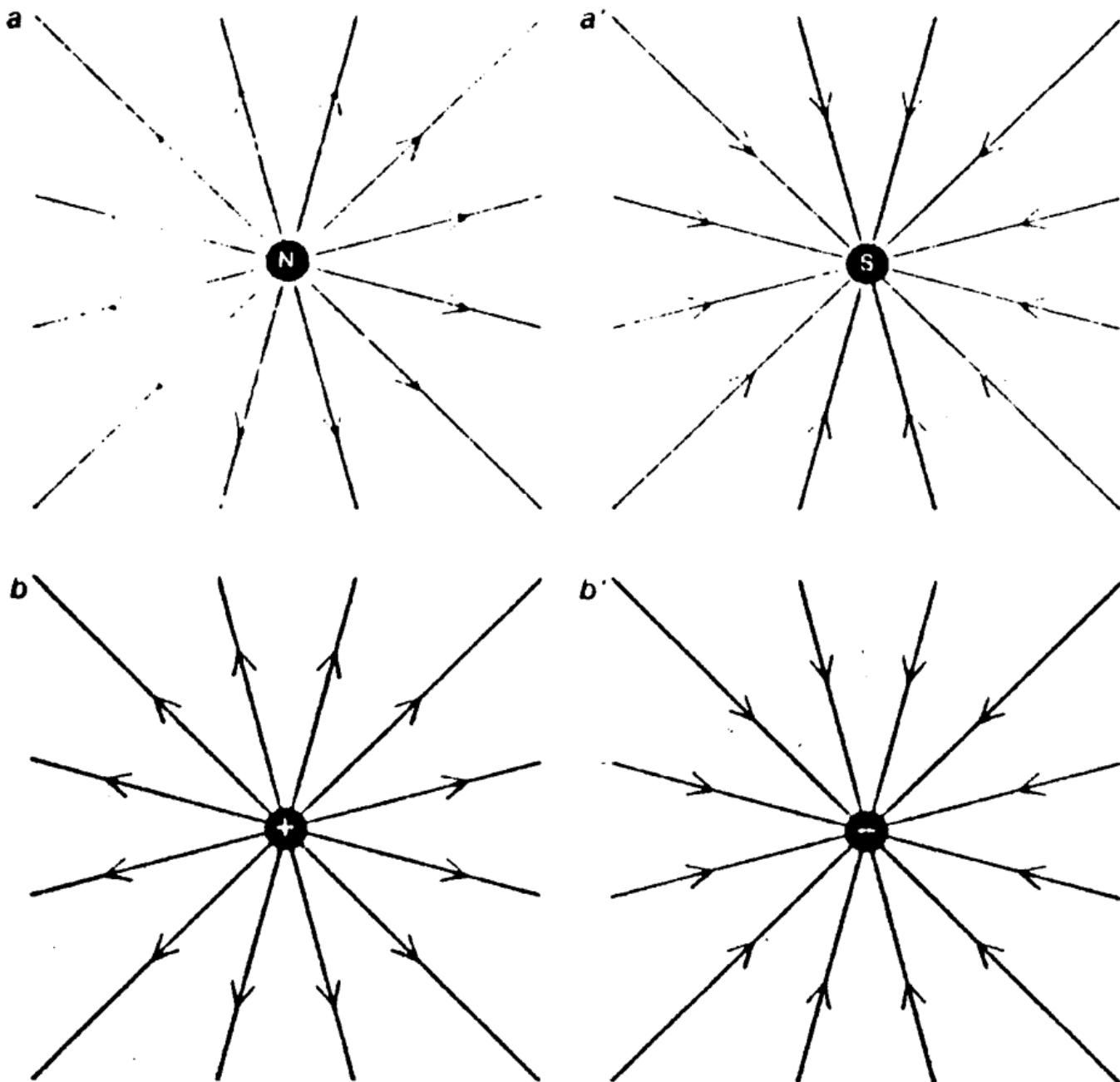
ELECTROMAGNETIC WAVE propagating in free space consists of oscillating electric and magnetic fields of equal intensity in a perfect state of balance. Such a wave can be created by an accelerated charged particle (a proton or an electron). It could also be created by an accelerated North or South monopole. In this diagram the electric field is vertical and the magnetic field horizontal.

Figure 16 - Electric and Magnetic Fields created by Magnetic Monopoles (66)



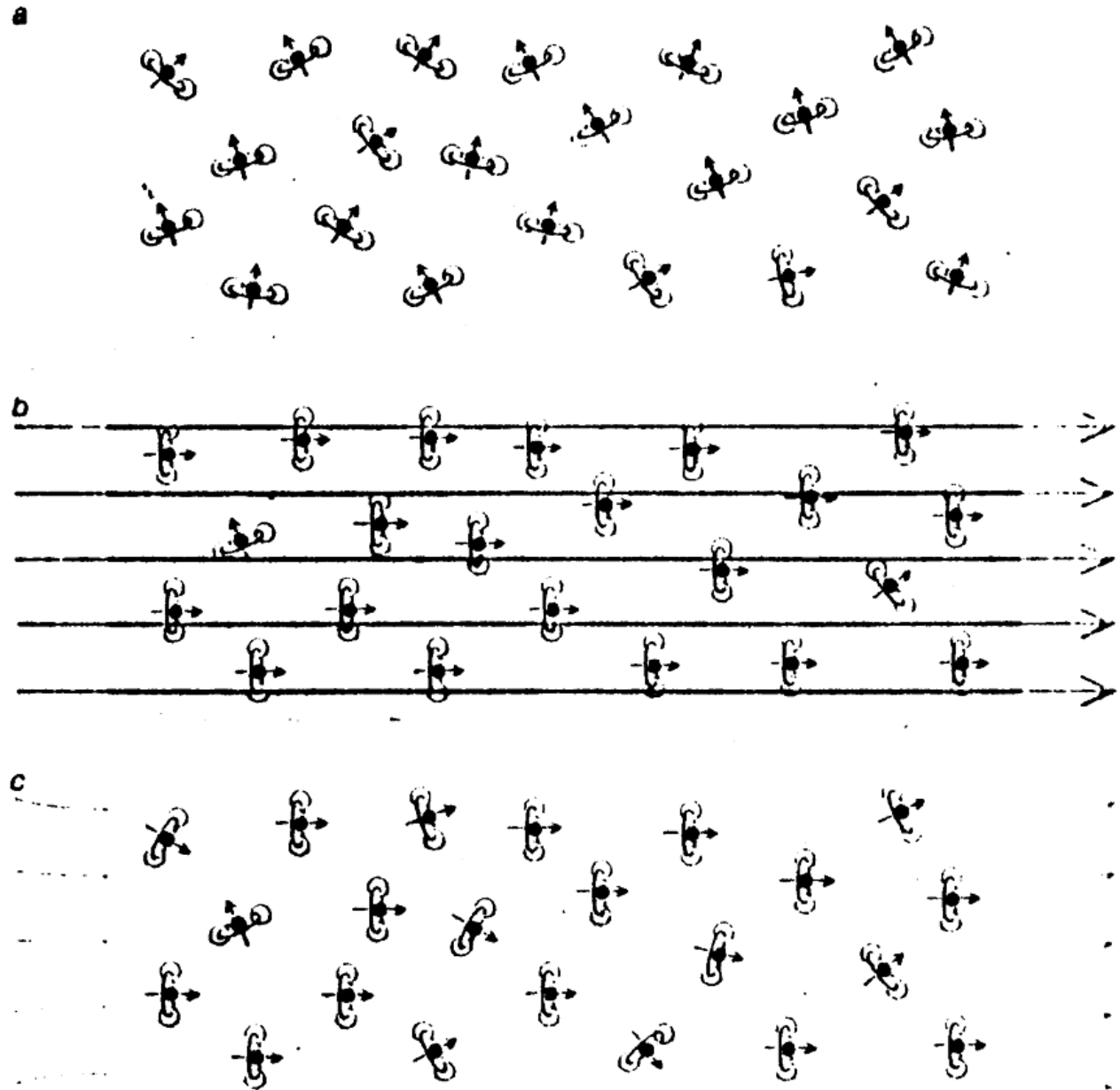
TIME REVERSAL would have a peculiar effect on an electrically charged particle moving through the magnetic field produced by a magnetic monopole. In (a), a proton is shown moving along a curved path through a perpendicular magnetic field generated by electric currents flowing in a pair of wire loops. If the direction of time is reversed (a'), both the currents (and therefore the magnetic field) and the motion of the proton would be reversed. The path of the proton, however, would be invariant: the particle would simply retrace the same path in the opposite direction. In (b), a proton is shown moving along a similar path through the magnetic field produced by an idealized array of North and South monopoles. In this case reversing time would leave the magnetic field unchanged (b'). Although the proton would reverse direction, it would not retrace its path; such a result would be a violation of the principle of time-reversal invariance.

Figure 17 - Time History of an Electrically-Charged Particle moving by a Monopole
(courtesy Scientific American, June '80 (66))



SYMMETRY between magnetic monopoles and electrically charged particles such as the proton extends in theory to their antimatter counterparts. A North monopole (*a*) would have as its anti-particle a South monopole (*a'*), just as the proton (*b*) has as its anti-particle the anti-proton (*b'*).

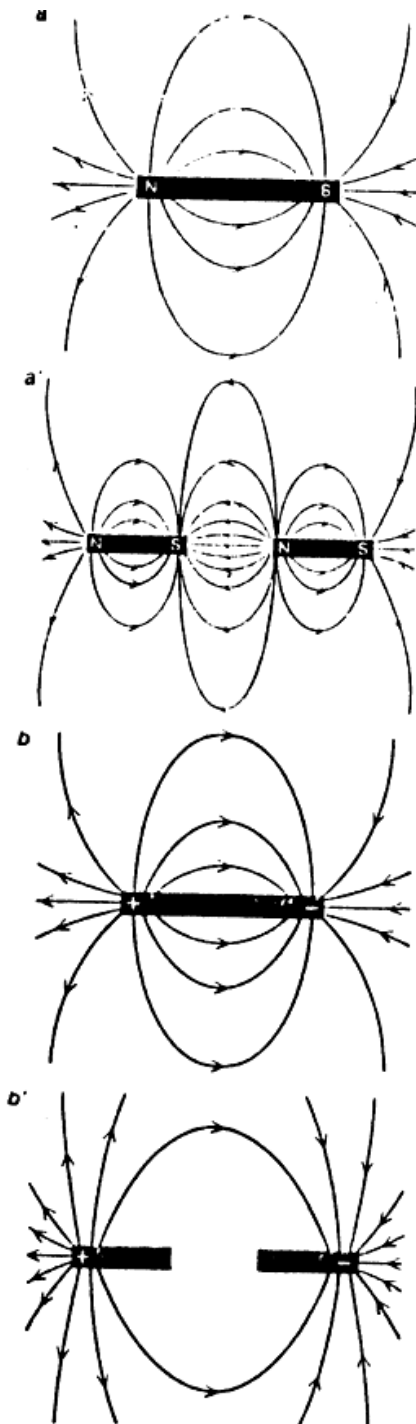
Figure 18 - Symmetry between Magnetic Monopoles and Matter/Anti-Matter
(courtesy Scientific American, June '80 (66))



ATOMIC MAGNETS are randomly oriented in an ordinary, nonmagnetic iron bar (a). The atoms can be aligned by the application of an external magnetic field (b). When the external field is removed (c), many of the atoms remain aligned, forming a permanent magnet. Cutting such a magnet in half has no effect on the atomic currents and hence does not serve to isolate the magnetic poles. For simplicity the bar is represented as having a single magnetic domain.

Figure 19 - Magnetic Orientation on an Atomic Scale

(courtesy Scientific American, June '80 (66))



DIPOLE FIELDS are set up by a bar magnet (a) and by an analogous structure consisting of an insulating rod with opposite electric charges deposited at the ends (b). When the magnet is cut in half, two smaller dipoles are created (a'). When the electric analogue is cut in half, the field remains dipolar because the electric charges that generate the field remain in place (b').

Figure 20 - Dipole Magnetic and Electric Fields (courtesy *Scientific American*, June '80 (66))

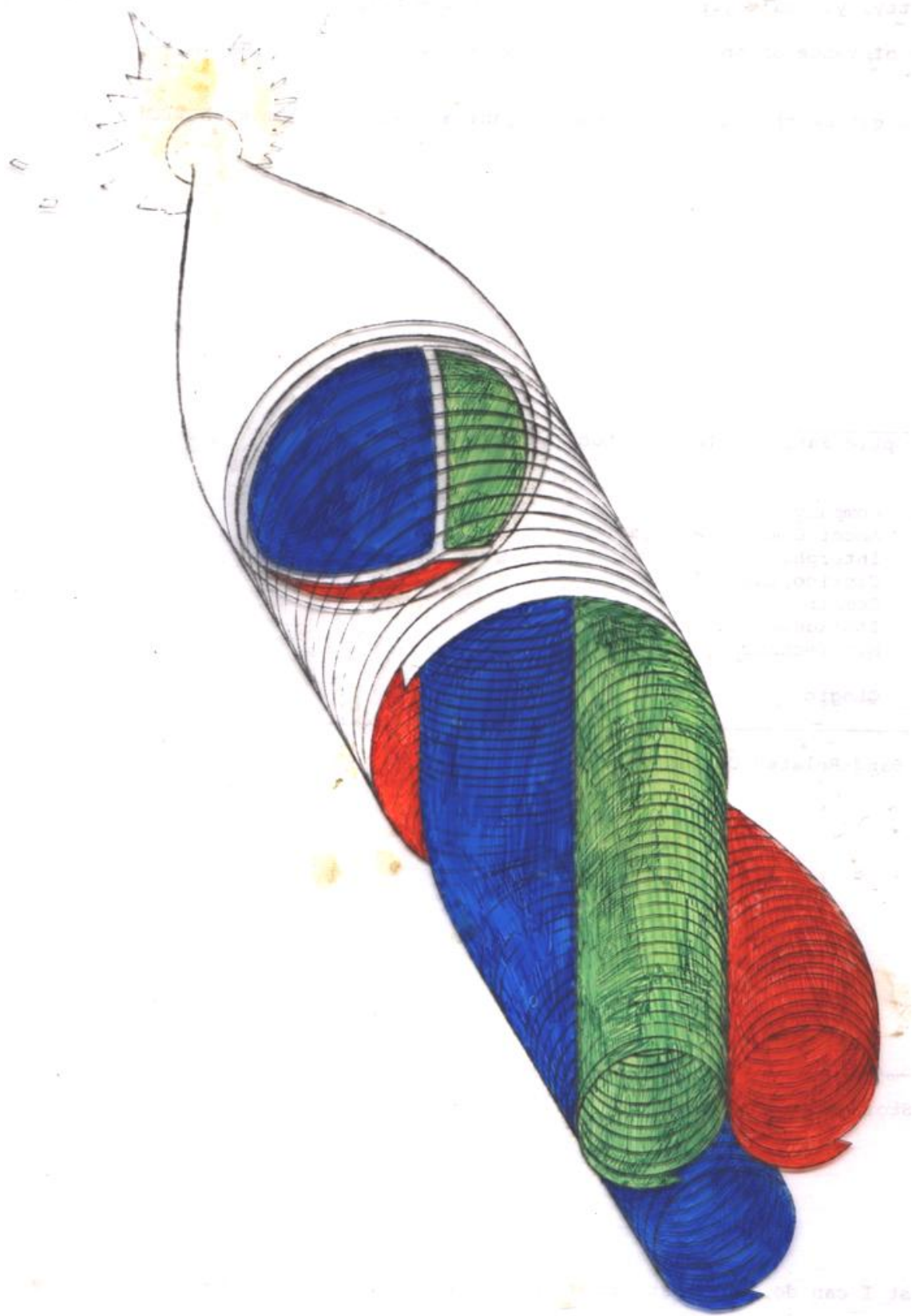


Figure 21 - artist's conception of field topology/dynamics of projected laser plasma

The hydrogenic nuclear bonding structure of the MOSS system can be expanded to set up a macroscopic bound state consisting of a **central Large Vehicle** and **several smaller satellite vehicles** that orbit around the larger vehicle. Larger vehicles may be constructed by stretching the smaller capped cone shaped vehicle at the point of interface between the lens and hull, increasing the diameter, at minimum increments, lengthening the hull to form a "cigar" shape. Analysis shows that certain hard-deformed nuclei have this "cigar" shape (26).

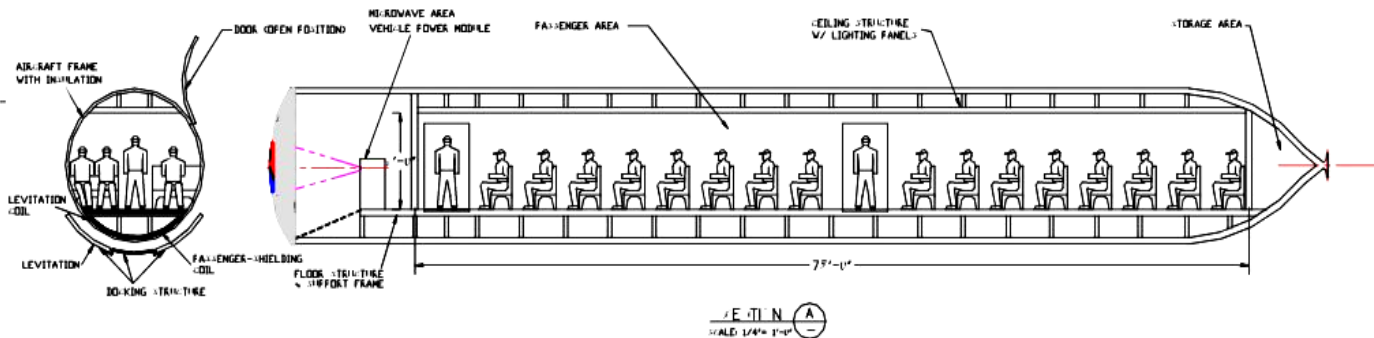


Figure 22 - conceptual drawing from UNITEL's Laser Mag-Lev mass transportation design

This essentially permanent or stable structure can be described as a prolate spheroid, with one long axis and two equal short axes. Specifically the cigar-shaped hard-deformed nuclei (which are massive at sub-nuclear scales) are found in U-235 and U-238 atoms (27).

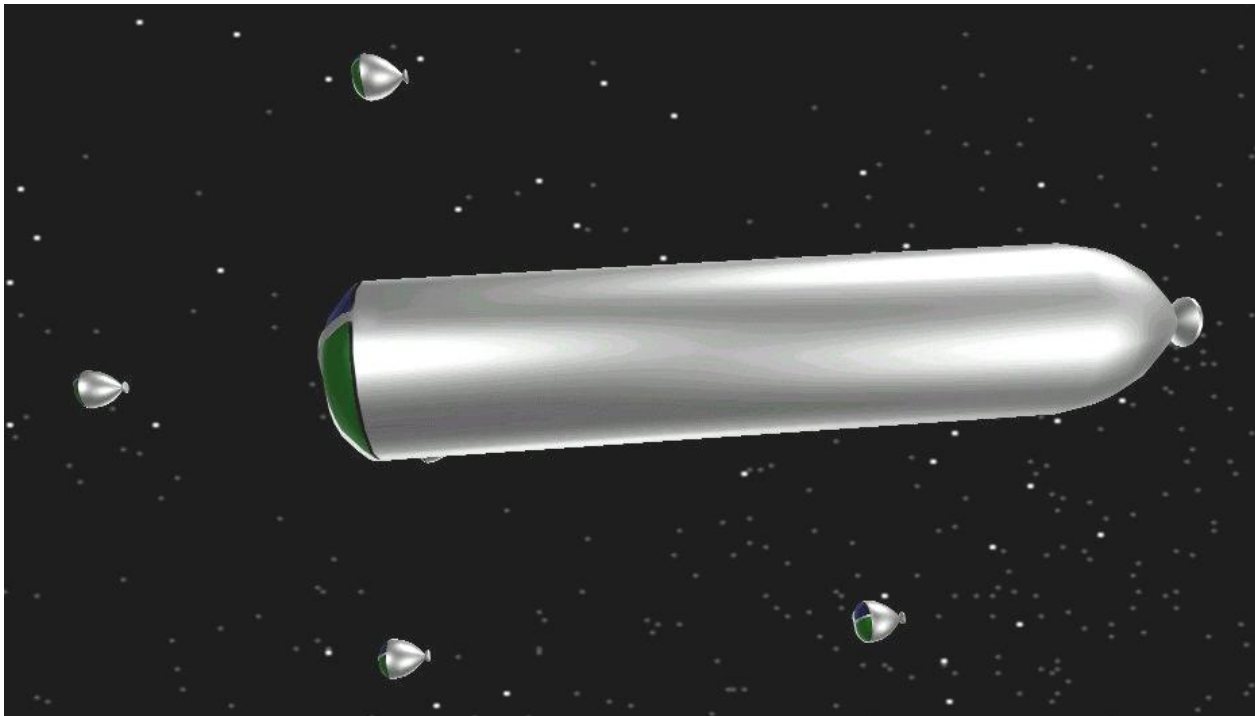


Figure 23 - Main Body Vehicle with multiple "drones" (courtesy A. Moore / UNITEL, Inc.)

The larger "mother ship" plays the role of an atomic nucleus, while the smaller "satellites" function as bound electron" orbiting around the larger vehicle, all of which move as one system (bound state) in outer space. The orbital attraction of the smaller vehicles to the mother ship can be varied over Macroscopic distances. Experiments performed at Texas A&M in 1986 with mother-daughter satellites in outer space revealed that broadcast microwave energy (832 Watts) can be transferred from the mother satellite to the daughter satellite efficiently. Subtle manipulation of the orbiting vehicle's (electron) cloud configuration allows us to move from one atomic state to another. There is a dynamic equilibrium in which the ZPE field stabilizes the electron in a set ground state orbit. This is why the electron's orbit does not decay in a nuclear bound state. The electron simultaneously absorbs a compensating amount of energy from the ZPE field.

The MOSS system allows the vehicle or group of vehicles traveling in a (atomic) bound state, to traverse the vastness of outer space using the **elastic tunneling** technique that is commonplace for particles at microscopic levels. Tunneling -- which is derived from quantum physics -- is not a new effect. Elastic tunneling is a quantum mechanical process whereby a particle travels through an insurmountable (potential) barrier and appears on the other side virtually unscathed by the probability distribution and the wave function. The process of tunneling plays a major role in today's science and technology. We would not have the tunneling electron microscope or several other semiconducting electronics devices if it weren't for this effect. Quantum tunneling is the basic mechanism of radioactive decay and is of central importance in nuclear fusion and some theories of cosmology. Several top physicists have described the "fabric" of outer space mathematically in quantum mechanical terms as a potential barrier through which **tunneling is possible over any Macroscopic distance up to the width of the Universe!**

According to **Gerald Feinberg**, "*the light speed barrier is a barrier consisting of two sides*" (28). Under classical conditions this is an impenetrable barrier. However **it is possible for our vehicle to tunnel elastically** -- in a multi-vehicle bound state or by single vehicle -- **through the light speed barrier by use of "camouflage" techniques**, enabling us to screen out the fabric of 4D spacetime.

As **Albert Einstein** stated in 1943: "*one way to cross the tremendous distances of space would be to alter the structure of space itself*". This is the jux or purpose of our technology we are presenting here, i.e., **altering the fabric of space could be accomplished by modifying the spacetime geometric matrix**. It is this matrix that gives us the illusion of form and distance. One method of changing the matrix (as our system does) is through the modification of frequencies controlling the mater-antimatter cycles. Einstein's premise was that "*time as well as space is a geometric concept*". Therefore if this matrix could be altered -- as we say we can with our MOSS system -- then **ALL of the Universe would become available to us at any single moment**. This technique of tunneling through spacetime by use of camouflage effectively gives our vehicle (with-payload) zero rest mass like a photon, the same technique that takes advantage of wave/particle (duality) relationships and interactions. The MOSS ship-antiship system can be considered to be similar to a **Cooper pair** whereas the pair is transferred in the preferred direction by simply changing their pair phase by just the amount required to match the pair phase on the side of the potential barrier to which they desire to tunnel to -- almost instantaneously -- over vast distances of spacetime.

The junction current density in the **Josephson theory** is a sinusoidal function of the phase difference. If the resulting phase doesn't match, the pair will be simply reflected back to where they came from. The transfer of the pair will give rise to a current after tunneling in the preferred direction. A special relationship between the Josephson frequency and microwaves exists.

Studies of the phenomenon of one-dimensional non-resonant tunneling were performed by **Olkhevsky**, et al in 1996 (29) through two successive potential barriers separated by an intermediate free region R by analyzing the relevant solutions to the Schrodinger equation. They found that the total traversal time is

independent not only of the barrier widths (**Hartman effect**) but also of the R-width so that the effective velocity in the region R between the two barriers can be regarded as infinite. This agrees with the results known from the corresponding waveguide experiments which simulated the tunneling experiment therein considered because of the formal identity between the Schrodinger and the Helmholtz equation.

Studies of Macroscopic quantum tunneling were also performed by **Chudnovsky**, et al in 1998 (**30**) of the magnetic moment in a single-domain particle placed above the surface of a superconductor. Such an arrangement allows one to manipulate the height of the energy barrier, preserving the degeneracy of the ground state. The tunneling amplitude and the effect of the dissipation in the superconductor were computed.

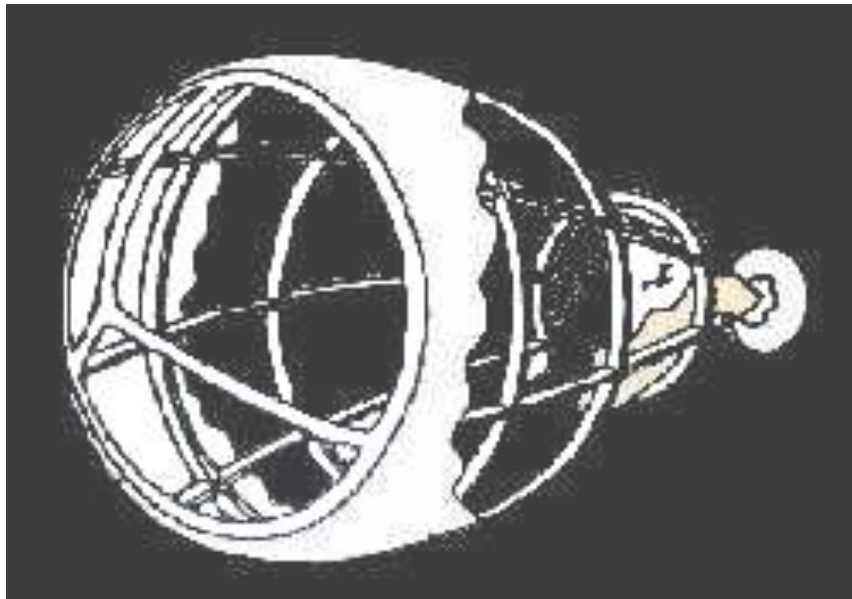


Figure 24 - cut-away drawing of UNITEL's helium gas-filled aircraft frame with smartskin & hull layers, tail piece.

2 - The Type VI Vehicle

The **UNITEL** aircraft will be specifically shaped. **Geometry has a great deal to do with quantum mechanics**. The geometrical "capped cone" tear-drop shape is the ideal electromagnetic shape and it represents what electricity and magnetism have in common. The microscopic monopole is electromagnetic in nature and exerts a powerful magnetic attraction. The geometrical "capped cone" or teardrop, zero degree angular excess shape of our vehicle is in the exact relativistic shape of a particle - the **General Vector Potential** (GVP) for all particles including the electron and photon (31).

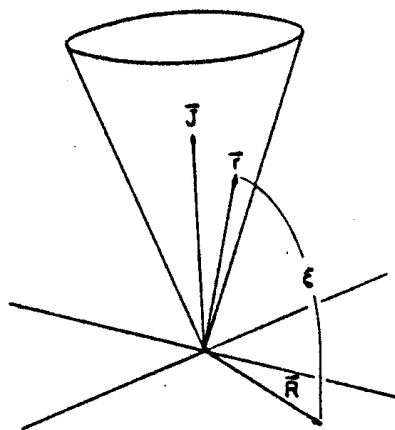


FIG. 1. A charged particle scattered by a fixed monopole moves on a cone whose axis is along the angular momentum, \vec{J} . Its position vector \vec{r} is related by Eqs. (9a) and (9b) to a vector \vec{R} , of the same length as \vec{r} , but lying in the plane perpendicular to \vec{J} .

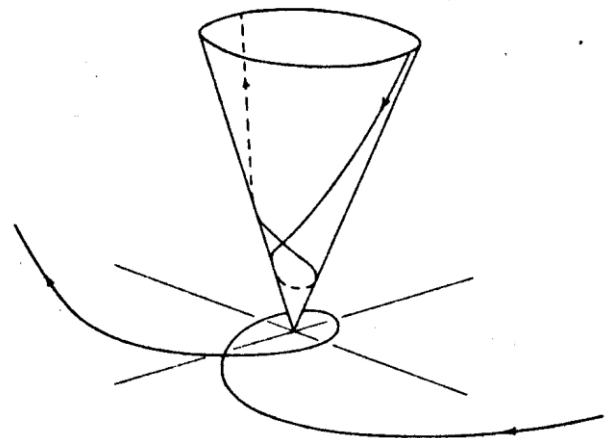


FIG. 2. While the position vector, \vec{r} , of the charged particle traces out its path on a cone, the related vector, \vec{R} , follows the path of a particle in an attractive inverse-square-law potential as shown.

Figure 25 - Geometrical Paths taken by a Charge Particle scattered by a Fixed Monopole

3 - Aircraft Frame and Hull Composition

The ship will be built using a standard aircraft frame similar to that of a helicopter. The hull of the vehicle will be composed of a laminated compositional arrangement of various metals, including composite niobium-tin-titanium-diamond on the exterior and a titanium substrate with laminated layers of carbon fiber. This fiber hull can be constructed by **Cincinnati Machine** (Cincinnati, OH) **Fiber Placement Plant**.



Figure 26 - Viper 3000 Fiber Placement System

UNITEL came close to acquiring a contract with a large European aerospace firm last fall (**Rolls Royce**) to construct and test prototypes of our proposed smartskin design that would be tailored to commercial and military jet aircraft applications. The construction of the small prototype -- a one square centimeter of smart skin material with two charge pins -- was to be subcontracted by **Applied Sciences** (Cedarville, OH) (<http://www.apsci.com>). The project was shelved because of the current airline economic conditions. We expect that we will continue the project as soon as economic conditions allow for R&D projects to be funded hopefully in the near future. There is much interest by the airline industry in the elimination of noise and contrail pollution by smart skin application to modify the combustor chamber and adjacent jet engine equipment in standard jet aircraft engines. Also military (stealth) applications of the smartskin will allow for reduction in radar and infrared signatures. To date, UNITEL continues to negotiate

with prospective financial backers of the continuation of applying smartskin technology to conventional aircraft as well as pursuing the construction of a full-sized prototype of its aerospace propulsion system.

Concerning **UNITEL**'s choice of materials in its aerospace vehicle's exterior charged hull construction, we have chosen **niobium-tin-titanium** for good reason. The following article exemplifies this fact extremely well:

[**http://enews.lbl.gov/Science-Articles/Archive/14-tesla-magnet.html**](http://enews.lbl.gov/Science-Articles/Archive/14-tesla-magnet.html) : "Is there a more rewarding thrill than to break a record? Whereas most of us must content ourselves with breaking personal bests, earlier this month the scientists and engineers of **Berkeley Lab's Superconducting Magnet Group** experienced the rush of shattering a world record. The team's newest niobium-tin dipole electromagnet reached an unprecedented field-strength of 14.7 Tesla. This is more than 300,000 times the strength of Earth's magnetic field. Niobium (Nb) has a body-centered cubic (bcc) crystal structure and a melting point of 2,468°C (4,474°F). Of the refractory metals, it has the lowest density and best workability; for this reason, niobium-based alloys are often used in aerospace applications. Because of its strengthening effect at elevated temperatures, its principal commercial use is as an additive in steels and superalloys. Niobium-titanium and niobium-tin alloys are used as superconducting materials." Of course it is our full intention to create a high-temperature Macroscopically observable superconducting state (MOSS) with our proposed vehicle and its projected laser plasma system.

Albeit the materials are similar (*i.e.*, the composition of Berkeley Labs 14.7 Tesla electromagnet and our proposed space vehicle's exterior charged smartskin), one main difference between the systems (electromagnet vs. aerospace vehicle) is that the magnet was super-cooled to avoid "quenching" or loss of superconductivity due to heat. In the design of the aerospace vehicle, however, it is a **high-temperature (3000°F)** superconducting system that will be the first of its kind to operate at room temperature and above. Only through real testing of working prototypes can we prove our design works. We may consider winding the niobium-tin-titanium wire as opposed to the layered "onion-skin" type of smartskin structure. We know one thing, though, and that is we definitely have to work with a high-temp design in this type of application (aerospace).

We contacted **Ron Hennes**, Composites Product Manager of Cincinnati Machine after the materials we received from their Corporate Secretary Helen Boerger directing us to Ron's department to pursue obtaining a price quote for our full-sized prototype of our aerospace propulsion vehicle. We decided that Cincinnati Machine's composite fiber hull would be stronger, more durable and lighter than a titanium-steel hull. We will be using a super-lightweight, titanium-aluminum aircraft type frame to mount the composite fiber hull with our smartskin attached to the outside of the composite fiber hull.

Edwin G. Schastee of **Tap-Ten Research Foundation International** (San Diego, CA) (<http://groups.yahoo.com/group/tapten>) suggested we fill the aircraft (tubular) frame with helium gas to make it even lighter. Remember, helium gas does everything that hydrogen gas does (such as providing lift) etc., except helium gas is non-volatile. The Zeppelin "Hindenberg" was supposed to switch to helium gas from hydrogen gas but didn't get the chance because of the explosion mishap back in the '30s. The whole system, which amounts to the on-board powerplant, control and other electronics equipment as the only payload weight for our proposed all-electric vehicle with Laser propulsion, is extremely lightweight; especially with a helium gas-filled frame (http://www.cinmach.com/products/adva_set.htm).

We placed a call to Cincinnati Machine to progress forward with exchanging more information concerning our prototype & associates etc. and Cincinnati Machine's capabilities/requirements/etc. so that

we can obtain a reasonably accurate price quote to undertake such a project. We announced that we are prepared to send Cincinnati Machine AutoCAD R14 drawings, requirements, prototype descriptions, etc., along with a list of contractors for their review.

We announced that Elliot Kennel is our POC at **Applied Sciences** (Cedarville, OH) and that they will be giving us a quote along with Cincinnati Machine's quote for the composite fiber hull. Applied Sciences will apply the smartskin layer to the exterior surface of the **UNITEL** prototype, which is roughly 5-ft diameter x 15 ft. long. We are hoping that the Cincinnati Machine Fiber Placement Group will work with Elliot and Applied Sciences, Inc. to construct the smartskin on our prototype hull composed of Cincinnati Machine's composite fibers. We can exchange information concerning the requirements from both firms in order to construct the prototype fully completed at Cincinnati Machine's facilities.

To get started, we sent Cincinnati Machine several AutoCAD drawings of the proposed prototype vehicle and we will supply the shop drawings with the specifications in the near future. We have Applied Sciences as the subcontractor on a previous contract to construct and test a smartskin prototype with Rolls Royce which entailed testing a piece of our smartskin that was one square centimeter with two charge (SDE) pins. Unfortunately, Rolls Royce suffered a heavy economic blow after the 9-11 WTO incident and our project was set aside.

At any rate, we will pursue the construction of a full-sized model of our all-electric (Laser) EM space vehicle with the composite fiber for our skin. The composite fiber hull will be lighter than titanium-steel but more durable and just as strong of a material. The smartskin layer would be adjacent (outside) of the composite fiber layer which will support the modulated system of **semiconducting diode elements (SDEs)** that provide the high volume of charge (close-adhering cloud of electrons in a Rayleigh-Stonely wave manner) to the exterior smartskin that is composed out of doped layers of niobium-tin-titanium-diamond.

Concerning the use of SDEs, we may be using more sophisticated emitters to instill on the hull surface certain desirable effects such as the **gravity emitters** described in the very important work recently done by **Dr. Raymond Y. Chiao** (abbreviated write-up of his March 23, 2002 Wheeler Symposium lecture, and a book chapter for Wheeler / Festschrift):

"Type II superconductors will be considered as Macroscopic quantum gravitational antenna, which can simultaneously also be used as efficient transducers for converting electromagnetic radiation into gravitational radiation and vice versa. A Meissner-like effect -- in which the Lense-Thirring field associated with a gravity wave is expelled from the interior of the superconductor -- is predicted. An analysis of a process of natural impedance matching in Type II superconductors such as YBCO based on the Ginzburg-Landau theory yields an estimate of the transducer conversion efficiency of the order of unity upon reflection of the wave. Thus efficient emitters and receivers of gravitational radiation can be constructed at microwave frequencies. A simple, Hertz-like experiment using YBCO and 12 GHz microwaves is being performed to test these ideas. Results of this experiment will be reported elsewhere" (see the June '02 issue of Scientific American).

We want to discuss the possibility of both firms (Cincinnati Machine & Applied Sciences) participating as active partners in construction and marketing of the prototype because of the high profit to be made in the transportation market. We are certain our propulsion system will work and we are prepared to construct our prototype at their facilities if we can insure the clean room atmosphere required in creation of our vehicle. **This is a very exciting project that will be a milestone in the progression of flight technology.** We are attempting to obtain a general price quote and/or a general estimate of what it would cost to construct our

vehicle's hull so we can announce the price quote in our contract with a potential financial backer. We all look forward to doing business with Cincinnati Machine & Applied Sciences and providing the possibility of several contracts to manufacture more prototypes of various sizes, etc. The aircraft frame will be made of lightweight tubular aluminum and filled with the nonvolatile helium gas that will make our vehicle even lighter. There is no payload or fuel weight except the powerplant and on-board control equipment. **The total weight of the entire vehicle should be only 300 to 400 lbs.**



Figure 27 - Fuselage Mandrels at Cincinnati Machine's plant

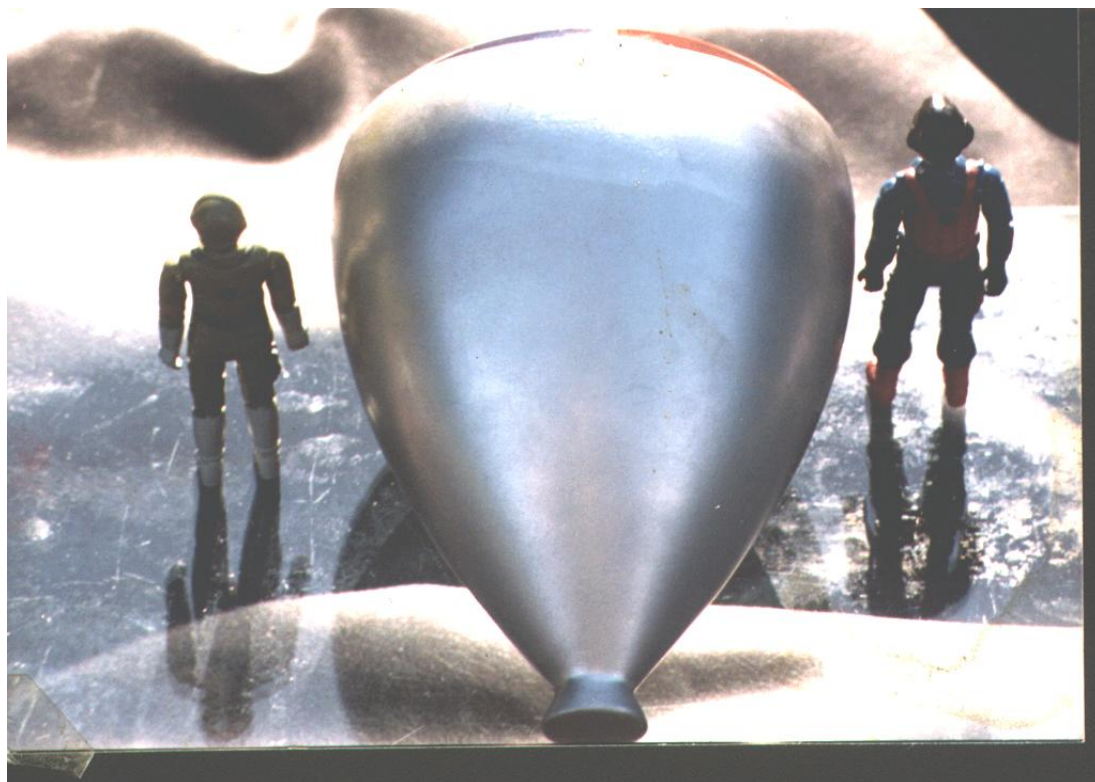


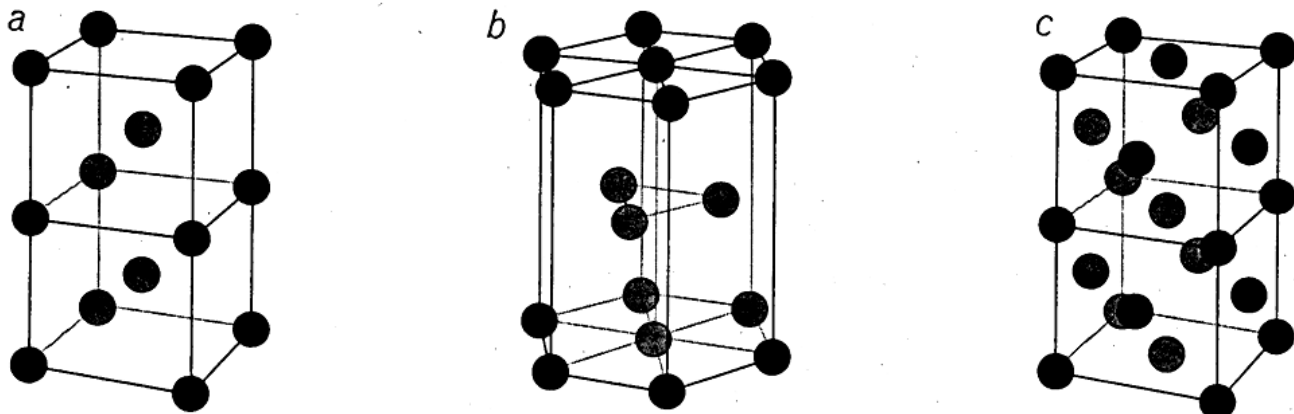
Figure 28 - scale model of UNITEL's proposed all-electric laser propulsion aerospace vehicle



Figure 29 - a collage of various pictures of the scale model

The last exterior layer outer laminate will be a specific form of **synthetic blue diamond** grown on the polished niobium substrate. Niobium, aluminum, nickel, and other shiny metals reflect 4D spacetime upon itself like an optical mirror in the visible spectrum where photosynthesis occurs (32). **UNITEL** plans to construct and test the laser system for these various effects. Another important aspect of **UNITEL**'s pulsed-chirped laser system is **efficiency**. **UNITEL**'s Type II-VI compound lens is similar in material make-up to **Fusion Lighting**'s (1995 DOE Annual Award Winner) Sulfur lamp

(<http://americanhistory.si.edu/lighting/sul.htm>), which illustrates the supreme synergetic relationship between sulfur and microwaves to produce synthetic solar light with full visible spectrum value. We have been told by Fusion Lighting that **UNITEL**'s laser lens may be a solid-state version of their microwave activated sulfur lamp. The sulfur atoms in **UNITEL**'s CdS doped RF-transparent glass crystallite is stimulated by the RF wavepackets and will produce the same quality synthetic solar light. One of their bulbs will replace 1000 standard light bulbs with an accompanied 2/3-power requirement. The **Red/Green/Blue** equal sections produce true electromagnetic wave packets that eliminates blurring and distortion over Macroscopic distances. All of these various different aspects show how advanced **UNITEL**'s laser system is.



THREE CRYSTAL STRUCTURES formed under different conditions of temperature and pressure by the atoms in solid helium are the "body-centered-cubic" structure (a), the "hexagonal-close-packed" structure (b) and the "face-centered-cubic" structure (c).

Figure 30 - Crystal Structures in Solid Helium

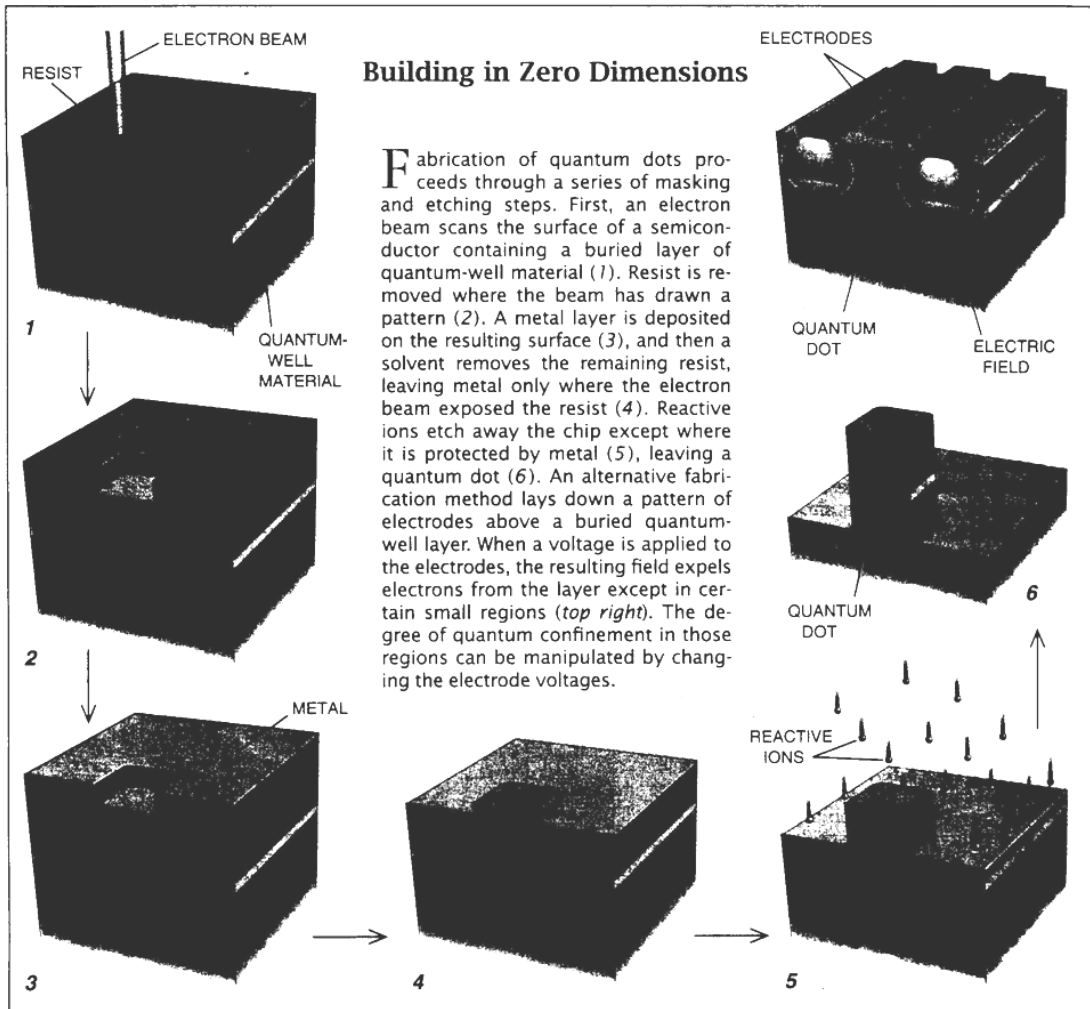


Figure 31 - Fabrication of "Quantum Dots"

(courtesy Scientific American, Jan '93)

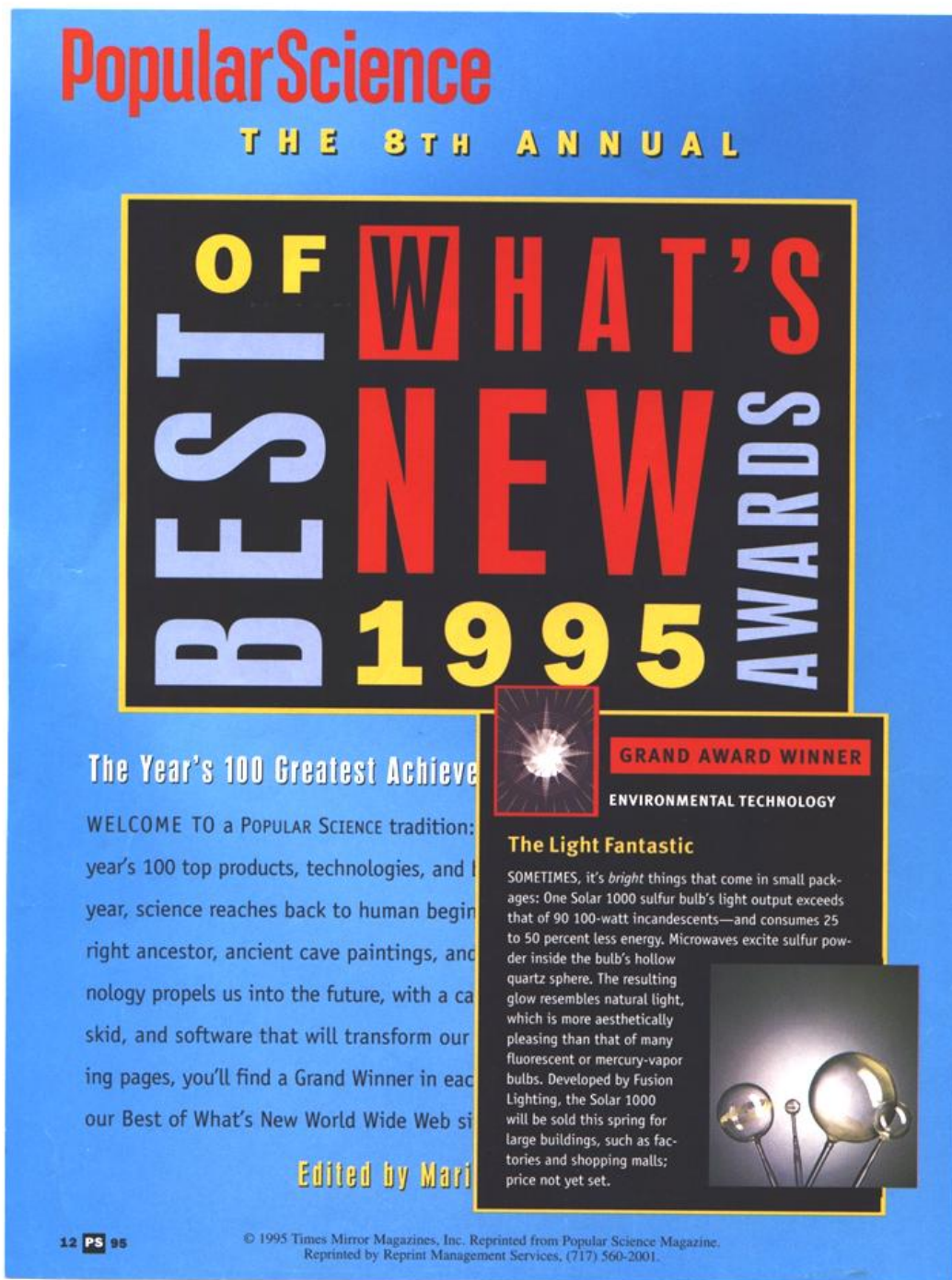
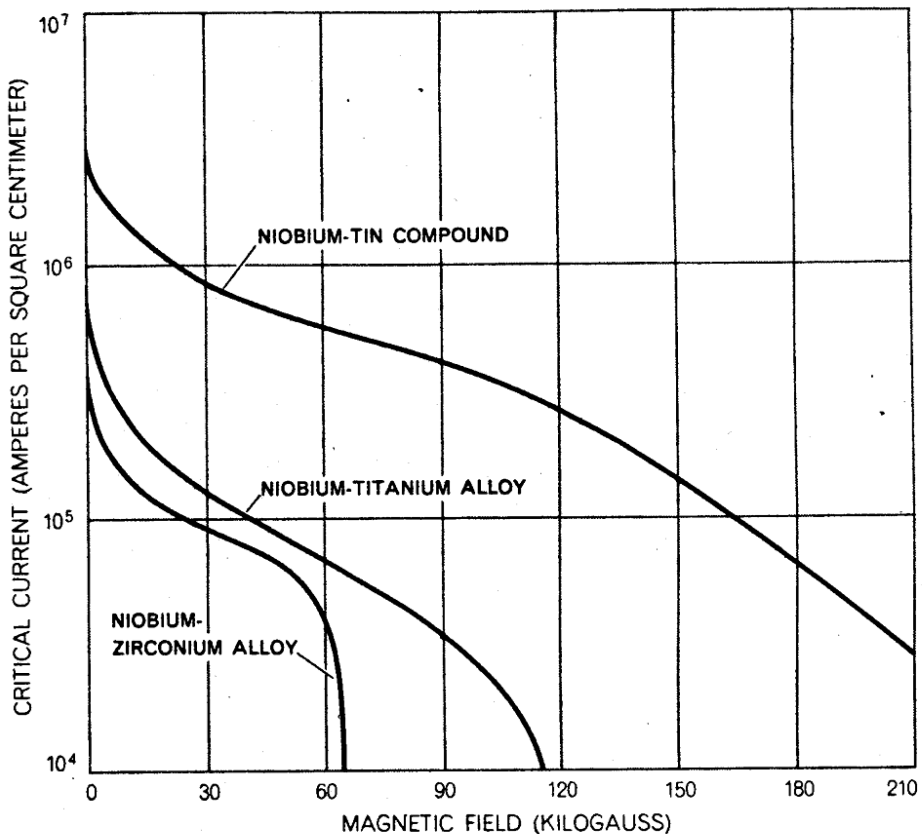


Figure 32 - Bright Light from Microwave-excitation of Sulfur Atoms

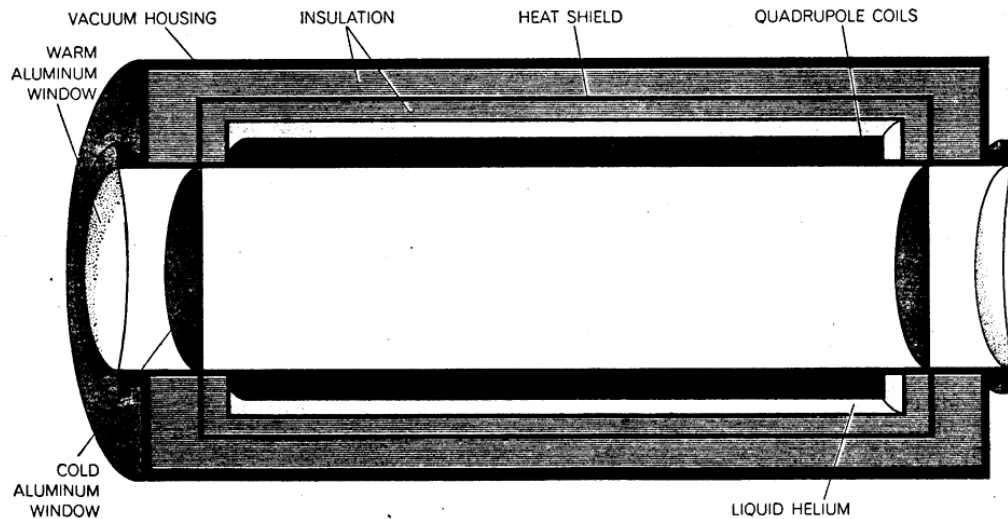
courtesy Popular Science, Dec '95

Unlike a wave reflected from other reflective surfaces such as water or glass, the wave reflected from a metal surface has almost the full intensity of the incoming wave (33). The hatch will be flush with the hull, being an active part of the charged hull system. The vehicle will have a standard type of aircraft frame with insulated interior.



CURRENT V. FIELD CURVES indicate the maximum current density that a short sample of a superconducting material will carry as a function of an applied magnetic field. The curves shown here represent the three most commonly used superconducting materials.

Figure 33 - Current Densities of some Superconductors (courtesy *Scientific American*, July '66 (37))

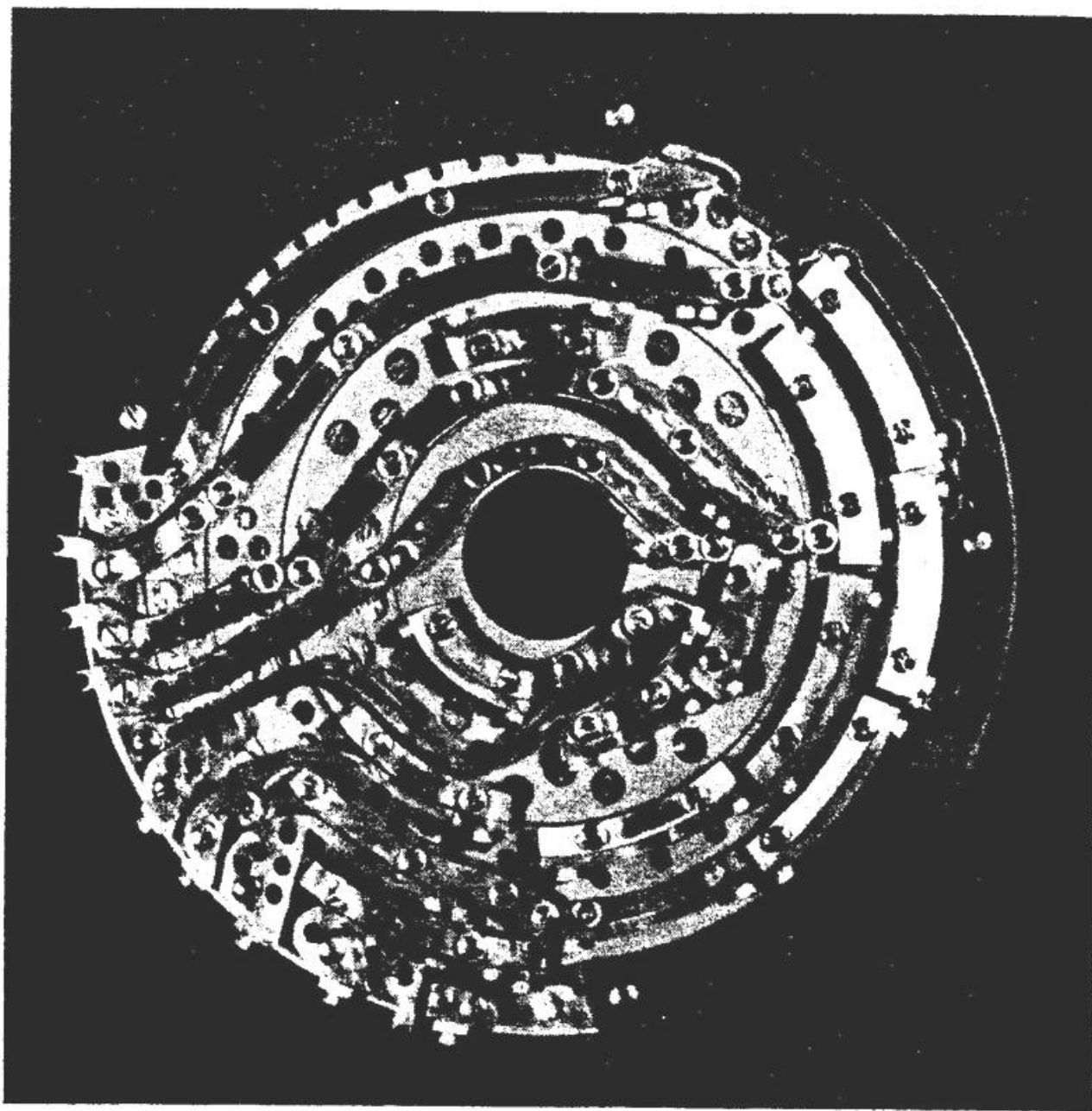


PROTON-FOCUSING MANET IS COOLED by installing it in a Dewar, an insulating vessel that contains liquid helium at 4.2 Deg.K. The foil windows reduce the flow of radiant energy into the cold bore.

Figure 34 - an example of Supercooling a Superconductor (courtesy *Scientific American*, July '66 (37))

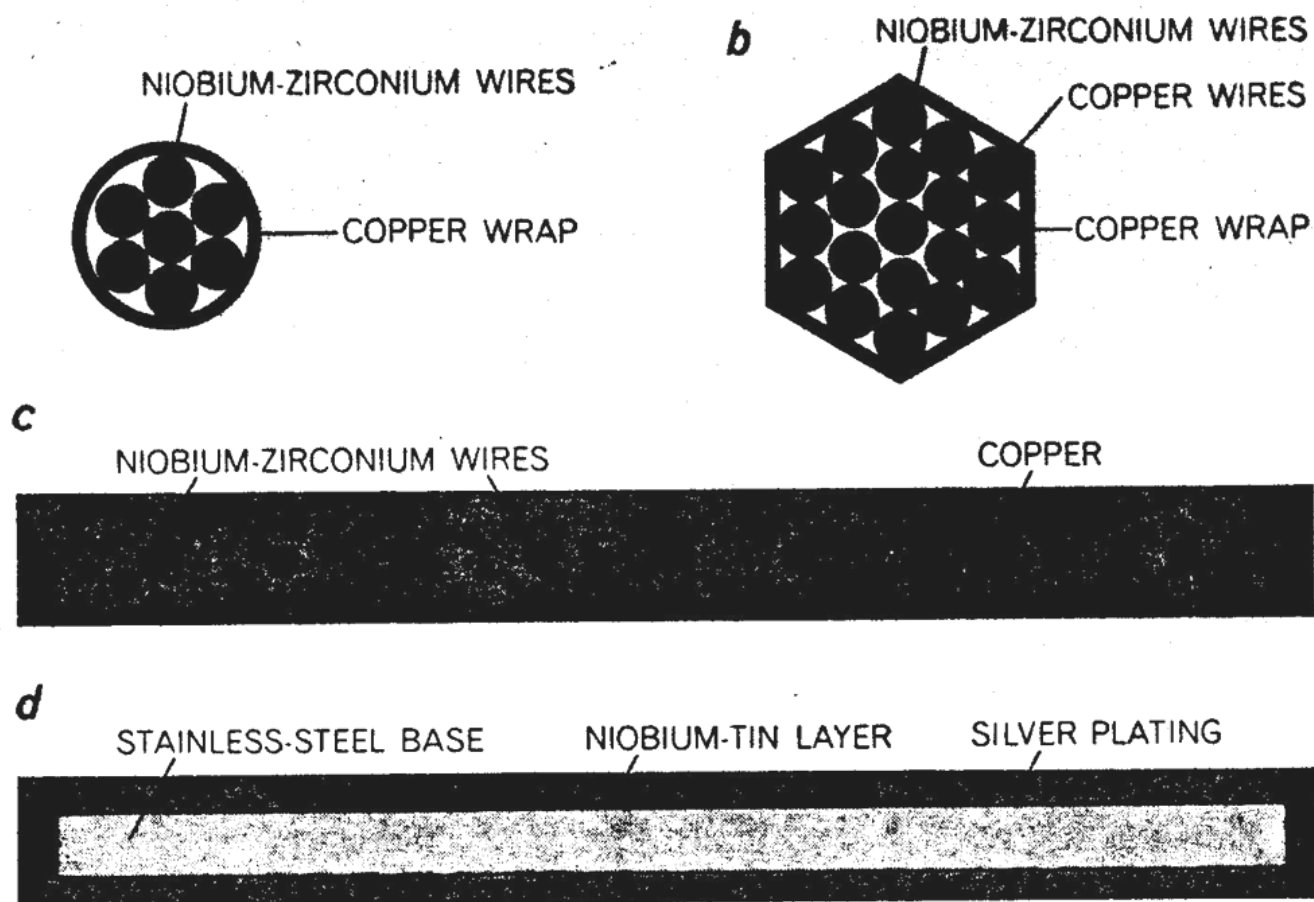


Figure 35 - Berkeley Lab's Superconducting Magnet Group's Cooling Chamber



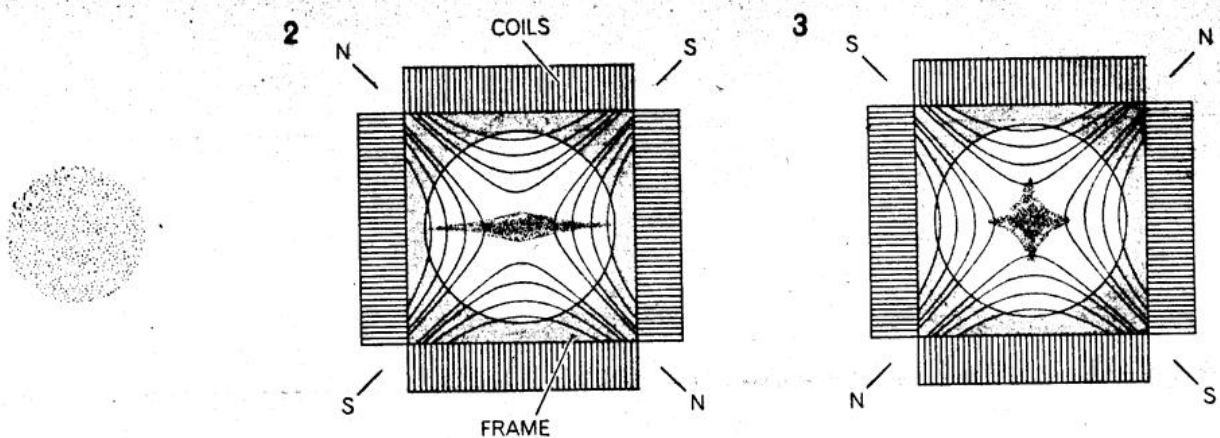
FOUR CONCENTRIC COILS are employed to generate the field inside the bore of this superconducting magnet, used at Brookhaven to measure the gyromagnetic ratio of the negative xi particle (Ξ^-). The four sections can be powered separately to produce a maximum field of 125,000 gauss. Short-circuiting switches that allow the magnet to operate without power once the field is established are housed in the insulating ring around the magnet.

Figure 36 - Cross-Section of a Laboratory Superconducting Magnet
(courtesy Scientific American, July '66 (37))



COMPOSITE SUPERCONDUCTORS commonly used in winding high-field magnets are shown in cross section. In each case the superconducting material is in color. The two cables (a, b) are composed of wires a hundredth of an inch thick. The two ribbons (c, d) are about half an inch wide and four-hundredths of an inch thick. They are not drawn to scale.

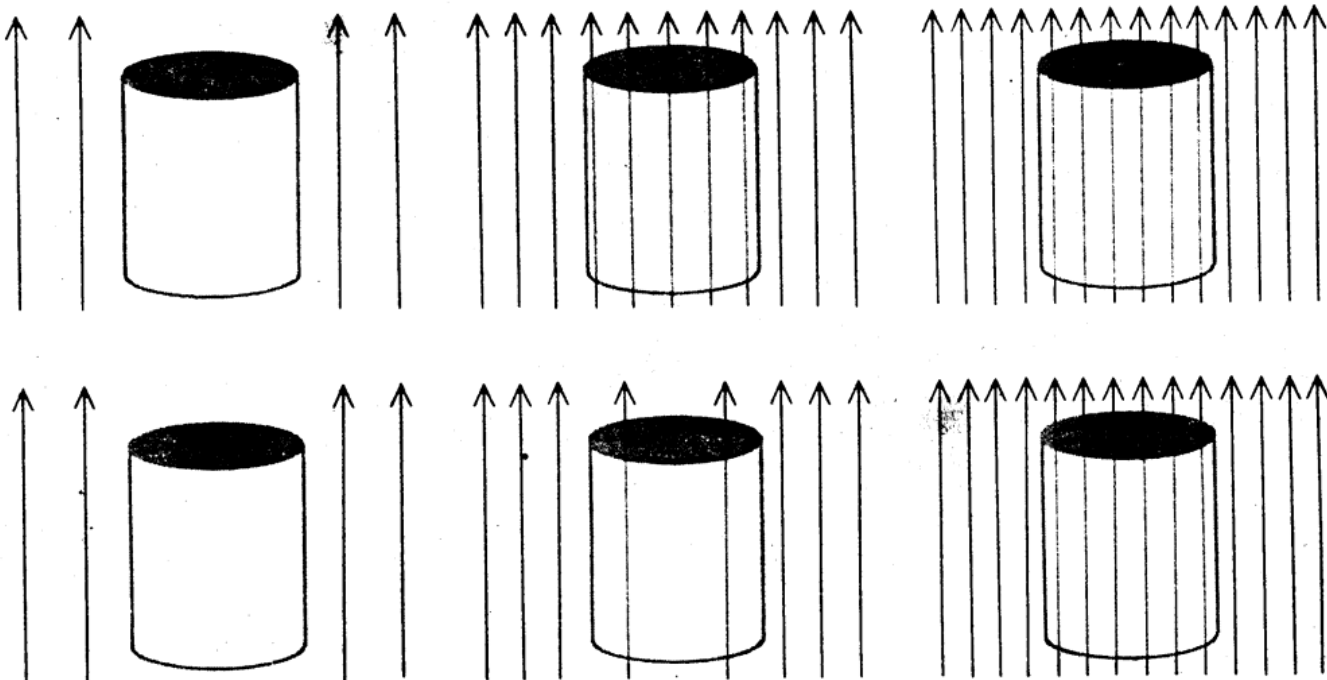
Figure 37 - Sample Composite Superconductors (courtesy Scientific American, July '66 (37))



BEAM OF PROTONS can be focused by a pair of superconducting quadrupole magnets in two stages. As the beam leaves the accelerator (1) it has a diverging circular cross section. The beam then enters the bore of the first magnet (2), where the magnetic field forces the protons to converge along a vertical plane and diverge

along a horizontal plane. The second magnet (3) is rotated 90 degrees with respect to the first and completes the focusing. Because of its higher current density, such a superconducting magnet has a field gradient (change in field intensity with distance) more than five times greater than a comparable conventional magnet.

Figure 38 - Focusing Particle Beams with Superconducting Magnets
(courtesy Scientific American, July '66 (37))



TWO TYPES OF SUPERCONDUCTOR can be distinguished by the way they behave in an external magnetic field (arrows). The Type I superconductor (top) totally excludes the magnetic field up to a certain point, called the critical field, whereupon the sample suddenly loses all trace of superconductivity and the field penetrates fully into the interior of the material (top center). The Type II

superconductor (bottom), predicted on theoretical grounds in 1957, excludes the magnetic field only until some lower critical field is reached, at which point partial field penetration takes place (bottom center). Beyond a second, upper critical field penetration is complete and the sample loses superconductivity (bottom right). The drawings represent portions of a theoretically infinite cylinder.

Figure 39 - "Type I" and "Type II" Superconductors (courtesy Scientific American, July '66 (37))

A hatch will be built to receive equipment and personnel. The hatch will be flush with the hull, being an active part of the charged hull system. The vehicle fuselage will be composed of an exterior charged "smart skin". This smart skin design is a laminated valent-donor, energy band gap, "mini" layers of a compositional arrangement of various metals to form p-i-n junction at the exterior surface area. The hull composition shall also have a system of high volume charge-junction semiconducting diode elements (SDE's) (34) controlled by the onboard very high-speed integrated circuitry (VHSIC) computer system. This VHSIC system will be modulated by the **central quantum computer HOLO-1**. The hull surface receives the charge with the desired harmonics input from the SDE system. The high volume of electrical power required for the external surface charge (and the rest of the ship's equipment) will be produced by an onboard intrinsic source.

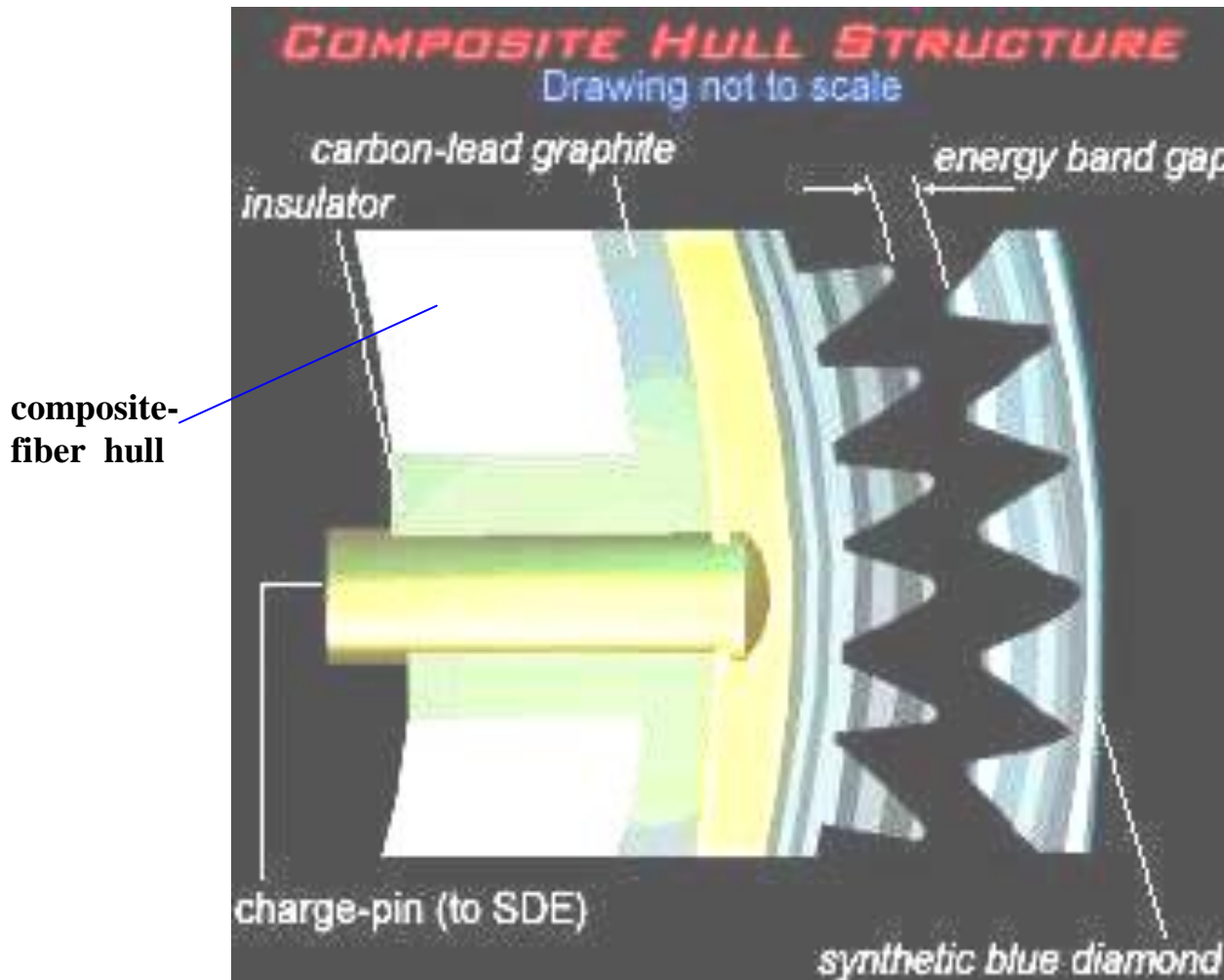


Figure 40 - hull cross-section illustration (courtesy A. Moore - UNITEL, Inc.)

The modulated charge is broken down and isolated by the consecutively decreasing donor layer composite structure of mini-bands that descends down to one-dimensional (atomic) thick layers. The last layer of p-doped synthetic blue diamonds (35) possesses strong semiconducting properties which can withstand more than 3000 degrees F and can be grown in large sheets (on the surface of the fuselage). An electric field surrounding a charged body is analogous in almost every respect to the gravitational field surrounding a massive body. Both fields cause other objects within them to move; gravity attracts massive objects, whereas the electronic fields can do both; repel or attract other objects (36).

4 - Exterior Charged "Smart Skin" Hull

The term “**smart skin**” refers to special types of composite hull structures. The **B-2** Stealth bomber uses smartskin technology to avoid radar detection and the retired **SR-71** Blackbird used a primitive form of smartskin that additionally reduced intense heat incurred at Mach 3+ speeds. **UNITEL**'s exteriorly charged vehicle will have the ability to bend or absorb radar to avoid radar detection with a high degree of radar invisibility or “cloaking”. Instead of reducing the radar signature to a small one, our design will completely **eliminate** radar signature. The process of applying a smartskin to the fuselage of an aircraft is highly sophisticated and requires a clean room environment.

A system of **semiconducting diode elements (SDEs)** will be used to charge the hull surface with controlled harmonics. The final layer of the smartskin will be composed of **synthetic blue diamond**, selected for its semiconducting properties and its ability to withstand more than 3000°F. The exterior surface charge will prevent the diamond layer from deteriorating through oxidation.

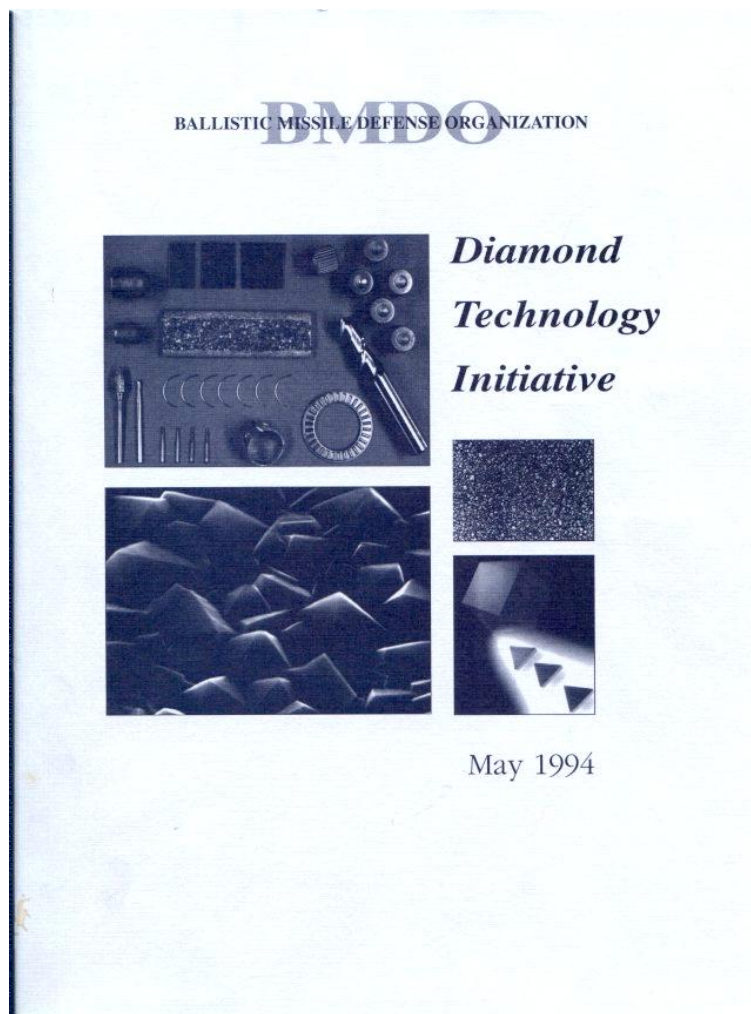


Figure 41 - Applied Sciences was a Phase III grant award winner of the '94 Diamond Initiative BMDO that was an effort to study possible applications of diamond semiconductor technology.

UNITEL's smartskin design will produce and support a close-adhering cloud of electrons. This is not a new technology. In 1967, a design was offered to NASA by **Avco** of Everett, NJ in order to screen out harmful rays and heat during re-entry into the Earth's atmosphere (**37**).

**Is this all
you think of
when you
think of
Avco?**



Think again. We are this. And much more. We are 25,000 people changing the way you live: an unusually broad range of commercial, defense and space capabilities now identified by this new symbol.



AVCO AEROSTRUCTURES DIVISION
(Structures for aircraft and space vehicles)

AVCO LYCOMING DIVISION
(Engines for utility aircraft and helicopters)

AVCO BAY STATE ABRASIVES DIVISION
(Grinding wheels and other abrasives)

AVCO NEW IDEA FARM EQUIPMENT DIVISION
(Specialized farm machinery)

AVCO BROADCASTING CORPORATION
(Radio and television stations)

AVCO ORDNANCE DIVISION
(Ammunition, fuzing devices)

AVCO DELTA CORPORATION
(Financial services)

AVCO RESEARCH AND DEVELOPMENT DIVISION
(Missile and space systems)

AVCO ELECTRONICS DIVISION
(Communications systems)

AVCO SPENCER DIVISION
(Heating boilers and sewage systems)

AVCO EVERETT RESEARCH LABORATORY
(High temperature gas dynamics, biomedical engineering, superconductive devices)

AVCO TULSA DIVISION
(Aerospace instrumentation)

You'll be hearing more about us.

AVCO CORPORATION, 750 THIRD AVENUE, NEW YORK, NEW YORK 10017

Figure 42 - the advertisement for the now-defunct AVCO taken from a 1966 magazine

Avco maintained that **an electron cloud would provide as much protection as a ten-foot thick lead wall.** Since the **UNITEL** aerospace vehicle is entirely electrical, we will not have the same problem as NASA who rejected the idea due to the volatile nature of their rocket propellants. We have modified the design of this superconducting magnetic system and applied it to the design of the exteriorly charged hull or fuselage in our all-electric propulsion system:

Avco considered in detail the problem of energy storage and concluded that there exists a fundamental relation between the energy that can be stored in a magnetic field and the weight of the structure required to support the magnetic forces. This relation states that the minimum magnet weight equals the energy stored in the field times the density of the magnet material divided by the tensile strength of the material. Under favorable conditions a magnetic energy-storage device for use in outer space could be about 10 percent as efficient a storage device as TNT. In a magnet, however, the stored energy can be converted directly into electrical energy rapidly and with high efficiency.

We can increase the amount of stored energy through our superlattice mini-band composite niobium-tin-titanium-diamond modulated SDE charged hull structure. We can control the production of vast amounts of energy on the hull surface via the **Stark ladder effect**. Each individual mini-band in the composite hull structure contains standing electromagnetic waves. We can control the release of electromagnetic waves to the surface by a specific frequency signal from by the computer-modulated SDEs which create an ordered flow of dielectric permitivity waves in the metal alloy. The standing electromagnetic waves couple to an external wave provided by the network of SDEs. Hopefully we will produce enough energy to provide propulsion by **mimicking a particle system** and perform **Macroscopic Quantum Tunneling (MQT)**.

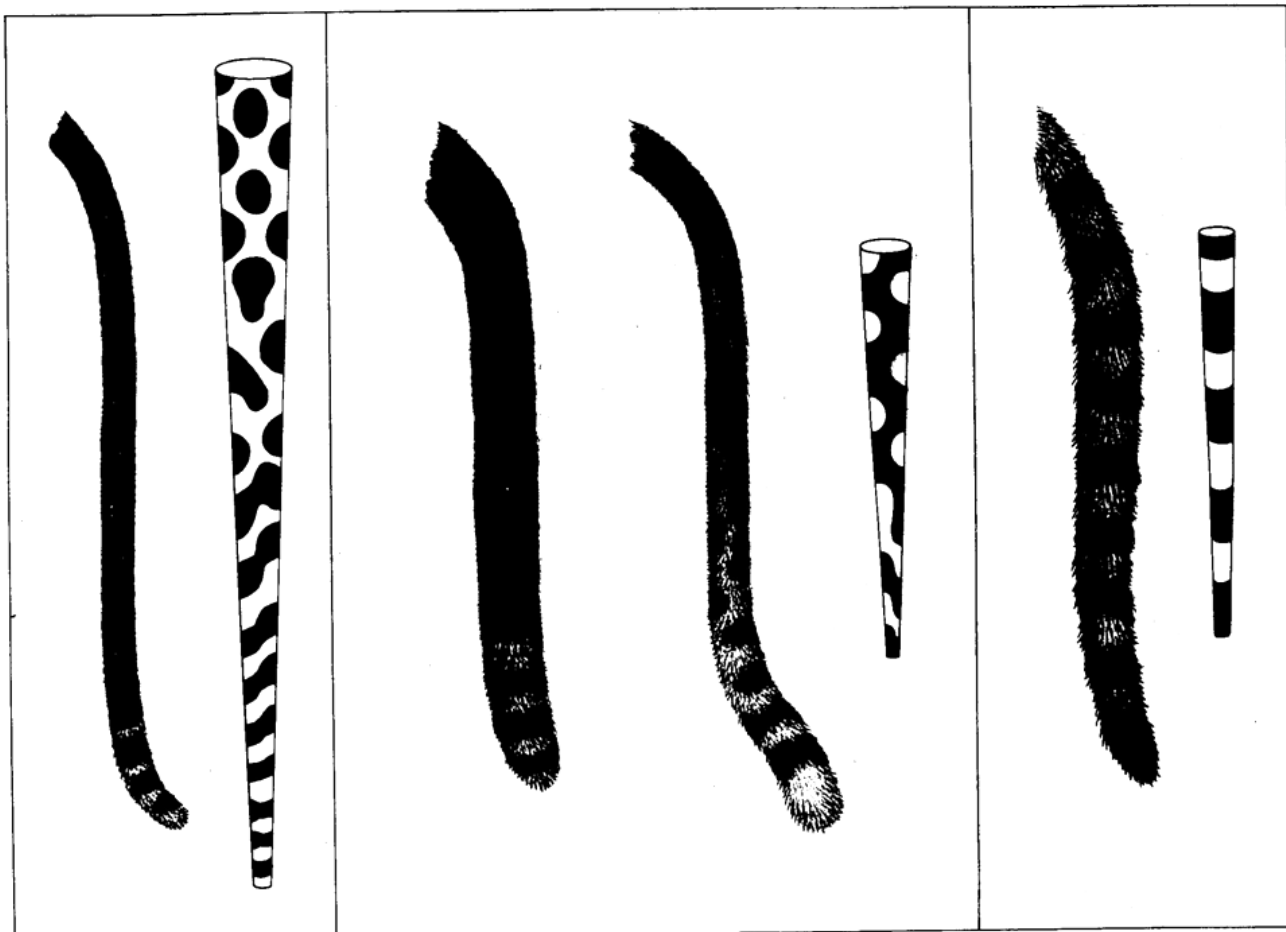
One of the most severe problems that will arise on long missions in outer space is that of protecting the crew from the intense flux of high-energy particles produced by Solar flares. The exteriorly charged magnetic radiation shielding will deflect the charged particles away from the space vehicle by charging the vehicle to a high electric potential. This is accomplished by surrounding the vehicle with a cloud of electrons moving in a magnetic field strong enough to keep the electron orbits close to the space vehicle. The exterior charge will allow safe re-entry of our space vehicle into the Earth's atmosphere. A large magnetic field will produce hydromagnetic drag in the cloud of ionized air the vehicle produces as it enters the atmosphere. With hydromagnetic braking, the kinetic energy of the vehicle would be absorbed through the magnetic field rather than through heating of the vehicle itself.

The close-adhering cloud of electrons would be as efficient as a ten-ft. thick lead wall. NASA turned down the now defunct Avco design because of the volatile nature of rocket booster propellants. NASA opted instead, as we know, to employ the tiled space shuttle vehicle still in use today. **UNITEL** is focusing on the **magnetic field storage of energy**.



Figure 43 -Berkeley Lab's Superconducting Magnet Group

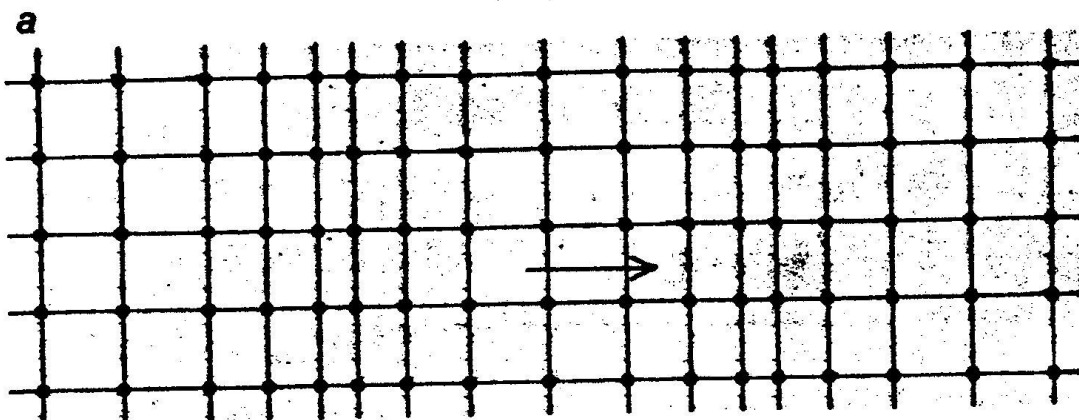
Our design of surface charge not only has the ability to screen out harmful effects but also can produce certain patterns analogous to those discussed in some of **Turing**'s papers which are called reaction-diffusion mechanisms (38) that interact at Planckian levels with the ZPE field. Two-dimensional complex multiple reaction-diffusion zones are formed out of the standing, negatively-charged acoustic surface waves (39) on the hull surface to interact with and extract vast amounts of abundant energy contained in the ZPE field required for tunneling.



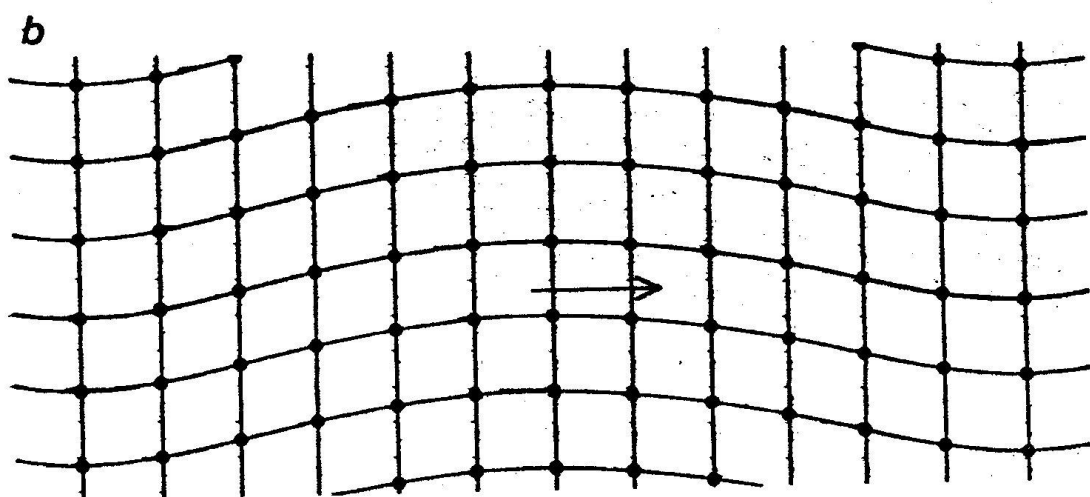
MATHEMATICAL MODEL called a reaction-diffusion mechanism generates patterns that bear a striking resemblance to those found on certain animals. Here the patterns on the tail of

the leopard (*left*), the jaguar and the cheetah (*middle*) and the genet (*right*) are shown, along with the patterns from the model for tapering cylinders of varying width (*right side of each panel*).

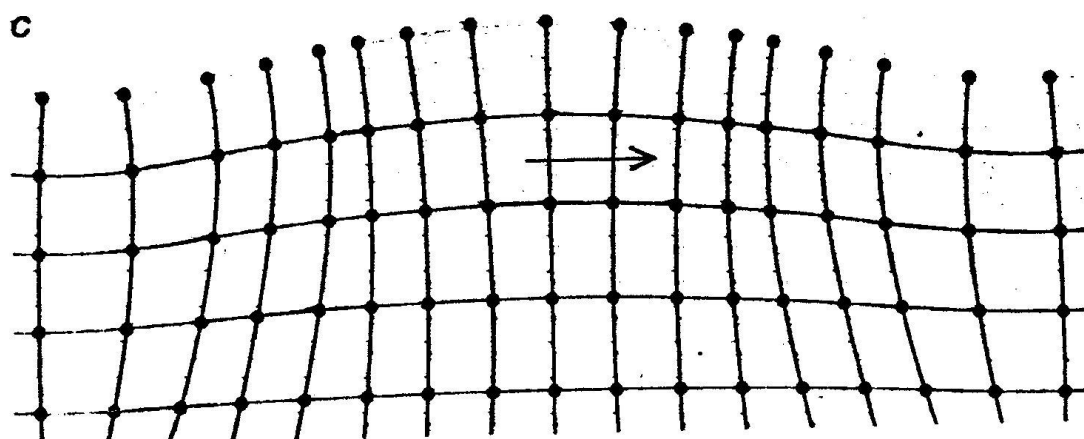
Figure 44 - Mathematical Model of a Reaction-Diffusion Mechanism
(courtesy Scientific American, Special Issue 1990 (38))



LONGITUDINAL WAVE is the simplest kind of acoustic wave that can travel through an elastic material. The material is alternately compressed and expanded as the wave passes.



TRANSVERSE WAVE, also known as a shear wave, provides a second way for acoustic energy to travel through a solid. Oscillations are at right angles to the direction of the signal.



RAYLEIGH WAVE, or acoustic surface wave, is a more complex wave that is found only near the free surface of a solid. Wave has both longitudinal and transverse components.

Figure 45 - examples of Acoustic Surface Waves (courtesy *Scientific American*, Oct '72 (25))

We can, by fluctuation, tunnel through the energy barrier of the ZPE field because the field consists in part of very strong fluctuations in probability density. It is our every intention to duplicate on the hull surface, patterns of the different modes that are found on the interactive surface of microscopic particles such as the electron.

We intend to produce fractional ($1/3e$) charges on the surface of our composite structure. This application would be slightly different but hopefully we can obtain the same results as did **George S. LaRue** et al in "***Observation of Fractional Charge of ($1/3e$) on Matter***" (40). "*Measurements on niobium spheres show unambiguously the existence of fractional (41) charges of $1/3e$. Charge changes of $1/3e$ on particular spheres when they contact other surfaces were continually observed. Of 21 new experiments, four charges of + $1/3$, four of - $1/3$, and thirteen of zero were found. Extensive measurements and critical analysis have assured us that the background forces are either negligible or have been measured and taken fully into account.*" It is apparent to us that we must incorporate niobium into our composite hull structure. It is important that we produce the fractional $1/3e$ charges (+, 0, -) on the hull surface to mimic the surface of an electron (42).

The use of niobium spheres by **Mead** and **Nachamkin** in their 1996 proposal for ZPE extraction of useful energy gives credence to application of niobium to produce fractional ($1/3e$) charge. The used "resonant dielectric spheres, slightly detuned from each other, to provide a beat-frequency downshift of the more energetic high-frequency components of the ZPE to a more easily captured form. Our proposal is similar except we are working with a (hemi-)spherical niobium alloy niobium in our prototype vehicle that is also the general vector potential shape for all particles. Our prototype is similar to a spherical shape but slightly different.



Stern view



Port Side View

Figure 46 - rear and side views of the UNITEL craft [scale model] (courtesy UNITEL, Inc. – May 2002)

The disk-shaped structure attached to the stern is designed to prevent cavitation or "pitting" of the hull surface. The vehicle is designed to focus surface charge energy to the stern where it is dispersed in a corona.

5 - Power Source

The **UNITEL** vehicle will be powered by a small intrinsic power source such as a proton/anti-proton exchanger. Although not the best option due to its large mass, the craft could carry a nuclear reactor such as are currently used in US military subs. **Michael McDonnough** (info@betavoltaic.com) may be a good contact for power-supplies for our quantum-spacecraft powerplant. He works with Betavoltaic cells which are a clean safe (<http://www.betavoltaic.com>) nuclear-battery.

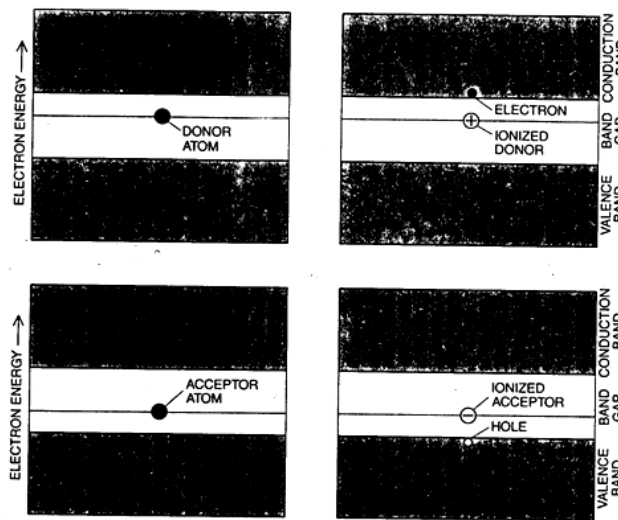


Figure 47 - front views of the **UNITEL craft [scale model]**

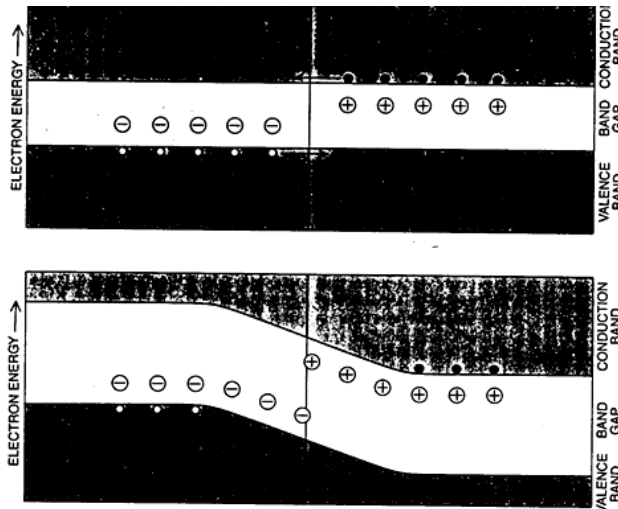
(courtesy of *UNITEL, Inc.*)

6 - Lens

The three-part free-standing laser lens will be placed in a polished titanium lens frame. The lens frame will attach to the front of the vehicle, being precisely congruent to the hull curvature. Each section of the lens will be tuned to emit a coherent beam of separate wavelengths of **Red**, **Green**, or **Blue**. The combination forms a true electromagnetic wave packet of synthetic solar (coherent) light.



SEMICONDUCTORS are materials in which a small amount of energy promotes electrons from a valence band in which electrons are bound to atoms to a conduction band in which electrons move freely. Two types of semiconductors are made by introducing impurities into an intrinsic semiconductor such as silicon. In *n-type* semiconductors (*top charts*), impurity atoms called 'donors' each give up an electron to the conduction band. The donors themselves become positive ions. In *p-type* semiconductors (*bottom chart*), impurity atoms called 'acceptors' each capture an electron from the valence band leaving a "hole". The hole -- or absence of an electron -- is in effect a positive charge. The donors themselves become negative ions.



P-N JUNCTION is the alteration of a semiconductor material from *p-type* to *n-type* in a narrow zone. At the time the junction first arises (*top drawing*), the *n* side has an excess of electrons and the *p* side an excess of holes. Electrons and holes then tend to diffuse. When an electron meets a hole (in an ideal semiconductor), they recombine. What remains (*bottom drawing*) are the ionized impurity atoms, which produce an electric field at and around the junction. This built-in electric field makes the *p-n* junction the central element in semiconductor electronics.

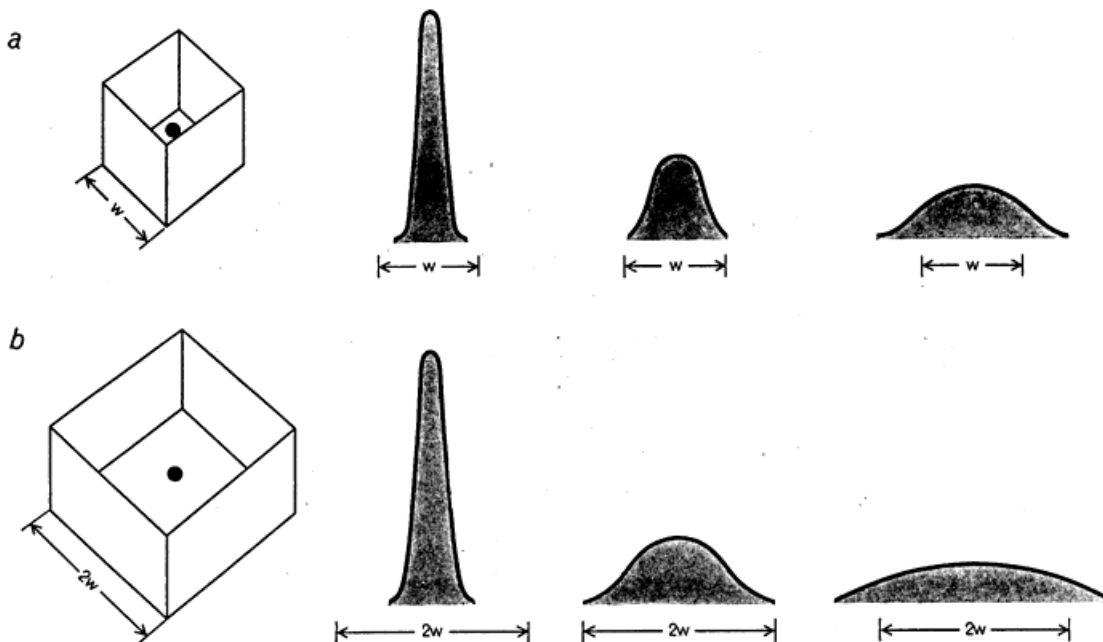
Figure 48 - "Doping" Semiconductors to create Junctions (courtesy *Scientific American, Oct'72 (25)*)

The beam will be projected from the three-part **Red/Green/Blue**, doped, periodically arrayed superlattice, RF-transparent, glass/CdS-CdTe:Te crystallite (A. Paul Alivisatos et al, Cal Berkeley, Type II-VI glass semiconductor compound crystallite) microwave-activated lens located in the forward area of the vehicle. The construction of our free standing three equal part **Red/Green/Blue** Type II-VI compound laser lens sections will require a chemical etching or electro-polishing process to eliminate excess material to produce the exact thickness of the required layer (down to nano-electronic tolerances).

To create our free-standing laser lens, each of the separate layers will be separately constructed and then “joined together” by thermal bonding methods. Each of the layers will be composed of three separate **Red**, **Green** & **Blue** sections with p-doped conduction, neutral intrinsic and n-doped valence layers. These layers form the p-n junction with an energy band gap to formulate the lasing process. They are:

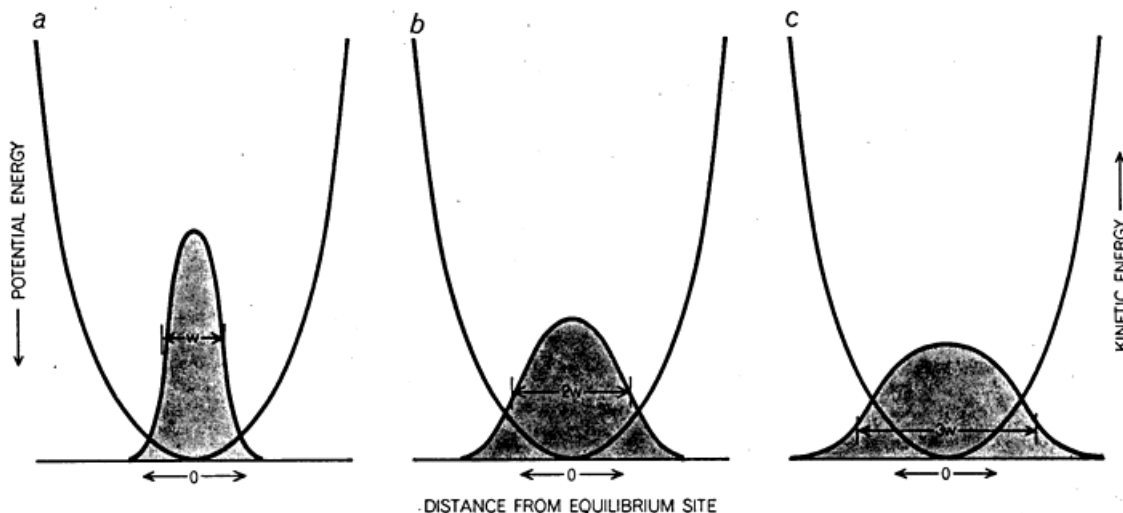
- 1). The conduction layer or outermost section of our laser lens structure will be composed of **tellurium doped cadmium telluride (CdTe:Te)**. The composition of the conduction layer will include the following p-dopants: copper, phosphorus antimony, arsenic & sodium.
- 2). The intrinsic or energy band gap layer shall be composed of **neutral cadmium sulfide**.
- 3). The valence layer is located in closest proximity to the RF lens activator (magnetron) and is composed of **cadmium sulfide**. The n-dopants to be used are: zinc, indium, aluminum or iodine.

NOTE: Lithium will be added to the conduction layer and silver will be added to the valence layer. Although both materials are difficult to work with, lithium is known for its reinforcement of its host Type II-VI compound material and silver lowers the lasing threshold.



ZERO-POINT MOTION of an atom in a crystal lattice is defined in quantum mechanics in terms of the atom's "wave function": a mathematical expression of the probability of finding the atom at a given point in space. The wave function is large in a region of space where there is a high probability of finding the atom and small where there is a low probability. In the diagrams at left two atoms are shown in imaginary boxes that have a depth corresponding to the atom's potential energy and a width corresponding to the

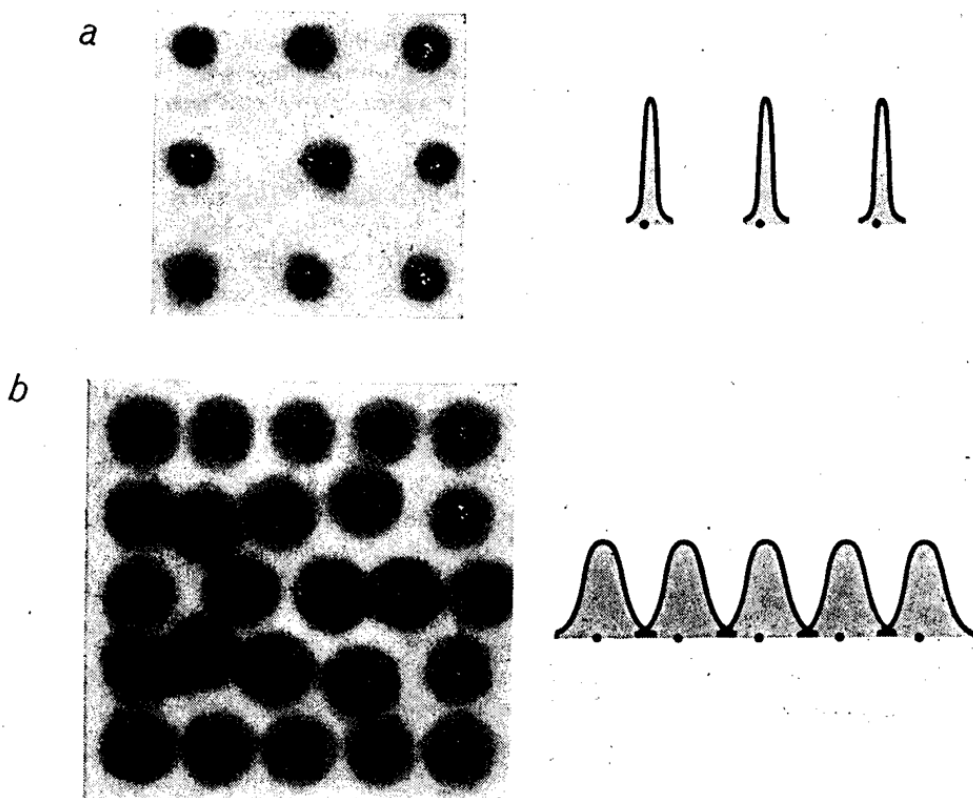
distance by which the atom is separated from its neighbors. For each atom a choice of three wave functions is represented by the curves at right. The kinetic energy, or energy of motion, of the atoms is inversely proportional to the width of the wave-function curves. In both cases the choice of the middle wave function is optimum; that is, it corresponds to the least total energy (potential energy plus kinetic energy) of the atom. The zero-point energy of the atom is the kinetic energy when it is at this lowest total energy.



POTENTIAL ENERGY of a particle in a crystal lattice is represented by a parabolic potential-energy curve (black) in which the particle is at rest at the bottom of the potential "well." The potential energy of the particle is directly proportional to the square of its distance from the center of the well (in classical terms) or to the square of the width of its wave function (in quantum-mechanical terms). Therefore the potential energy of the particle can be made

arbitrarily small by reducing the width of the wave function. Reducing the width of the wave function, however, has the effect of increasing the zero-point kinetic energy of the particle, which varies inversely as the square of the width of the wave function. For example, the wave-function curve in *a* (color) has the smallest potential energy and the largest kinetic energy of the three curves shown, whereas the reverse is true of the wave-function curve in *c*.

Figure 49 - Zero-Point Motion and Energies of a Particle in a Crystal Lattice
(courtesy *Scientific American*, (82))



CORRELATION of the motion of helium atoms, arising from their large zero-point motion, complicates the theoretical treatment of solid helium. In these diagrams the wave functions of the atoms are represented by intensity of color (*left*) and by the corresponding wave-function curves (*right*). In a normal crystal lattice (*a*) the atoms are well localized at their equilibrium sites; there is little correlation of the motion of neighboring atoms and their wave functions do not overlap. In the solid helium crystal lattice (*b*) the atoms are not well localized; their motion is highly correlated (*arrows*) and their wave functions overlap.

Figure 50 - Wave Functions of Solid Helium Atoms (courtesy Scientific American, (82))

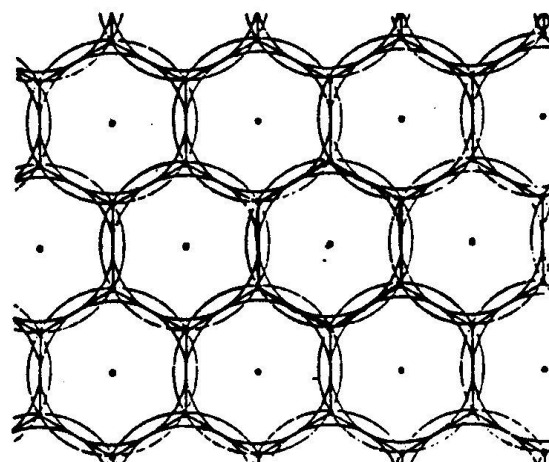


Figure 51 - close hex-pac of II-VI semiconductor compound structure (Wurzite) of lens showing overlapping, interlocking borders

The forward positioned microwave activated lens support frame will be attached at the end of the conical RF waveguide which is also attached at the opposite (rear) end to a square RF magnetron horn. This is similar to an ordinary microwave relay system where the RF signal wave packet is flat before leaving the horn. The RF wavepackets become parabolic in shape when they leave the horn as a traveling wave. The conical waveguide acts as an extension to the square horn. Square or rectangular horns are required to produce circular RF wavepackets. In the generic patent design the lens design is parabolic -- or more precisely a "paraboloidic" shape -- to receive the traveling wave lens activating microwave packet from an internal excitation source. The curved lens hence matches the microwave signal's parabolic shape as in a television antenna receiving dish. The free-standing, three-part laser lens receives the microwave signal like a "hand-in-a-glove". For the purposes of testing simple versions of the patent, we have developed the **"Prototype 1-A"**. We must mate the square horn to the conical RF oscillating chamber to match the circular 2-D pi-mode microwave signal to the flat three-part **Red/Green/Blue** laser lens.

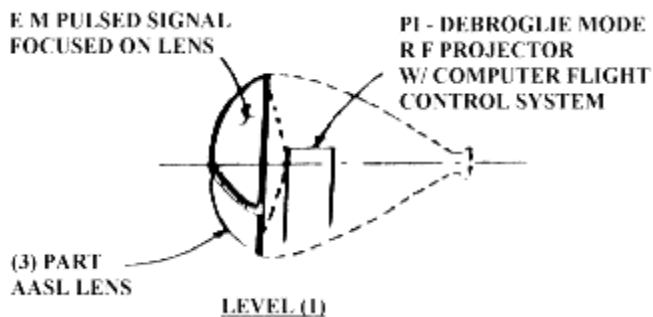


Figure 52(A) -Beam Structure of Potential EM Wells (Level 1)

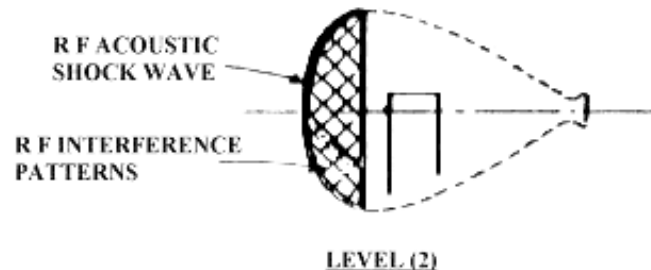


Figure 52(B) -Beam Structure of Potential EM Wells (Level 2)

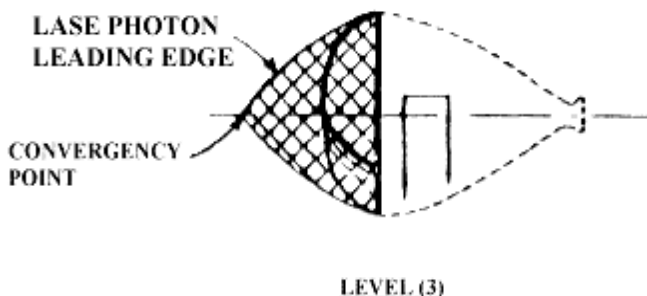


Figure 52(C) -Beam Structure of Potential EM Wells (Level 3)

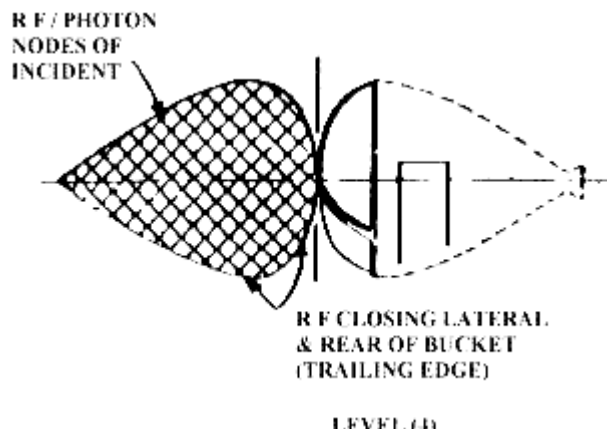


Figure 52(D) -Beam Structure of Potential EM Wells (Level 4)

The RF oscillator magnetron will be variably-pulsed to be used as a mechanical stress modulator that causes the forward mounted laser lens to lase. We have chosen the beacon ku-band tube-type, tunable, pulsed **VMU-1255 magnetron** built by CPI / Beverly Microwave Division (Beverly, MA). The VMU-1255 magnetron has a frequency output of 16.25 GHz with a peak power of 500 Watts. The high frequency and low wattage output should be optimal for non-destructive laser activation capabilities.

The pulsed magnetron will operate in the pi-mode (43) and be mode-locked to activate the laser lens so that the positive (+) areas of the pulsed projected microwave packets activate the **Blue** 1/3 section of the lens. The negative (-) area of the RF wavepackets activates the **Red** 1/3 lens section and the neutral (o) area will activate the **Green** lens section.

Type II-VI compound/glass
Crystallite Lens section

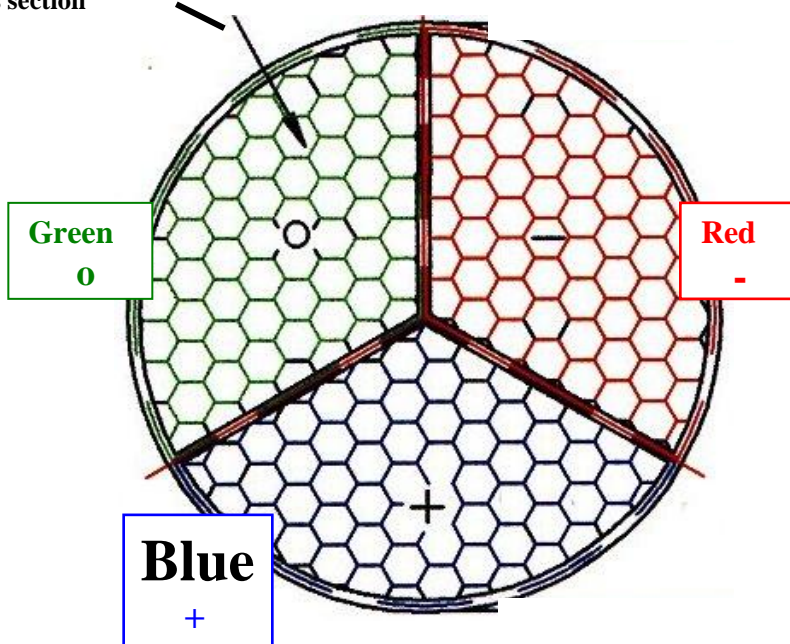
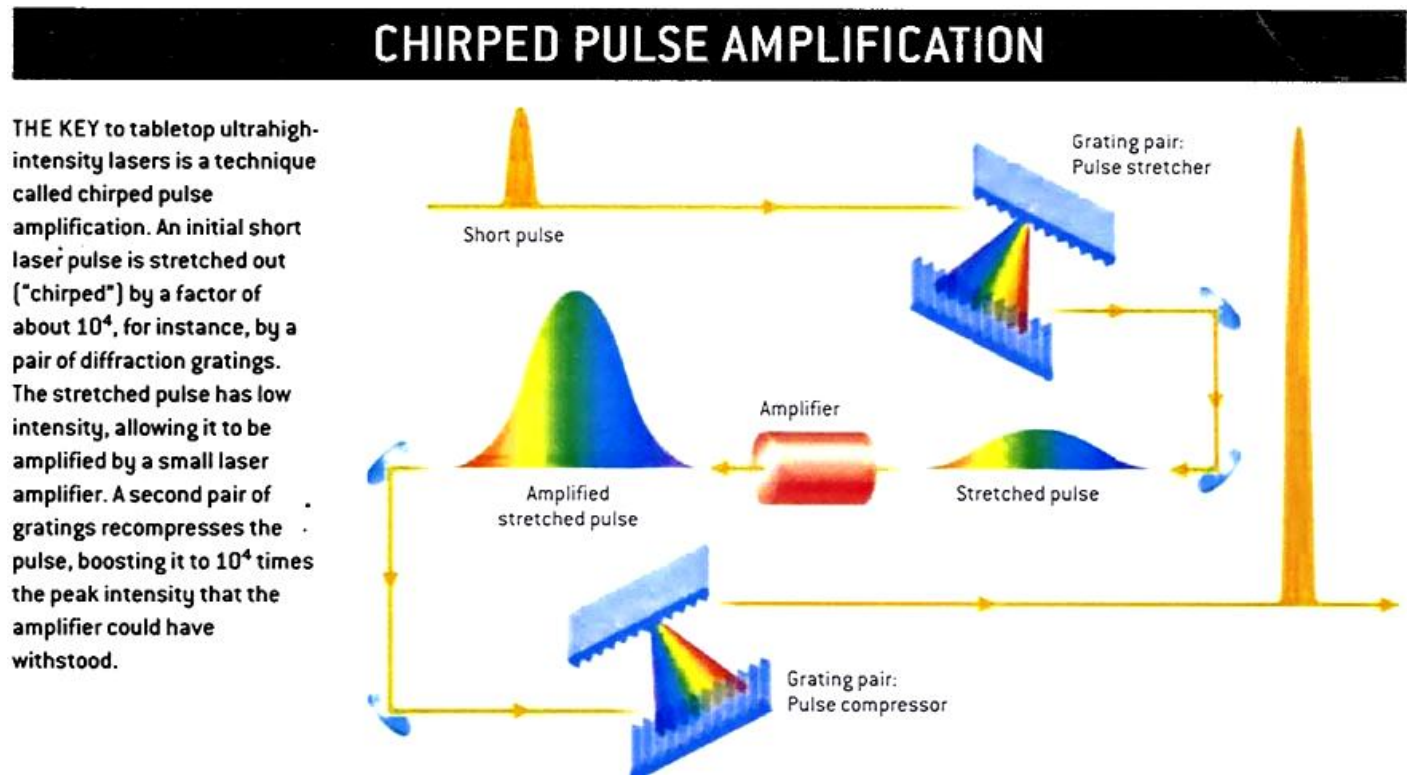


Figure 53 - the Charge-Color Placement in the Lens

The circular RF wavepackets will also be left- and right-hand circularly polarized at the horn. This means that the device will require an antenna attached to the horn. The left- and right-hand polarization is analogous to Faraday rotation of laser beams where left and right hand components of circularly polarized light are of equal amplitude. The lens will emit one (white) ellipse per cycle in the projected laser plasma.

Excitons are coupled to the acoustic shockwave projected by the magnetron creating **mechanical stress modulation** of the lens (44). The crystal lens is piezoelectric and required for mechanical stress modulation. An example of mechanical stress modulation occurs in a record player. The phonograph needle is attached to a piezoelectric quartz crystal. As the needle vibrates across the grooves in the record, phonons are created. The phonons couple with electrons and are channeled in the form of an electric signal to the speakers. This principle will be used to control lasing, navigation, and data storage with the **UNITEL** lens.

An RF pulse compression chamber is to be attached to the horn so that we may compress or "chirp" the signal (45).

**Figure 54 - Chirped Pulse Amplification**(courtesy of [Scientific American, May'02 \(99\)](#))

Radar-chirping and **phase-conjugate steering techniques** are important to **UNITEL**'s aerospace flight propulsion system. Design and fabrication of the RF compression chamber and oscillating cavity (horn) will be completed by the contractor and manufacturing consultant who will work in a consulting capacity to refine the overall design of the lens activating system. This will include working in concert with the lens fabrication contractors as a consultant to coordinate the construction of the lens that will be matched to the RF lens activation equipment. The crystal MBE growers are to act as subcontractors to produce our Type II-VI compound laser lens.

In **UNITEL**'s "Prototype 1-A" drawings [see the "Documents" section at the end of the book], dimensions "A" and "B" of the RF waveguide details are to be determined (along with the overall thickness) of the lens by sizing and functional dynamics of the lens activating magnetron. The waveguides are attached together and to the magnetron. The laser lens is attached to the conical waveguide at the forward mounted position.

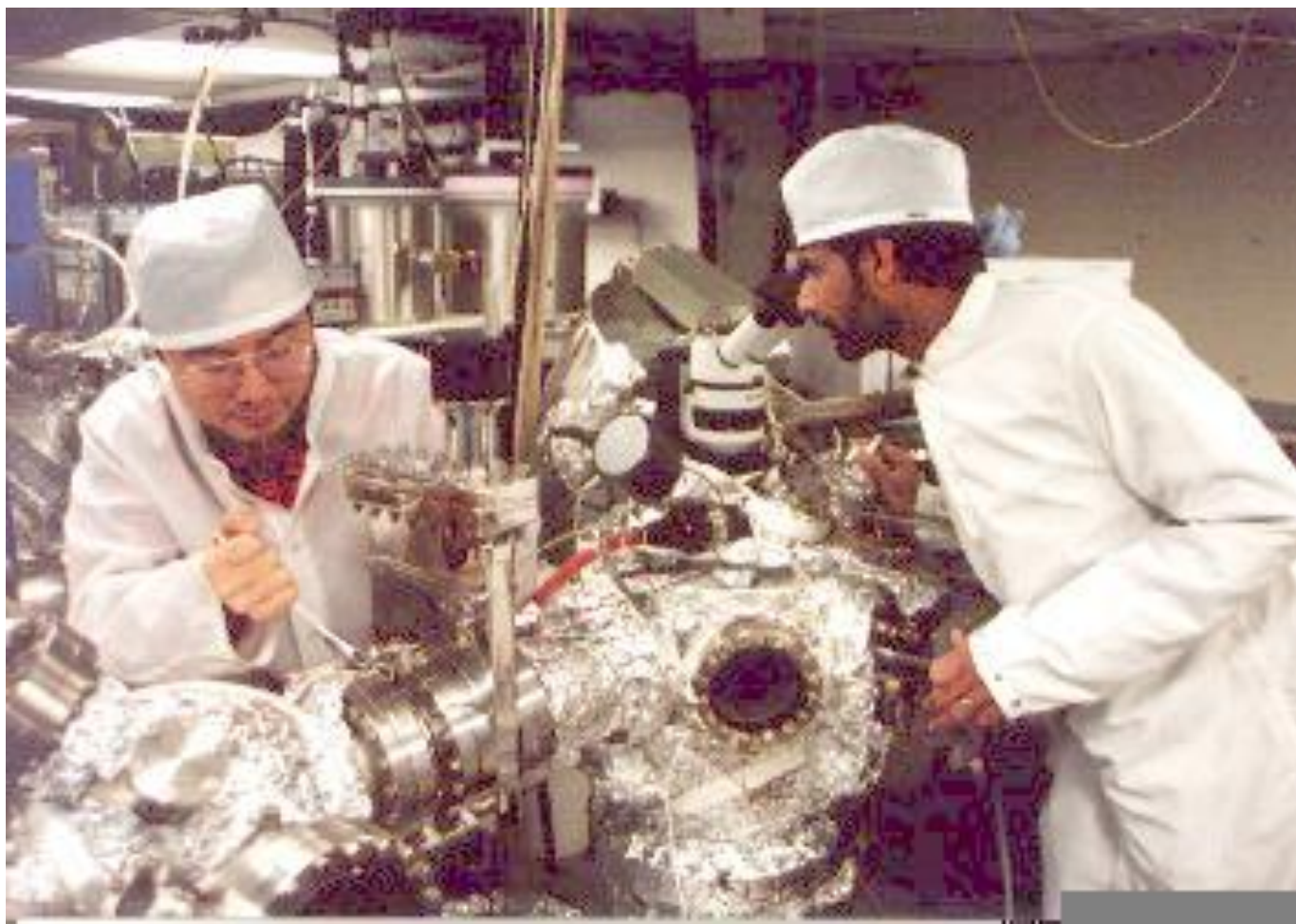
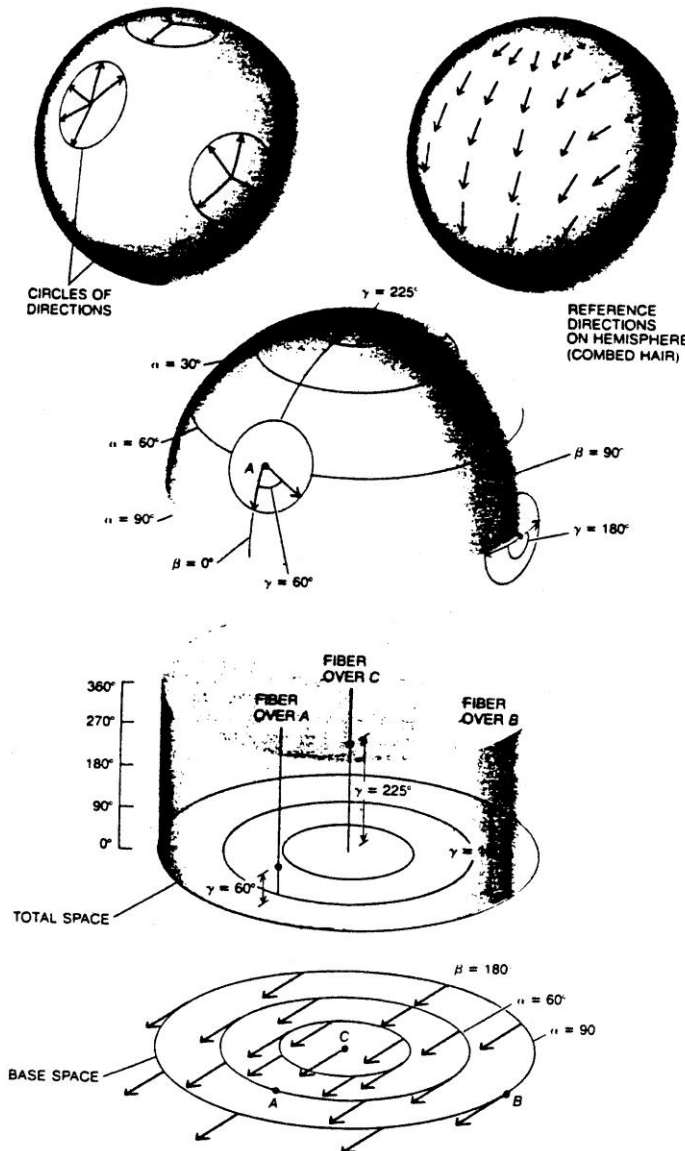


Figure 55 - Dr. Sivananthan (Director/UIC Microphysics Labs) and co-worker using MBE equipment that will be used in producing UNITEL's lens

These circular pi-mode wavepackets are produced in the square horn and then introduced into the conical waveguide that is congruent with the lens support frame. The overall dimensions are reliant on the design factors concerning the lens thickness and its distance from the laser lens activating magnetron that will be determined by the lens and microwave system fabricators. Both the square horn and the conical waveguide are to be composed of high polished aluminum. The fabrication of the lens support frame shall be of high-grade polished titanium alloy steel. A thermal expansion gap coefficient allowance is to be included in the fabrication of the lens support frame. All component parts, including the square and conical waveguides and lens support frame (excluding lens sections), shall be fabricated and assembled with the RF compression chamber and the lens activating magnetron system by a designated fabricator. Once fabricated and assembled, the system will be shipped to a testing facility for the detection of certain desired effects.

The free-standing RGB lens acts much like a large pixel. Each separate, equal 1/3 section is activated by mechanical RF-modulation to generate 255 lumens. This produces an over-all white (monochromatic) laser light beam. This will be a true electromagnetic wavepacket that is effectively a (smoothly varying) **potential electromagnetic well** at one ellipse per cycle (46). The crystallite lens is paraboloidically curved and serves as a **fiberbundle** attachment point of the projected beam with string-like effects to the vehicle (47) and

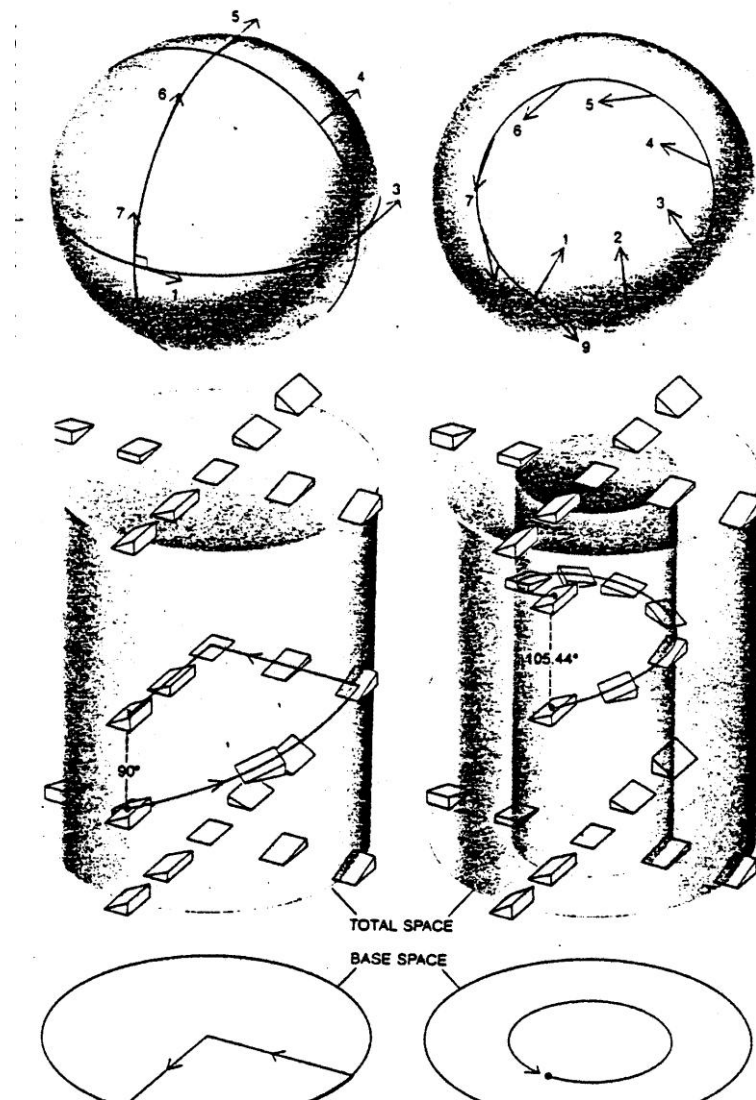
provides a path for a quantum parallel transport mechanism (affine connection) that automatically aligns all particles in the beam in one direction (magnetization). The particles then move up the projected beam, without resistance, in a superfluidic manner. The projected plasma will exhibit string-like effects, whereby the exteriorly charged vehicle will commute up the string (48).



BUNDLE OF DIRECTIONS on the surface of a sphere is an important example of a fiber bundle. At each point on the sphere there is a circle of directions along which one can look the surface. To label these directions with angles, one must assign a reference direction to each point. If the reference directions could be assigned everywhere in a continuous manner, one could "comb the hair" on the sphere. But that is not possible; there must always be a "cowlick". Hair can be combed, however, over any region smaller than the entire surface. For example, on a flat map of the northern hemisphere the description "downward and to the left" specifies a direction at each point and so defines a continuous set of reference directions on the hemisphere. A picture of the bundle of directions on the hemisphere appears on the vertical coordinate line above the corresponding point on the map, and at a height that corresponds to the angle the direction makes with the reference direction. Heights '0' and '360' correspond to the same direction. The total space of the bundle is a cylinder where points at the top and bottom of each vertical fiber are identical. The arrows that represent the reference directions on the map are parallel; but their counterparts do not represent parallel transport.

Figure 56 - a Fiber Bundle on a sphere

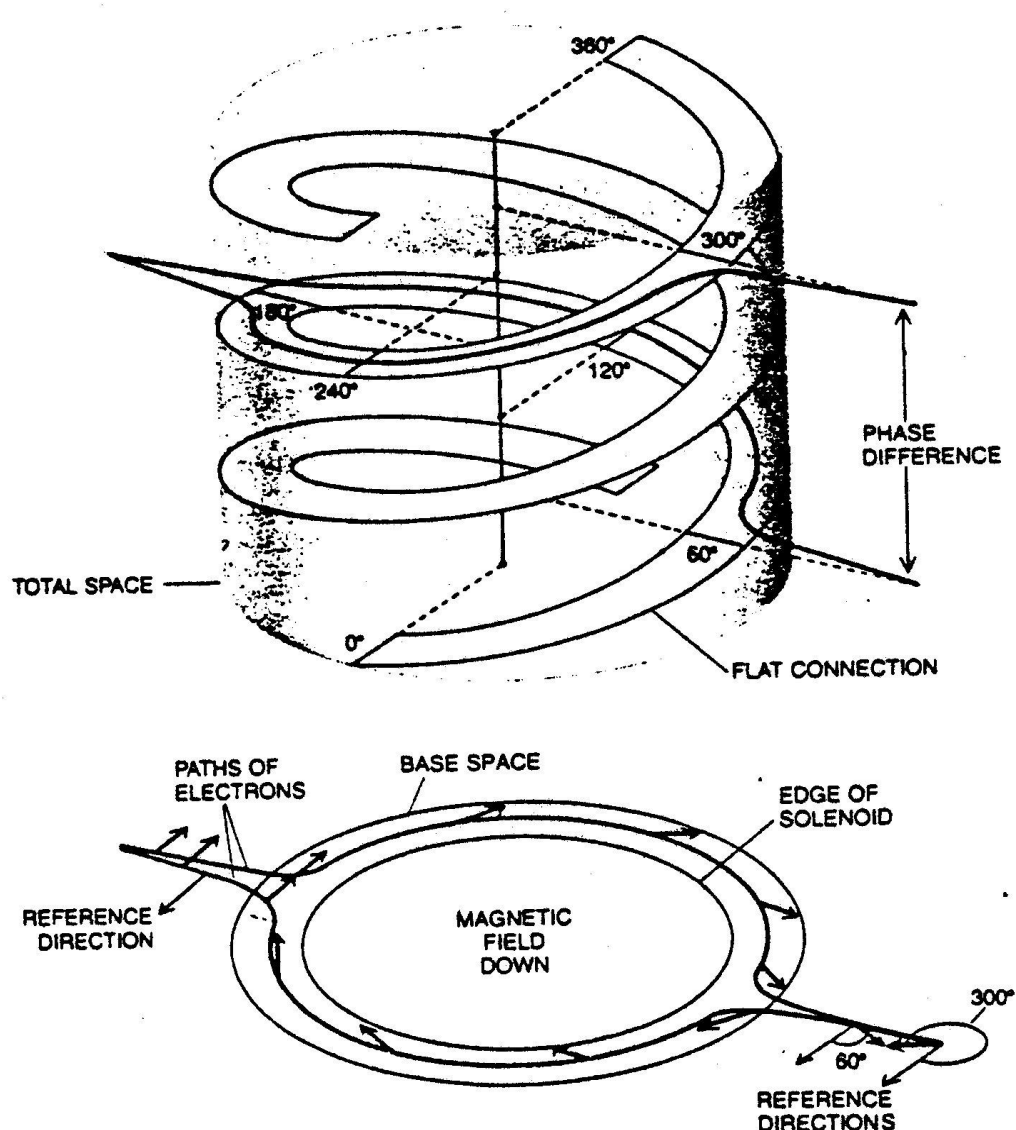
(courtesy Scientific American, July '81 (17))



LIFTING A PATH in a fiber bundle is a means of finding a path in the total space starting at a given point and lying directly above the path in the base. For the bundle of directions on the surface of the sphere, parallel transport of directions on the surface gives a unique lifting for every path. The bundle of directions over the northern hemisphere can be represented as a cylindrical total space. Each direction is at a height corresponding to the angle it makes with the hemisphere. For the path around the spherical geodesic triangle, the reference directions point South along the meridian at the start of the path. The angle between the transported direction and the tangent to a geodesic is constant. On the first leg of the triangle, the geodesic curves with respect to the reference direction so that the angle between the transported direction and the reference direction increases at a constant rate. Along the second and third legs of the triangle, the transported direction maintains a 180-degree angle with the reference direction. When the arrow returns to its starting point, its direction has changed by 90 degrees -- the angular excess of the closed triangular path. The changes in transported directions are plotted as a lifted path in the bundle of directions on the hemisphere. For the path around the 45-degree latitude, the transported direction begins 180 degrees away from the reference direction and increases its angle with the reference direction at a constant rate. A connection can define a path-lifting rule without reference to parallel transport by assigning planes to every point in the total space. The lifted path must be tangent to the planes. The slopes of the planes are the same for all points along a single fiber, but they vary continuously from fiber-to-fiber; the planes are never vertical. Such a collection of planes is called a 'connection in the fiber bundle'.

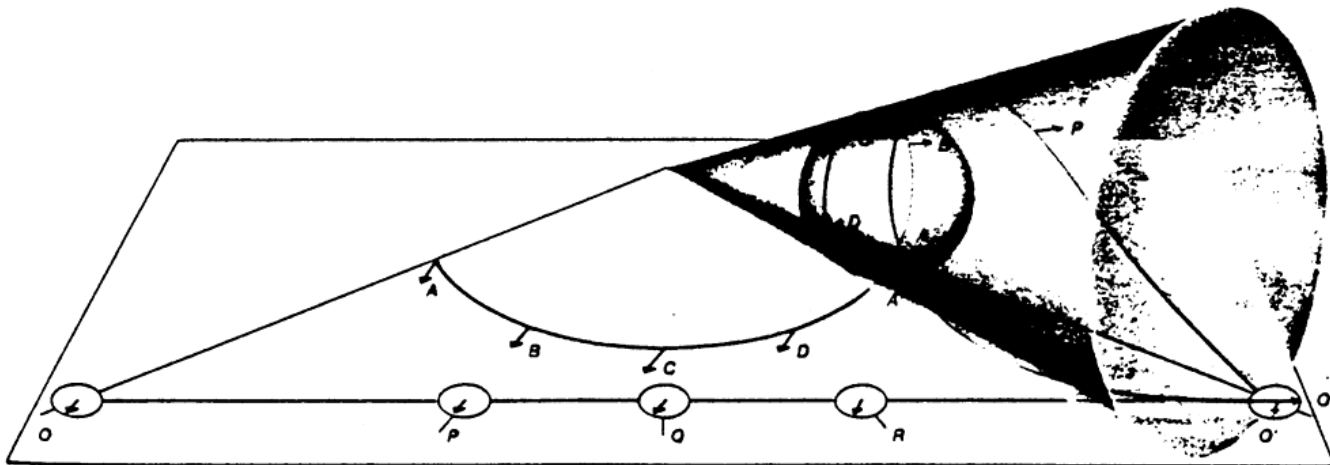
Figure 57 - Geometrical Paths in a Fiber Bundle

(courtesy Scientific American, July'81 (17))



FIBER BUNDLE of phase angles over a cross section of the Abaronov-Bohm experiment is almost exactly like the fiber bundle of directions on the surface of a spherically domed cone. Over each point in the base the fiber in the total space represents the possible phase angles (from 0 to 360 degrees) of the electron at that point. For an appropriate choice of magnetic-field intensity the connection defined in the bundle of phases by the magnetic vector potential field is identical with the connection given by parallel transport on the domed cone. The curvature of the connection corresponds to the magnetic field in the solenoid. The region inside the solenoid corresponds to the spherical dome. There the rule for lifting a path is the same as the parallel-transport rule on the surface of the sphere, and it can be described by the same system of sloping planes (not shown). The region outside the solenoid corresponds to the truncated cone. There the connection is flat. The sloping planes are tangent to a family of spiral ramps that fill up the total space. The phase shift in the base is represented by the rotating arrows.

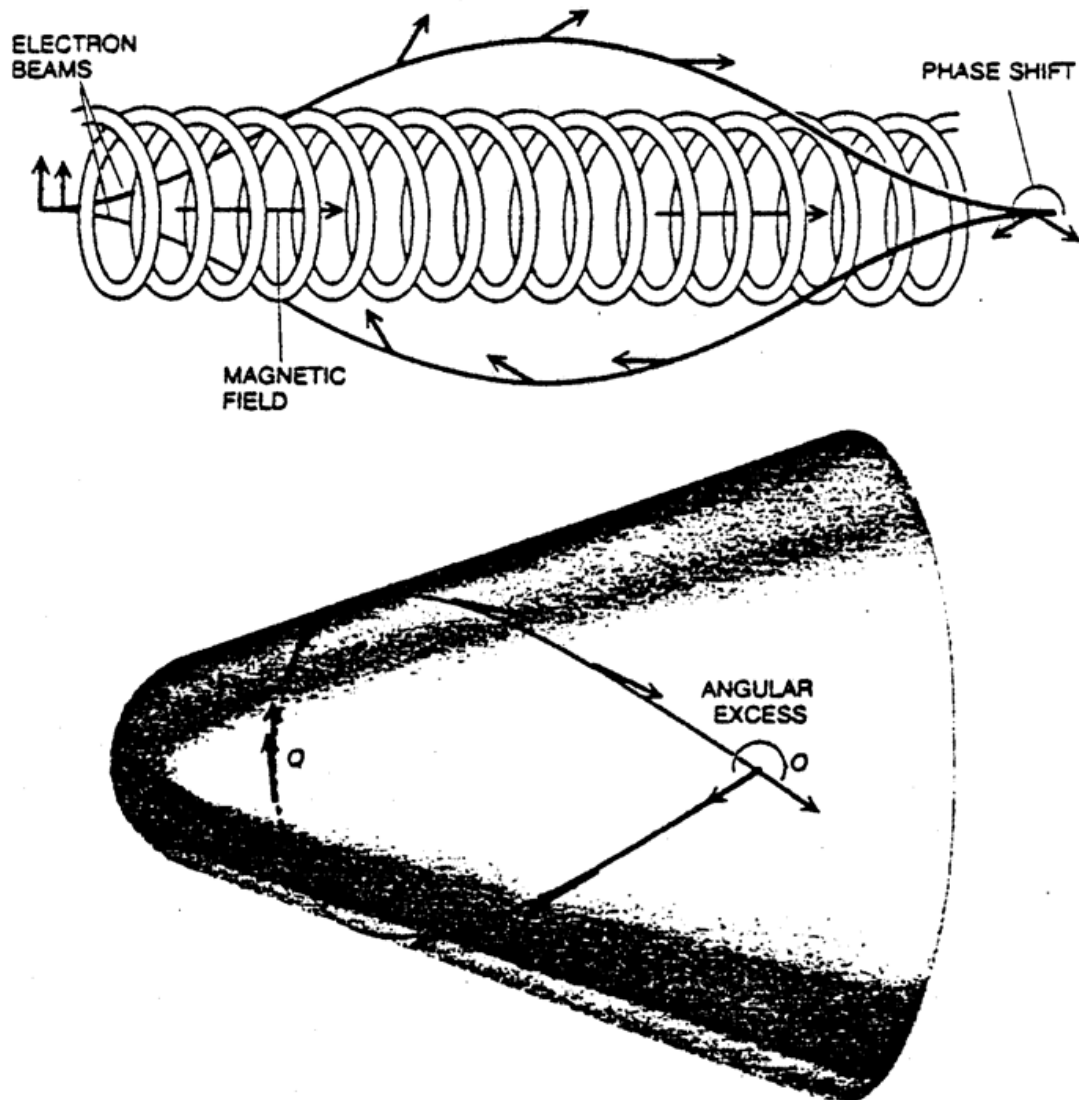
Figure 58 - The above illustration is comparable to UNITEL's projected, pulsed-chirped, spiraling laser plasma. The spiraling path of parallel transport produces the same results as Cal Berkeley's "Racetrack" design of arrayed coils in their accelerator for their 14.7-Tesla magnet. (courtesy of *Scientific American*, July'81, (17))



PARALLEL TRANSPORT carries a direction along any curve in a plane so that an arrow points in the same direction everywhere on the curve. To extend the idea to parallel transport along a curve on a surface that is not planar, one can imagine that parallel directions in the plane are printed onto the surface as the surface rolls on the plane -- without slipping or twisting about the vertical -- so that the point of tangency always remains on the curve. To roll a sphere along one of its circles of latitude, it is convenient to draw a cone tangent to the sphere along the circle. As the cone rolls on the plane, the sphere rolls along the circle of latitude. When a surface is rolled along a straight line in the plane, the curve printed onto the surface is a geodesic. If a geodesic is printed on to a cone of sufficiently small vertex angle, it can circumscribe the cone and intersect itself at an angle called the 'angular excess' -- a measure of the curvature by the path.

Figure 59 - the above illustration is comparable to **UNITEL**'s design for an all-electric space vehicle which utilizes the "capped-cone" (or teardrop) shape, which is the General Vector Potential for all particles and a mathematical identity of 137.

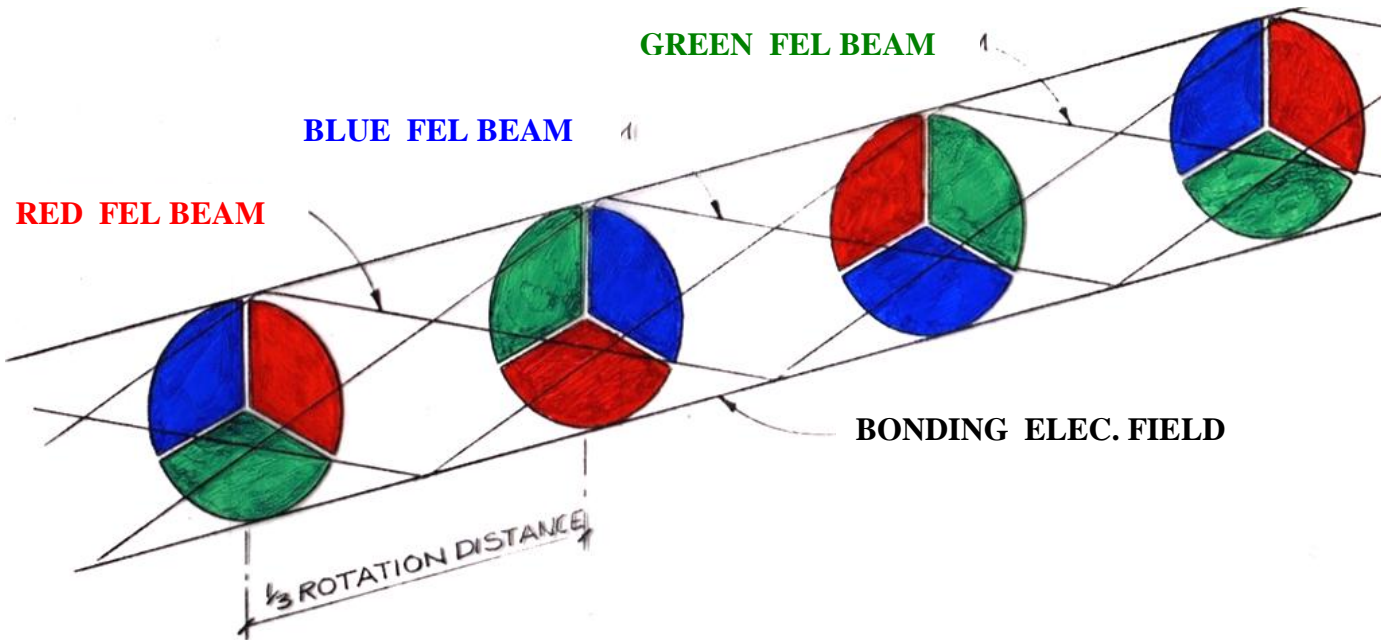
(courtesy of *Scientific American*, July 1981, (17))



PHASE SHIFT of the electron beams in the Abaronov-Bohm experiment can be modeled by the parallel transport of a direction on the surface of a truncated cone capped with a spherical dome. The shifting of phase along each beam is represented by the rotation of an arrow. The two partial beams begin in phase. The phase is then retarded along the colored path and advanced along the black path. The phases shift even though the magnetic field along both paths is zero; the shifts are directly proportional to the magnetic field between the paths. On the domed cone the geometry of the conical region is like the geometry of a plane: the region can be slit longitudinally and unrolled onto a plane without stretching or compressing. Parallel transport along two paths around the cone, however, will not lead to the same direction when the paths meet again, even though the curvature along both paths is zero. The paths shown form a curve that is a self-intersecting geodesic; the arrows represent the direction tangent to the curve. Because the tangent direction undergoes parallel transport along a geodesic the angular excess of the curve is identical with the angle at which the two paths meet. The angular excess measured in radians is equal to the total curvature of the region between the paths. The curvature is concentrated on the dome, just as the magnetic field is confined to the solenoid.

Figure 60 - the above illustration is comparable to UNITEL's teardrop-shaped vehicle.
(courtesy of Scientific American, July'81 (17))

The current in the projected superconducting laser plasma “string” produces electric and magnetic fields that -- in empty space -- would propagate away from the string as electromagnetic waves. But interstellar and intergalactic space is not exactly empty. It is filled with a dilute gas of electrons and charged atoms that prevent waves from leaving the vicinity of the string (49). The **fiber bundle** attachment is the starting point for the path of parallel transport of the projected laser plasma charged particles and is a superconducting system that will produce **quantum topological** and **superfluidic MagnetoHydroDynamic** effects (50).



Partially overlapping sections of a three-part field through projection as found in a Hilbert space of sections. Successive one-third turns match the internal rotation of the isotopic spin of a Hadron and the color rotation of a Baryon from Red-to-Green, to Blue, and back to Red again. These rotations give the projected plasma field a net color (white). When colors are changed, a virtual particle must be emitted that will re-adjust the colors of the plasma field to maintain net color. This process is produced by the resonance interference pattern of the desired quanta.

Figure 61 - the above illustration depicts the 720° timing with internal laser plasma beam structure and rotation of the equally proportioned Red, Green & Blue sections. Each section undergoes two complete (360°) rotations. The $1/3$ individually colored sections are like pistons, complete with firing order and BDC & TDC in a conventional three-cylinder gas motor.

The final step in the lens construction process after the blank (valence, intrinsic & conduction) p-i-n layers are thermally bonded is the exterior surface layer of each separate Red, Green & Blue lens sections will be electro-polished to the exact overall thickness. The final or last layer will be made of p-doped Cadmium Telluride (CdTe:Te), using vapor deposition growth technique **Molecular Beam Epitaxy** (MBE). The last layer will be one-molecule thick. This is to ensure chromaticity or the ability for the lens to have

the ability to produce coherent or lased light. All other components of our proposed model of the Type VI System are readily available as standard items.

The **acoustoelectric** effect is the appearance of a DC electric field when an acoustic wave propagates in a medium containing mobile charges. It is an example of the general phenomenon of "wave-particle drag" of which the operation of a linear accelerator and the motion of driftwood toward a beach are other examples. It can be quite strong in the piezoelectric materials CdS and CdTe. Concerning the piezoelectric properties of these type II-VI semiconducting compounds, the wave and mobile charges interact through the electric field arising from the strain associated with the wave. This interaction is significant when the electric field is longitudinal, *i.e.* parallel to the wave propagation direction. Because the interaction of the passage of an acoustic wave through the medium causes a periodic spatial variation of the potential energy of the charge carriers. If the mean free path l of the carriers is small compared to the acoustic wavelength λ -- as is the case for most of the usual (ultrasonic) frequency range -- this results in the bunching of the carriers in the potential-energy troughs. Since the wave is propagating, it drags the "bunches" along with it. This is the origin of the acoustoelectric field and clearly causes attenuation of the wave. The stronger the effect, the stronger the bunching.

The foregoing discussion suggests that if an external electric field were applied to the sample to give carriers a drift velocity n_d greater than the drift velocity n_s the carriers should drag the wave, *i.e.* the wave should be amplified. This conjecture was verified experimentally on CdS samples at frequencies of 15 and 45 MHz by Hutson, McFee and White in 1962. They found acoustic gain for shear waves at fields greater than 700 V/cm at which field n_d equals the shear wave velocity. For not-too-large acoustic wave amplitudes, it was possible to account quite well for the size of the gain and its variation with frequency, etc, with a linear phenomenological theory taking into account the currents and space charge produced by the piezoelectric fields that accompany the acoustic wave. The gain (called the **acoustoelectric gain**) is found to be low at low frequencies (less than the conductivity relaxation frequency s/e), where the carriers can redistribute themselves quickly enough to essentially cancel out the piezoelectric field. It peaks at the frequency for which the acoustic wavelength is of the order of the Debye length where the bunching is optimum.

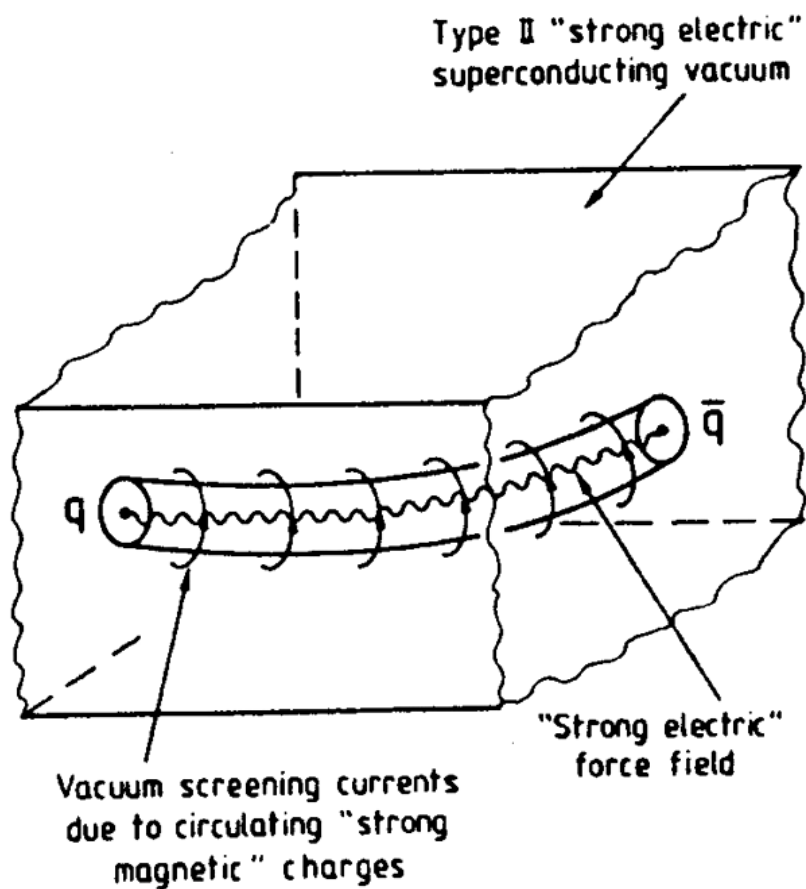
In the fairly strong piezoelectric material such as CdS, acoustoelectric gains as high as 40 dB/cm have been found, leading to consideration of this effect for practical use as an amplifier (acoustoelectric amplifier). This type of amplification has been found particularly useful for amplification of **acoustic surface waves (SAWs)**. Because the amplitude of a SAW decays exponentially with distance below a free surface, the surface acts as a waveguide for such a wave. SAWs at microwave frequencies are easily introduced into a piezoelectric material by coupling in microwaves within our freestanding periodically arrayed superlattice laser lens. A similar transducer such as LiNbO₃ can reconvert the SAWs into microwaves. The SAW velocity being smaller by a factor of 105 than electromagnetic wave velocity, a short length of a SAW-propagating material is useful as a delay line and for various types of signal processing. For maximum utility, the losses of the SAWs in the guide are conveniently overcome by incorporating acoustoelectric gain. If the piezoelectric material is insulating, this is easily accomplished by providing a conducting layer. The conduction layer CdTe is used to support both the SAW and the electrons drifting in the electric field.

As a special case for this, a single large wave the interaction of its piezoelectric field with its own carrier bunches results in the generation of a dc current -- called the acoustoelectric current -- flowing in opposite direction opposite to the useful or Ohmic current and may result in the generation of the second harmonic. When an outside acoustic wave is not introduced, application to a highly conducting sample of CdS, for example, of a field high enough to make $n_d > n_s$ will in a short time make the current will drop to a much smaller value and remain there. In this theory acoustic gain, then, may be thought of as due to an excess of stimulated phonon emission by the carriers over absorption.

UNITEL will be testing mixtures of the same Type II-VI compound semiconductors as described in the patent with various types of glass, including RF transparent and armor plate varieties. In 1980 **A.I. Ekimov** and his colleagues at the *Ioffe Physical-Technical Institute* in St. Petersburg, Russia discovered distinctively different optical spectra from samples of glass containing the Type II-VI compound semiconductor cadmium sulfide or cadmium selenide. The samples had been subjected to high temperature. Ekimov suggested that the heating caused the nanocrystallites of the semiconductor to precipitate in the glass and that **quantum confinement of electrons in these crystallites caused the unusual optical behavior**. This is valid proof that a much thicker and more rugged laser lens can be constructed from a glass Cds-CdTe mixture for aerospace purposes.

Ekimov's work set a precedent for work later performed by groups of researchers at **Corning Glass**, **IBM**, **City College of New York** with more elsewhere. Many experiments were performed with recorded data for the correct glass preparation techniques and convincingly demonstrate quantum confinement. **Luis E. Brus** and colleagues at **Bell Labs** were making colloidal suspensions of nanocrystallites by precipitating from solutions containing the elements that make up semiconductors. A dramatic shift in fundamental absorption energy to higher energies suggested quantum confinement. **A. Paul Alivisatos** and staff at the **University of California at Berkeley** and other researchers all over the world have expounded on this approach. **Michael L. Steigerwald** of Bell Labs and others have used an organic "soap bubble" wrapping known as a reverse micelle to stabilize the surface of a semiconductor. Research groups at the **University of California at Santa Barbara** and the **University of Toronto** are stuffing clusters of atoms into nanometer-scale cavities of Zeolites, a technique that confers the advantage of precise dimensional control of constructing the lens.

The lens will emit coherent monochromatic laser light from the three separate **Red**, **Green** & **Blue** sections forming an overall white light. The paraboloidal curve serves as the base or point of attachment for a light string. This curved lens provides the uplifting path for parallel transport superconducting mechanism that attaches the light beam to the vehicle. This is the fiber bundle connection of the projected light string to the vehicle. The dielectric and ZPE forces play an important role in producing the particle pair mode from this arrangement so as to become a **gigantic** electron-hole or electron-positron pair at Macroscopic scales. The glass mixture will provide the ruggedness required for aerospace propulsion.



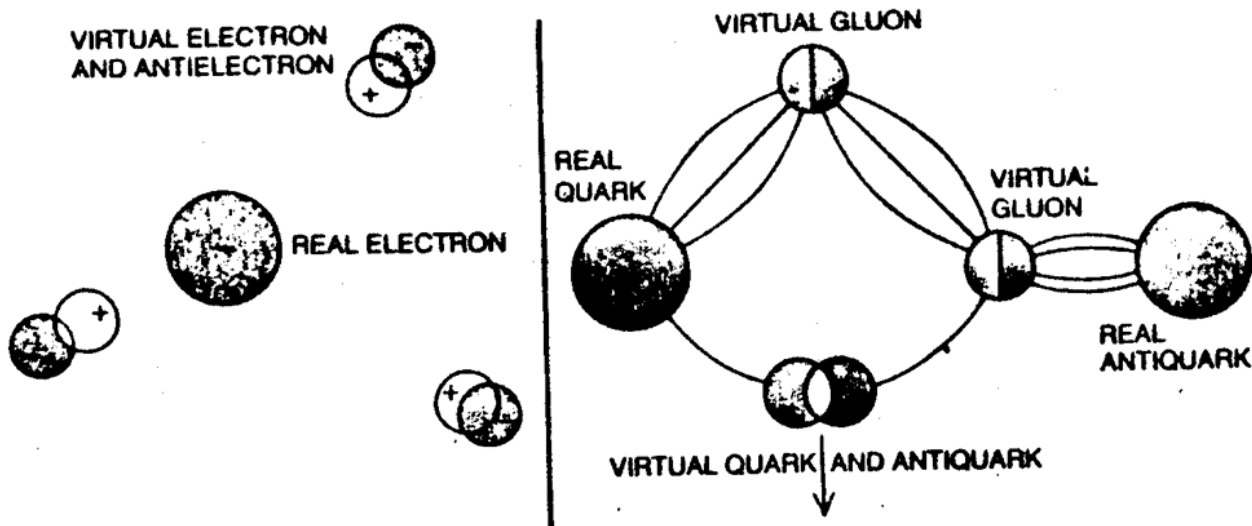
A chunk of vacuum illustrating its possible 'type II superconducting' property with respect to the strong interaction.

Figure 62 - Type II "Strong Electric" Superconducting Vacuum (69)

7 - Control and Navigation

An on-board computer, **UNITEL**'s quantum computer design **HOLO-1** will efficiently control the array of semiconducting diode elements (SDEs) via a digital relay system. Quantum computers are ideal for managing quantum systems. The network of SDEs work unitarily and provide the ability to "chirp" the entire system in a precise variable pattern. Technically this is referred to as a **phase conjugate steering technique (51)**.

In addition to providing a protective shield, the close-adhering cloud of electrons will flow over the hull in acoustic surface waves or **Rayleigh-Stonely** waves. Three modes of acoustic surface wave will be used to control the ship: running, standing, or retarded mode. The retarded mode would slow the vehicle through interaction with the ZPE while the running mode would reduce friction for high-speed travel. The standing mode could be used when the ship is hovering.

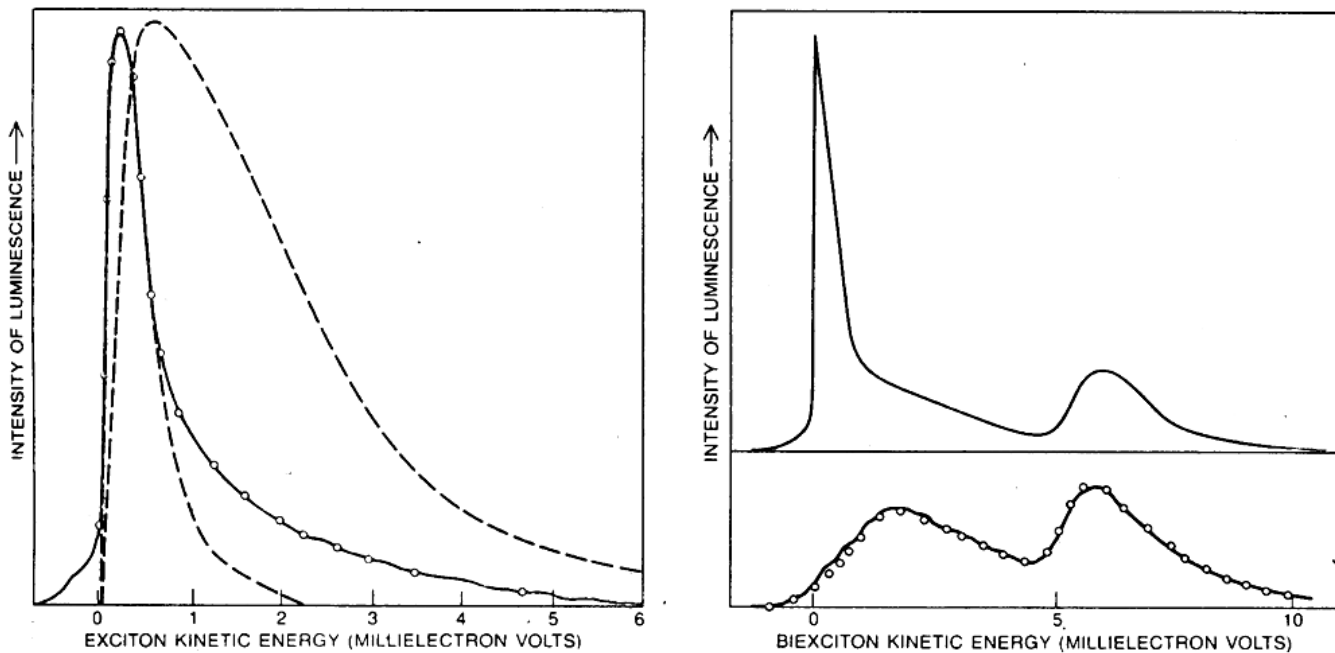


POLARIZATION OF THE VACUUM explains to some extent the peculiar force law that seems to allow quarks complete freedom of movement within a hadron but forbids the isolation of quarks or gluons. In quantum electrodynamics (*left*) pairs of virtual electrons and anti-electrons surround any isolated charge, such as an electron. Because of electrostatic forces the positively charged antielectrons tend to remain nearer the negative electron charge and thereby cancel part of it. The observed electron charge is the difference between the "bare" charge and the screening charge of virtual antielectrons. Similarly, pairs of virtual quarks diminish the strength of the force between a real quark and a real antiquark. In quantum chromodynamics, however, there is a competing effect not found in quantum electrodynamics. Because the gluon also has a color charge (whereas the photon has no electric charge), virtual gluons also have an influence on the magnitude of the color force between quarks. The gluons do not screen the quark charge but enhance it. As a result the color charge is weak and the quarks move freely as long as they are close. At long range infinite energy may be needed to separate two quarks.

Figure 63 - Quantum ChromoDynamics (QCD) vs. Quantum ElectroDynamics (QED)
(courtesy *Scientific American*, June'80 (66))

The fact that atoms or particles can exist on a Macroscopic scale has been proven recently by the creation of a **Bose-Einstein condensate**; a proven MOSS system. **Eric A. Cornell** et al at the **National Institute of Standards and Technology** (NIST) (Boulder, CO) along with the **University of Colorado** in June 1995, formally created a Bose-Einstein Condensate.

The condensate can be thought of, as atoms that act like ice cubes in a tray. Each individual ice cube would lose their individual identities and act as an organized whole similar to the way photons in laser light march in coherent (in step) fashion. They would in effect, act like "one giant atom".



BOSE-EINSTEIN CONDENSATION may account for the anomalous shape of the two luminescence spectra shown here. The condensation is predicted from the quantum-mechanical distribution of excitons and biexcitons, which are both classified as bosons, among the energy states available to them at low temperatures. At the left is the luminescence spectrum for a dense gas of excitons in cuprous oxide. The distribution of the particle velocities that can be inferred from the spectrum (color) closely matches the distribution predicted by Bose-Einstein statistics (open circles). The semiclassical distributions shown for two possible temperatures (black) can fit portions of the observed spectrum, but the overall match is not as precise as it is if Bose-Einstein statistics is assumed. The data were collected by Hulin,

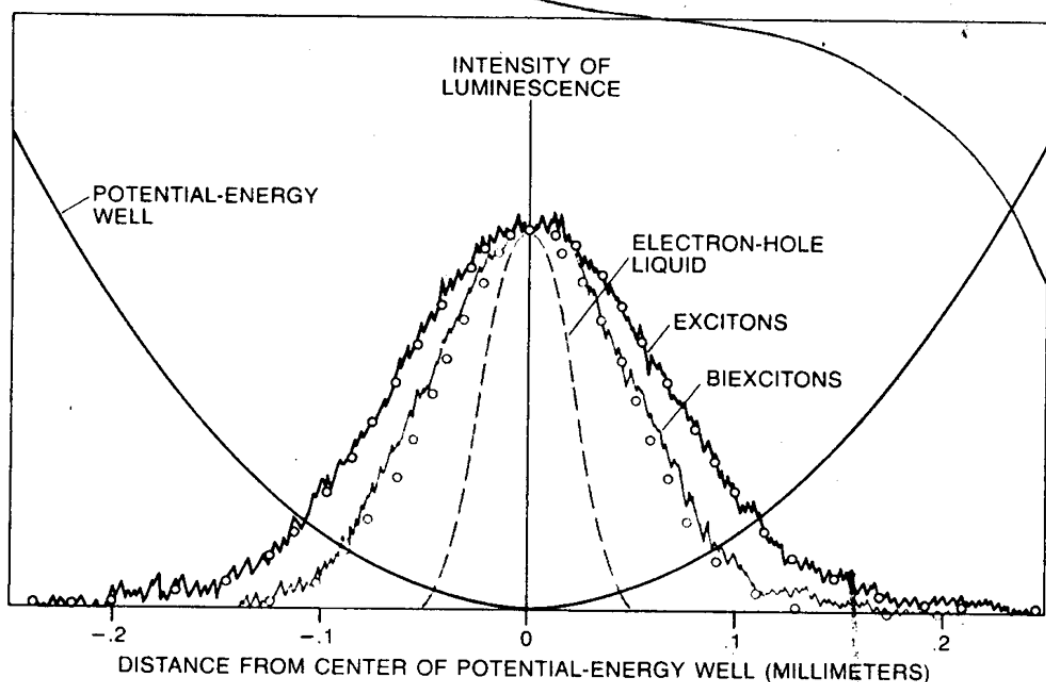
Claude Benoit à la Guillaume and Mysyrowicz at Paris. At the right is the luminescence spectrum for a biexciton gas in copper chloride (CuCl). The black curve is the spectrum obtained from a relatively rarefied gas of biexcitons generated by a laser at low power, and it agrees well with the velocity distribution of the biexcitons that is calculated from a semiclassical distribution (open circles). The colored curve is the spectrum obtained at higher laser power; it shows a large increase in the biexciton luminescence at low energy. The spectral peak is sharp, which indicates all the biexcitons have nearly the same kinetic energy. Such a spectrum is expected from a Bose-Einstein condensate. The data were collected at Indiana University by Lloyd L. Chase, Nasser Peyghambarian, Gilbert Grynberg and Mysyrowicz.

Figure 64 - Luminescence Spectra of a Biexcitonic Gas
(courtesy Scientific American, March'84)

Research since 1995 in Bose-Einstein Condensates (BECs) have produced much valuable information that can be directly correlated to **UNITEL**'s all-electric quantum electromagnetic laser propulsion system and vehicle. The BEC state is one which a cloud of atoms is cooled to near-absolute-zero temperature and subsequently fall into the same quantum state and act as a single entity. **Andre Mysyrowicz** pointed out the fact that **a BEC could more easily be produced by trapping excitons than hydrogen atoms (52)**. **Excitons** (or an electron-hole pair) are considered synthetic hydrogen atoms and are hence much more stable than hydrogen atoms. Excitons have been produced at **room temperature** and **last for hours** rather than a billionth of a second. Consequently, a BEC would be relatively easy to produce a BEC with the exact

same characteristics that are found in the BECs that we are discussing, concerning the various properties such as tunneling BECs, etc. Size does not matter as a BEC can be as big as a battleship. Excitons are produced in CdS with much supportive evidence derived from physically observed research. **UNITEL**'s research into the various methods to produce a large diameter lens for aerospace applications.

During **UNITEL**'s Director-of-Engineering **Larry Maurer**'s recent visit to UIC Microphysics Lab in Chicago, he discussed the idea of possibly using glass mixed Type II-VI compound crystallites with **Paul Boirus**, Physicist / UIC MP Labs. The question of the existence and availability of RF-transparent glass was asked of Paul and his reply was 'Yes', that **RF-transparent glass was in existence and readily available**. We propose in the design of our crystallite lens to be made of RF-transparent glass with embedded multiple arrayed quantum dots composed of CdS & CdTe, RF-transparent crystallites composed of glass and/or plastics, and "knitting" smaller MBE grown sections together. All of these methods are under consideration. The p-i-n layers will be precisely placed together with the surface of the outermost layer to be MBE grown to ensure chromaticity or coherency (lasing) capability of the light emitted from the beam. This method of construction was suggested to **UNITEL** by **Michael deBruzzii**, of **EMI-MBE** Equipment Manufacturers. The completed individual layered **Red, Green & Blue** crystallite sections will be tuned to interact and respond to the pulsed-chirped shockwaves emitted as traveling RF microwave packets.



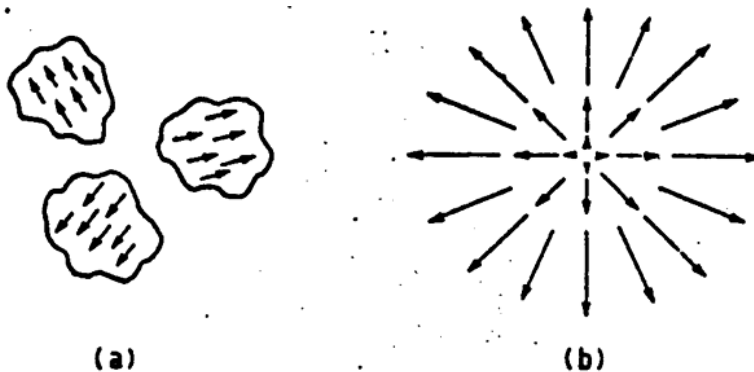
VOLUME OF THE LIGHT-EMITTING REGION of the potential well associated with each peak in the luminescence spectra shown in the illustration on the preceding page confirms the presence of the biexciton gas and the electron-hole liquid. The graphs show that exciton luminescence is emitted from the greatest volume. Because the mass of the biexciton is twice the mass of the exciton, it is predicted that the luminescence from biexciton decay (open circles in color) should be emitted from a region whose diameter is $\sqrt{2}/2$, or about .7, times the diameter of the region associated with exciton decay (open circles in black). The graphs show the data are in accord with the prediction. The volume of the region that emits luminescence characteristic of the electron-hole liquid is even smaller (broken curve), which indicates condensation from the gas to the dense, liquid phase. The data were collected by Gourley and Wolfe.

Figure 65 - Potential Energy Wells in Excitons, Biexcitons, and Electron-Hole liquids
(courtesy *Scientific American*, March'84)

Recent studies of BECs have produced information regarding MACROscopic tunneling and the specific electromagnetic frequencies that maintain quantum coherence so that the system will not decohere into the Macroscopic level. This effect can be compared to quantum computing and **Peter Shor**'s algorithm that keeps the quantum computer from decohering into the macroscopic level.

The **sonic analogue of a gravitational black hole** in dilute-gas Bose-Einstein condensates was investigated by **L. J. Garay** et al (53). It was shown that there exist both dynamically stable and unstable configurations which the BEC in the hydrodynamic limit exhibited a behavior completely analogous to that of gravitational black holes. The dynamical instabilities involve creation of quasi-particle pairs in positive and negative energy states just as in the well-known suggested mechanism for black hole evaporation. They have also simulated the creation of a stable sonic black hole by solving the full **Gross-Pitaevskii** equation numerically for a condensate in which its characteristic parameters are changed adiabatically. This was absolute proof that a sonic black hole could in this way be created experimentally with state-of-the-art or planned technology.

In the application of **synthetic gravity black hole**, ours is much like a **Kerr-Schwartschild black hole** in that it is both rotating and electrically charged. The rotation adds an entire extra degree of freedom or dimension. One can easily visualize the strength of attraction that takes place with that kind of gravitational force contributing to the immense pulling power. **Marek Artur Abramowicz** explains in detail in his paper (54) that the centrifugal forces of a spiraling (rotating charged) black hole are pushing inward rather than outward as **UNITEL**'s Director-of-Research **Michael Miller** described in the Type II Propulsion system in 1983. In the application of synthetic gravity black hole, ours is much like a Kerr-Schwartschild black hole in that it is both rotating and electrically charged (55). The rotation adds an entire extra degree of freedom. The end-point of the projected charged particle beam is charged rotating and will exhibit similar effects by electromagnetically attracting our vehicle to the end point. According to the laws of physics for a string requires at least one end-point must move at the speed-of-light, which the end-point of the **UNITEL** plasma is moving near or at the speed-of-light.



Impressions of (a) Higgs fields in causally separated domains pointing in different internal group directions causing (b) a monopole to be formed where they meet. Note that the value of the Higgs field goes to zero in the center.

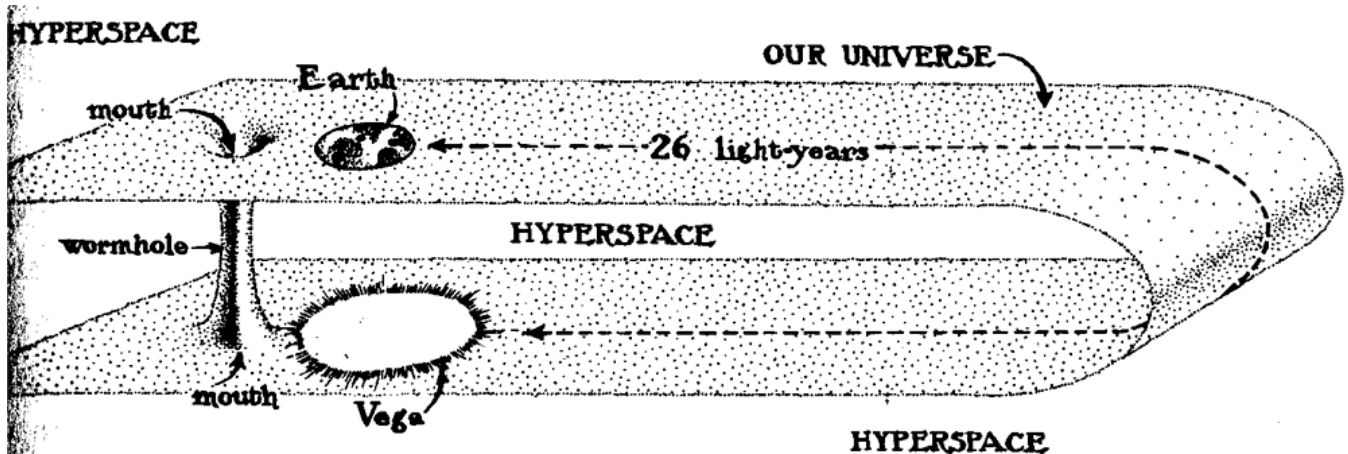
Figure 66 - the above illustration (a) also represents the electromagnetic radiative properties of the primary colors Red, Green & Blue that radiate 90° orthogonal from one another.

It was shown that through a super-radiant Rayleigh scattering, a strong far off resonant pump laser applied to a BEC can induce a non-demolition coupling of the many-mode quantized vacuum field to the

BEC (**56**). This effective interaction will force the total system of the BEC plus the light field to evolve from a factorized initial state to an ideal entangled state and thus result in the quantum decoherence in the BEC. Since the effective coupling coefficients were mainly determined by the **Rabi frequency** of their pump laser, it was proven that the quantum decoherence process could be controlled by adjusting the intensity of the pump laser. To study the physical influence of decoherence of the BEC, the team investigated how the coherent tunneling of BEC in a well-separated tight double wall is suppressed by the effectively-entangled vacuum modes in their test lab.

It was discovered that in sound waves and supernovas in BECs in 1995 the BEC would collectively go from a low-density state to a high-density state, forming molecules which would then release excess heat and cause the BEC to blow apart like a supernova. It's an analogue of the Josephson effect in the study of BECs and coherently propagating matter wavepackets that either repulse -- with holes trapped in the BEC -- or attract. In these experiments de Broglie wave interference patterns were clearly observed.

We have shown the feasibility of our proposed space vehicle and projected field and that **it is one gigantic tunneling BEC that won't decohere**. Production and testing of small prototypes is the next obvious step that is needed before constructing a full-sized working prototype. **UNITEL**, Inc. along with contracted affiliates intends to build a space vehicle whose design is based on **UNITEL**'s patented design that will have the capability to explore the vast reaches of outer space. It is common knowledge that in order to explore the distant regions of the Universe, it would have to be done with a space vehicle that travels faster than the speed-of-light in 4D spacetime or -- in our case -- **tunnel** through the potential barrier composing the distance between the target destination and Earth instead of going the "long way" in 4D spacetime around the barrier. **The ONLY realistic way to travel the vastness of space is to tunnel on a macroscopic level with a vehicle of our type of quantum design.** **UNITEL**'s aerospace vehicle's design is accepted by several accredited individuals in the world's prominent aerospace organizations that believe that tunneling through the potential barrier of the fabric of 4D spacetime in Hyper-Space is the only acceptable method that has the potential of traveling to the nearest solar systems with habitable planets, etc.



4.1 A 1-kilometer-long wormhole through hyperspace linking the Earth to the neighborhood of Vega, 26 light-years away. (Not drawn to scale.)

Figure 67 - a "wormhole" in Hyper-Space

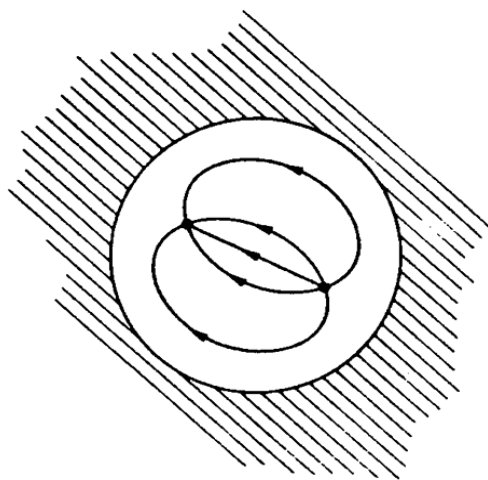
(courtesy Kip Thorne, *Hyperspace*)

The exterior surface charge will protect the diamond layer from deteriorating by oxidation. The whole laminated composition of the exterior charged fuselage can be tuned to produce a large increase in frequency and amplitude for the production of an intense electrical charge. The network of charge junction SDE's work unitarily by computer modulation with the capability to "chirp" (as in RF compression or radar chirping) the entire system in a precise variable pattern by use of a digital delay system attached to the computer modulating system.

The ideal exciter for the ion-acoustic mode in air could be a waveform which rapidly shifts or chirps its frequency (57). The ratio of the **golden section (0.618...)** and the **Fibonacci series** are associated with growth and self-organization by activating a three-dimensional projection of a natural hyperspatial form such as our projected, spiraling, pulsed laser plasma, a certain desired effect may arise. The specific effect that we will produce will be the excitation of the space around the vehicle(s), produced by the helical-rotating laser beam produced and directed directly in front of the ship. The excited space produces the viscoelastic liquid field (rubber elasticity = entropy elasticity) in the surrounding area of the spaceship and generates a constant acceleration.

The projection of a vortex oriented orthogonally to four-dimensional spacetime appears as the logarithmic spiral whose characteristic rate of expansion, or contraction, is in the ratio of the golden mean. This may be why logarithmic imploding vortices in experiments would interact and possibly orthorotate the ZPE flux from an induced hyperspatial resonance. A waveform that rapidly changes in its frequency such that the length between adjacent zero crossings is in the ratio of the golden mean called the "Fibonacci chirp" and may be an activator of a natural hyperspatial resonance.

Excitons are bound electron-hole pairs, analogous to the binding between an electron and a proton in a hydrogen atom. **Uchida** (1967) reported that excitonic peaks appear at room temperature in the PC spectrum of CdS crystals with very high sulfur content (58). Because of the close similarity to hydrogen atoms, excitons have been considered to be "synthetic" hydrogen atoms. Excitons have five times the mobility of hydrogen atoms and last for hours rather than a billionth of a second as hydrogen atoms do. This allows easier production of a Bose-Einstein condensate state in our projected laser plasma. **UNITEL**, Inc.'s variable EM emitter/monochromatic laser lens is modulated to produce biexcitonic gasses within the lens in sufficient amounts. The biexcitonic gases are then scattered by the phonons produced by the incoming RF shockwaves projected from the magnetron within the piezoelectric crystal (59). After lasing occurs, the biexcitonic gases are then trapped in the pulsed laser plasma potential EM wells with leading and trailing-edge dynamics. The 3-part red/green/blue lens will emit a steady stream of spiraling, bead-like, true electromagnetic wavepackets at one ellipse per cycle. The spiraling wavepackets are a mixture of three separately color-charged (+) Red, (0) Green & (-) Blue excitons. The RF microwaves also trapped in the projected wavepackets produce Fresnel-type interference patterns that confine the excitons. The RF microwaves perfectly replace or mimic ferromagnet flux lines, which flow towards the vehicle. The exciton mechanism in a superconductor phonon-mediated electron-electron interaction is replaced by excitons. As in the case of phonons, the excitons cause the electrons to attract, forming bound states known as **Cooper pairs** (60).



A quark and anti-quark pair, each carrying a strong charge, may create a "bubble" within the non-perturbative QCD vacuum (shown shaded). Strong force-field lines may be confined to the interior of the bubble where the vacuum structure is altered.

Figure 68 - a quark-antiquark "bubble"

(78)

The trapped biexcitonic gasses act in the same manner as Cooper pairs. Cooper pairs (or phonons) cannot operate in a vacuum but excitons can. The (semi-) transparency of the laser lens adds conduction to exciton current. The specifically described curve on the “capped cone” fiber bundle technology freestanding, three-part laser lens provides a stress-gradient on the excitons. This forces the excitons to the lens’s surface in a unitary manner and couple to the pulsed lasing/RF shockwaves .

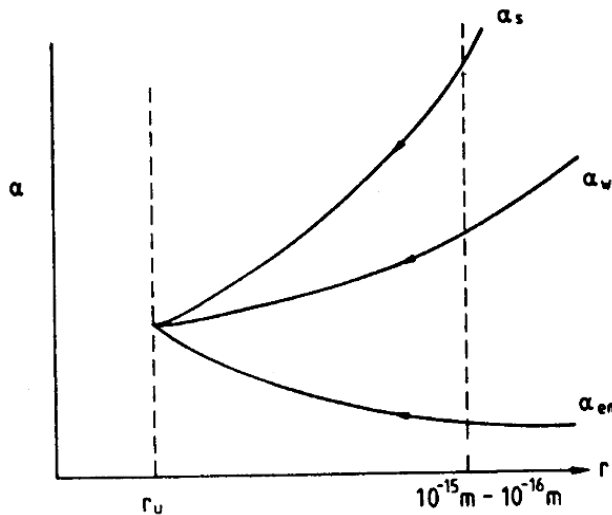


Figure 16. Variation of the strong, weak and electromagnetic fine structure constants with interparticle separation r , showing possible convergence of values at $r = r_\nu$.

Figure 69 - Dependency of "Fine Structure" Constants on inter-particle Separation Distances (78)

In 1993 **Pfeiffer** and his colleagues demonstrated that a quantum-wire laser has an unusual property: it emits photons that arise from the recombination of excitons. In a conventional semiconductor laser or even in a quantum-well laser on the other hand, the densely-packed excitons interact and disrupt the relatively weak pairing between electron and hole. The resulting electron-hole plasma still generates photons but from the mutual annihilation of free electrons and free holes, rather than from the recombination of electrons and holes already paired together in excitons.”

Adiabatic approximation: (also called molecular approximation) is generally applied to slow collisions. It is based on the physical assumption that the collision process evolves sufficiently slowly in time that the electrons are able not only to adjust continuously to the changing internuclear separation, but also to take energy from, and give energy to, the kinetic energy of nuclear motion. In this way, the electronic motion acts as a potential for the nuclear motion, which supplements the repulsive internuclear coulombic potential. The adiabatic electronic state is defined as the eigenfunction of the electronic Hamiltonian '**H**':

$$H \ 5\Sigma_1 (\underline{p_i^2} \ 2\underline{z_{ij}} \ \underline{e^2} \ 2\underline{z_{je}} \ 1 \ \Sigma_e^2) \angle \mathbf{m}_e \ r_{jp} \ r_{it} \ r_{ji} \ r_{ij}$$

where ' r_{ij} ' and ' r_h ' are the respective distances of the i-th electron to projectile and target nuclei, and ' \mathbf{m}_e ' is the electronic mass. '**H**' includes the kinetic of each electron along with its potential energy of attraction to both nuclei and, finally, the inter-electron repulsive term between each pair of electrons.

8 - Lamb Shift

Starting from the late 1940s, **Willis E. Lamb** and his colleagues carried out a series of experiments in which the fine structure was studied by radio-frequency spectroscopic of the transitions $2S\frac{1}{2}$, $2P\frac{1}{2}$, $2P\frac{3}{2}$. He confirmed that the fine structure of the $2P$ state is accurately given by the Dirac theory, and in fact used his measurements to obtain a more precise value for ' a' . A more dramatic finding for which Lamb received the Nobel Prize was that $2S\frac{1}{2}$ and $2P\frac{1}{2}$ levels for $n = 2$ are not, in fact, degenerate (61). The $2S\frac{1}{2}$ state was found to be shifted upward by 1060 MHz. The displacement -- known as the Lamb shift -- is dominantly due to radiative coupling of the electron with the vacuum field.

The discovery of the Lamb shift played a central role in the development of **Quantum ElectroDynamics (QED)**. Experiments and calculations on the fine structure and the Lamb shift in hydrogen have undergone continuing refinement. Experiment and theory have been pushed to an accuracy of about 11 kHz (or 1 part in 10^5) are in good agreement. The term fine structure is used in somewhat different context with respect to molecular spectra. There it refers to the rotational structure of an electric or vibrational molecular band.

The term is descriptive because the structure only becomes apparent when the spectrum is observed with moderate resolution. Molecular structure can also exhibit hyperfine structure arising from nuclear-electronic interactions. Although magnetic dipole interactions tend to be most important for free atoms, molecular hyperfine structure is often dominated by the electric quadrupole interaction.

9 - Polarized Beam

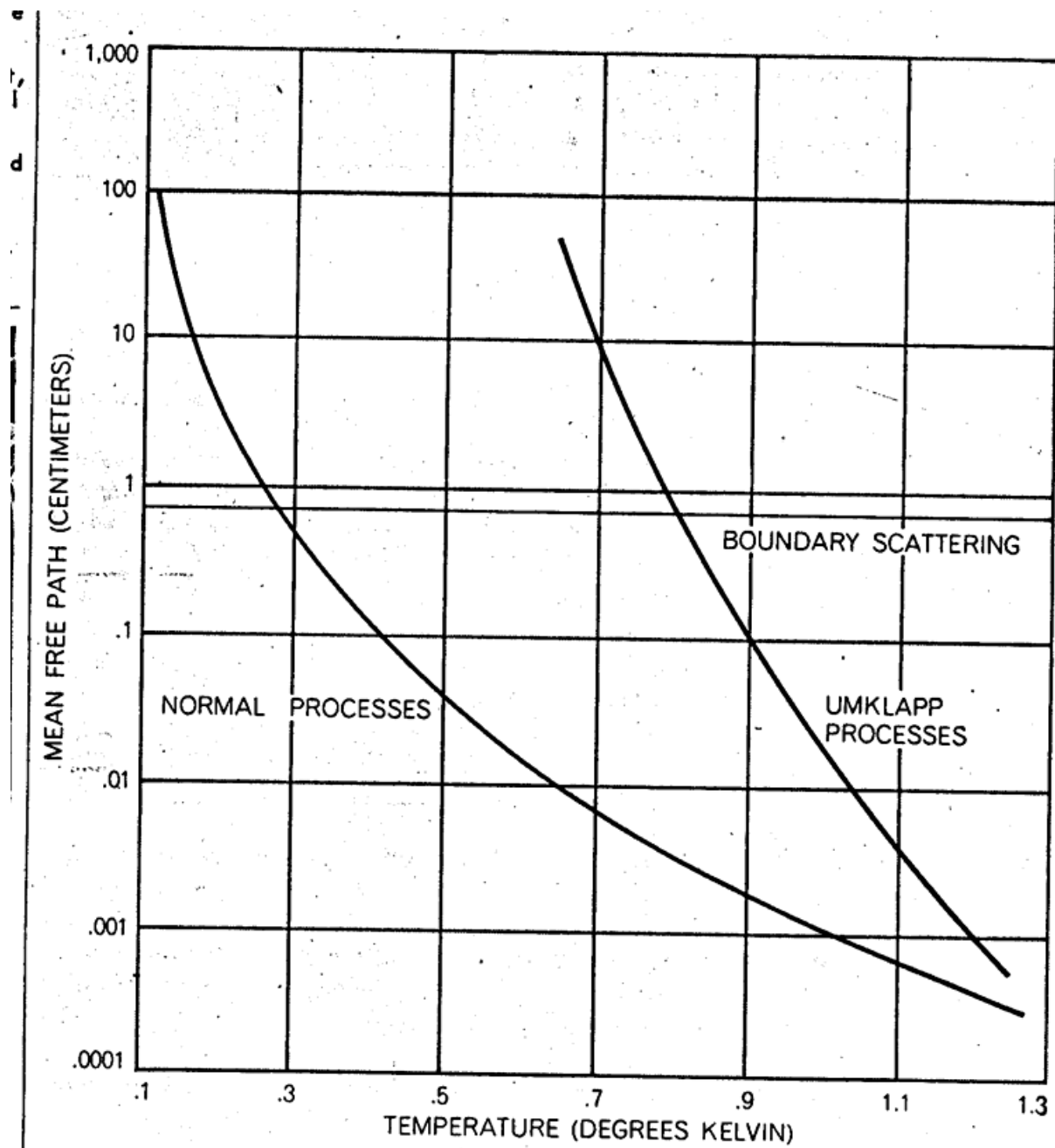
The **paraboloidal-curved AASL lens** provides a stress-energy gradient (62) producing a change in energy of the excitons per unit distance created in the crystallite Type II-VI compound lens. It is also a motive force on the excitons as is the applied periodic alternation in electric potential (63). The trapped excitons assume the role of hydrogen atoms and have **five times** the mobility and a lifetime of **hours** rather than a billionth-of-a-second. The projected potential electromagnetic wells are, therefore, ponderomotive phase-spaces of extremely dense hydrogenic nuclear structure with a vacuum expectation charge value.

The pressure exerted as tension on the crystallite lens by the acoustic wavepacket forces the excitons to attach to the shock-wave that slows down the lasing photons (leading-edge wave) so that (64) charge/vibrational transference of information goes from the quasi-level -- or phase-space oriented oscillating gas of polarized excitons -- to the coherent photon wave (65). The curved AASL lens effectively takes on the role of a hadron face (66).

The projected, pulsed, true “white light” charged particle beam automatically rotates to produce the helically wound plasma, with a beaded structure that is patterned after a microscopic “string”. The beaded electromagnetic wavepackets (67) will assume the character of a light string that can be described as “beads on a chain”. The projected potential electromagnetic wells in the beam are modulated in a computer-coded manner to produce left-handed Larmor precession, mimicking the rotation of frustrated overlapping wave sections of closed Wilson-loop plaquettes (68) in a hadron string.

High frequency harmonics create electro-optical effects such as the magneto-optical Faraday polarized states of photons (three-part overlapping integrity pattern); clocking controls the Larmor precession in odd-numbered precessing “frustrations” (half-twists). These half-twists (69) connect electric (three-parts) and magnetic (three-parts) fields through the six-tensor GVP shape of the projected potential electromagnetic wells. The wells are electromagnetic wavepackets with smoothly varying sides that are a 3D mirrored shape of the vehicle.

Color-mixing the **Red**, **Green** & **Blue** beams to form the white light source and an increase in current flow of heat by wave propagation (discussed later along with “second sound”) of the microwave current trapped in the electromagnetic potential wells forces flux-bundles to grow in energy until the flux-bundles begin to jump (*i.e.* the vehicle moves or commutes up the projected string) over pinched or pinning barriers (70). This process is known as **flux-jumping** and the mixing of colors (RGB) excites or enhances this effect.



CONDITIONS FOR SECOND SOUND in solid helium at a density of .205 gram per cubic centimeter can be obtained from this plot of the phonon mean free path versus the temperature for various types of phonon-scattering processes. At this density solid helium has a hexagonally close-packed crystal structure; the curves shown in the graph refer to a single crystal approximately five millimeters in diameter. Boundary scattering and umklapp scattering are called thermally resistive processes; normal scattering is a nonresistive process. The conditions for second sound (normal mean free path much greater than resistive mean free path) are satisfied for this particular sample between about .4 and .9 degree K.

Figure 70 - Phonon-Scattering Processes in Solid Helium (courtesy *Scientific American*, May'70 (82))

We will control the frequency dependency of the friction force using Landau-Zener transitions for **fast** and **slow acceleration**. Non-linear dependence of the friction force on the velocity results in significant physical consequences that are due to the formation of local non-equilibrium (GVP shape) structure caused by bunching of particles. The friction force is a function of velocity. If an atom is moving along the field gradient for a long time, the dissipative forces caused by the friction force essentially influence the kinetics of the motion. In the case of deceleration, the distribution function of the electric field becomes stationary. This will allow a **hover mode** of our vehicle. A characteristic of particle velocity undergoes strong modulations caused by the gradient force. The deceleration (or acceleration) occurs because of the hysteresis effect in the gradient force. The friction force is therefore a product of the gradient force (71). A better name for the molecular friction is the **hysteresis effect**.

The polarized diamagnetic biexcitonic gas is trapped in the charged pulsed coherent white light plasma. The biexcitonic gas becomes very dense when confined in the projected, pulsed, spiraling electromagnetic potential wells in the beam due to momentum.

The first polarization experiments were carried out with polarized beams produced in nuclear reactions or by nuclear scattering. Much larger intensities and better control over the beam polarization have become available by the development of polarized ion sources. One scheme that is in use employs a beam of neutral, polarized atoms, produced by substrate separation in an inhomogeneous magnetic field or by optical pumping methods. The polarization of the atomic electrons is then transferred to the nucleus by use of the hyperfine interaction. Subsequent ionization (both negative and positive ions are available) prepares the beam for injection into an accelerator. In this manner, polarized beams of protons, deuterons, ${}^3\text{He}$, ${}^6\text{Li}$, ${}^7\text{Li}$, and ${}^{23}\text{Na}$ have been prepared.

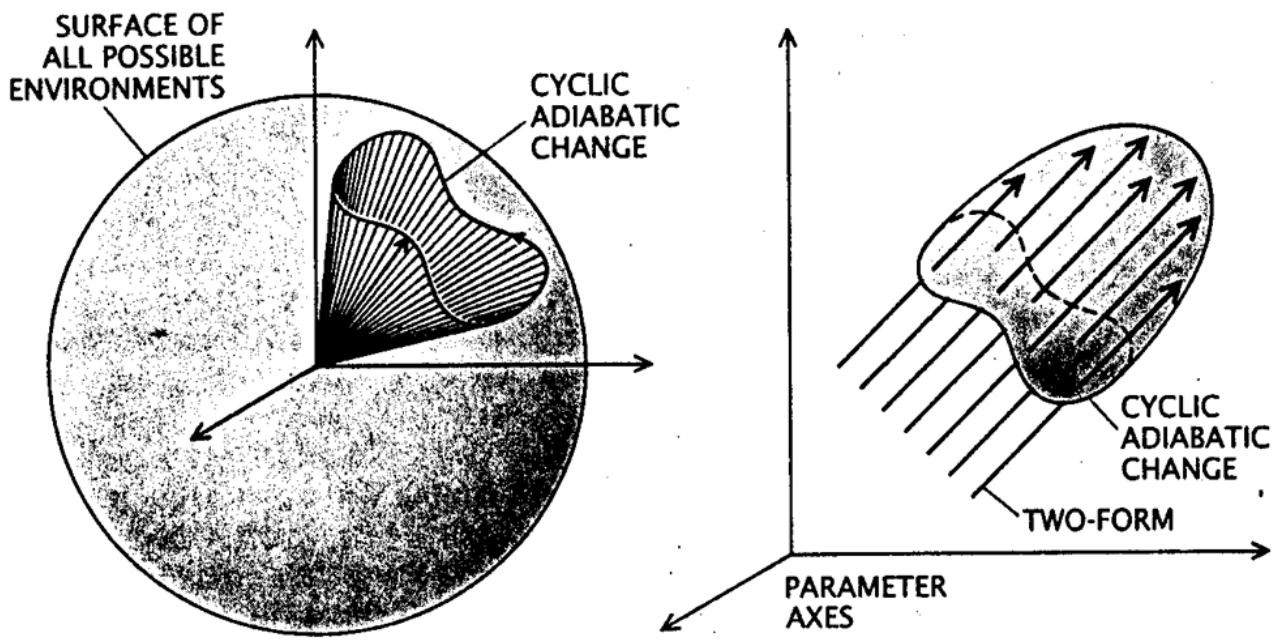
Another scheme that has been applied to produce polarized protons and deuterons uses hydrogen atoms in the metastable $2s$ state ("Lamb shift" polarized ion source).

This seemingly small difference in physics leads to a major difference in the way that the lasers radiate. As the intensity of an ordinary semiconductor laser is increased (say, by boosting the current), the energy of the photon emissions from a free-electron-hole plasma is reduced (72). This phenomenon -- called **band-gap renormalization** -- causes the laser's emission frequency to shift downward, which could inhibit the performance if the laser is being used for spectroscopy or to transmit information. In the intense confinement of a wire or dot, on the other hand, the excitons do not fragment; so the frequency remains stable when input current -- and therefore output power -- is increased.

At low temperatures excitons are less able to penetrate the narrower, higher-energy parts of the wire; thus, these narrow areas become *de facto* barriers along the wire. They wall off sections of the wire creating a string of dots. In addition to this fixed magnetic backdrop, **NMR** procedures also utilize varying electromagnetic fields. By applying an oscillating field of just the right frequency (determined by the magnitude of the fixed field and the intrinsic properties of the particle involved), certain spins can be made to flip between states. This feature allows the nuclear spins to be redirected at will.

For instance, protons (hydrogen nuclei) placed within a fixed magnetic field of 10-Tesla can be induced to change direction by a magnetic field that oscillates at about 400 megahertz -- that is, at radio frequencies. While turned on, usually only for a few millionths of a second, such radio waves will rotate the nuclear spins about the direction of the oscillating field which is typically arranged to lie at right angles to the fixed field. If the oscillating radio-frequency pulse lasts just long enough to rotate the spins by 180 degrees, the excess of magnetic nuclei previously aligned in parallel with the fixed field will now point in the opposite,

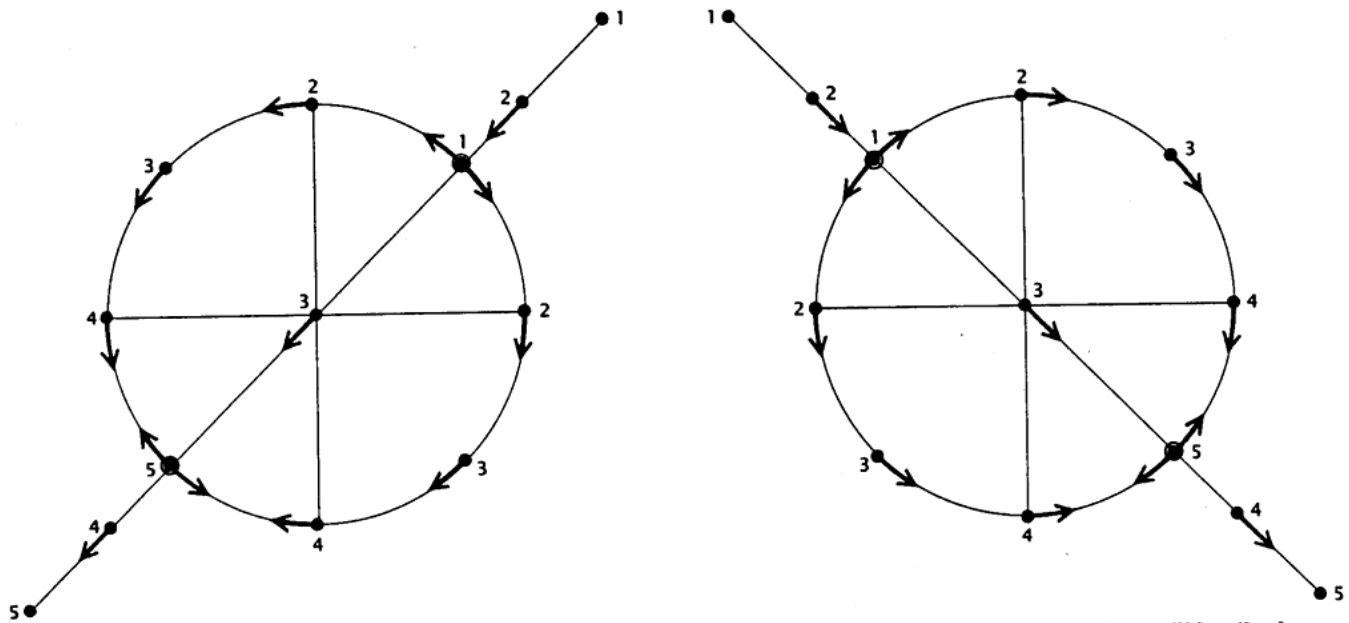
anti-parallel direction. A pulse of half that duration would leave the particles with an equal probability of being aligned parallel or anti-parallel.



GEOMETRIC PHASE of a quantum system whose environment has undergone a cyclic adiabatic change can be derived by plotting all possible environments of the system in a frame of reference whose axes are parameters: the physical variables that describe the environment. A cyclic adiabatic change is then represented as a closed curve in the "parameter space". In the simplest case the geometric phase is given in terms of the area of any surface the curve encloses. If the surface is spherical (*left*), the area is equivalent to the solid angle subtended by the curve. The geometric phase can be more readily generalized to parameter spaces with more than three dimensions if it is expressed in terms of a mathematical quantity called a "two-form" (*right*). A two-form can be thought of as representing the flux -- or flow -- of a quantity through space. The geometric phase can then be calculated by integrating (or summing) the two-form over any surface that "catches" all the two-form flux through the circuit.

Figure 71 - Adiabatic Changes in Quantum Systems

(courtesy *Scientific American, Dec'88*)



SUPERPOSITION of two oppositely directed circular motions can result in linear motion. Summing the coordinates of the red and the blue points, which are tracing concentric circles of equal radius, yields the coordinates of a third point (green) that slides back and forth along a line. The direction of the line depends on the relative phases of the two circling points. If the two points start their motions in the upper right-hand quad-

rant of the coordinate system (left), the line will be tilted at an angle of 45 degrees. If they start in the upper left-hand quadrant (right), however, the angle will be 135 degrees. A similar principle explains how two superposed states of circularly polarized light rotating in opposite senses can result in linearly polarized light. As with the moving points, the relative phases of the states determine the light's direction of polarization.

Figure 72 - Changing Circularly-Polarized Light into Linearly-Polarized
(courtesy *Scientific American*, Dec'88)

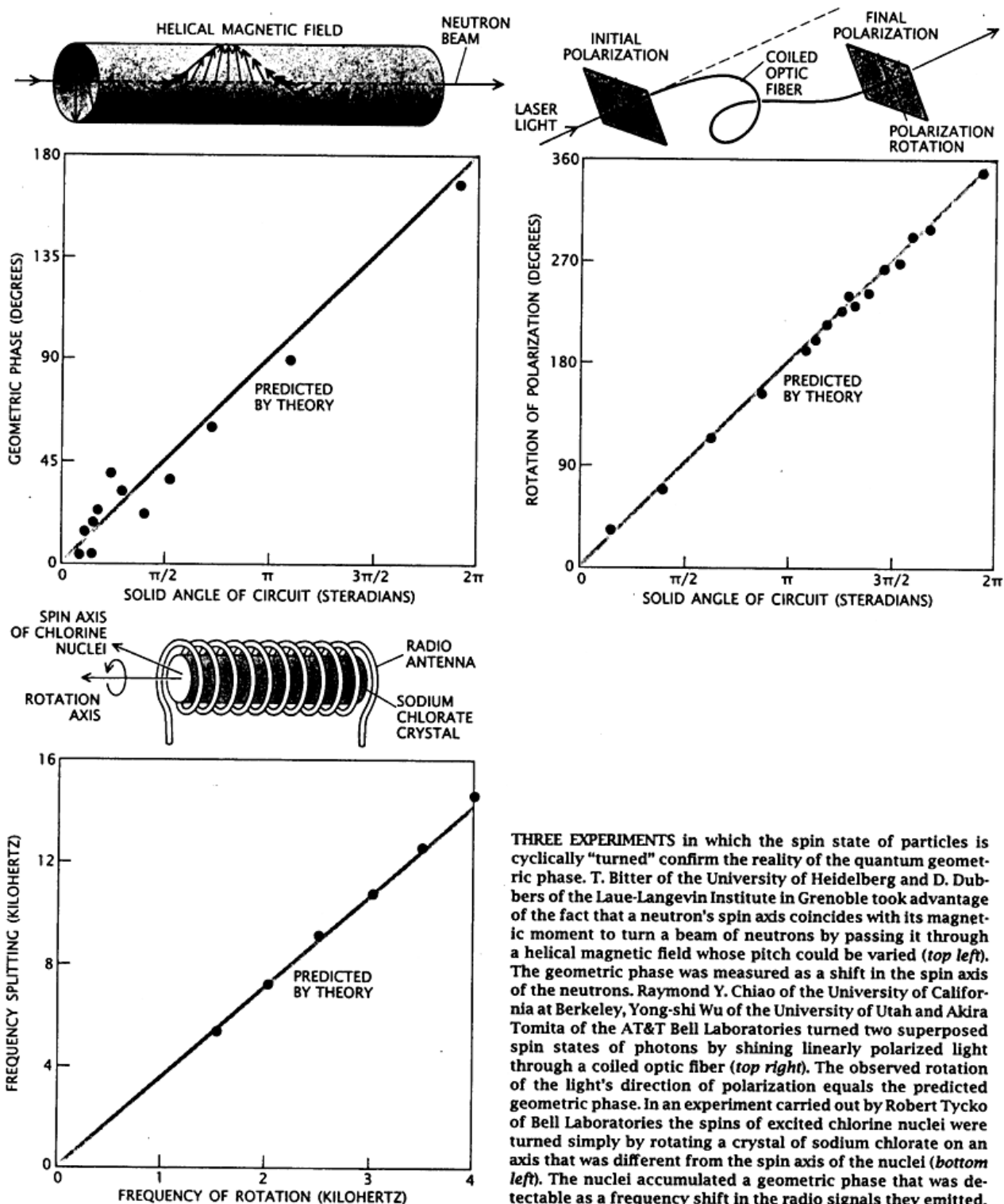
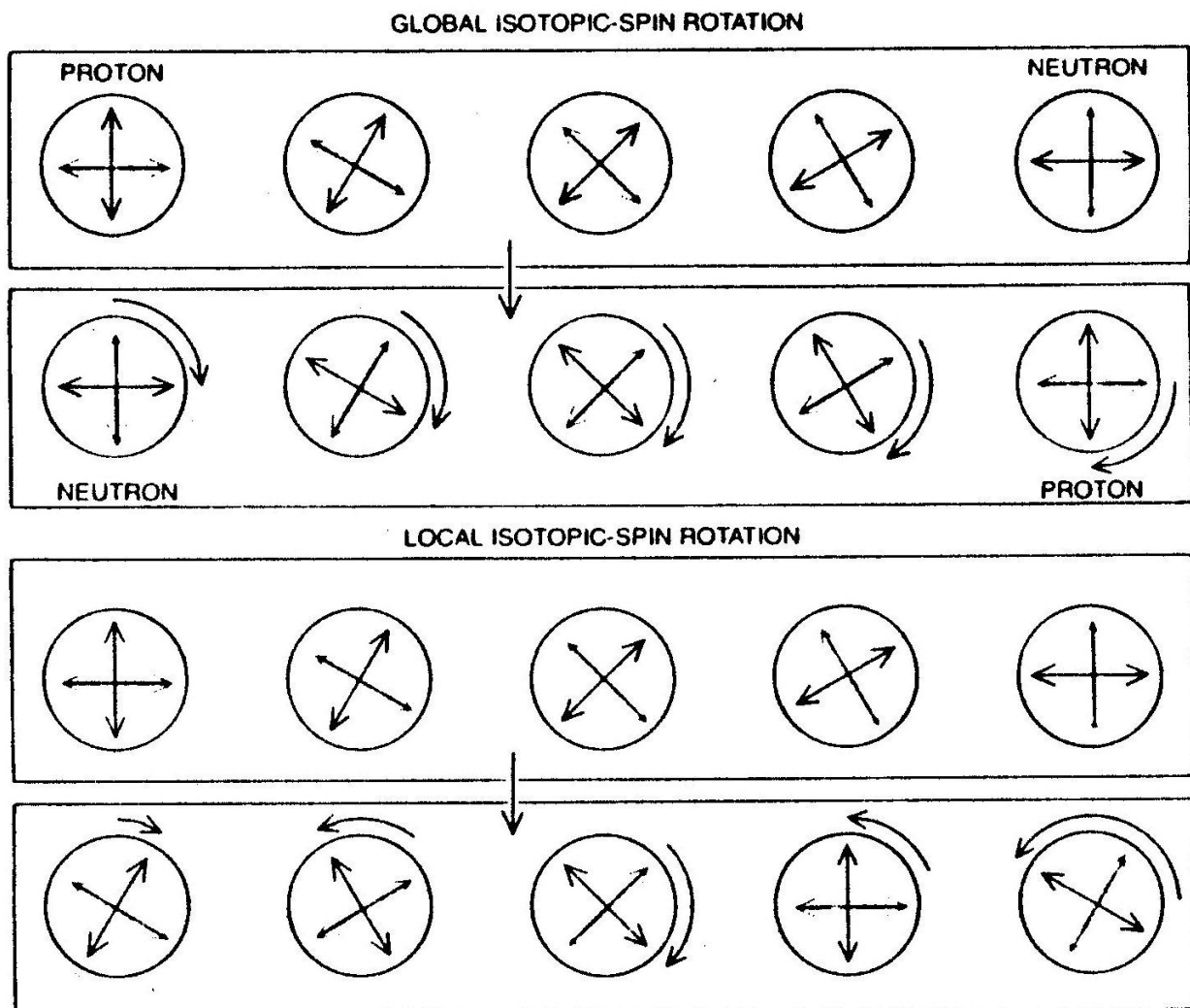
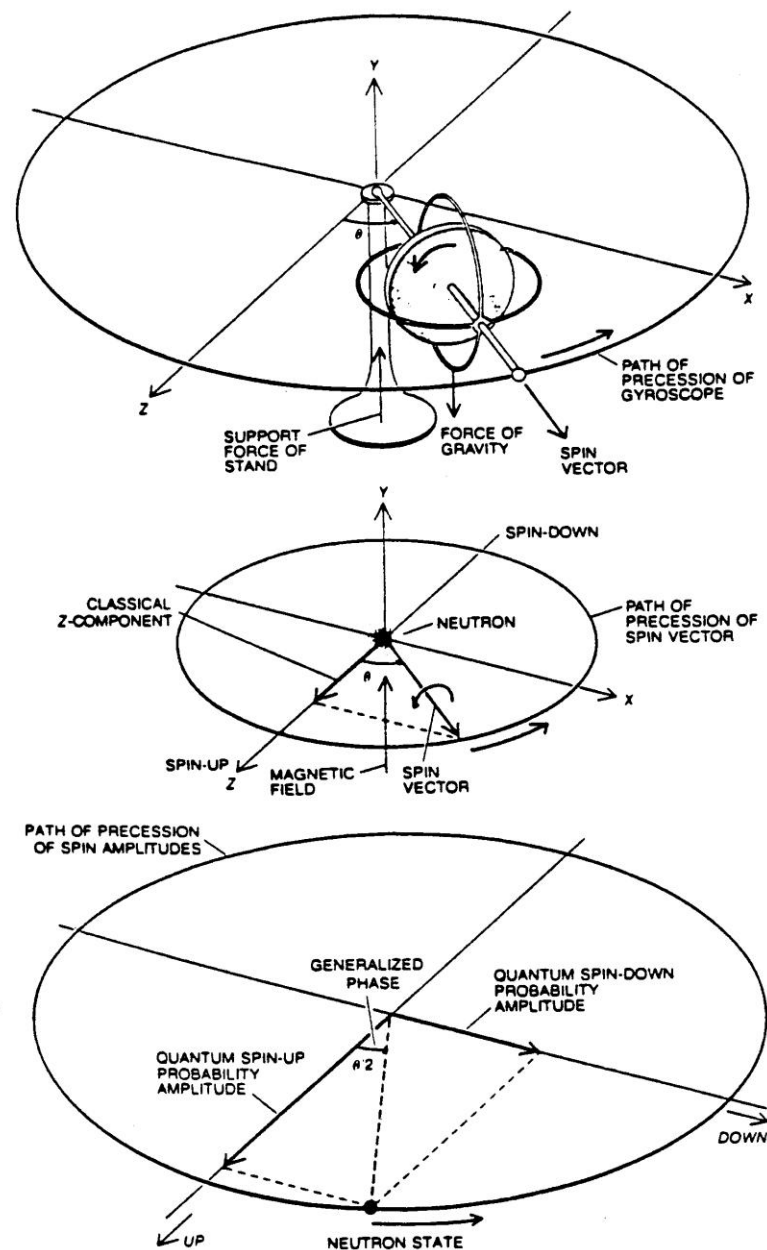


Figure 73 - the Quantum Geometric Phase (courtesy *Scientific American*, Dec'88)



ISOTOPIC-SPIN SYMMETRY serves as the basis of another gauge theory, first discussed in 1954 by C.N. Yang and Robert L. Mills. If isotopic-spin symmetry is valid, the choice of which position of the internal arrow indicates a proton and which a neutron is entirely a matter of convention. Global symmetry (*upper diagram*) requires the same convention to be adopted everywhere, and any rotation of the arrow must be made in the same way at every point. In the Yang-Mills theory, isotopic spin is made a local symmetry (*lower diagram*) so that the orientation of the arrow is allowed to vary from place-to-place. In order to preserve the invariance of all observable quantities with respect to such local isotopic-spin transformations, it is necessary to introduce at least 6 fields corresponding to 3 mass-less vector particles (or vector bosons). One of these particles can be identified as the photon. The other two carry electric charge. The theory has been influential but it was unrealistic in its original form. It makes protons and neutrons indistinguishable and predicts mass-less charged particles that do not exist.

Figure 74 - Isotopic-Spin Symmetry in another Gauge theory
(courtesy Scientific American, June'80 (66))



PRECESSION OF THE SPIN VECTOR of a neutron in a magnetic field resembles the precession of a gyroscope in a gravitational field. The magnetic torque on the spinning neutron causes it to precess at a rate proportional to the strength of the field and independent of the orientation of the neutron. If the initial direction of the neutron's spin vector is called "up", and if the field is perpendicular to it, precession through an angle of 180 degrees will make the spin vector point down. At intermediate angles classical physics predicts that the component of the spin vector measured along the z-axis is equal to the perpendicular projection of the vector on to the axis. In quantum mechanics the component of the spin measured along any axis can have one of only two values: $+1/2$ or $-1/2$ Planck's constant \hbar . What changes during precession is the probability of detecting a neutron in the spin-up state ($+\hbar/2$) or the spin-down state ($-\hbar/2$). Each probability is determined by squaring a probability amplitude whose value can be either positive or negative. Hence the quantum-mechanical precession of a neutron can be graphed as a rotation of the neutron state in an abstract space whose coordinate axes are the probability amplitudes of the spin-up and spin-down states of the spin vector.

Figure 75 - a Neutron's Spin Vector in a Magnetic Field (courtesy Scientific American, July'81 (47))

In this fashion we can control the strength of magnetization by manipulating the alignment of all particles, along with feathering the signal to slow the attraction down for instant response of the vehicle to projected field interactions.

A **spin packet** is a group of spins experiencing the same magnetic field strength. In this example, the spins within each grid section represent a spin packet. In the uplifting spiraling pathway of parallel transport (73) mechanism in the projected plasma, the spins of the three separate biexcitonic gasses (from the individual **Red**, **Green** & **Blue** sections) are automatically aligned in one direction. Nuclear magnetic resonance operates on quantum particles in the atomic nuclei within the molecules of the fluid. Particles with "spin" act like tiny bar magnets and will line up with an externally applied magnetic field. Two alternative alignments (parallel or anti-parallel to the external field) correspond to two quantum states with different energies. One might suppose that the parallel spin corresponds to the number **1** and the anti-parallel spin to the number **0**. The parallel spin has lower energy than the anti-parallel spin by an amount that depends on the strength of the externally applied magnetic field.

At any instant in time, the magnetic field due to the spins in each spin packet can be represented by a magnetization vector. The size of each vector is proportional to ($N_+ - N_-$). The vector sum of the magnetization vectors from all of the spin packets is the net magnetization. In order to describe pulsed NMR, it is necessary from here on to talk in terms of the net magnetization (74). Adapting the conventional NMR coordinate system, the external magnetic field and the net magnetization vector at equilibrium are both along the Z-axis.

At equilibrium, the net magnetization vector lies along the direction of the applied magnetic field \mathbf{B}_0 and is called the equilibrium magnetization \mathbf{M}_0 . In this configuration, the **Z** component of magnetization \mathbf{M}_Z equals \mathbf{M}_0 . \mathbf{M}_Z is referred to as the longitudinal magnetization. It is possible to change the net magnetization by exposing the nuclear spin system to energy of a frequency equal to the energy difference between the spin states (75). If enough energy is put into the system, it is possible to saturate the spin system and make $\mathbf{M}_Z = \mathbf{0}$.

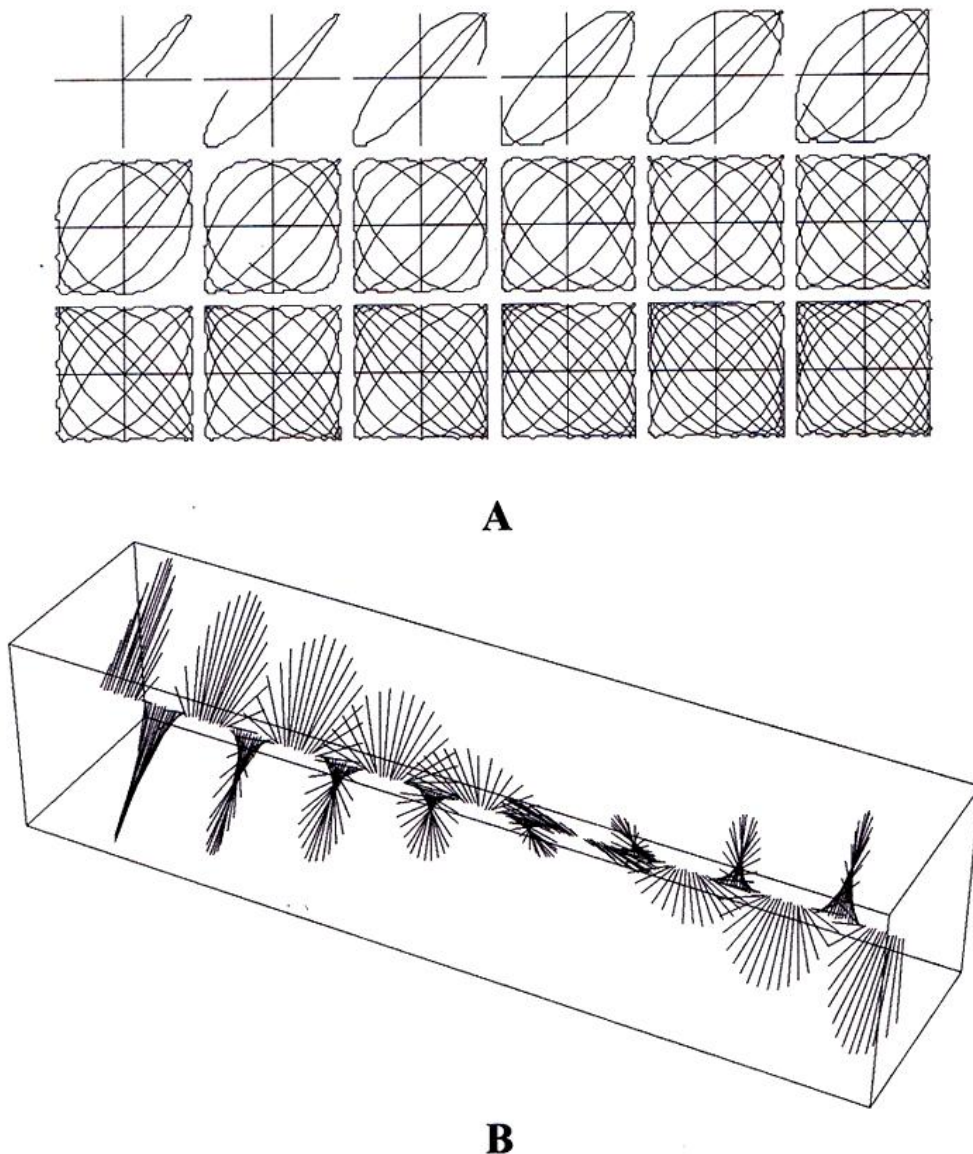
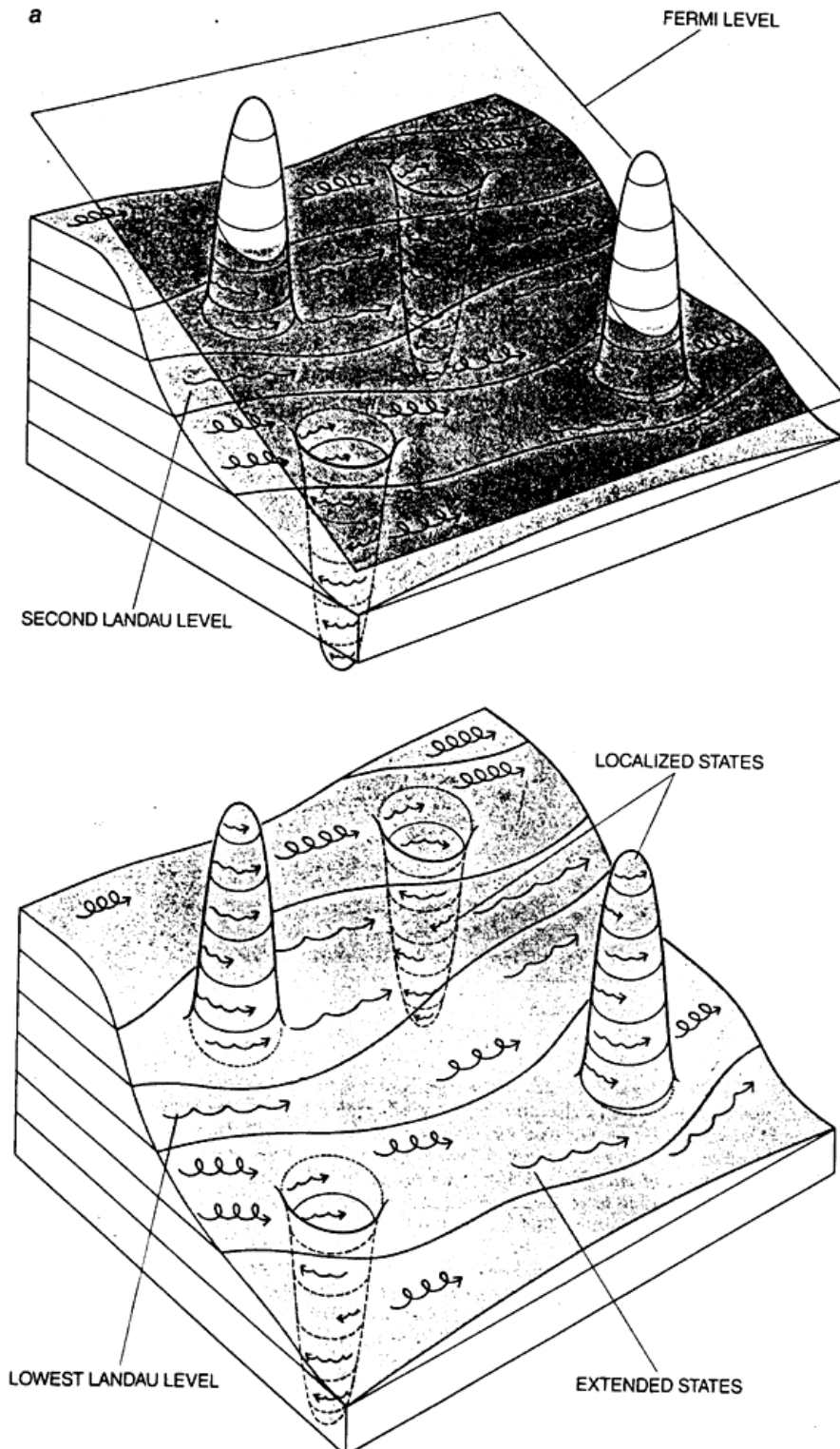


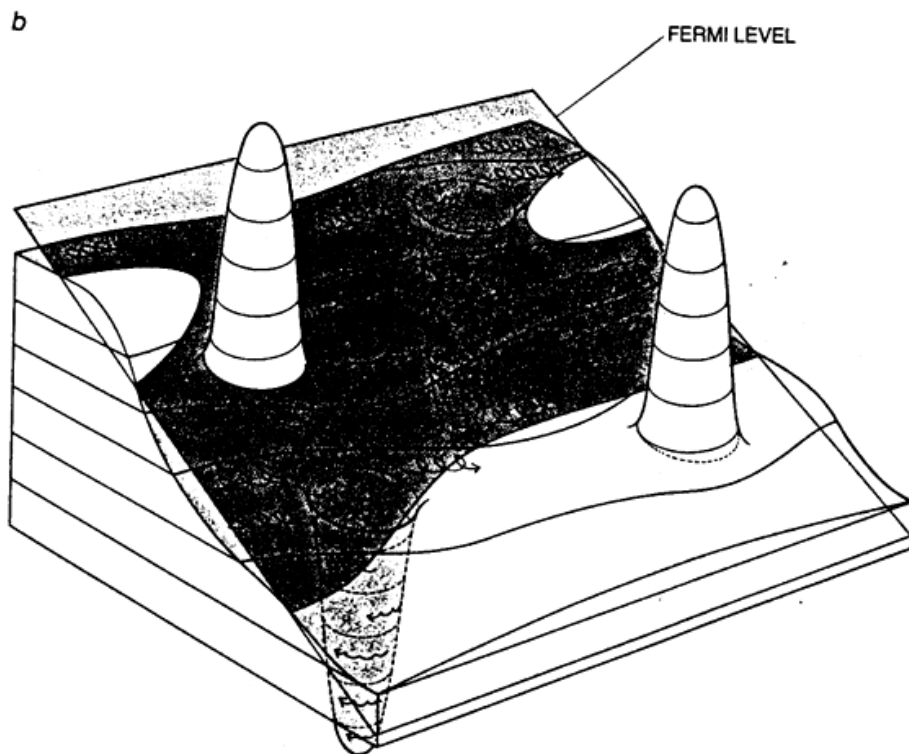
Fig 4.9 A Lissajous patterns representing the polarized electric field over time, viewed in the plane of incidence, resulting from the two orthogonal s and p fields, which are out of phase by the following degrees: 0, 21, 42, 64, 85, 106, 127, 148, 169 (top row); 191, 212, 233, 254, 275, 296, 319, 339, 360 (bottom row). In these Lissajous patterns, the plane polarizations are represented at 45 degrees to the axes. B: representation of a polarization modulated beam over 2π in the z -direction. These are $SO(3)$ $Q^i(\omega, \delta)$ in C representations over 2π , not an $SU(2)$ $Q_i(\psi, \chi)$ in C^* over π .

Figure 76 - the electric field produced by Orthogonal 's' and 'p' fields
(courtesy Terence W. Barrett)



GEOMETRIC REPRESENTATION of the energy of electrons confined to a two-dimensional layer in a strong magnetic field illustrates the difference between localized and extended states and explains the quantized Hall effect. The vertical axis represents the energy, within a small section of a sample, of electrons in two Landau bands. Peaks and valleys in the electric potential are due to impurities spaced randomly within the sample. Electrons move in cycloidal paths parallel to contour lines (lines of constant electric potential); hence closed contours around peaks and valleys indicate localized states, in which electrons orbit within a small region of space, and open contours indicate extended states, which may stretch from one end of the sample to the other. At low temperatures electron states whose energy lies below the local Fermi level (*colored plane*) are filled (shad-

Figure 77(A) - Electrons confined to a 2-dimensional layer in a strong Magnetic Field -- Part 1
(courtesy Scientific American,)



(ed region) and others are empty. The surfaces of electron energy and the local Fermi level are tilted from the horizontal because of a voltage difference (the Hall voltage) between the two edges of the sample. When the Fermi level is in a region of localized states (a), the quantized Hall effect occurs; the Hall resistance (the Hall voltage divided by the current flow) is not affected by small changes in such parameters as the strength of the magnetic field or the number of electrons in the layer. For example, a small change in the Fermi level would not change the Hall resistance because it would not affect electrons in the extended, current-carrying states. When the Fermi level is in a region of extended states (b), on the other hand, a small change in its height does indeed affect the current flow by emptying or filling some of the extended states, and the quantized Hall effect does not occur.

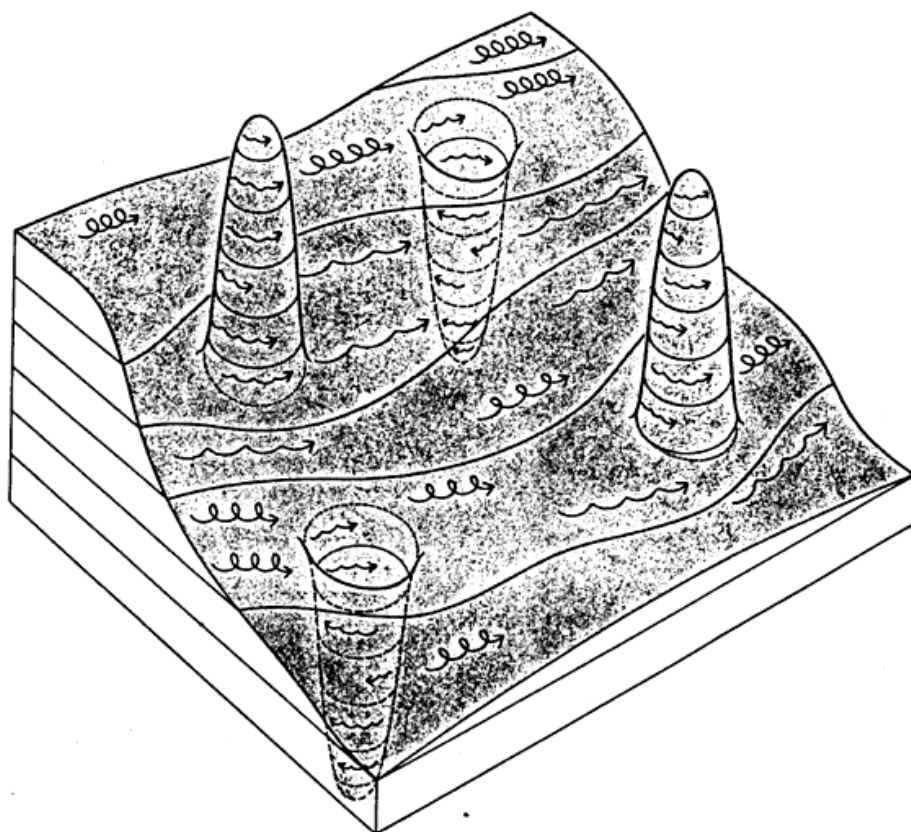


Figure 77(B) - Electrons confined to a 2-dimensional layer in a strong Magnetic Field -- Part 2

The time constant which describes how M_Z returns to its equilibrium value is called the spin lattice relaxation time (T_1). The equation governing this behavior as a function of the time t after its displacement is:

$$M_Z = M_0 [1 - e^{-t/T_1}]$$

T_1 is therefore defined as the time required to change the Z -component of magnetization by a factor of e .

If the net magnetization is placed along the $-Z$ axis, it will gradually return to its equilibrium position along the $+Z$ axis at a rate governed by T_1 . The equation governing this behavior as a function of the time t after its displacement is:

$$M_Z = M_0 [1 - 2e^{-t/T_1}]$$

The spin-lattice relaxation time (T_1) is the time to reduce the difference between the longitudinal magnetization (M_Z) and its equilibrium value by a factor of 'e'. A BEC can be produced with an excitonic gas trapped in a potential electromagnetic well that is produced in our pulsed laser plasma (Free Electron Laser pulsing technique) (76). The biexcitonic gasses or individual excitons are produced in CdS via the mechanical stress modulation from the RF shockwaves from the magnetron.

The cross-section of the proposed paraboloidically-curved free-standing RF-activated laser lens shown depicts the "stress-gradient" that forces the excitons to couple to the RF (shock) wavepackets that are then trapped in the potential electromagnetic wells in the pulsed projected laser plasma. The curve is the stress gradient for excitons to couple to external electromagnetic wave then trapped in the projected, pulsed potential electromagnetic wells in the beam (77).

UNTEL intends to build a spaceship of this design to explore the vast reaches of outer space with the capability of performing Macroscopic quantum tunneling (78). This is the ONLY way that is realistic and has the potential of traveling to the nearest planets, etc.

If the net magnetization is placed in the XY-plane it will rotate about the Z-axis at a frequency equal to the frequency of the photon that would cause a transition between the two energy levels of the spin. This frequency is called the Larmor frequency.

In addition to the rotation, the net magnetization starts to de-phase because each of the spin packets making it up is experiencing a slightly different magnetic field and rotates at its own Larmor frequency. The longer the elapsed time, the greater the phase difference. Here the net magnetization vector is initially along $+Y$. For this and all de-phasing examples think of this vector as the overlap of several thinner vectors from the individual spin packets. The time constant which describes the return to equilibrium of the transverse magnetization M_{XY} is called the spin-spin relaxation time, T_2 .

$$M_{XY} = (M_{XY0}) e^{-t/T_2}$$

T₂ is always less than or equal to **T₁**. The net magnetization in the **XY** plane goes to zero and then the longitudinal magnetization grows in until we have **M₀** along **Z**. Any transverse magnetization behaves the same way. The transverse component rotates about the direction of applied magnetization and de-phases. **T₁** governs the rate of recovery of the longitudinal magnetization.

In summary, the spin-spin relaxation time **T'** is the time to reduce the transverse magnetization by a factor of e. In the previous sequence, **T₂** and **T₁** processes are shown separately for clarity. That is, the magnetization vectors are shown filling the **XY**-plane completely before growing back up along the **Z**-axis. Actually, both processes occur simultaneously with the only restriction being that **T₂** is less than or equal to **T₁**.

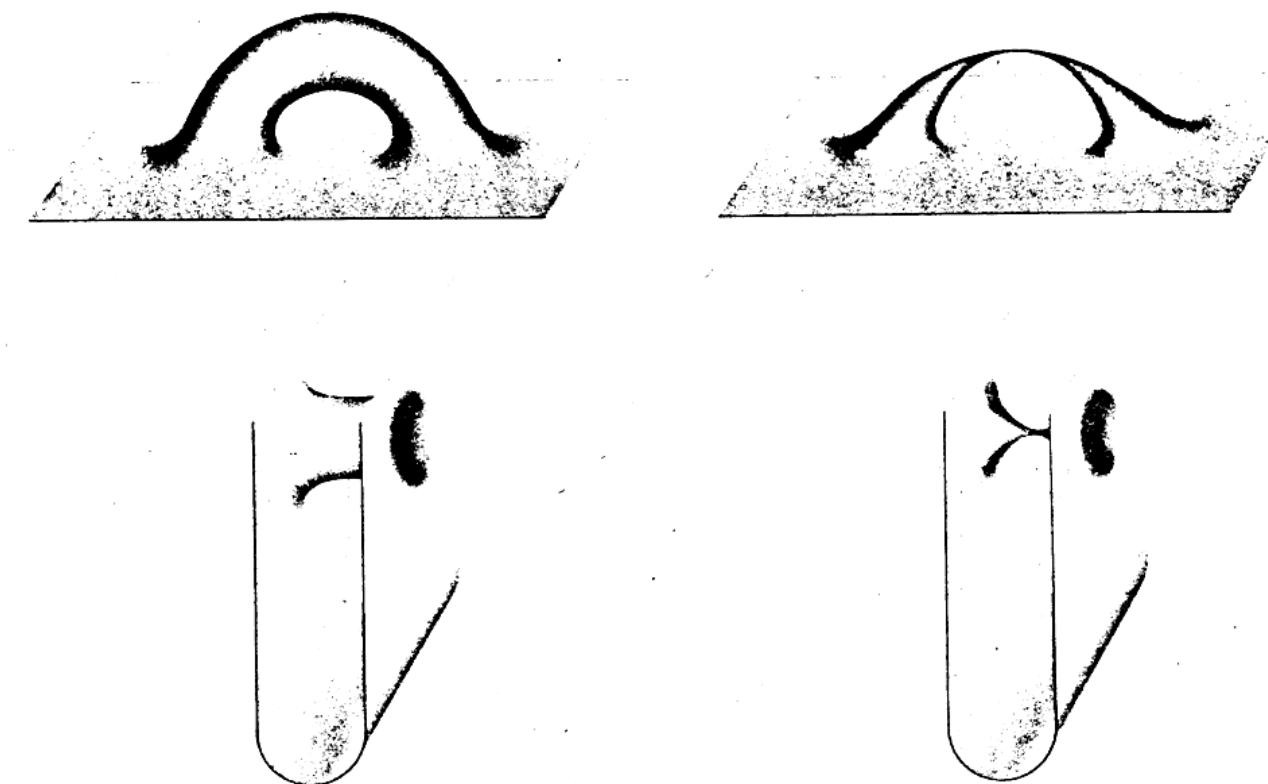
Two factors contribute to the decay of transverse magnetization:

- 1). molecular interactions (said to lead to a pure **T₂** molecular effect)
- 2). variations in **B₀** (said to lead to an inhomogeneous **T₂** effect)

The combination of these two factors is what actually results in the decay of transverse magnetization. The combined time constant is called **T₂-star** and is given the symbol **T₂***.

10 - Macroscopic Quantum Tunneling

Our aerospace propulsion system features two modes of transportation. **(1) Electromagnetic Laser Propulsion** will be used for short-range travel while **(2) Macroscopic Quantum Tunneling** will allow us to travel throughout the Universe. This design is the only realistic and feasible method of traversing the vast distances of the Universe to regions that would be unattainable using conventional technology or even a propulsion system capable of traveling at the speed-of-light. Even at light speed it would take a hundred years to even get to the closest star. All of the designs such as the "Light Sail" that include hibernation and long-term living systems are unfeasible.

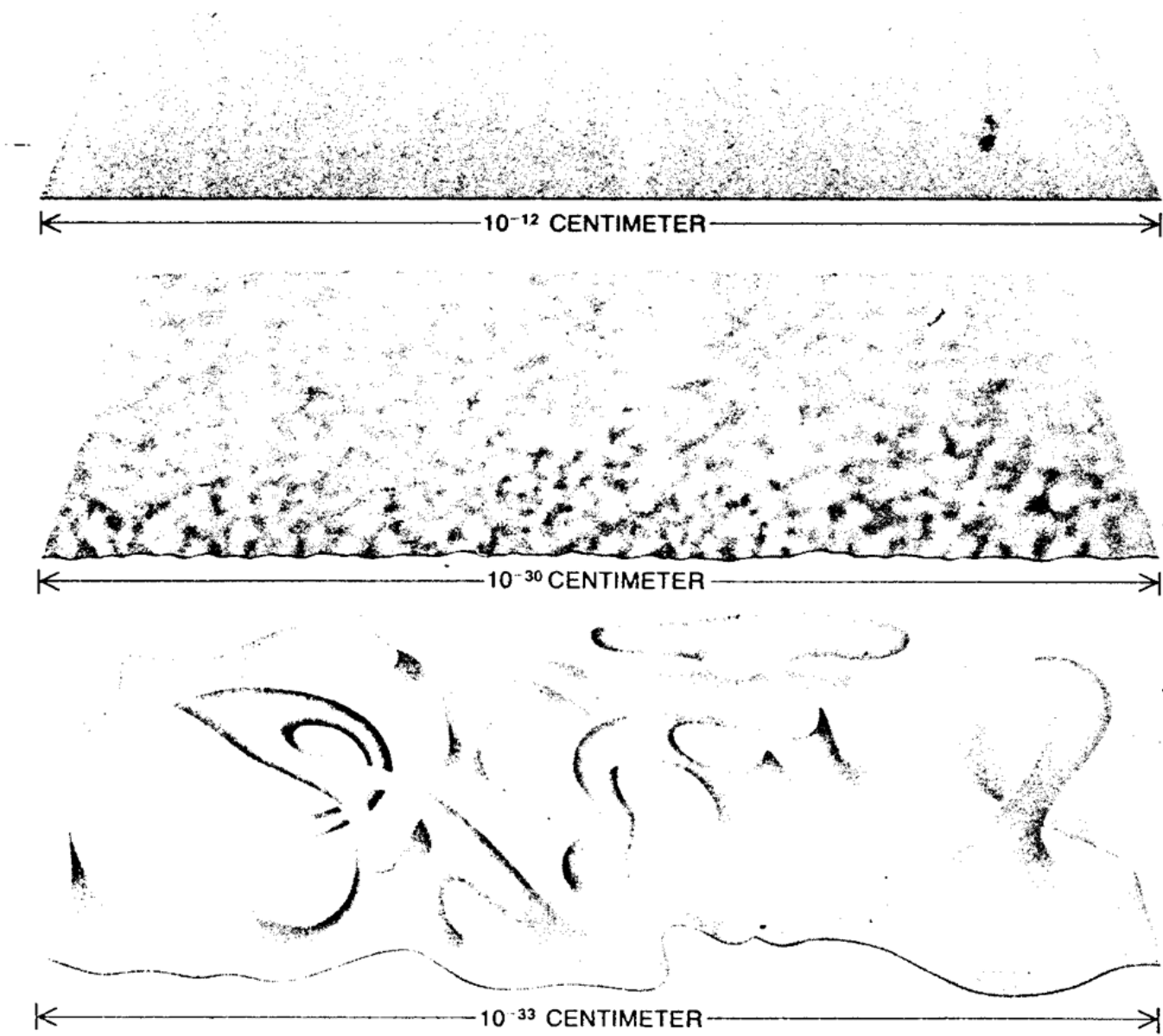


DISTANT REGIONS OF THE UNIVERSE could in principle be connected by a wormhole, suggesting that faster-than-light communications might be established. Actually the scheme cannot work. In the drawing of a wormhole (upper left), the distance between the holes in the "outside world" is comparable to the distance through the "throat". In the wormhole at the (lower left), the outside distance is much greater. In the lower drawings the space represented by the plane appears to be bent. But that is only because it is viewed from the perspective of a higher-dimensional space; it would appear approximately flat to an observer living in the plane. Whether -or-not the "throat" is a shortcut, it is not possible to pass through it. The reason is that a wormhole invariably connects two black holes. The throat "pinches off" (as is shown at the right), and anything that enters it is crushed to infinite density before reaching the other side.

Figure 78 - FTL using a "Wormhole" (courtesy *Scientific American*, Dec'83 (88))

The MOSS vehicle (or group of vehicles that assume the role of an atomic bound state) will take advantage of the wave/particle relationship on a Macroscopic scale and tunnel through the fabric of 4D spacetime as it is found throughout the universe and emerge unscathed at the destination point or chosen

location in spacetime in a very short period of time. During tunneling while inside the barrier, a particle -- or in this case our ship -- can be considered to be traveling at the speed-of-light.



QUANTUM VACUUM, as envisioned by John Archibald Wheeler in 1957, becomes increasingly chaotic as one inspects smaller regions of space. At the scale of the atomic nucleus (*top*) space looks very smooth. At dimensions of 10^{-30} centimeter (*middle*) a certain roughness in the geometry begins to appear. At the scale of the Planck length, 1,000 times smaller still (*bottom*), the curvature and the topology of space are continually undergoing violent fluctuations.

Figure 79 - John Wheeler's depiction of Quantum Vacuum Fluctuations
(courtesy Scientific American, Dec'83 (88))

While inside the barrier (Hyper-Space), its kinetic energy would be negative. Velocity would then be proportional to the square root of a negative number. Hence, it is impossible to ascribe a "real velocity" to the particle (or ship) while tunneling inside the barrier. According to theory, an increase in the width of a

barrier does not lengthen the time needed by the particle or wavepacket to tunnel through it (79). It is not hard for one to visualize that for a starship tunneling through the barrier of outer space, one will arrive at a distant solar system much faster than one would by going across the vastness of outer space by any other conventional means (even if they were traveling at the speed-of-light). So in this fashion we say that our vehicle appears to have a **superluminal** capability or faster-than-light drive. By this statement, however, we do not want to be misunderstood as implying we are disobeying the Law of Special Relativity. We freely acknowledge that one cannot travel faster than the velocity of light in Real-Space. Our traditional 3D concept of "speed" is all-but-eliminated in Hyper-Space.



DIMENSIONALITY OF SPACE is put into question by the possibility that spacetime has a complex topology. The surface shown is two-dimensional, but its topological connections give it the appearance of a three-dimensional object. It is conceivable that three-dimensional space perceived at a macroscopic scale actually has fewer dimensions but is topologically convoluted.

Figure 80 - Topology of Space (courtesy *Scientific American*, Dec'83 (88))

In the book "**Hyperspace**" by **Michio Kaku** [Oxford University Press (1994), pg. 227], the author explains how the fictional starship "Enterprise" would tunnel through the fabric of outer space to get to the distant star Alpha Centauri from planet Earth: *"Imagine sitting on a rug and lassoing a table several feet away. If we are strong enough and the floor is slick enough, we can pull the lasso until the carpet begins to fold underneath us. If we pull hard enough, the table comes to us and the distance between the table and us disappears in a mass of crumpled carpeting. Then we simply hop across this carpet warp. In other words, we hardly moved; the space between us and the table has contracted, and we just step across the contracted distance."* Dr. Kaku's simple description is a good example of UNITEL's space vehicle tunneling through the potential barrier of outerspace.

The Special Relativity Law states that the velocity of light is the maximum velocity of all, which is true for 4D spacetime or Real-Space. UNITEL proposes with their space propulsion system that interstellar travel could be performed in a matter of **a few days** with the Hyper-Space MQT mechanism employed whereby the method of plunging into Hyper-Space is realized. The UNITEL's Type VI MOSS Vehicle requires the three-part laser lens to produce specific quantum effects in order to be used for propulsion. MOSS pertains to a system that is observable on a large-scale, yet bound to the same quantum laws as a subatomic particle. The fact that atoms or particles can exist on a Macroscopic scale was recently proven with the creation of a Bose-Einstein condensate, a proven MOSS system. UNITEL's Type VI vehicle is itself a MOSS system. The physical space in which we live in -- 4D spacetime -- is described by **Yoshinari Minami** in 1993 (80) as three-dimensional (3D) space ($x=x^1$, $y=x^2$, $z=x^3$) plus the time ($w=ct=x^0$), where c is the velocity-of-light. [The four coordinates are denoted as x^i ($i=0,1,2,3$).]

Quantum tunneling is an effect whereby an object passes through the barrier by its wave function. Forming a fine-grained structure as a many-particle system implies a matter wave. We need the technology to form a fine-grained structure and the solution of the spaceship wave function. We produce the fine-grained structure by our interactive composite wave structure via the acoustic surface wave (Rayleigh-Stoney) and projected three-part field plasma. On a subatomic level quantum mechanics describes the light string that is part of a quantum particle system -- such as an electron-positron or electron-hole pair -- where only one endpoint is required by quantum law to be moving at the speed-of-light (81).

Heat can flow without resistance through the RF-transparent & activated crystallite lens as a wave (82). The combined energy of the RF lens activating shock wave packets traversing the AASL lens is the same as the combined energy of the wave packets afterward. Similarly the combined momentum is the same after traversing the lens. Heat flow by wave propagation through the lens and up the RF-confined and driven superfluidic plasma with parallel transport does not lose energy or momentum and is carried almost instantaneously to the other end of the projected "string" (83). This behavior of heat flow by wave propagation is characteristic of thermal waves, which were originally called "second sound" waves that are analogous to first sound, or acoustic waves. The projected and pulsed shock-wave packets produce a gas of phonons that transport thermal energy by diffusion throughout the interior of the crystallite AASL laser lens. Second sound is propagated in the gas of phonons in the AASL lens (84) and the laser lens provides the mean free path or direction of flow of kinetic energy, like water running down a hill.

The projected plasma of the laser assumes the role of a Macroscopic light string. Our vehicle will traverse the light string (85) like a particle such as an electron or photon. This can be considered electromagnetic propulsion because we utilize a quantum mechanical function intrinsic to monopole, in order to generate a strong magnetic attraction. There has been a great deal of controversy concerning the monopole effects that we say is an integral part of the design of our vehicle. The controversy mainly concerns the fact that a monopole itself has never been physically observed. Dr.'s **Raymond Chiao** and

Akira Tomita, however, were able to measure quantum **monopole**-like effects in an experiment in 1986 (86). They were able to physically apply these effects to optical fibers & RF waveguides. It is our contention that we want to apply these same monopole effects to our spiraling laser field.

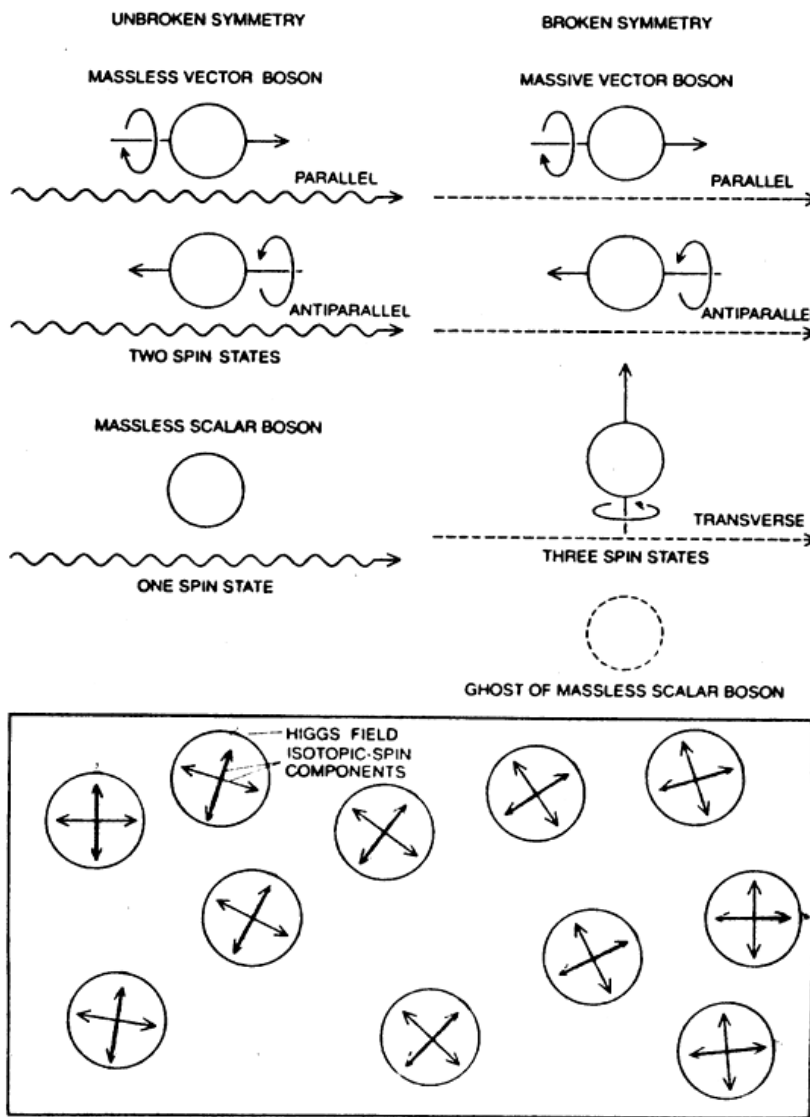
For traveling vast distances, that are normally unattainable with conventional technology, such as from Earth to the nearest solar system, our ship will tunnel elastically, meaning that the tunneling object will emerge on the other side of the barrier virtually unscathed. Tunneling is a commonplace phenomenon at sub-nuclear levels and occurs in semiconductors, nuclear fusion, and the tunneling electron microscope. According to the WKB approximation the tunneling probability on the Macroscopic level is zero. **It is UNITEL's contention that the WKB Approximation does NOT apply to our system.**

Let us now suppose that space is an infinite continuum (87) that can be considered to be a potential barrier. This assumption enables us to apply a continuum mechanics to the so-called "vacuum" of space. This means that space can be considered as a kind of transparent elastic field. From the continuum mechanics, the quantity of strain gives the deformation of space and the quantity of curvature gives the deformation of curved space. A Minkowski graph bears curves that represent the positions of objects in space as a function of time; the curves are called "World Lines". Spacetime -- instead of being a featureless arena for physics -- is itself endowed with physical properties. The relation between the amount of matter and the degree of curvature is simple in principle but complicated to calculate. Twenty functions of the coordinates of a point in spacetime are needed to describe the curvature at that point. Ten of the functions correspond to a part of the curvature that propagates freely in the form of gravitational wave (or "ripples of curvature"). The other ten functions are determined by the distribution of mass, energy, momentum and internal stresses in the matter as well as by Newton's gravitational constant **G** (88).

The entire mass of the Earth induces a spacetime curvature that is about a billionth the curvature of the earth's surface. At the exteriorly charged surface of our vehicle's hull, an electromagnetic wave that is emitted is converted into photons with a thermal energy spectrum (or in other words, into black-body radiation characteristic of a certain temperature). The ground-state fluctuations of the harmonic oscillators give the vacuum field a residual energy or the zero point energy. Curvature influences the spatial distribution of the quantum field fluctuations and -- like acceleration -- can induce a non-zero vacuum energy. Because the curvature can vary from place-to-place, the vacuum energy can also vary, being 'positive' in some places and 'negative' in others. Spacetime resists bending, so energy is required to force it to bend. Particle production -- which directly relates to our goal of fooling Mother Nature into thinking our ship is a quantum particle system -- is maximized where the curvature of spacetime is greatest and changing most rapidly.

Dr. Raymond Y. Chiao has proven that the particle wavepacket has a dramatic effect on tunneling technology. The **General Vector Potential (GVP)** or capped-cone shape of our vehicle interacts with the projected laser field with quantum effects on a Macroscopic scale. The "conclusive evidence given for faster-than-light transmission of smoothly varying functions such as that of a particle wave packet" means that it is indeed possible for an object to have a velocity greater than that of light" (89) [see http://lal.cs.bry.edu/ketav/issue_3.2/Lumin/lumin.html]. This directly relates to the topological shape possibly having a stabilizing effect on the tunneling object, thereby obtaining the same results in lieu of having to produce massive and destructive amounts of energy. The GVP shape for electricity and magnetism is the shape for all particles. This exterior charged vehicle produces the smoothly varying functions and is exactly that of a particle wave packet. In other words, the charge surrounding the vehicle is the same as the particle wave packet that Dr. Chiao describes in his article. Hence, our specifically shaped vehicle, -- as described in our patent with 10 claims -- whereby this physical shape represents the GVP for all particles and its projected string-like plasma produces a specific collection of quantum harmonic

oscillators in the form of overlapping fermions that are impressed on the fabric of 4D spacetime. The result will be the same: spacetime becomes the quantum object on a Macroscopic level. Our vehicle will be able to interact in the visible spectrum at Planckian levels as one gigantic free-particle with the mathematical identity of 137, and commutes up the projected laser plasma string (90).

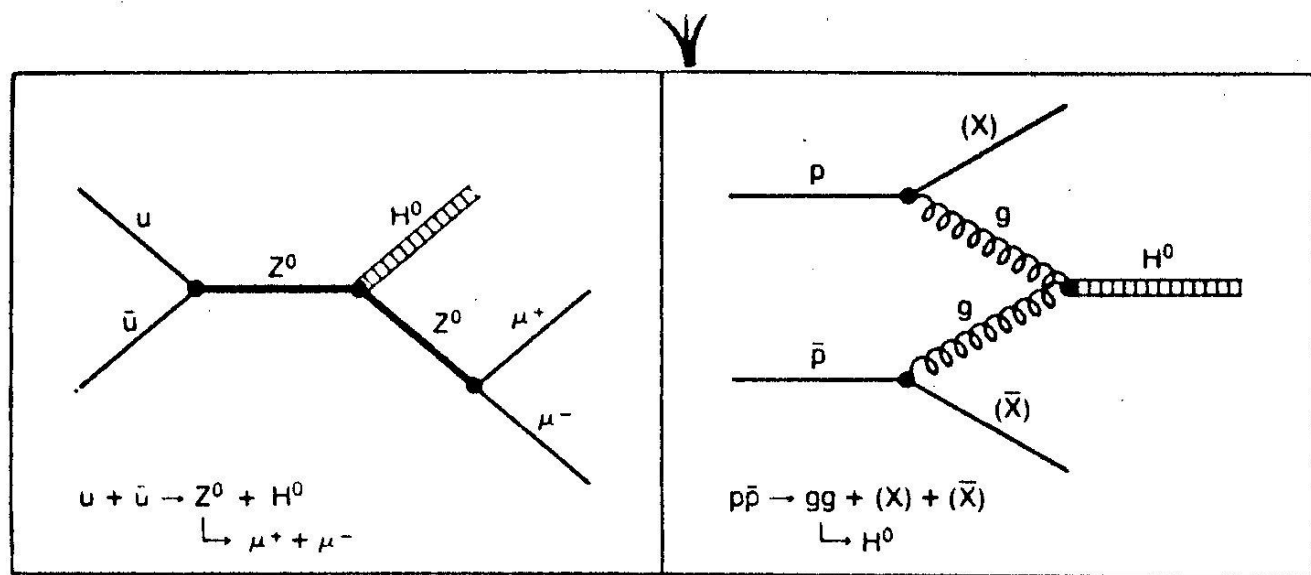


HIGGS MECHANISM can lend mass to the photonlike vector bosons of the Yang-Mills theory.

HIGGS MECHANISM can lend mass to the photon-like vector bosons of the Yang-Mills theory, thereby making the theory making realistic. The mass-less bosons have three3 possible spin orientations (parallel, anti-parallel, and transverse to the direction of motion), but only two of these are observable. The transverse state does not exist, a peculiarity of all mass-less particles which move with the speed-of-light. If the Yang-Mills particles were to acquire a mass, the transverse state would become observable; and this added mode of motion must have some source. In the Higgs mechanism, the source is an extra scalar field corresponding to a mass-less spin-zero boson. The Yang-Mills particle is said to "eat" the Higgs boson, which thereupon becomes an unobservable "ghost". The Higgs field also provides a frame of reference (gray arrows) in which protons can be distinguished from neutrons. The arrow of the Higgs field rotates along with the other arrows in a guage transformation, and so there is no absolute orientation but the relative orientation of the isotopic-spin arrows can be measured with respect to the Higgs arrow. The symmetry of the theory -- which without the Higgs mechanism would have abolished all differences between the proton and neutron -- has not been lost but only hidden.

Figure 81 - Broken & UnBroken Symmetry of the Boson (courtesy *Scientific American*, Dec'03 (66))

The geometrical structure of the Universe is extremely sensitive to the value of the vacuum energy density. So important is this value that a mathematical constant, proportional to the vacuum energy has been defined. It is called the **cosmological constant**: $8\pi G / x c^4$, x = **vacuum energy density** (91). The only way to establish an absolute measure of energy is by using gravity. In General Relativity, energy (and mass) is the source of gravitational fields in the same way that electric charge is the source of electric fields in the Maxwell theory of electromagnetism. An energy density of any kind -- including that produced by fluctuations in the vacuum -- generates a gravitational field that reveals itself as a change in the geometry of spacetime. The production of a Higgs' field should have a particularly dramatic effect on the energy density of the vacuum state (92).



HIGGS BOSON might also make its first appearance in the colliding-beam experiments at CERN or Fermilab. The discovery of this massive, uncharged particle (designated H^0) is considered the ultimate test of the "standard" unified theory linking electromagnetic interactions and weak interactions. Two processes that might lead to the production of Higgs bosons are illustrated. At the left a Higgs boson is created in association with a neutral intermediate vector boson. At the right a Higgs boson arises from the fusion of two gluons emitted during a grazing collision between a proton and an antiproton. (Gluons are the intermediary particles of the strong force that is thought to hold the quarks together inside the particles of the nucleus.)

Figure 82 - the Higgs Boson

(courtesy *Scientific American*, Dec'80 (66))

Concept of Space

As eloquently described by **Yoshinari Minami** in 1993 (80), "space" can be considered as a kind of transparent elastic field. From the continuum mechanics, the quantity of **strain** gives the deformation of space and the quantity of **curvature** gives the deformation of curved space. The properties of space in general are characterized by the distance between two infinitesimally near points in space. The square of the infinitesimal distance ds between two infinitely proximate points x^i and $x^i + dx^i$ is given by the equation of the form:

$$ds^2 = g_{ij} dx^i dx^j \quad (1)$$

where \mathbf{g}_{ij} is a metric tensor. The metric tensor \mathbf{g}_{ij} determines all the geometric properties of space. Although the metric tensor is a function of a space coordinate in Riemannian space, the metric tensor is constant in flat space. The metric tensor of flat space (*i.e.*, Minkowski space) is labeled as the well-known “**Minkowski metric**”.

An external physical action, such as the existence of a mass or electromagnetic energy, yields the structural deformation of space. The degree of geometrical and structural deformation of space can be expressed by the quantity denoting the change of the metric tensor, *i.e.* $(\mathbf{g}_{ij}' - \mathbf{g}_{ij})$. From the above concept, the following equation can be obtained:

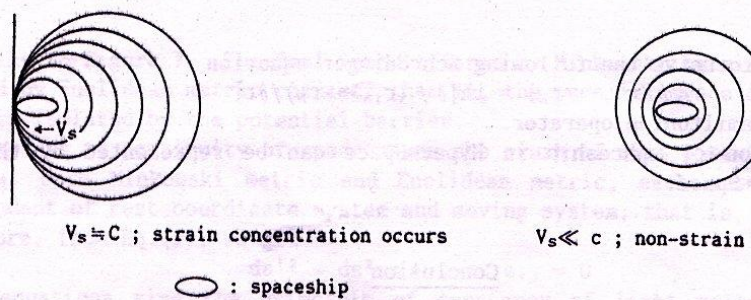
$$ds'^2 - ds^2 = (\mathbf{g}_{ij}' - \mathbf{g}_{ij}) dx^i dx^j = 2e_{ij} dx^i dx^j \quad (2)$$

where e_{ij} is a strain tensor.

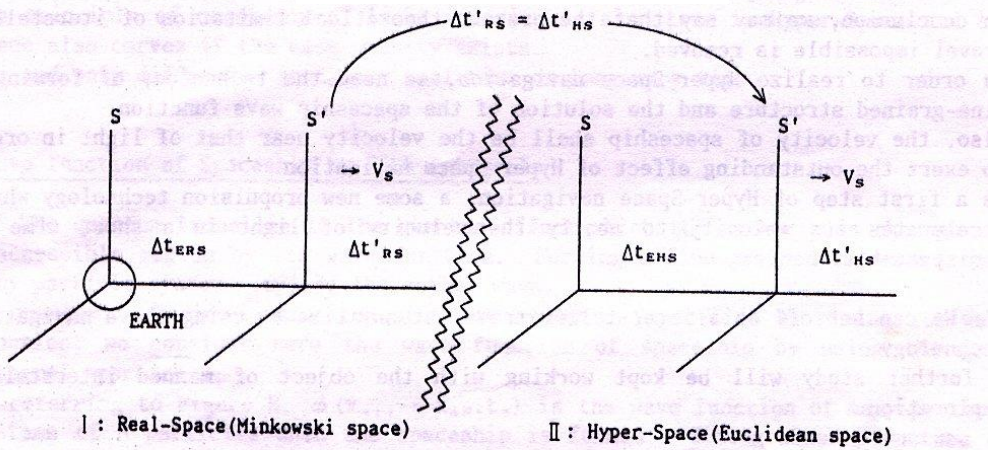
Equation (2) indicates that a certain geometrical structural deformation of space is described by the concept of the strain. In a word, the change of metric tensor due to the existence of mass or electromagnetic energy yields the strain field of e_{ij} , and this strain of space shows some type of structural deformation of space.

The rate of deformation (*i.e.*, strain rate) rather than deformation plays a significant role. In order to keep the continuity of space, the velocity of moving matter in space does not exceed the strain rate of space itself (*i.e.*, the velocity-of-light). The strain rate of space is the velocity-of-light which is derived from the propagation velocity of the gravitational field. Although the spaceship can approach the velocity-of-light as a strain rate of space, it can not only become the velocity-of-light but also cannot exceed it. If the spaceship exceeds the velocity-of-light, the crack occurs and spacetime as a continuum will be fractured. The velocity-of-light gives the critical state to space.

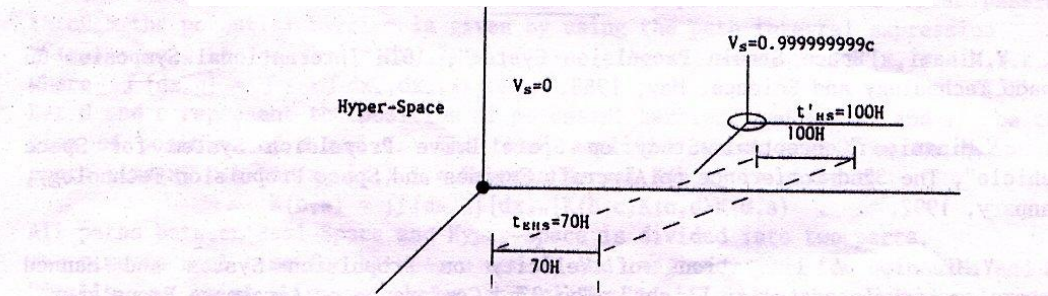
In general, a means to avoid the fracture of the continuum for external load is a deformation. A deformation gone beyond the bounds of the above critical state causes a crack, which may lead to the fracture of space. **Figure 83(a)** shows that if the velocity of the spaceship V_s is almost equal to c , a strain concentration of space occurs in front of the spaceship. Here we divide space into two types. The actual physical space in which we live in is a Minkowski space and the world is limited by Special Relativity. This space maintains the continuity constant: we define it as “**Real-Space**”. Next, if the crack occurs and the continuity of space is fractured; we define it as “**Hyper-Space**”.



(a) Deformation of Space



(b) Transition from Real-Space to Hyper-Space



(c) Comparison of Elapsed Time between Real-Space and Hyper-Space

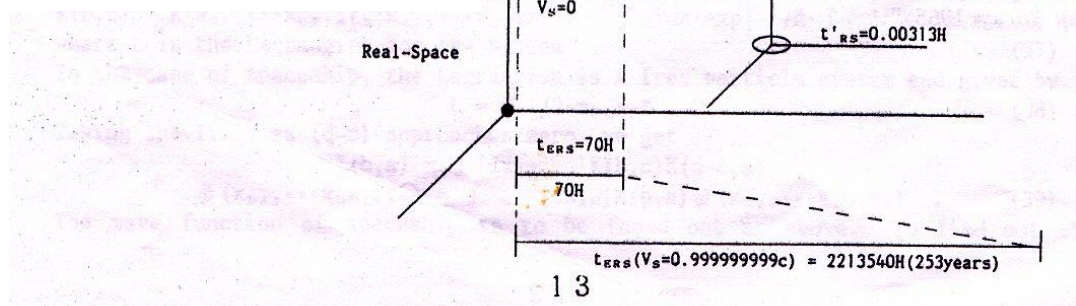


Figure 83 - Transitioning from Real-Space to Hyper-Space (courtesy Yoshinari Minami (80))

Characterization of Hyper-Space

The properties of Hyper-Space is analogous to that of Minkowski Space. As previously mentioned, the properties of space are determined by a metric tensor, which defines the distance between two points. Let us put $\mathbf{x}^1, \mathbf{x}^2, \mathbf{x}^3$ for $\mathbf{x}, \mathbf{y}, \mathbf{z}$ and \mathbf{x}^0 for $c\mathbf{t}$. For the Minkowski space the distance \mathbf{S} is given by:

$$\mathbf{S}^2 = \eta_{ij} \mathbf{x}^i \mathbf{x}^j = -(x^0)^2 + (x^1)^2 + (x^2)^2 + (x^3)^2 = -(ct)^2 + x^2 + y^2 + z^2 \quad (3)$$

where η_{ij} is the Minkowski metric and c is the velocity of light.

It is a feature of Minkowski space that the square of the time coordinate $\mathbf{x}^0 = ct$ is a minus sign. Equation (3) indicates the properties of actual physical space limited by Special Relativity. In order to bring the properties of Hyper-Space close to that of Minkowski space, the minus sign of the time component of the Minkowski metric ($\eta_{ij} = -1$) is changed to the plus sign ($\eta_{ij} = +1$) while keeping other components of the Minkowski metric unchanged. The mathematical details are aptly described by Minami in his paper (80). The results of his derivations are the Lorentz transformation of Hyper-Space corresponding to that of Real-Space.

Hyper-Space Navigation

Suppose the spaceship accelerates in Real-Space and achieves a quasi-light velocity ($V_s \approx c$) and plunges into Hyper-Space. In Real-Space we have

$$\Delta t'_{RS} = \Delta t_{ERS} [1 - (V_s/c)^2]^{1/2} \quad (4)$$

where $\Delta t'_{RS}$ is the time shown by a clock on the spaceship and Δt_{ERS} is the time of an observer on Earth. From Figure 83(b), after plunging into Hyper-Space the spaceship keeps the quasi-light velocity and takes the S' -coordinates. The elapsed time in the spaceship shall be continuous. Considering the continuity of spaceship time between Real-Space and Hyper-Space, $\Delta t'_{RS} = \Delta t'_{HS}$. It follows that

$$\Delta t'_{ERS} = \Delta t_{EHS} ([1 + (V_s/c)^2]^{1/2} / [1 - (V_s/c)^2]^{1/2}). \quad (5)$$

Equation (5) is the time transformation of Earth time between Real-Space and Hyper-Space. In the case where $V_s = 0.999999999c$, one second in Hyper-Space corresponds to 31,622 seconds in Real-Space. More of this is summarized in Figures 83(c) and 84(a).

Interstellar Flight by Hyper-Space Navigation

Figure 84(b) shows the realistic method for interstellar travel. Two kinds of navigation systems are required. The first is the spaceship acceleration and deceleration in Real-Space. The second is Hyper-Space navigation. In Real-Space, a gap between spaceship time ($\Delta t'_{RS}$) and Earth time (Δt_{ERS}) rapidly increases in proportion to the navigation time. Therefore -- to avoid this gap -- after achieving quasi-light velocity the navigation time shall be shortened and the spaceship shall plunge in Hyper-Space immediately.

Many-Particle Systems

A factor which isolates Real-Space from Hyper-Space is a usual real time and imaginary time. Such a state may be analogous to a state of de Sitter space. In general when a diverse two kinds of space co-exist or adjoin, a potential barrier shall exist to isolate these two kinds of phase space. The spaceship shall therefore overcome this potential barrier. Its energy can be shown to be $\mathbf{V}_{\mathbf{R-H}} = \frac{1}{2} \mathbf{M}_{\mathbf{PL}} \mathbf{c}^2 = \mathbf{9.9 \times 10^8 J}$.

When the spaceship reaches the velocity-of-light, a space as a continuum reaches at the limit of the values -- i.e., a "fracture point" -- and begins the "crack". To fracture a space, the spaceship gives its kinetic energy to the space as an external force. And if this energy exceeds the crack energy of space, then the crack begins.

Suppose that a spaceship of mass M is formed a fine-grained structure of N Plank masses, then $M = N m_{PL}$. It shall maintain the shape as a many-particle system to recreate the structure of the spaceship existing in the initial state. It is necessary to subdivide the spaceship into the size of mass which recreated the initial structure. It is impossible to recreate if it is subdivided into the size of an atom or a molecule. Therefore the spaceship is composed of Planck mass of N particles. It is necessary for the spaceship to be formed as a fine-grain structure in order to treat the spaceship as a many-particle system. Thus we can apply a **quantum tunneling** effect to the ship.

Penetration of the Potential Barrier by Quantum Tunneling

Let us suppose that the thickness of the potential barrier is a Planck length. This assumption is something like the potential thickness of as a de Sitter cosmological model. The Planck length is considered as a fundamental constant of space-time. By method of a fine-grained structure technology, the mass of the spaceship is subdivided into the Planck mass of N .

Even if the energy of each particle is less than the potential barrier, the particle can tunnel through the barrier by the quantum tunneling effect. By the quantum tunneling effect, the spaceship as a many-particle systems can plunge into Hyper-Space without the fracture of space even if its velocity is less than the velocity of light ($V_s \ll c$). In the case of the energy of particle less than potential barrier ($E < V$), the transmissivity T is given by

$$T = [1 + V^2 \sinh^2 \alpha d / 4 E (V-E)]^{-1}, \quad \alpha = [2m (V-E)^{1/2} \hbar] \quad (6)$$

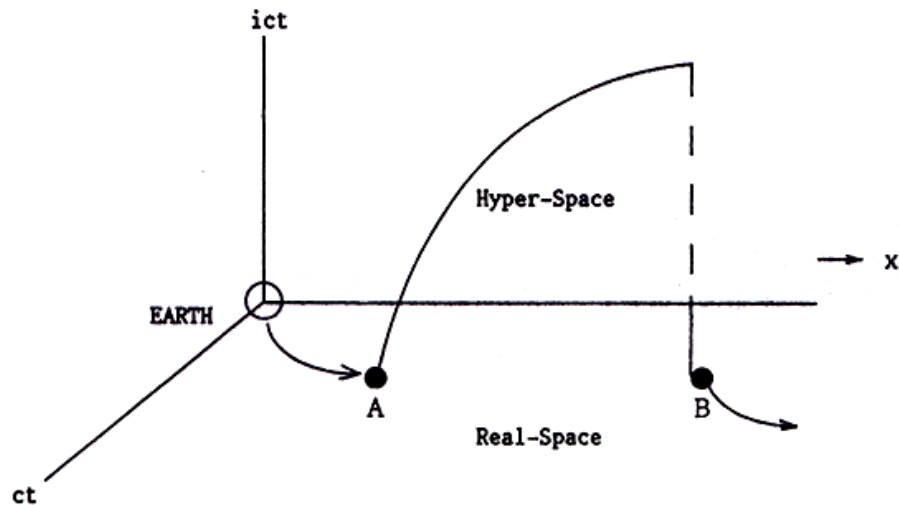
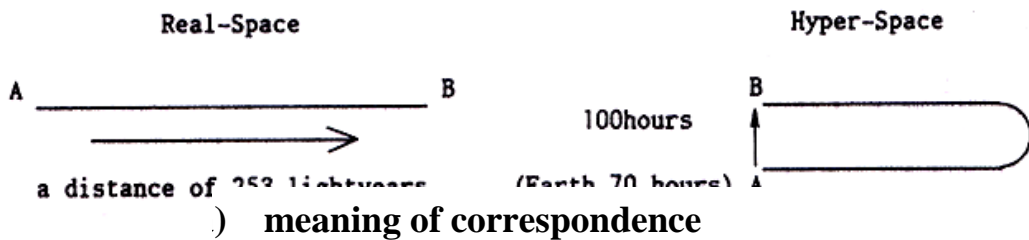
where $m(kg)$ is the mass of the particle, $V(J)$ is the height of the potential barrier, $E(J)$ is the energy of the particle and $d(m)$ is the thickness of the potential barrier.

If $\alpha d < 1$, the following approximate equation is obtained

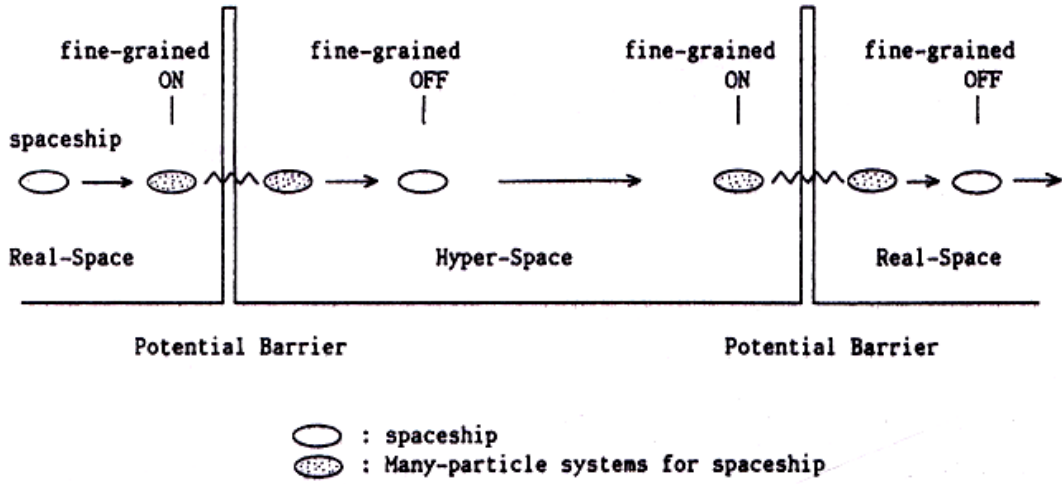
$$T = [1 + V^2 m d^2 / 2 E \hbar^2]^{-1} \quad (7)$$

If the shape of the potential barrier is not a square potential but like the Gaussian shape, we get by the WKB approximation:

$$T = \exp \left\{ -2 \int_a^b [2m (V(x) - E)]^{1/2} / \hbar dx \right\} / \exp(-2 \alpha d). \quad (8)$$



) Interstellar Travel by Hyper-Space Navigation



) Navigation Scenario of the spaceship

Figure 84 - Interstellar Travel by Hyper-Space Navigation (courtesy Yoshinari Minami (80))

With the help of Eqs. (6) - (8), we can estimate the transmissivity.

Substituting the following values for Eqs. (6) and (7),

$$\mathbf{V} = \frac{1}{2} \cdot m_{PL} c^2 = 9.9 \times 10^8 \text{ J}, d = L_{PL} = 1.6 \times 10^{-35} \text{ m}, V_s = 0.999999999c,$$

$$E = \frac{1}{2} \cdot m_{PL} V_s^2 = 9.8999999 \times 10^8 \text{ J}, V-E \approx 41.98 \text{ J},$$

we have $\alpha d = 4.5 \times 10^{-5} < 1$, and hence we get $T = 0.8$.

If we use Eq. (8), the result is $T = e^{-2\alpha d} = 0.99991 \approx 1$.

In the case of WKB approximation -- in which the potential energy changes slowly as a function of position -- the spaceship composed of many-particle systems can tunnel through this potential barrier and plunge into Hyper-Space. And also, in the case of square potential, almost particles can tunnel through this potential barrier. As can be seen from above, the transmissivity depends on the mass. If the mass $m = 10m_{PL}$, $100m_{PL}$, $1/10 m_{PL}$, and $1/100 m_{PL}$, the transmissivity T becomes $T = 0.28$, 0.038 , 0.975 and 0.9975 respectively. Therefore the large mass cannot tunnel through the potential barrier. Anyway, the quantum tunneling effect has the advantage of plunging into Hyper-Space without the fracture of space.

Navigation Scenario between Real-Space and Hyper-Space

Figure 84(c) shows navigation a scenario of a spaceship passing a through Hyper-Space region. Although the spaceship is a mass body of M , at a certain time the spaceship forms a fine-grained structure as a many-particle systems of $m_{PL} \times N$. The wave function of the spaceship is required at that time. After that, the spaceship composed of many-particle systems plunges into Hyper-Space. Then, the spaceship turns off the fine-grained structure technology and continues to travel in Hyper-Space. In order to jump out from Hyper-Space, the spaceship turns on a fine-grained structure technology again and plunges into Real-Space by quantum tunneling effect. After that, the spaceship turns off a fine-grained structure technology again, then decelerates and continues travel.

According to the quantum mechanics, a passage through a narrow region makes the future position uncertain. From the uncertainty principle, we have:

$$\Delta P \Delta x = \hbar, \quad (9)$$

Where ΔP is the uncertainty in the momentum, and Δx is the uncertainty in the region. From Eq. (29), we get

$$\Delta V = \hbar / (m \Delta x), \quad (10)$$

where ΔV is the velocity uncertainty, and m is the mass of the particle.

We can say that a passage through a narrow region (Δx) causes a velocity uncertainty (ΔV) whose size is Eq. (10). Let us now apply the Planck unit to the above equation. Substituting the Planck mass and Planck length as thickness of the barrier for Eq. (10), we get:

$$\Delta V = \hbar / (m_{PL} L_{PL}) = \hbar / [(\hbar c / G)^{1/2} \cdot (G \hbar / c^3)^{1/2}] = \hbar / (\hbar / c) = c . \quad (11)$$

Eq. (11) indicates that even if the velocity of many-particle systems (i.e., the spaceship) is less than the velocity-of-light, the spaceship may achieve the velocity-of-light c by passing through the potential barrier. Therefore, the spaceship may keep the velocity-of-light in Hyper-Space. A range of velocity V_s is c .

Hence, we may also consider that even if the spaceship is at rest, by turning on a fine-grained structure technology the spaceship can plunge into Hyper-Space. Therefore it may not be necessary to accelerate the spaceship to the velocity near that of light!

The time of passing through the potential barrier, we get

$$t = L_{PL}/c = (G \hbar / c^3)^{1/2} / c = (G \hbar / c^5)^{1/2} = t_{PL} . \quad (12)$$

Namely, the passing time is **Planck time** itself.

In addition, we have another form of the uncertainty principle, that is,

$$\Delta E \Delta t = \hbar , \quad (13)$$

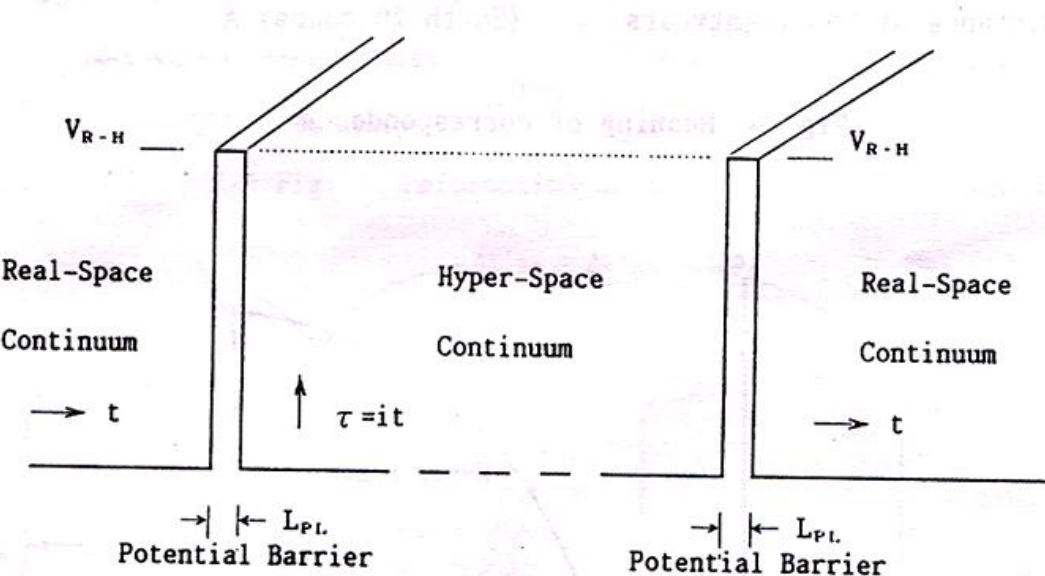
where ΔE is the uncertainty in the energy, and Δt is the uncertainty in the time.

Substitution of Planck time into Eq. (11) gives $\Delta E = 1.9 \times 10^9$ J. This value is Planck energy E_{PL} .

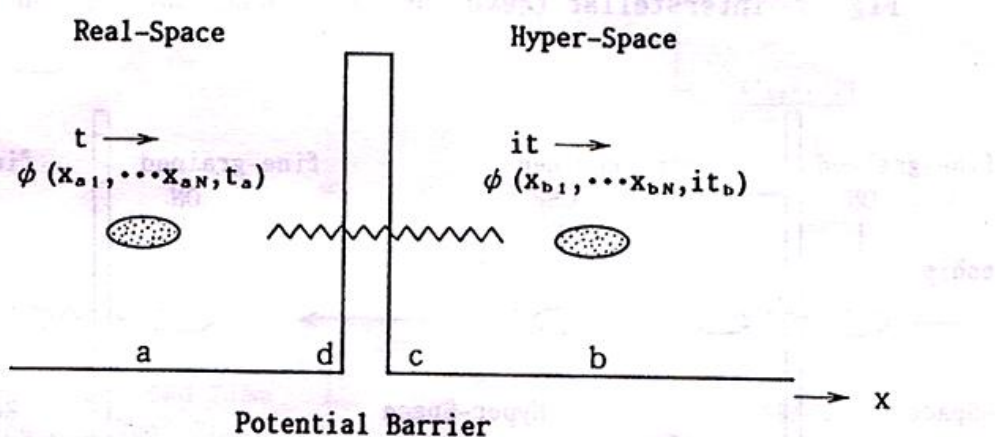
If the above huge energy can be derived from passing through the potential barrier, we can avoid the following difficult problems:

- 1) The mass of any object would become infinite ($m \rightarrow \infty$) at near the velocity of light and the structure of the spaceship or crew would be broken.
- 2) How can we get a power source of vast energy to accelerate any object to near the velocity-of-light?

Finally, let us supplement the properties of Hyper-Space with a few more words on referring to **Figure 85(a)**. The real-space offered by Minkowsky metric and Hyper-Space offered by Euclidian metric co-exist; that is, the parallel space exists. And each space is isolated by the potential barrier.



(a) Properties of Hyper-Space



(b) Wave Function of the spaceship

Figure 85 - 'Time' and 'Imaginary-Time' in Real-Space and Hyper-Space

(courtesy Yoshinari Minami (80))

Now, both Minkowski metric and Euclidian metric, each metric is identical, independent of rest coordinate system and moving system; that is, $\eta_{ij}' = \eta_{ij}$. Therefore, we get:

$$\mathbf{ds}'^2 - \mathbf{ds}^2 = \mathbf{0}, \mathbf{e}_{ij} = \mathbf{0}. \quad (14)$$

These equations give the principle of constancy of light velocity and Lorentz transformations. In this respect, although the Hyper-Space is the space which is fractured its continuity, this cleft space shall also be a continuum. The principle of constancy of light velocity is also true in Hyper-Space is the space which is fractured its continuity, this cleft space shall be also continuum. The principle of constancy of light velocity exists. The one and only difference is either real-time or imaginary-time.

Wave Function of the Spaceship by Path Integrals

The quantum tunneling is the quantum effect which the matter pass through the inaccessible region by its wave function. Forming a fine-grained structure as a many-particle systems implies the matter wave. In quantum mechanics, since the state of the system is specified by giving its wave function, we consider here the wave function of the spaceship by using the path integral approach. On referring to **Figure 85(b)**, $\phi(\mathbf{x}_{a1}, \dots, \mathbf{x}_{aN}, t_a)$ is the wave function of the many-particle systems of N particles when the spaceship has formed a fine-grained structure at point \mathbf{a} .

The wave function $\phi(\mathbf{x}_{b1}, \dots, \mathbf{x}_{bN}, it_b)$ of many-particle systems after passing through the potential barrier is given by using the path integral expression:

$$\phi(\mathbf{x}_{b1}, \dots, \mathbf{x}_{bN}, it_b) = \int_{-\infty}^{+\infty} [d\mathbf{x}_{aN}] K(\mathbf{x}_{b1}, \dots, \mathbf{x}_{bN}, it_b; \mathbf{x}_{a1}, \dots, \mathbf{x}_{aN}, t_a) \phi(\mathbf{x}_{a1}, \mathbf{x}_{aN}, t_a) \quad (15)$$

where $f[d\mathbf{x}_{aN}] = \int \dots \int d\mathbf{x}_{aj} d\mathbf{x}_{a2} \dots d\mathbf{x}_{aN}$.

Let \mathbf{d} and \mathbf{c} represent the position of the potential barrier, and let t_d and t_c be the time of position of \mathbf{d} and \mathbf{c} . The total amplitude which goes from the point in space-time (\mathbf{x}_a, t_a) to (\mathbf{x}_b, it_b) , i.e. Feynman Kernel $K(\mathbf{b}, \mathbf{a})$ is given by $K(\mathbf{b}, \mathbf{a}) = \int \int [d\mathbf{x}_{cN}] [d\mathbf{x}_{dN}] K(\mathbf{b}, \mathbf{c}) K(\mathbf{c}, \mathbf{d}) K(\mathbf{d}, \mathbf{a})$ is given by:

$$K(\mathbf{b}, \mathbf{a}) = \int \int [d\mathbf{x}_{cN}] [d\mathbf{x}_{dN}] K(\mathbf{b}, \mathbf{c}) K(\mathbf{c}, \mathbf{d}) K(\mathbf{d}, \mathbf{a}) \quad (16)$$

All paths between Real-Space and Hyper-Space are divided into two parts.

The time is real-time for between \mathbf{a} and \mathbf{d} , and imaginary-time for between \mathbf{c} and \mathbf{b} .

Finally, as a point \mathbf{d} comes closer and closer to point \mathbf{c} , the real time t gets closer and closer to imaginary-time it (i.e., analytic continuation).

Each kernel is represented as follows:

$$\begin{aligned} \mathbf{K}(\mathbf{d}, \mathbf{a}) &= \mathbf{K}(x_{d1}, \dots, x_{dN}, t_d; x_{a1}, \dots, x_{aN}, t_a) = \\ &\quad \int_a^d dx \cdot \exp [i/\hbar \cdot \int_{ta}^{td} dt L(x, x, t)], \\ \mathbf{K}(\mathbf{b}, \mathbf{c}) &= \mathbf{K}(x_{b1}, \dots, x_{bN}, it_b; x_{c1}, \dots, x_{cN}, it_c) = \\ &\quad \int_c^b dx \cdot \exp [-1/\hbar \cdot \int_{tc}^{tb} dt L(x, x, it)], \end{aligned} \quad (17)$$

where \mathbf{L} is the Lagrangian for the system.

In the case of the spaceship, the Lagrangian is a free particle system and given by:

$$\mathbf{L} = \sum \frac{1}{2} \cdot m_{PL} x_N^2. \quad (18)$$

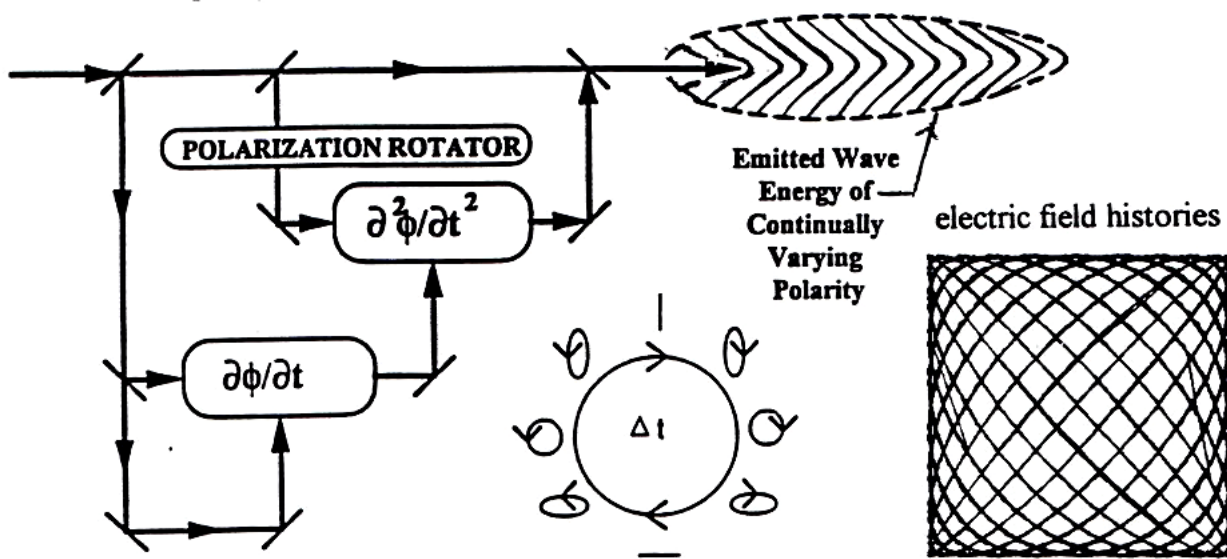
Taking the limit as $(\mathbf{d} \rightarrow \mathbf{c})$ approaches zero, we get:

$$\begin{aligned} \mathbf{K}(\mathbf{b}, \mathbf{a}) &= \int [dx_{d \rightarrow c, N}] \mathbf{K}(\mathbf{b}, \mathbf{c}) \mathbf{K}(\mathbf{d} \rightarrow \mathbf{c}, \mathbf{a}) \\ \phi(x_{b1}, \dots, x_{bN}, it_b) &= \int_{-\infty}^{+\infty} [dx_{aN}] \mathbf{K}(\mathbf{b}, \mathbf{a}) \phi(x_{a1}, \dots, x_{aN}, t_a). \end{aligned} \quad (19)$$

The wave function of the spaceship is to be found out as above. To find out the kernel is equal to solve the following Schrodinger equation:

$$\mathbf{H} \phi(r_1, \dots, r_N) = i\hbar [\partial \phi(r_1, \dots, r_N) / \partial t], \quad (20)$$

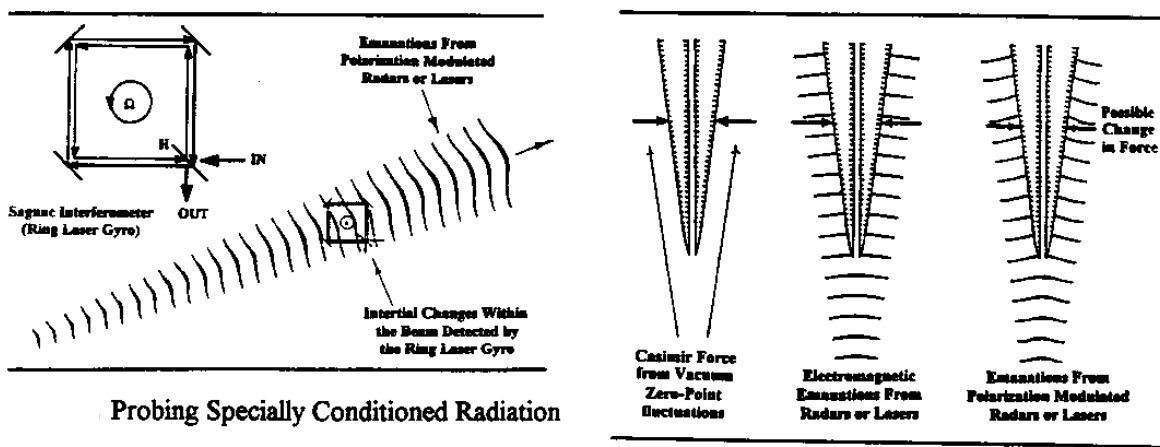
where ' \mathbf{H} ' is the Hamiltonian operator. The wave function of the spaceship in Hyper-Space can be represented by the wave function in Real-Space. A plunging into Hyper-Space characterized by Euclidian space and makes this method of Interstellar flight possible. And in a short time.



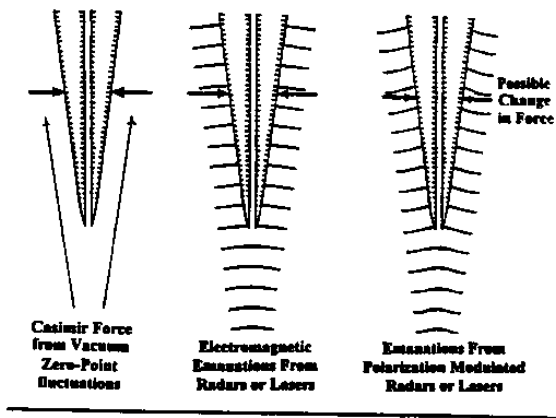
Specially conditioned em fields of SU(2) symmetry and nonabelian form can also be created, , by driving alternating current through a toroid with single windings. The resulting magnetic and electric fields do not extend significantly outside the toroid, but its geometry and the alternating current flow produces overlapping A vector potential patterns which extend outward from the toroid over significant distances and combine into "phase factor" waves which represent disturbances in A vector potential. The

Figure 86 - Polarization Modulation of Ordinary Electromagnetic Radiation

(courtesy Yoshinari Minami ([11](#)))



Still another method would be to detect the influence of specially conditioned em radiation on the measured Casimir force between two closely spaced plates. For any influence that would change ZPE distributions or patterns in the vicinity of the plates would cause a change in measured Casimir force.



Casimir Force Experiment

Expanded Maxwell Equations for Specially Conditioned Em Radiation

Figure 14 - Maxwell Equations

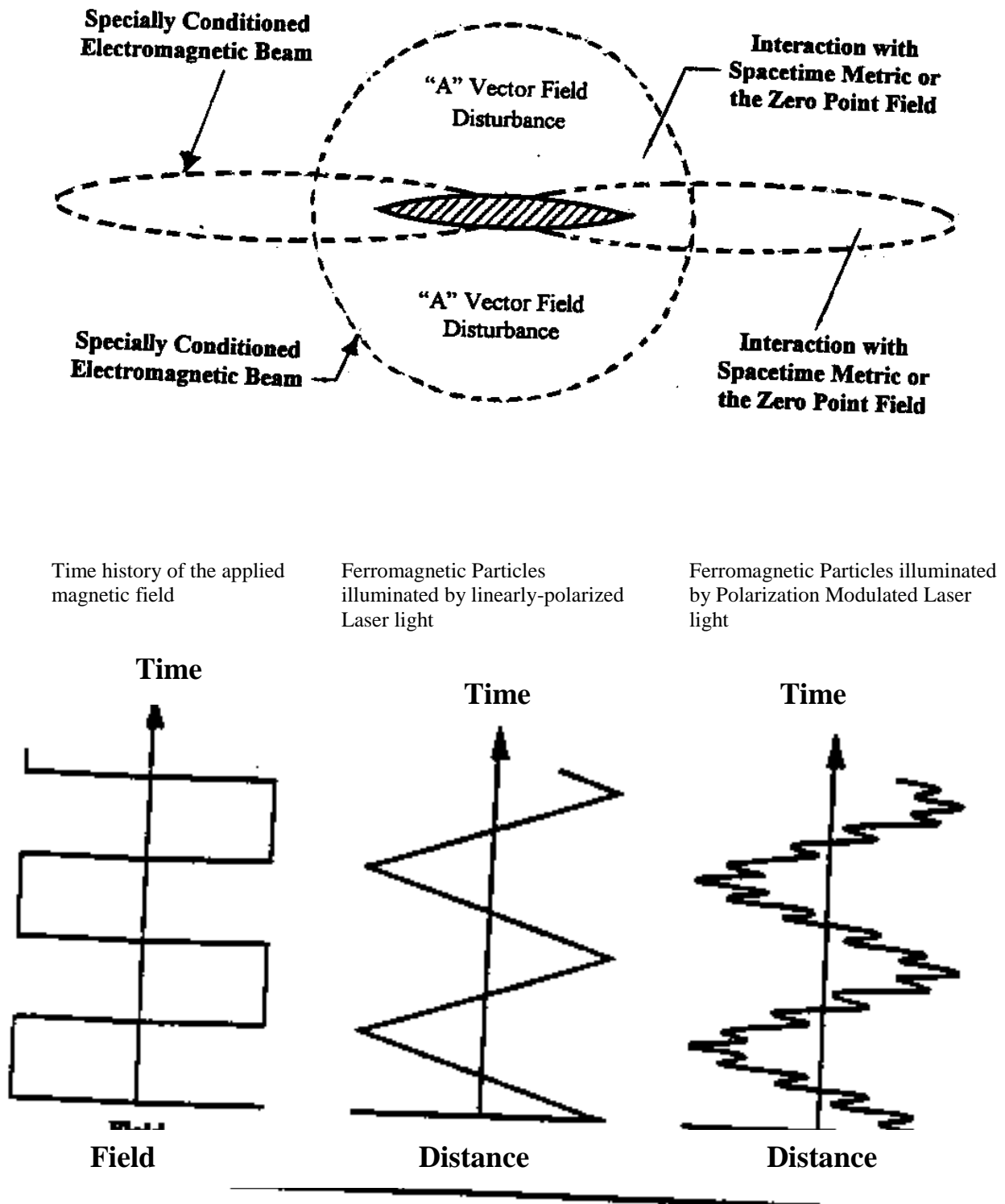
| | $U(1)$ $\left(\right)\left(\right)\left(\right)\left(\right)\left(\right)-$ | $SU(2)$ $\left(\right)\left(\right)\left(\right)\left(\right)\left(\right)\left(\right)\left(\right)\left(\right)\left(\right)\left(\right)\left(\right)\left(\right)-$ |
|---------------|---|---|
| Coulomb's Law | $\nabla \cdot E = J_0$ | $\nabla \cdot E = J_0 - iq(A \cdot E - E \cdot A)$ |
| Ampère's Law | $\frac{\partial E}{\partial t} - \nabla \times B + J = 0$ | $\frac{\partial E}{\partial t} - \nabla \times B + J + iq(A_0 E - EA_0) - iq(A \times B - B \times A) = 0$ |
| Gauss's Law | $\nabla \cdot B = 0$ | $\nabla \cdot B + iq(A \cdot B - B \cdot A) = 0$ |
| Faraday's Law | $\nabla \times E + \frac{\partial B}{\partial t} = 0$ | $\nabla \times E + \frac{\partial B}{\partial t} + iq(A_0 B - BA_0) + iq(A \times E - E \times A) = 0$ |

A = Vector Potential

A_0 = Magnitude of Vector Potential

Figure 87 - Probing Specially-Condition EM Radiation

(courtesy of Yoshinari Minami (11))



Ferromagnetic Aerosol Experiment

Figure 88 - Experiment to Detect Interaction with the ZPE (courtesy Yoshinari Minami (11))

Vacuum Field Perturbation

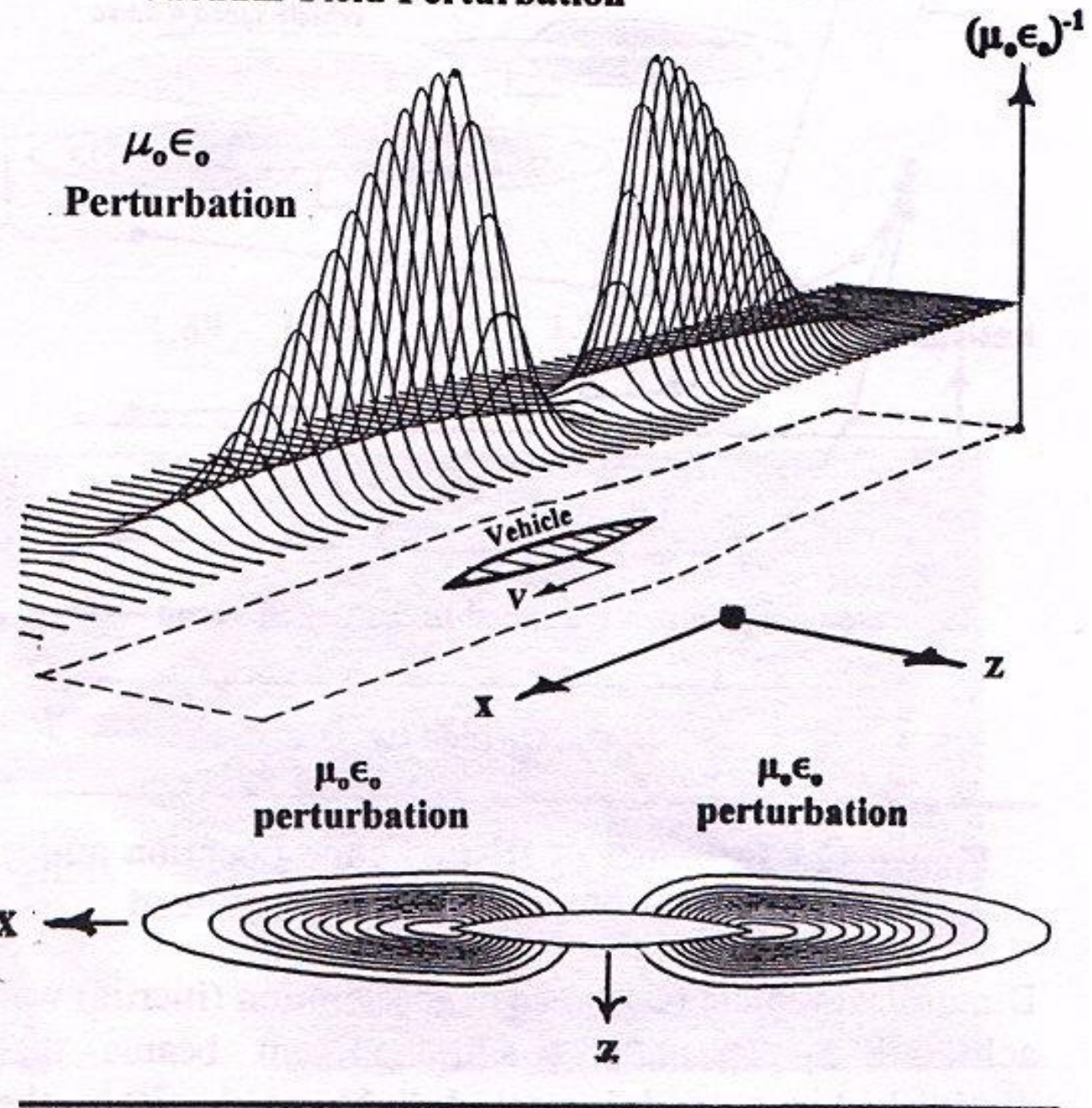
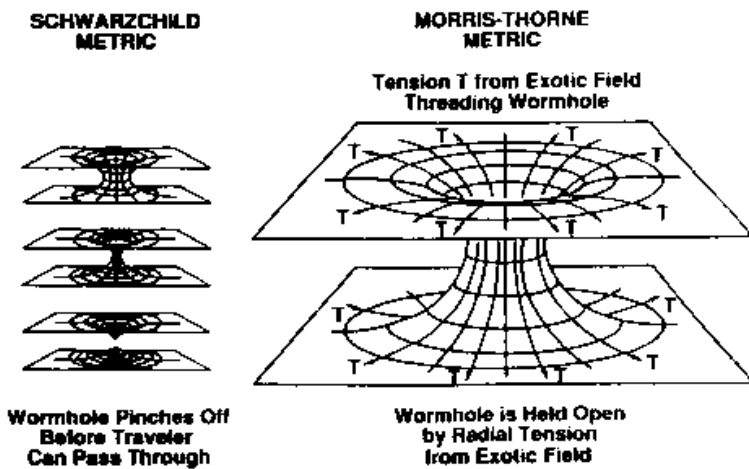
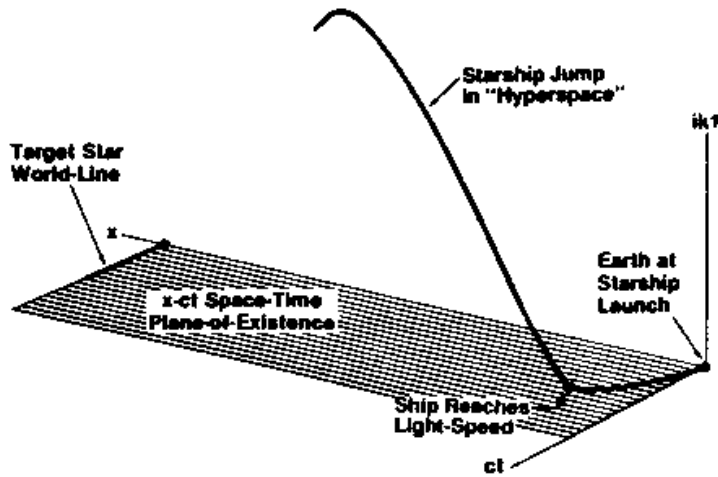


Figure 89 - Topology of Vacuum Field Disturbance (courtesy H.D. Froning, Jr. (10))



Morris-Thorne Space Tunnel

Froning (Reference 28) has shown solutions to the Einstein Special Relativity equations that allow faster-than-light travel within a realm of existence that has space but not time. Such a realm, which can be visualized as rising "above" the spacetime realm of existence of our material world, could presumably be entered if a ship could reach and rapidly surpass light-speed. Figure 6 shows that a superluminal starship would traverse enormous interstellar distances within such a realm; with its flight path arcing above the length and breadth of spacetime just as the flight path of aircraft arc above the length and breadth of earth.



Space - Time - Tau Travel in "Hyperspace"

Figure 90 - Special Relativity Solutions that permit FTL Travel
(courtesy H.D. Froning, Jr. (10))

In order to realize Hyper-Space navigation, the **UNITEL** design employs the technology of forming a fine-grained structure and thus provides the solution of the spaceship wave function. As an important step of Hyper-Space navigation, our propulsion technology -- which accelerates its velocity to nearly the velocity-of-light in a short time -- is invaluable. We can set off on an interstellar travel at any time by using the navigation technology just discussed. **UNITEL**'s electromagnetic propulsion ship and its attached field will generate abruptly-opposed electromagnetic bucking waves, denoting a direct interaction with the ZPE. Acting as a single "giant electron", the **UNITEL** aerospace vehicle will tunnel through the fabric of space-time to arrive at a calculated destination. In this manner, our vehicle will demonstrate superluminal or faster-than-light capabilities.

The use of abruptly-opposed electromagnetic fields was identified as the trigger to induce the orthorotation of the ZPE flux, and it could result in a hyperspatial vortex ring structure that was given the name scalar waves. All particles and microscopic systems arise from the nonlinear self-interaction with the ZPE. Scalar fields fill the Universe and mark their presence by affecting the properties of elementary particles (93). The **UNITEL** vehicle with its charged hull surface and projected laser plasma will polarize the scalar field underlying the elementary particles in our Universe and organize the quantum fluctuations coherently to make them large enough to alter physics locally and at our destination in order to provide instantaneous translation from one space-time coordinate to any other.

Our entire universe is merely a Guth-type faster-than-light inflation of a quantum fluctuation in the primordial before the Big Bang (one of decillions of such bangs), scalar field involving a Higgs-type mass generation (94). Two photons can interact with opposite circular polarizations (orientation of field vector **E**) to produce a neutrino if they run into one another. This is similar to abruptly opposed (counter-rotating 3-wave mixed) electromagnetic Bucking waves. Neutrinos (3) all have an intrinsic rest mass. Here is how photon's energy may not only be expressed as a mass but also in addition all three neutrinos have three distinct masses that may vary due to exterior influences. This is a mass screening mechanism at work. **UNITEL** has more specific details and how they are implemented in our aerospace technology; **E=MC²** and **M=e** over **C²** **C²**, is a head-on counter-rotating vector product that is also the precise Schrodinger probability wave-section for the photon and explains the existence of -- and nature of -- "time" (95).

The dielectric polarizable medium (ZPE) is similar to what **I.J.R. Aitchison** (96) said in pg. 368: "90% of the analogous Lamb Shift in muonic helium is due to vacuum polarization. Vacuum polarization - Consider a test charge '**q**' in a polarizable dielectric medium such as water. If we introduce another test charge '**-q**' into the medium, the electric field between the two test charges will line up the water molecules (which have a permanent electric dipole moment)." The helically wound, pulsed projected plasma field aligns the trapped particles and biexcitonic gasses in a ramp-like manner. Aligning the particles is very similar to a common magnet where all the particles are lined up.

In all dipolar media the effect of the polarization of the vacuum is always to reduce the apparent charge at larger distances or alternatively to increase it at smaller ones. This is because the electric field will always line up the dipoles in the same way. Vacuum polarization produces an anti-screening effect; *i.e.* the effective weak and strong fine structure constants. A flux line in a Type II superconductor can originate from or be terminated by a magnetic monopole. **Niobium** is a natural Type II superconductor. It is important also to mention that our propulsion field is **non-Abelian**. Non-Abelian fields interact directly with the vacuum as Abelian fields do not.

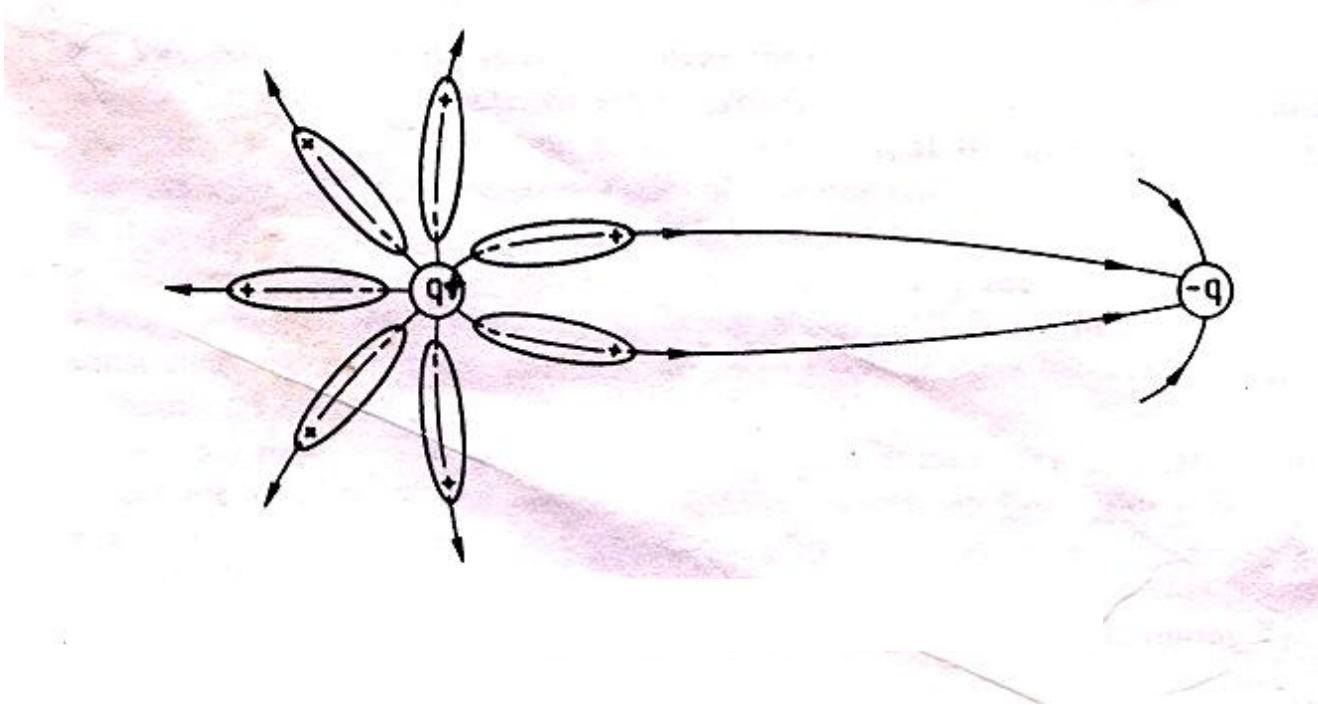


**Figure 91 - Screening of Charge in a Dipolar Medium
(96)**

The usual mean-field description of trapped atomic Bose-Einstein condensates predicts the existence of **solitons** (97) in one-dimensional and quasi-one-dimensional confinement. If the net atomic pair interaction is attractive, these solitons (98) appear as coherently propagating matter wavepackets. If it is repulsive, soliton behavior is seen in the motion of ‘holes’ in the condensate density, the velocity of which is determined by the phase difference between adjoining pieces of condensate in analogy to the familiar Josephson effect.

UNITEL continues to progress with world recognition for the proposed all electrical propulsion system. It is well known as a *buzzword* in international aerospace circles concerning MQT aerospace propulsion applications. UNITEL was one of the pioneers in applying MQT to its propulsion system design beginning in 1982. UNITEL has been recognized by the IAA-IAF (International Astronautical Association-International Astronautical Federation <http://www.iafastro.com>) as a feasible design and has given much credit to UNITEL for Macroscopic Quantum Tunneling (MQT) applications.

11 - Conclusions

We have accumulated enough useful data to validate funding for R&D of this breakthrough science. We are convinced that present-day fabrication & manufacturing technologies have matured to allow theory to evolve into machine. Advanced computer modeling will be extensively used to minimize unforeseen delays in construction and testing of our initial prototypes. **Tim Ventura** (<http://tventura.hypermart.net>) recently contacted us about his "Biefeld-Brown Effect Generator" that partially proved certain portions of our aerospace theories.

Electromagnetic Laser Propulsion can be applied today to mass-transit and atmospheric/near-Earth flight requirements. For interstellar travel via **MQT**, however, additional research into Hyper-Space navigation and biological effects need to take place which is outside the scope of this book. As we mentioned in the "Foreword", if any *revolutionary* effort were that 'easy' then everybody would be doing it already!



Figure 92 - photo of "Lifter" (Biefeld-Brown Effect) (courtesy Tim Ventura, May 2002)

12 - References

- 1)** The "**Acousto-Electromagnetic Hologistic Resonant System**" was patented on March 28, 1989 under **U.S. Patent** number **4,817,102** with ten (10) claims by Messrs Maurer and Miller. This invention was patented internationally under the patent cooperation treaty. International patent application number **PCT/US89/01268** was approved and patents issued on September 11, 1990 as international patent number **89906639.3**. The countries approving the patent are: Austria, Belgium, France, Germany, Italy, Japan, Korea, Luxembourg, The Netherlands, Sweden and The United Kingdom. A separate patent was actively pursued in Japan. Japanese patent application number **1-506249** was approved on August 8, 1994 with the issuance of patent number **1,864,717** to Messrs Maurer and Miller. The patent rights to the generic patent were assigned to **UNTEL**, Inc. by the inventors to promote the development, marketing and licensing of products -- such as the aerospace propulsion system and quantum computer HOLO-1 -- that could be derived from the generic patent.
- 2)** "Polarizable-Vacuum (PV) Representation of General Relativity" and "Can the Vacuum be Engineered for Spaceflight Applications", **H.E. Puthoff**, Institute for Advanced Studies at Austin, Austin, TX, USA February 2000, "Gravity As A Zero-Point-Fluctuation Force", *Physics Review A*, 39, 2333 (1989);
- 3)** "Transport properties in a spin polarized gas, III". **C. Lhuiller**, *J. Physics (Fr.)*, 1983, v.44, # 1, p.1. "The Effects of Spin In Gasses", **Franck Laloe** and **H. Freed**, *Scientific American*, 258:4, April 1988, pp. 94-101.
- 4)** **Gerard t'Hooft**, Physicist, Utrecht, Netherlands, published articles; *Scientific American*, June 1980, *Physica Scripta* Vol. 25, 1:2 January 1982, *Nuclear Physics* 1971 B35:167, *Nuclear Physics* 1974 B79:276, *Nuclear Physics* 1971 B33:173, *Nuclear Physics* 1974 B72:461, *Nuclear Physics* 1974 B75:461.
- 5)** "Quantum Gravity", **Bryce DeWitt**, *Scientific American*, December 1983, pg. 123.
- 6)** "The Superconducting Supercollider", **Jackson** and **Tigner**, *Scientific American*, May issue, 1983, pg. 70.
- 7)** "Nothing's Plenty: The Vacuum In Modern Quantum field Theory", **I.J.R. Aitchison**, *Contemporary Physics*, 1985, Vol. 26, No. 4, pg. 383.
- 8)** Higgs' Particle- (Cooper Pair), pairs of bound electrons which occur in a superconducting medium according to the Bardeen-Cooper-Schrieffer (BCS) theory of superconductivity and as observed in the Josephson Effect. **Bleany & Bleany**, *Electricity and Magnetism*, Oxford press, 3d edition, 1976 pp.423-424. Bardeen-Cooper-Schrieffer, *Physics Review* Vol.108, No.5, December 1957.
- 9)** **K. Enquist and D.V. Nanopoulos** (1984).
- 10)** "Theoretical and Experimental Investigations of Gravity Modifications by Specially Conditioned EM Radiation", **H.D. Froning, Jr.** and **T.W. Barrett**, presented to Space Technology and Applications International Forum (STAIF) January 2000; "Interstellar Studies-The Role In Astronautical Progress and The Future Of Flight", **H. D. Froning, Jr.**, McDonnell-Douglas Space Systems Co.

Huntington Beach, CA, presented to 40th Congress of the International Astronautical federation 7-15 October (1989) Malaga, Spain; "Use of Vacuum Energies For Interstellar Space Flight", **H.D. Froning, Jr.**, Journal of the Interplanetary Society (1986) Vol.39, pp. 410- 415; "Requirements For Rapid Transport To The Further Stars", **H.D. Froning, Jr.**, *Journal Of The British Interplanetary Society*, Vol. 36 (1983) pp. 227-230.

- 11) "Spacefaring to the Farthest Shores- Theory and Technology of a Space Drive Propulsion System", **Yoshinari Minami**, *Journal Of The British Interplanetary Society*, Vol. 50, pp. 263-276, 1997; "Space Drive Force Induced By A Controlled Cosmological Constant", **Yoshinari Minami**, presented to the 47th International Astronautics Congress, Bejing, China, October, 1996; "Possibility Of Space Drive Propulsion", **Yoshinari Minami**, NEC Corporation, Yokohama, Japan, presented to the 45th Congress of the International Astronautical Federation, October, 1994, Jerusalem, Israel; "Hyper-Space Navigation Hypothesis For Interstellar Exploration", **Yoshinari Minami**, NEC Corporation, Yokohama, Japan, presented to the 44th Congress of the International Astronautical Federation, October, 1993, Graz, Austria.
- 12) "Nothing's Plenty: The Vacuum In Modern Quantum field Theory", **I.J.R. Aitchison**, *Contemporary Physics*, 1985, Vol. 26, No. 4, pg. 367.
- 13) **Color-Gluonic Inter-quark Binding force:** the three-part color force acting between quark-antiquark in a meson or among the three quarks in a baryon is the most powerful force known, being fully 39 orders of magnitude greater than the that of gravity and much stronger than the electromagnetic and nuclear binding forces. For quarks that are at relatively great distances from one another, the color force between them becomes constant at the very large value of 16 tons. This is so, even if the quarks are separated by an infinite distance. On the other hand, when quarks are very near one another, their individual color fields begin to overlap and this process partially cancels the color bond between them; the bond strength varying as the inverse square of the distance for closely adjacent quarks. The particles or quanta of the color force are known as gluons and there are eight of them. See; "Gauge Theories of the Forces Between Elementary Particles", **Gerard t'Hooft**, *Scientific American*, June, 1980.
- 14) **Quark:** one of the hypothetical basic particles, having charges whose magnitudes are 1/3 or 2/3 of the electron charge, from which many of the elementary particles may, in theory, be built up; for example, baryons. Such as the neutron and proton may be formed from three quarks and mesons from quark-antiquark combinations. The baryons and mesons together form a group known as the hadrons.
- 15) **Magnetic Monopoles:** hypothetical particle carrying magnetic charge; it would be a source of a magnetic field in the same way that a charged particle is a source for an electric field. **P.A.M. Dirac**, *Proceedings of Royal Society* (1931) *Physical Review* (1948) No.7, Vol.74, pg. 817.
- 16) "Electromagnetic Flight", **John Joanopolis** (MIT), *Scientific American*, 1973; also see <http://www.geocities.com/Tokyo/Island/2589/nmt/bullet.html>
- 17) "Fiber Bundles and Quantum Theory", **Herbert J. Bernstein** and **Anthony V. Phillips**, *Scientific American*, 245:1, July 1981, pp.123-137.
- 18) **Crystallite lens:** is a three-part **red**, **green**, **blue** doped, periodically arrayed superlattice, RF-transparent, glass/CdS-CdTe:Te crystallite, Type II-VI glass semiconductor compound crystallite.

A. Paul Alivisatos et al, The Alivisatos Group, Dept. of Chemistry, University of California at Berkeley, Berkeley, CA, USA (see: www.cchem.berkeley.edu/~pagrp/publications.html)

- 19) "Shock Waves Excited by a Relativistic Charged beam in Media with Dissipation", **V.K. Grishin**, *Fizika*, Vol. 38, No. 3 (1983) pp.18-22.
- 20) "On the Structure of a Shock Wave in a Magnetized Plasma", **A.V. Danilov**, *Fizika*, Vol. 37, No.1 (1982) pp.108-110.
- 21) "Experimental and Theoretical Investigation of Free Exciton Transport in Si", **Hilmer** et al, *Physics Review B*, Vol. 20 (1987) pg. 523.
- 22) **Raymond Y. Chiao**, *Scientific American*, July 1996.
- 23) **Mysyrowicz** et al., *Physics Review B*, Vol. 28, No. 6 (1983) pg. 3590.
- 24) "Gauge Theories of the Forces Between Elementary Particles", **Gerard t'Hooft**, *Scientific American*, June, 1980, pp. 108-121. "Collective Model of Hadrons", **Heinz Pagels**, *Physics Review D*, 14:10, 10 November, 1976; "Magnetic Monopole Interactions", **O'Raifeartaigh** et al, *Physics Review D*, 20:8, 15 October 1979; "Dual Symmetric Theory of Hadrons/Mesons", **David Susskind**, *Nuovo Cimento*, 69:3, October 1970; "Theory of Quark Confinement Based on an Analogy with the Theory of Magnetic Monopoles", **Sugawara**, *Physics Review D*, 14:10, 15 November, 1976.
- 25) "Acoustic Surface Waves", **Gordon Kino** and **John Shaw**, *Scientific American*, 222:4, October 1972, pg.57.
- 26) "The Size and Shape of Atomic Nuclei", **Michael Baranger** and **Raymond N. Sorenson**, *Scientific American*, August 1969.
- 27) "Laser Separation Of Isotopes", **Richard N. Zare**, *Scientific American*, 236:2, February 1977, pg. 94.
- 28) "Light", **Gerald Feinberg**, *Scientific American*, 219:3, September 1968, pp. 50-59.
- 29) "Superluminal Effects for Quantum Tunneling Through Two Successive Barriers", by **Vladislav S. Olkhovsky**, **Erasmo Recami**, **Giovanni Salesi**.
- 30) "Macroscopic Quantum Coherence in a Magnetic Nanoparticle above the Surface of a Superconductor", **Eugene M. Chudnovsky** (Lehman College, CUNY), **Jonathan R. Friedman** (SUNY - Stony Brook).
- 31) "Fiber Bundles and Quantum Theory", **Herbert J. Bernstein** and **Anthony V. Phillips**, *Scientific American*, 245:1, July 1981, pp.123-137.
- 32) "How Light Interacts With Living Matter", **Victor Weiskopf**, *Scientific American*, Vol. 219, No. 3, September issue, 1968, pg. 60.
- 33) "How Light Interacts With Living Matter", **Victor Weiskopf**, *Scientific American*, Vol. 219, No. 3, September issue, 1968, pg. 74.

- 34)** "A Solid State Source Of Microwaves", **Raymond Bowers**, Scientific American, 215:2, August 1966, pp. 22-31; "Signal Processing In Acoustic Surface-Wave Devices", **G.S. Kino** and **N. Mathews**, IEEE Spectrum, Vol.8, No. 8, August 1971, pp. 22-35.
- 35)** "Diamond Film Semiconductors", **Michael W. Geis** and **John C. Angus**, Scientific American, October 1992, pp. 84-89.
- 36)** "The Electrification of Thunder Storms", **Earle R. Williams**, Scientific American, Vol. 259, No. 5, November issue, 1988, pg. 91.
- 37)** "Advances in Superconducting Magnets" by **William B. Sampson**, **Paul P. Craig** and **Myron Strongin**, Scientific American, July 1966, pg.123.
- 38)** "How the Leopard gets its Spots", **James D. Murray**, Scientific American, Special Issue, 1990, pp. 39.
- 39)** "Rayleigh and Lamb Waves: Physical Theory and Applications" , **I.A. Viktorov**, Plenum Press, 1967; "Microwave Semiconductor devices and Their Circuit Applications" , **N.A. Watson**, McGraw-Hill, New York, NY, 1969; "Acoustic Surface Waves", **Gordon S. Kino** and **John Shaw**, Scientific American, 227:4, October 1972, pp.51-69.
- 40)** "Observation of Fractional Charge of $(1/3)e$ on Matter", **George S. LaRue**, et al, Physics Review Letters, Vol 46, No 15, 13 April 1981, pg. 967.
- 41)** "Communication By Laser", **Stewart E. Miller**, Scientific American, 214:1, January 1966, pp. 19-27: "Traveling Wave tubes: Coupled Cavity high powered TWTs", Electrical Engineers Handbook, Fink, pp. 9-43.
- 42)** "Fractional statistics and the Quantum Hall effect", Daniel Arovas, **J. R. Schrieffer** and **Frank Wilzcek**, Phys Rev Lett, Vol 53, No. 7, 13 August 1984, pp. 722-723.
- 43)** **Pi mode of RF magnetron** (3-vaned spoke pattern in most magnetrons), Electronics Engineers Handbook, Fink, pp. 9-47. **deBroglie mode**: the deBroglie RF microwave mode is analogous to Faraday rotation of laser beams where left- and right-hand components of circularly polarized light are of equal amplitude. These two states of circular polarization travel at different velocities. The resulting change of phase between them causes their sum to produce a state of linear polarization rotated with respect to its initial orientation.
- 44)** **Mechanical Stress Modulators**, Electronics Engineers Handbook, Fink, pg. 14-59. Also see: Figures 13-86, 13-76, 14-12. Traveling wave tubes: coupled-cavity high-power TWTs, pp.9-43; "For high average or peak power there are a variety of all-metal slow-wave circuits which have low RF losses and high heat dissipation by thermal conduction. The circuits are equivalent to a series of cavities, similar to Klystron cavities, mutually coupled to propagate a traveling wave."
- 45)** "Acoustic Surface Waves", **Gordon S. Kino** and **John Shaw**, Scientific American, 227:4, October 1972, pg. 53.

- 46)** "On the Structure of a Shock Wave in a Magnetized Plasma", **A.V. Danilov**, Vestnik Moskovskogo Universiteta, Fizika, Vol. 37, No. 1, 1982, pp. 108-110; "Modulation of Laser Light", **Donald Nelson**, Scientific American, 218:6, June 1968, pg. 21.
- 47)** "Fiber Bundles and Quantum Theory", **Herbert J. Bernstein** and **Anthony V. Phillips**, Scientific American, 245:1, July 1981, pp.123-137.
- 48)** "A Possible mechanism For formation Of Ball Lightning", **G.A. Yorob'ev**, Sov Physc Tech Phys, 28:4, April 1983, pg. 521.
- 49)** "Cosmic Strings", **Alexander Vilenkin**, Scientific American, November 1987, pg.100.
- 50)** "Fiber Bundles and Quantum Theory", **Herbert J. Bernstein** and **Anthony V. Phillips**, Scientific American, Vol. 245, No.1, July issue, 1981, pp. 123-137.
- 51)** "Charge Datapoint Systems (the Enormous Theorem) Kalaedoscope Effect (In Phased Array Radar) On the Structure of the Finite Order", **Richard Brauer**, Proceedings of the International Congress of Mathematics, Vol. 1 (1954) pp. 209-217; "Side Looking Airborne Radar", **Jensen et al**, Scientific American, Vol. 237, No. 4, October 1977, pp. 84-95.
- 52)** "New Approach To The Exciton-Phonon Problem", **Oswald et al**, Physics Review B, Vol. 28, No. 6, 15 September, 1983.
- 53)** "Black Holes in Bose-Einstein Condensates", **L. J. Garay, J. R. Anglin, J. I. Cirac, P. Zoller**.
- 54)** "Black Holes and the Centrifugal Force Paradox", **Marek Artur Abramowicz**, Scientific American, March 1993, pp. 73-80; "Excitonic Matter", **James P. Wolfe & Andrew Mysyrowicz**, Scientific American, March 1984, pg.98.
- 55)** "The Search For Black Hole", **Kip S. Thorne**, Scientific American, 231:6, December 1974, pp. 32-43; "The Membrane Paradigm For Black Holes", **Richard H. Price and Kip S. Thorne**, Scientific American, 258:4, April 1988, pp. 69-77.
- 56)** "Controlling Decoherence in Bose-Einstein Condensation by Light Scattering Far Off Resonance", **C.P.Sun** (Report-no: ITP (CAS)-QP (AMO)-2000/5).
- 57)** "The Mystery Of The Cosmological Constant", **Larry Abbott**, Scientific American, 258:5, May 1988, pp. 106-113.
- 58)** "Photoacoustic and Thermal Wave Phenomena in Semiconductors", **Andreas Mandelis**, North Holland, New York, pg. 376.
- 59)** "Exciton Transport In Cu₂O: Phonon Wind vs Bose Condensation", **Mysyrowicz et al**, Physics Review Letters, 77, 895 (1996); **N.A. Gippius et al**, General Physics Inst. RAS, Moscow, Russia, presented to the American Physical Society March 1997.
- 60)** Encyclopedia of Modern Physics, Academic Press, 1990, pg. 248.

- 61)** "Nothing's Plenty: The Vacuum In Modern Quantum field Theory", **I.J.R. Aitchison**, Contemporary Physics, 1985, Vol. 26, No. 4, page 371. "Strain Confinement and Thermodynamics of Free Excitons in a Direct Gap Semiconductor", **A. Mysyrowicz, D. P. Trauernicht and J. P. Wolfe**, Physics Review B, 28:6, 15 September, 1983, pg. 3590.
- 63)** "Energy States and Bloch States for an Accelerated Electron in a Periodic Lattice", **Churchill and Holstrom**, Physica Scripta, 1982, pg. 27.
- 64)** "Optimal Control of the Wavefront and Temporal Profile of Optical Radiation Propagating in a Non-Linear Medium", **Karamzin et al**, Fizika, 37:4, 1982, pp. 18-21.
- 65)** "Optical Phase Conjugation", **Vladimer V. Shkunov and Boris Ya. Zel'dovich**, Scientific American, 253:6, December 1985, pp. 54-59.
- 66)** "Gauge Theories of the Forces Between Elementary Particles", **Gerard t'Hooft**, Scientific American, June 1980, pp. 108-121
- 67)** "Dual-Symmetric Theory of Hadrons/Mesons", **D. Susskind**, Nuovo Cimento, Vol. LXIX, No. 3, 1 October, 1970.
- 68)** "Topology of Fiber Bundles", **Steenrod**, Princeton University Press, Princeton, NJ, 1951; "Confinement in Topology in Non-Abelian Gauge Theory", **Gerard t'Hooft**, Proceedings of the 19th International University Physics Conference, Schmalding, Germany, February 20 - March 1, 1980.
- 69)** "Magnetic Monopoles, Fiber Bundles and Gauge Fields", **Chen Ning Yang**, Institute of Theoretical Physics, Stony Brook, New York, NY, USA, Annals of the New York Academy of Sciences, Vol. 294, Nov 1977, pp. 86-97.
- 70)** "Time-Dependent Superposition of Spinners", **Badurek**, Physics Review Letters, 51:12, 1983, pg. 1015.
- 71)** "Kinetic Phenomena of Atomic Motion in a Light Field", **A.P. Kazantsev et al**, J. Opt. Soc. Am. B, 2:11, November 1985, pp. 1731-1742.
- 72)** "Free Electron Lasers and Their possible Applications", **A.N. Didenko and A. V. Kozhevnikov**, Plenum Publishing C., 1983, pg. 221.
- 73)** "Observation of Berry's Topological Phase by Use of an Optical Fiber", **Akira Tomita and Raymond Y. Chiao**, Physics Review Letters, 57:8, 25 August, 1986, pp. 937-940.
- 74)** "Quantum Description of High-Resolution NMR in Liquids", **Maurice Goldman**, Oxford Press, 1988.
- 75)** "Instabilities and Chaos of a Solid State NMR Laser With Injected Signals", **E. Brun et al**, Physica Scripta, T113, 1986, pp.119-123.
- 76)** "Free Electron Lasers", **Henry P. Freund and Robert K. Parker**, Scientific American, April 1989, pp. 84-89.

- 77)** "Strain Confinement and Thermodynamics of Free Excitons in a Direct Gap Semiconductor", A. Mysyrowicz, D. P. Trauernicht and J. P. Wolfe, Physics Review B, 28:6, 15 September, 1983, pg. 3590.
- 78)** "Nothing's Plenty: The Vacuum In Modern Quantum field Theory", I.J.R. Aitchison, Contemporary Physics, 1985, Vol. 26, No. 4, pg. 365.
- 79)** "Electron tunneling Theory in Non-Linear transport in Junctions in Microstructures", Feuchtwang et al, NATO Research Grant Division, Grant No. 1902, Scientific Affairs Division, Brussels, Belgium.
- 80)** "Hyper-Space Navigation Hypothesis for Interstellar Exploration", Yoshinari Minami, NEC Corporation, Yokohama, Japan, IAF-IAA 44th Congress of the International Astronautical Federation, Graz, Austria, Oct. 16-22, 1993, No, IAA.4.1-93-712.
- 81)** "Theory of Quark Confinement Based on an Analogy with a Theory of Magnetic Monopoles", Physics Review D, Vol. 14, No. 10, 15 November, 1976, pg. 2771.
- 82)** "Second Sound in Solid Helium", Bernard Bartman and David J. Sandiford, Scientific American, Vol. 222, No. 5, May 1970, pp. 92-101; "Entropy Waves or Second Sound", Cecil T. Lane, Superfluid Physics, McGraw-Hill Book Co., 1962.
- 83)** "Space-Time Local Symmetry of String Field Theory", Tamiaki Yoneya, Physics Review Letters, Vol. 55, No. 18, Oct 28, 1985, pg.1828.
- 84)** "Temperature Pulses In Dielectric Solids", C.C. Ackerman and R.A. Guyer, Annals of Physics, Vol. 50, No.1, Oct 15, 1968, pp.128-185; "Second Sound in Solids", L.V. Pitaevskil, Soviet Physics Uspekhi, Vol. 11, No.3, Nov/Dec 1968, pp. 342-344.
- 85)** "Particles, Sources and Fields", J. Schwinger, Addison Wesley, Reading, MA, Vol 1 (1970), Vol 2 (1973).
- 86)** "Observation of Berry's Topological Phase by use of an Optical Fiber", Raymond Y. Chiao & Akira Tomita, Physics Review Letters, 57: 8, Aug 25, 1986, pp. 937- 940.
- 87)** Steven Weinberg, Scientific American, July 1974, pg. 56.
- 88)** "Quantum Gravity", Bryce DeWitt, Scientific American, December 1983, page 114.
- 89)** "Faster Than What?", Raymond Chiao, Scientific American, July, 1996.
- 90)** "Quantized Singularities in the Electromagnetic Field", P.A.M. Dirac, Proceedings of the Royal Society, A133(1931) pp. 60-72; "The Theory of Magnetic Pole", P.A.M. Dirac, Physics Review, Vol. 74, No. 7, October 1948, pp. 817-283.
- 91)** "The Mystery of the Cosmological Constant", Larry Abbott, Scientific American, 258:5, May 1988, pg. 110.
- 92)** Gerard t'Hooft, Nuclear Physics, 36:19, 10 May 1976.

- 93) "Generation of Electromagnetic Waves by Gravitational Waves in Electric and Magnetic Fields", **Grigor'ev**, Vestnik Moskovskogo Universiteta Fizika, Vol. 37, No. 3, 1982, pp. 34-38.
- 94) "Four-Component Electromagnetic Fields and ElectroDynamics", **M.T. Teli**, Pramana, 24:3, March 1985, pg.485.
- 95) "Dual Resonance Model of Elementary Particles", **J. H. Schwartz**, Scientific American, Feb 1975, pp. 63-65.
- 96) "Nothings Plenty", by **I.J.R. Aitchison**, Contemporary Physics, 1985, Vol. 26, No 4, pg. 333.
- 97) "Soliton Dynamics in the Collisions of Bose-Einstein Condensates: an Analogue of the Josephson Effect", by **William P. Reinhardt** and **Charles W.Clark**, J Phys B: at Mol Opt Phys, 30 No 22 (28 Nov 1997) L785- L789.
- 98) "Solitons", **Claudio Rebbi**, Scientific American, February 1979, pg. 92
- 99) "Extreme Light", Scientific American, May 2002, pp.80+ .

13 - Supplemental Documents

page

132 ... A - UNITEL's Type VI MOSS Prototype Vehicle AutoCAD Drawing 1-of-7

133 ... B - UNITEL's Type VI MOSS Prototype Vehicle AutoCAD Drawing 2-of-7

134 ... C - UNITEL's Type VI MOSS Prototype Vehicle AutoCAD Drawing 3-of-7

135 ... D - UNITEL's Type VI MOSS Prototype Vehicle AutoCAD Drawing 5-of-7

136 ... E - UNITEL's Type VI MOSS Prototype Vehicle AutoCAD Drawing 6-of-7

137 ... F - UNITEL's Type VI MOSS Prototype Vehicle AutoCAD Drawing 7-of-7

138 ... G - UNITEL's HOLO-1 Lens Composition AutoCAD Drawing 3-of-4

139 ... H - UNITEL's HOLO-1 Lens Composition AutoCAD Drawing 4-of-4

140 ... I - UNITEL's Space Shuttle Prototype AutoCAD Drawing 1-of-2

141 ... J - UNITEL's Space Shuttle Prototype AutoCAD Drawing 2-of-2

142 ... K - the challenging UNITEL Material-Sciences R&D Effort

143 ... L - comparing the semiconductor properties of Silicon (Si) with HgCdTe

144 ... M - Facilities Researching Advanced Semiconductor Fabrication Technologies

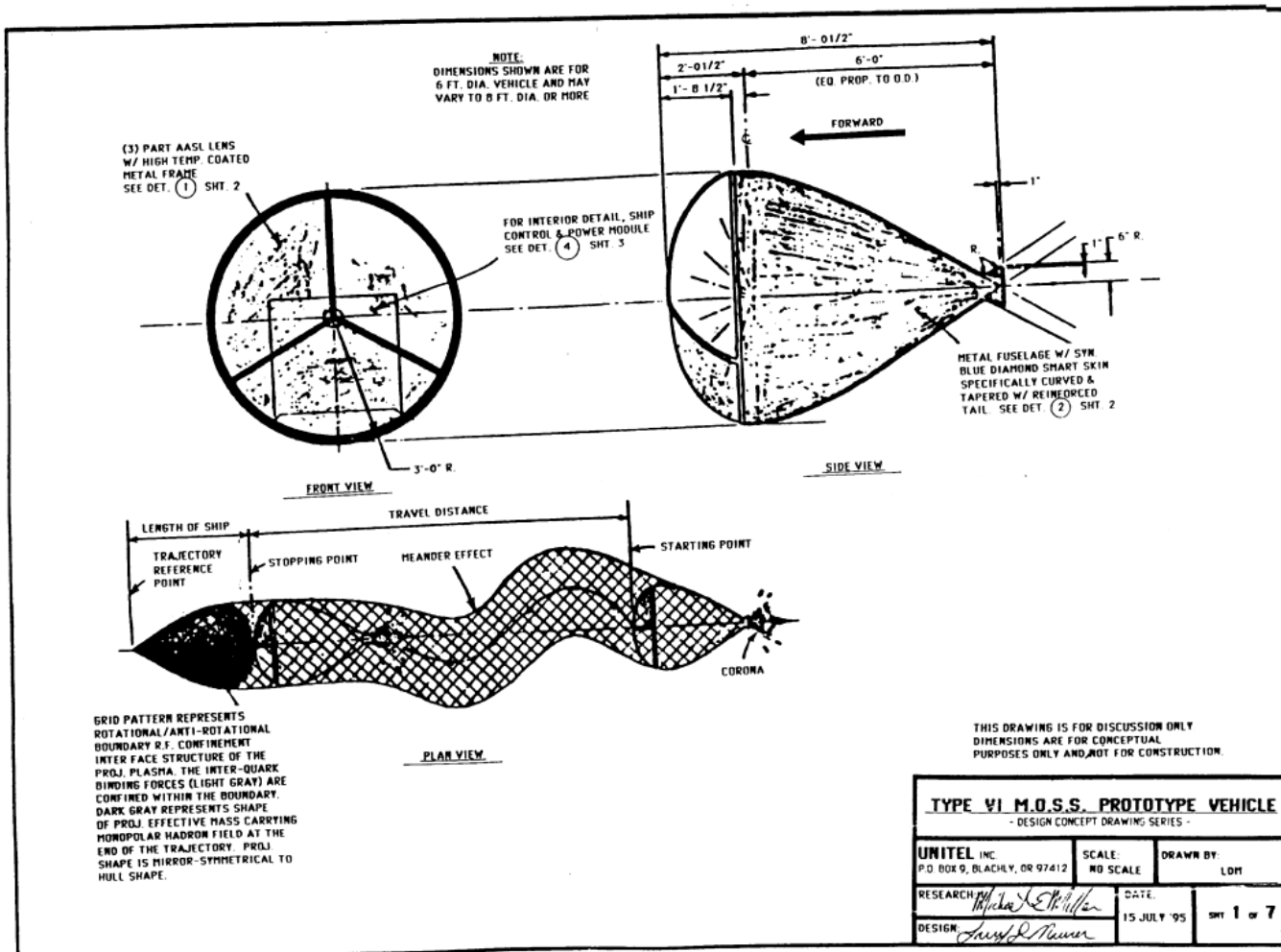
145 ... N - the Cover of the Japanese Patent awarded to UNITEL

146 ... O - January 2000 Space Technology and Applications International Forum

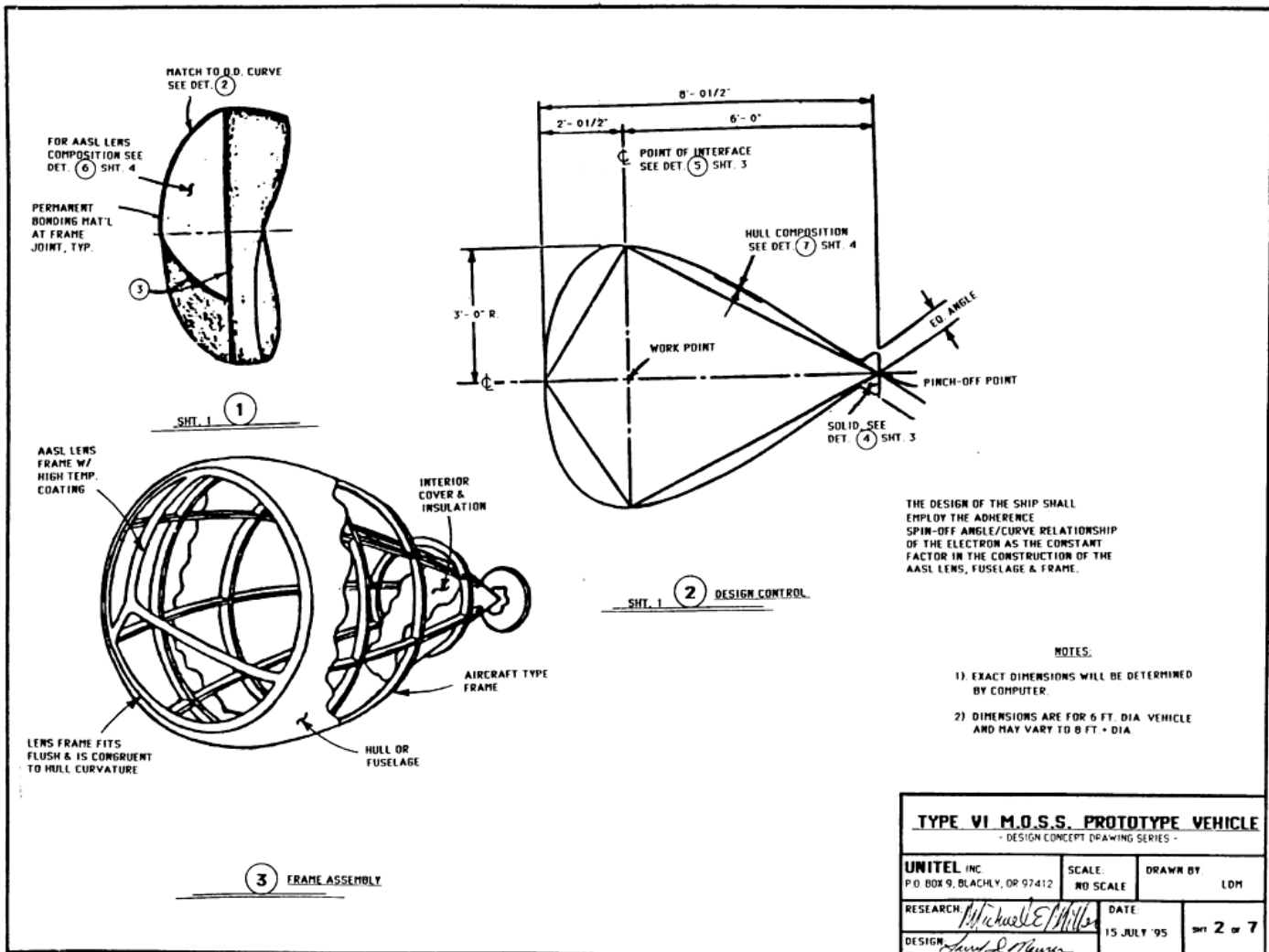
147 ... P - July 2000 AIAA/ASME/SAE/ASEE Joint Propulsion Conference & Exhibit

148 ... Q - a letter to UNITEL from Boeing Aerospace and Electronics

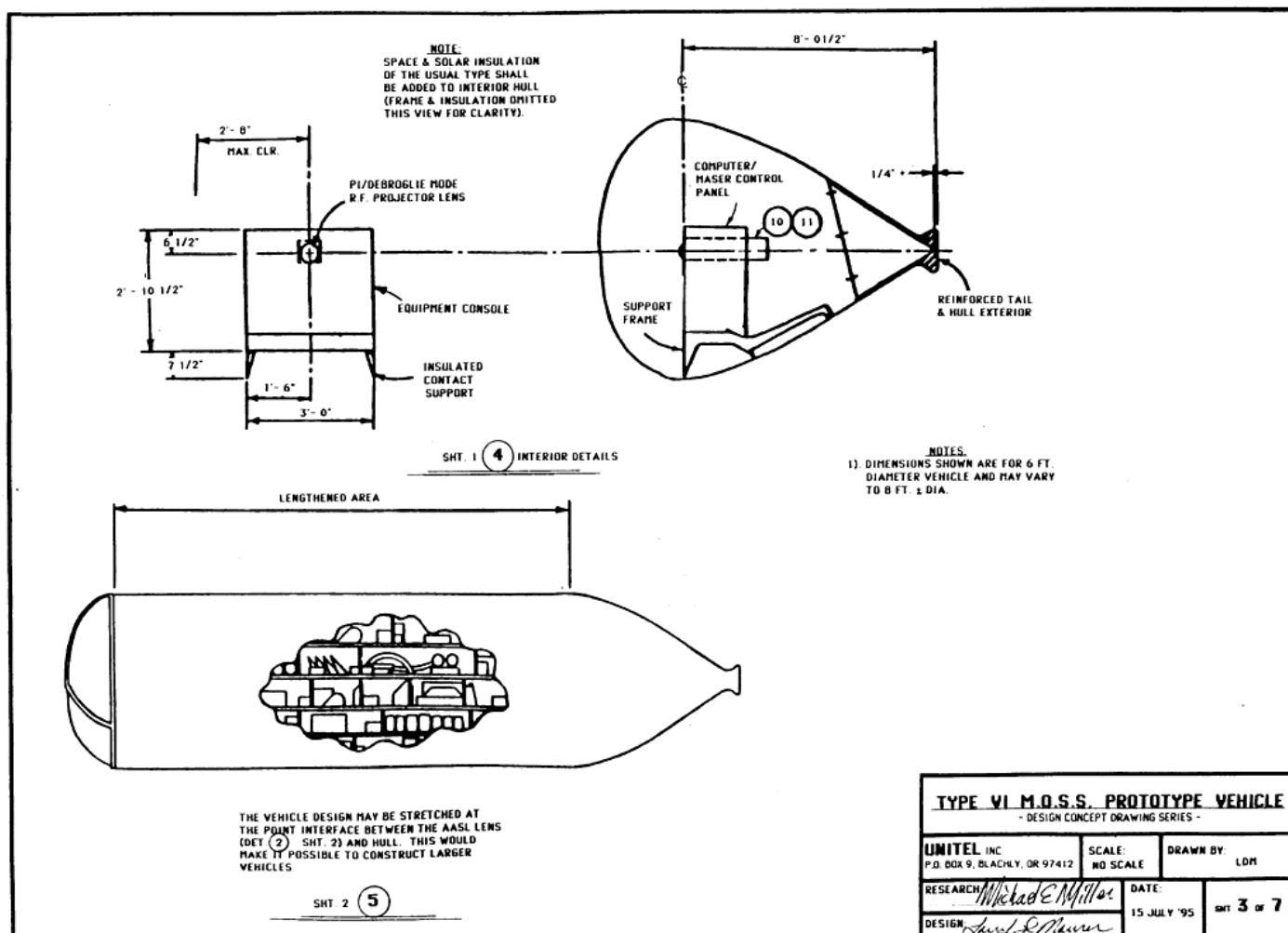
149 ... R - October 1993 Congress of the International Astronautical Federation



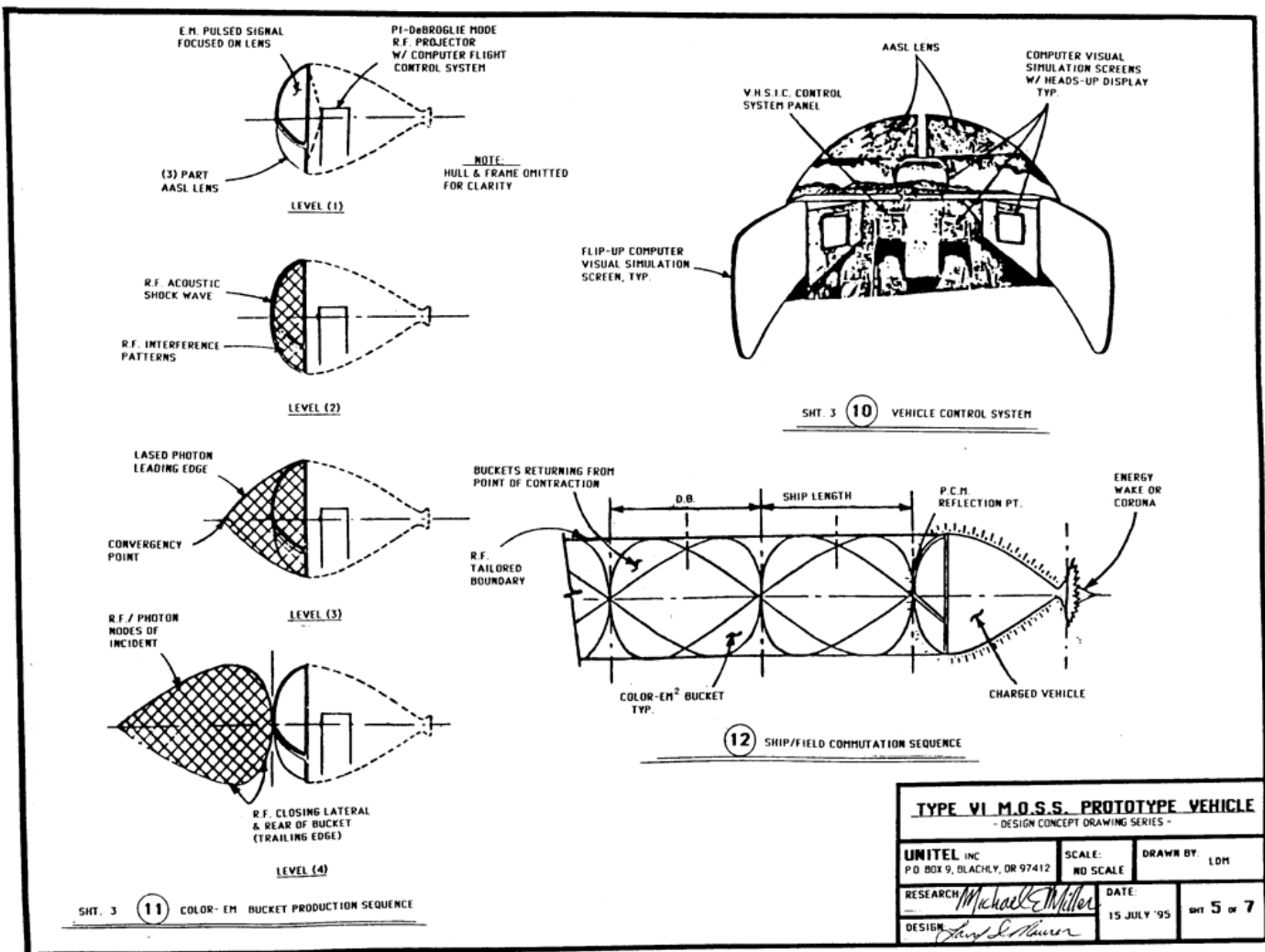
Document A - UNITEL's Type VI MOSS Prototype Vehicle AutoCAD Drawing 1-of-7



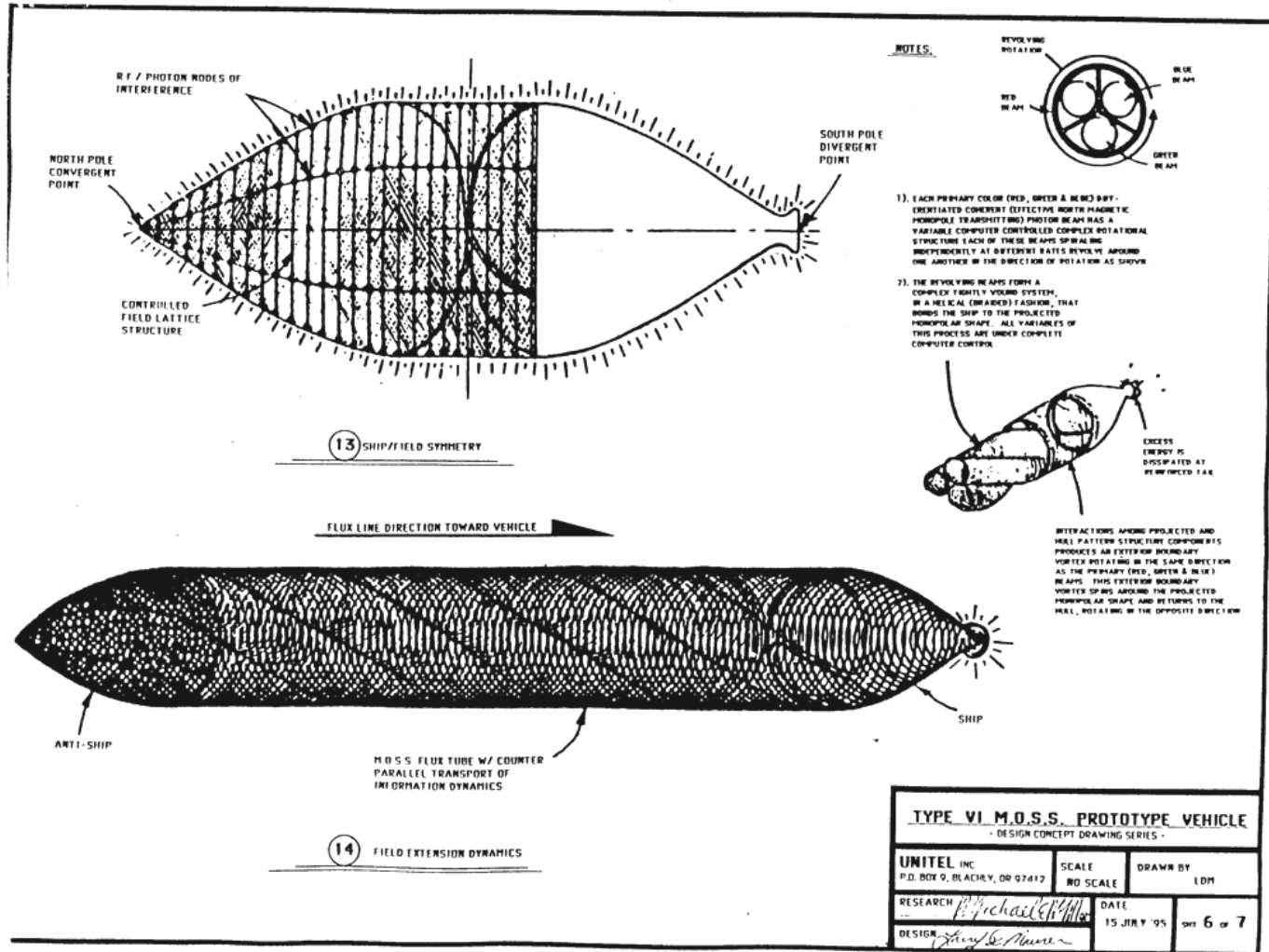
Document B - UNITEL's Type VI MOSS Prototype Vehicle AutoCAD Drawing 2-of-7



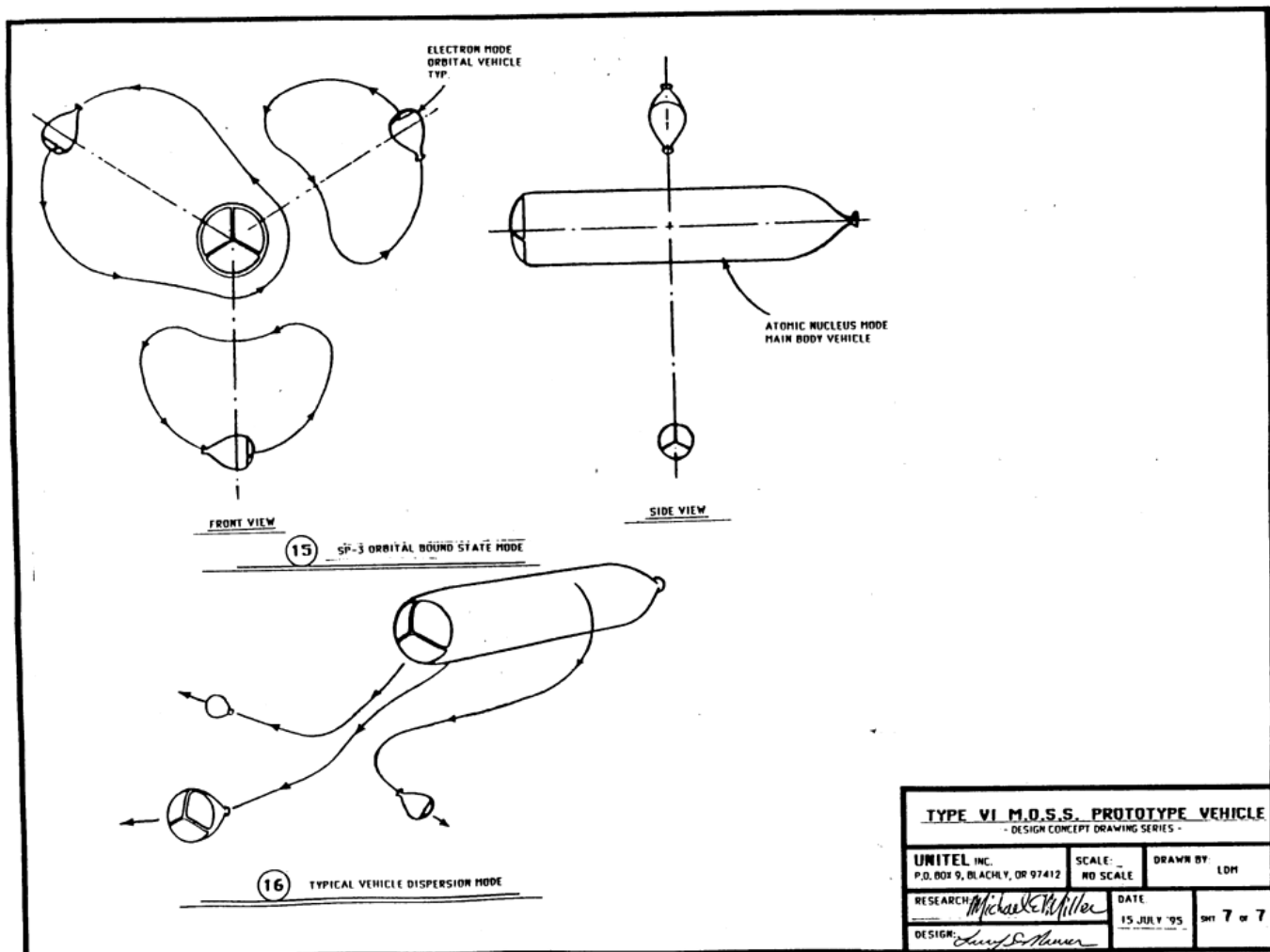
Document C - UNITEL's Type VI MOSS Prototype Vehicle AutoCAD Drawing 3-of-7



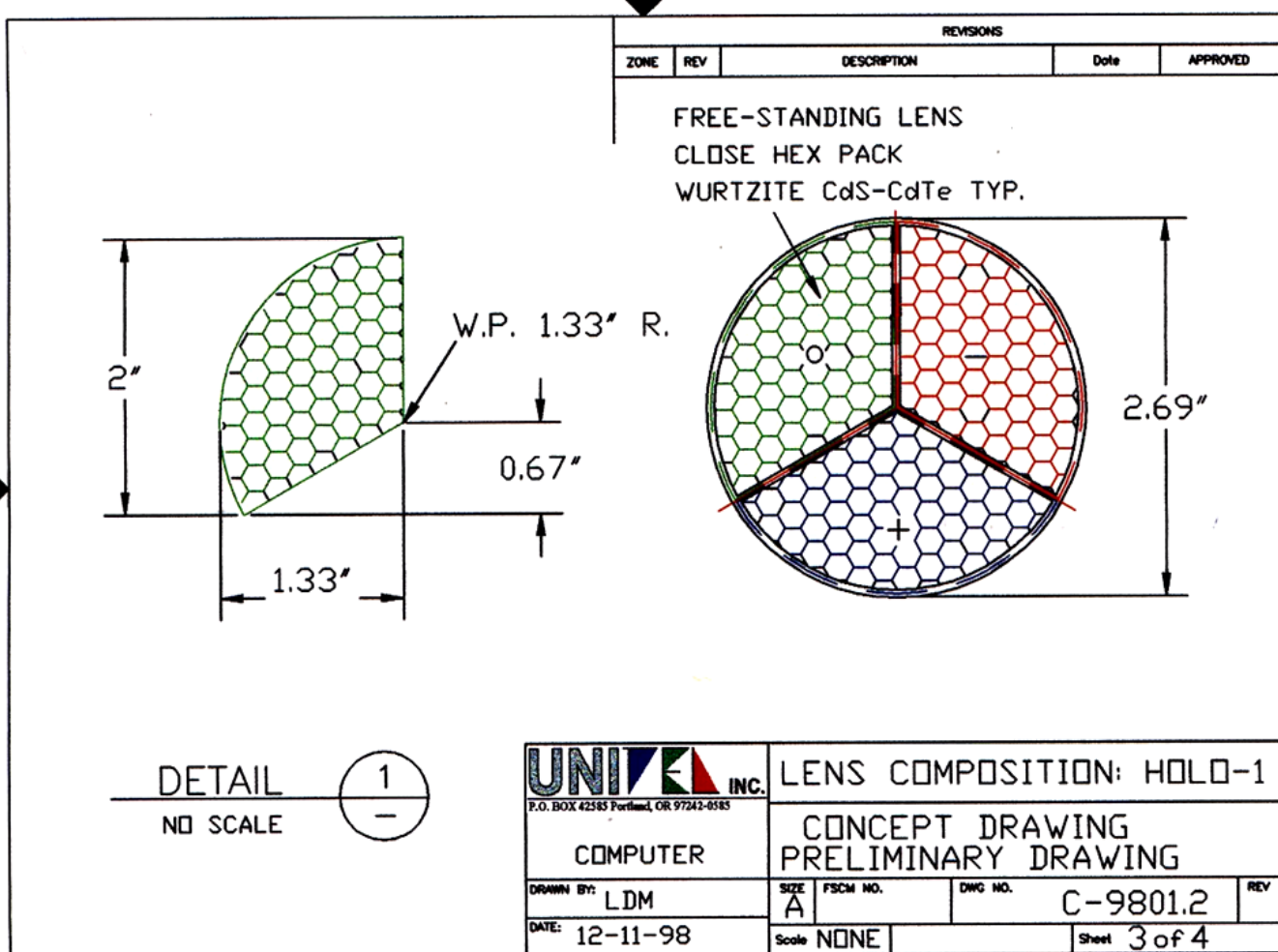
Document D - UNITEL's Type VI MOSS Prototype Vehicle AutoCAD Drawing 5-of-7



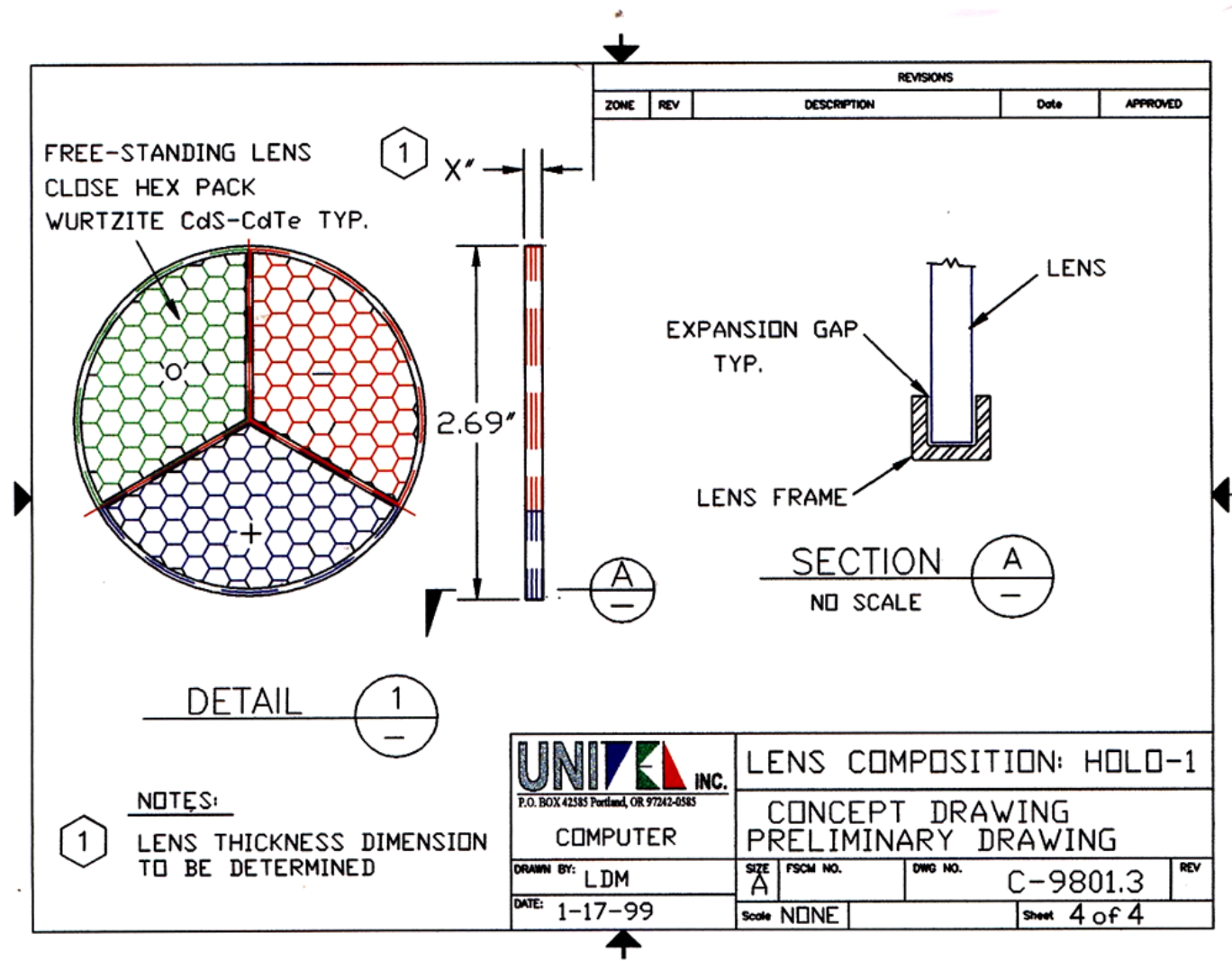
Document E - UNITEL's Type VI MOSS Prototype Vehicle AutoCAD Drawing 6-of-7



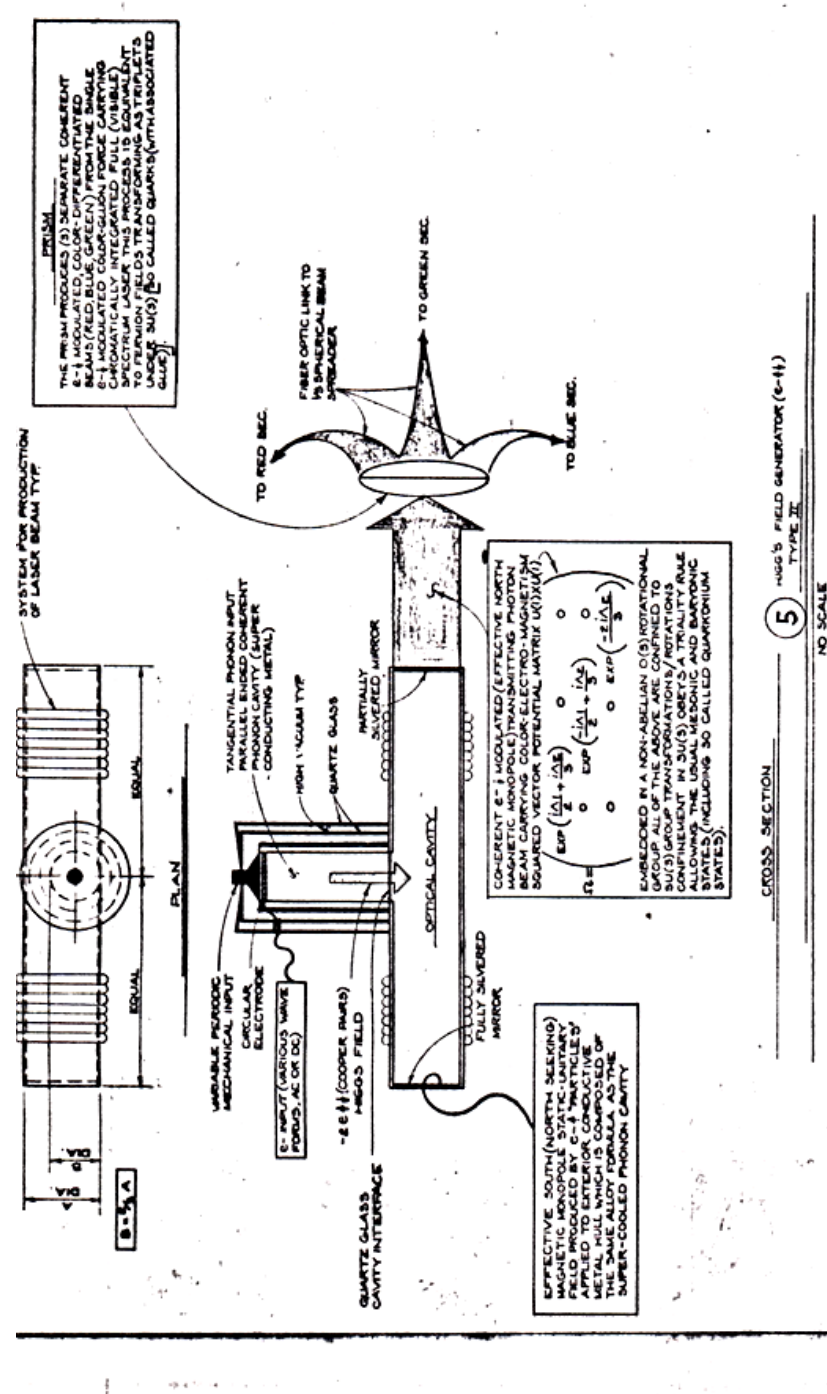
Document F - UNITEL's Type VI MOSS Prototype Vehicle AutoCAD Drawing 7-of-7



Document G - UNITEL's HOLO-1 Lens Composition AutoCAD Drawing 3-of-4



Document H - UNITEL's HOLO-1 Lens Composition AutoCAD Drawing 4-of-4

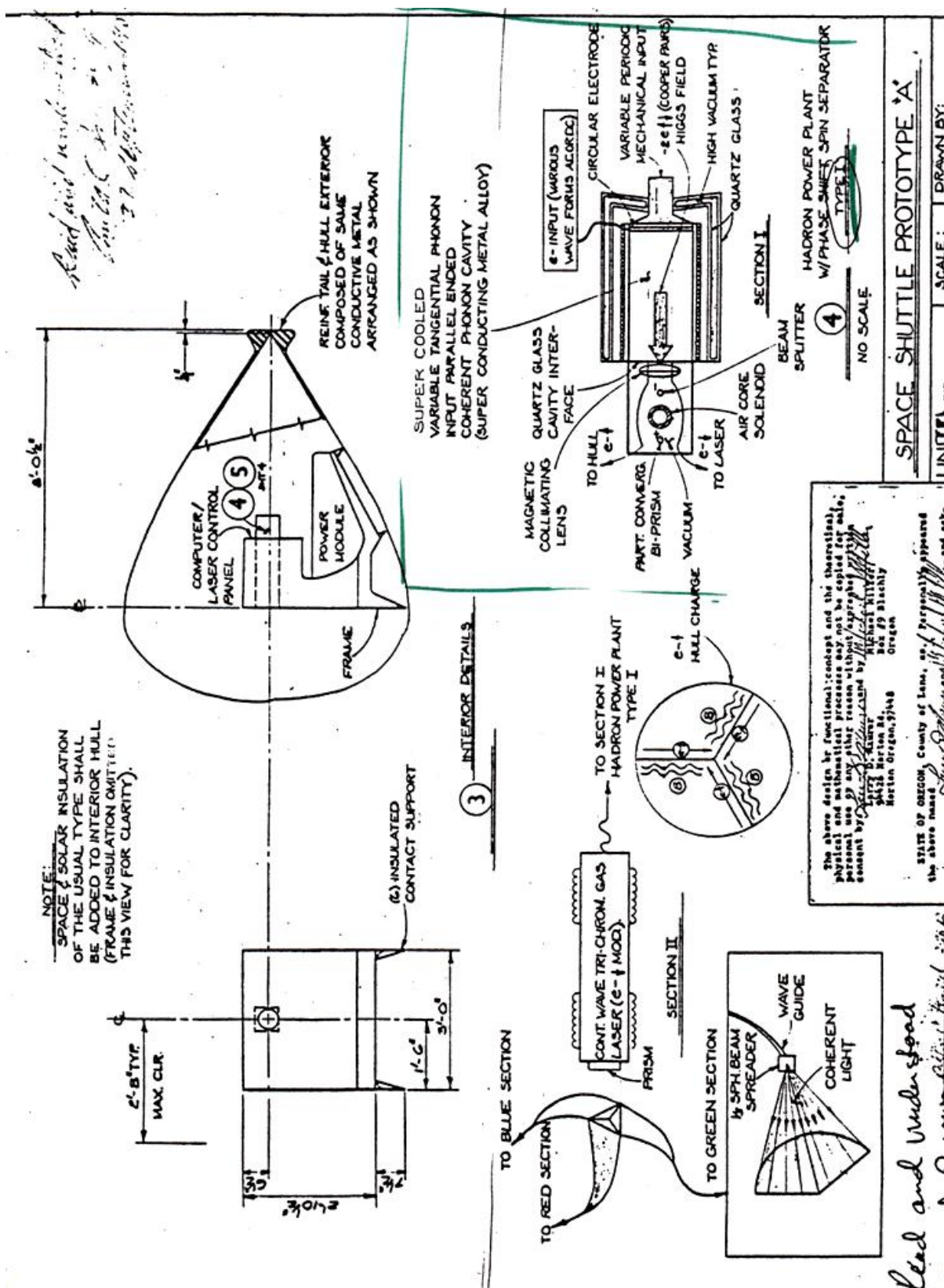


Document I - UNITEL's Space Shuttle Prototype AutoCAD Drawing 1-of-2

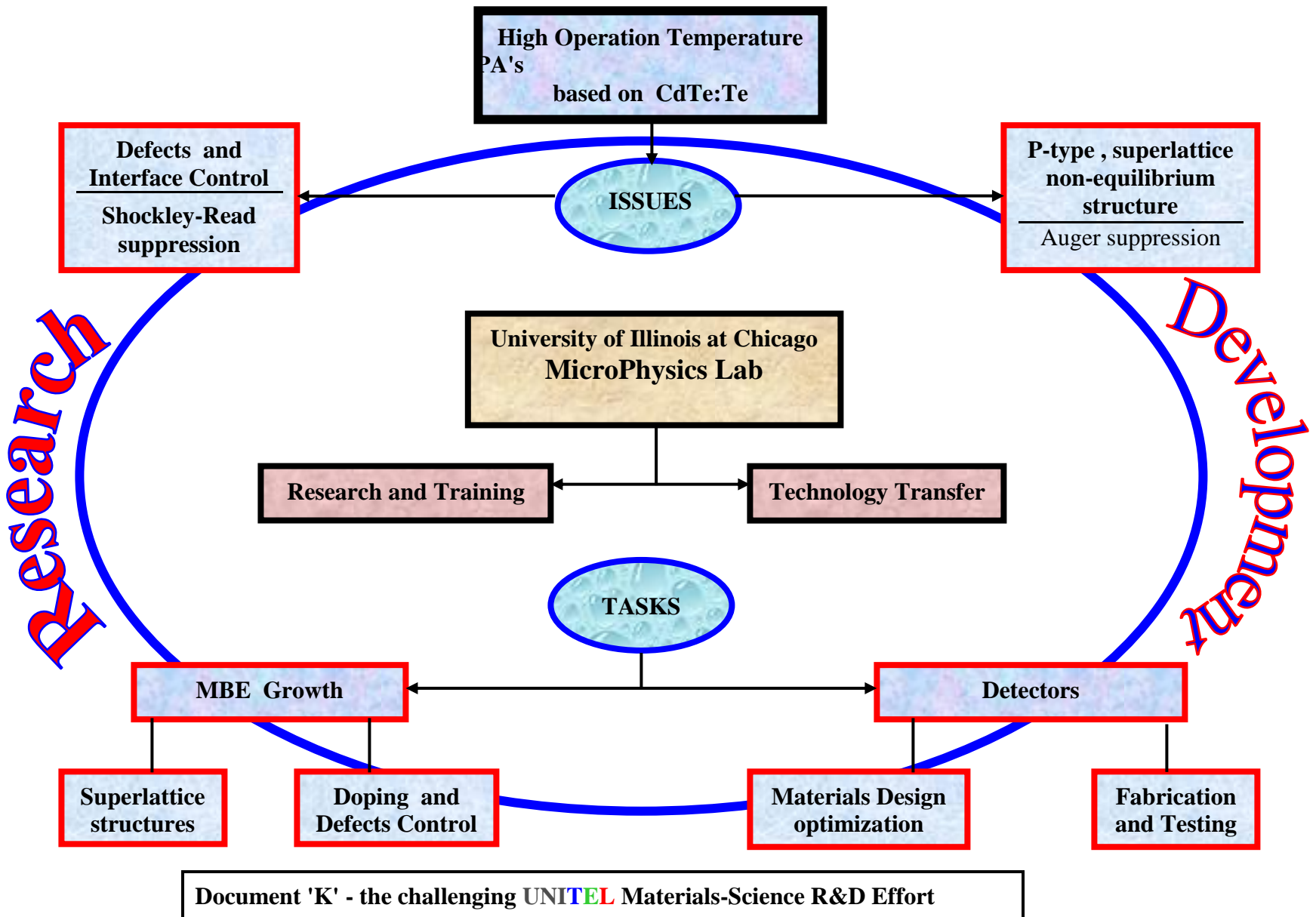
The above design or functional concept and the theoretical physical and mathematical processes may not be copied or reproduced, used or in any other reason without expressed consent by Larry D. Burton, and by Michael William,
Horton Rd., Portland, Oregon, 97248
Box #918818

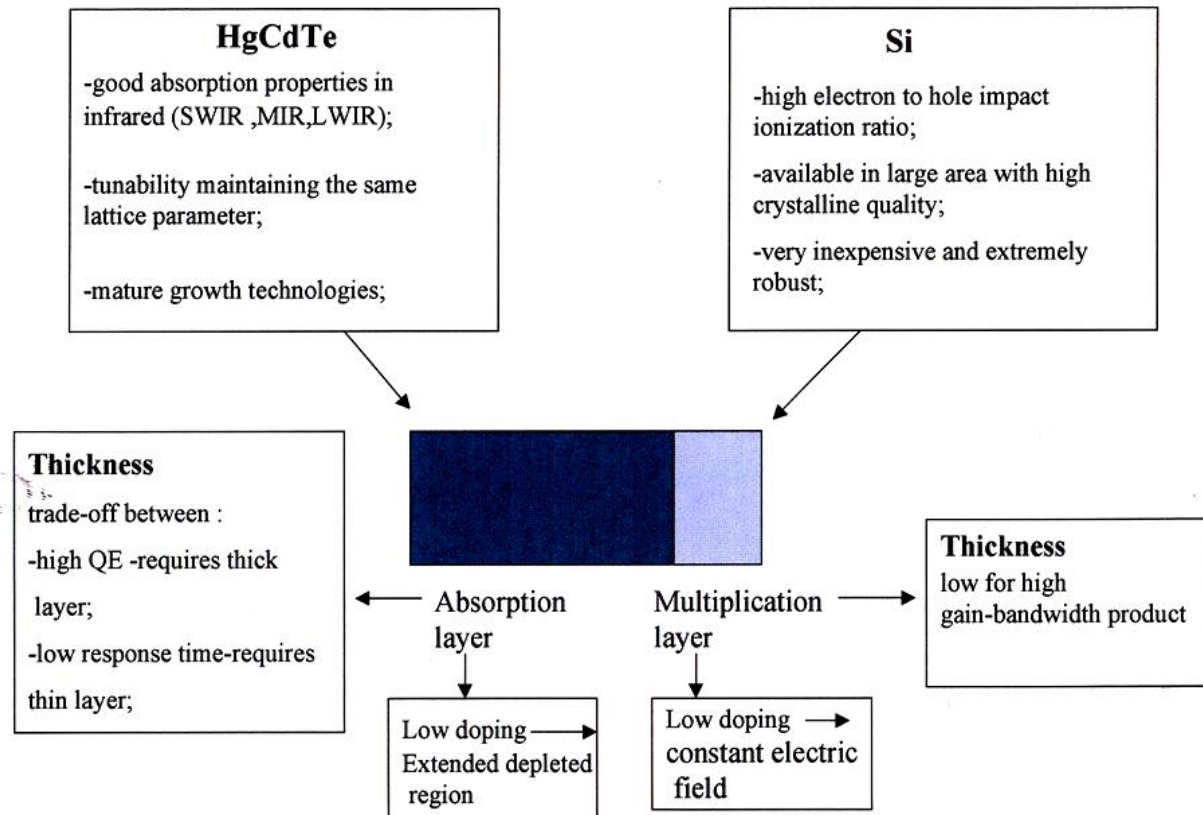
SPACE SHUTTLE PROTOTYPE

| UNITED NO. | DATE | SCALE: | DRAWN BY: |
|------------|------|--------|-----------|
| 1000000000 | 1981 | NOTED | JARRY D M |



Document J - UNITEL's Space Shuttle Prototype AutoCAD Drawing 2-of-2





Microphysics Lab.

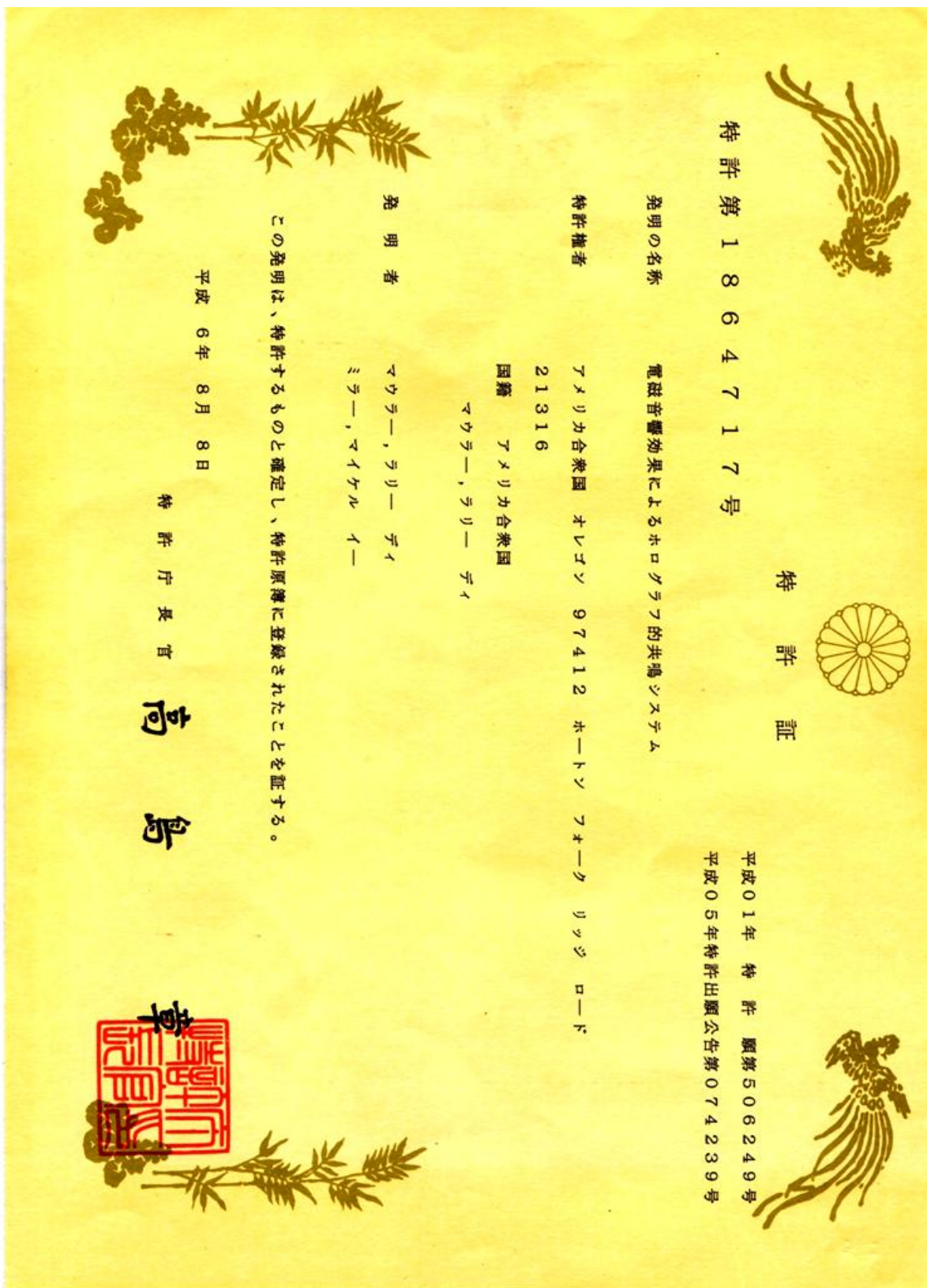
University of Illinois at Chicago

| |
|--|
| Document L - comparing the semiconductor properties of Silicon(Si) with HgCdTe |
|--|

.es

<http://www.darpa.mil/eto/ULTRA/98Overview/index.html>

| | |
|---|---|
| <u>Modeling Zinc Blend Alloys of Group IV Elements</u> | SRI International |
| <u>Sub-Micron Lithography with the Atomic Force Microscope</u> | Stanford University |
| <u>Column IV Heteroepitaxy for Silicon-Based Nanoelectronics</u> | Stanford University |
| <u>Electronic Properties of SiGeC Epitaxial Layers (ASSERT)</u> | Stanford University |
| <u>Nano-Fabrication of Quantum Devices on Silicon</u> | Stanford University |
| <u>Novel Silicon-Based Single Electron Nanodevices</u> | State University of New York, Stony Brook |
| <u>Ultra-sensitive Laser Ionization Technique for Real-time Analysis-control (ULTRA)</u> | SVT Associates |
| <u>Novel Array Architectures</u> | University College London |
| <u>Fabrication of Hetero-Channel Silicon MOSFETs with 10 nm Channel Length (DURIP)</u> | University of Maryland, College Park |
| <u>Self Assembled Quantum Dots For Large Scale Memory Devices</u> | University of California, Santa Barbara |
| <u>Microfabricated Multifunctional Scanned Probes for Nanometer Topography and High Frequency Fields</u> | University of Delaware |
| <u>Metal Silicide Source/Drain MOSFETs for Nanoscale CMOS</u> | University of Illinois |
| <u>Negative Differential Resistance (NDR) Devices and Their Digital Applications</u> | University of Michigan |
| <u>Tunneling Devices and Their Applications in Ultrafast and Superdense Digital Circuits</u> | University of Michigan |
| <u>Magnetization Controlled Resonant Tunneling in Rare Earth Arsenide / III-V Heterostructures</u> | University of California Santa Barbara, Quantum Institute |
| <u>Silicon-Based Nanoelectronics Using Quantum-Dot Cellular Automata</u> | University of Notre Dame |
| <u>Process Modeling and In-Situ Sensor Feedback Based Adaptive Control of Molecular Beam Epitaxy and Ion-Assisted Reactive Etching of Advanced Semiconductor Structures</u> | University of Southern California, Louisiana State University |
| <u>Silicon and Germanium Thin Film Chemical Vapor Deposition, Modeling, and Control (MURI)</u> | University of Texas, Austin |
| <u>Self-Assembly Based Approaches to Microelectronic Fabrication and Devices: Surface Passivation, Soft</u> | Yale University |



Document N - the Cover of the Japanese Patent awarded to UNITEL

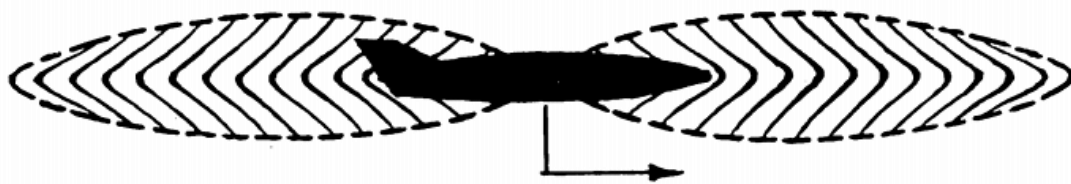
Theoretical and Experimental Investigations of Gravity Modification by Specially Conditioned EM Radiation

H.D. Froning¹

T.W. Barrett²

¹*Flight Unlimited, 5450 Country Club Drive, Flagstaff, AZ 86004*

²*BSEI, 1453 Beulah Road, Vienna, VA 22182*



SPACE TECHNOLOGY AND APPLICATIONS
INTERNATIONAL FORUM (STAIF-2000)
"Bridging the Future-Space Station and Beyond"
January 30-February 3, 2000

Flight Unlimited

Document O - January 2000 Space Technology and Applications International Forum

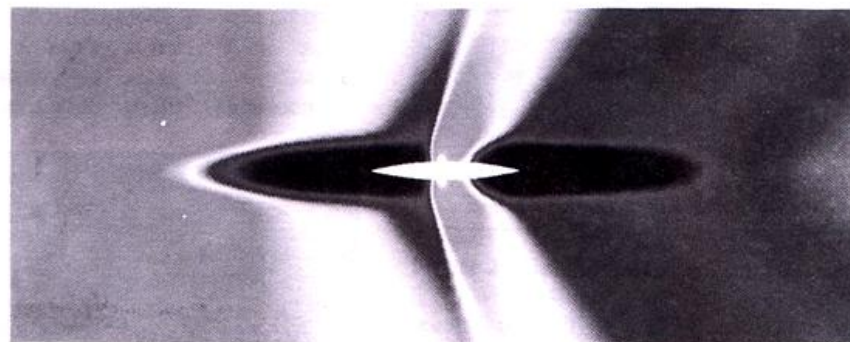


AIAA 2000-3478

Preliminary Simulations of Vehicle
Interactions with the The Zero-Point Vacuum
by Fluid Dynamic Approximations

H. David Froning, Jr.
Flight Unlimited
Flagstaff, AZ

R.L. Roach
Ramat Hashron
Israel



**36th AIAA/ASME/SAE/ASEE
Joint Propulsion Conference & Exhibit
17-19 July, 2000/Huntsville, AL**

For permission to copy or to republish, contact the American Institute of Aeronautics and Astronautics,
1801 Alexander Bell Drive, Suite 500, Reston, VA, 20191-4344.

Document P - July 2000 AIAA/ASME/SAE/ASEE Joint Propulsion Conference & Exhibit

Boeing Aerospace & Electronics
P.O. Box 3999
Seattle, WA 98124-2499

17 November 1989
2-1150-4000-166

Unitel, Inc.
P. O. Box 11291
Eugene, Oregon 97440

Attention: Larry Maurer

BOEING Subject: Proprietary Information Agreement
BAE/PIA-89-1925

Enclosed are two copies of the subject agreement executed on behalf of Boeing Aerospace and Electronics. Pursuant to your request, we have deleted any references to the Government (paragraphs 2 and 3.E).

Following signature by an authorized representative of Unitel, Inc., please fill in the effective date and forward a fully executed copy to the attention of Contracts Records, Mail Stop 18-30.

Please refer any questions or comments to E. J. Valley, telephone (206) 773-7395 (Mail Stop 87-49).


W.C. Hart
Contracts Manager
RESEARCH AND ENGINEERING

Enclosures

Document Q -- a letter to UNITEL from Boeing Aerospace and Electronics



IAA.4.1-93-712

**HYPER-SPACE NAVIGATION HYPOTHESIS
FOR INTERSTELLAR EXPLORATION**

Yoshinari Minami
NEC corporation, Yokohama, JAPAN

**44th CONGRESS OF THE
INTERNATIONAL ASTRONAUTICAL FEDERATION**
October 16–22, 1993 / Graz, Austria

For permission to copy or republish, contact the International Astronautical Federation,
3-5, Rue Mario-Nikis, 75015 Paris, France

Document R - October 1993 Congress of the International Astronautical Federation

14 - the 'UNITEL Team'

UNITEL CORPORATE MEMBERS

Larry D. Maurer, Secretary-Treasurer, Director - Engineering Dept.
Michael E. Maurer, President, Director - Research
Andrew C. Moore, Vice President - Computer Dept.
Ernest S. Brown, Vice President - Computer Dept.
R. Bryan Workman, Vice President - Communications
Douglas Starfield, Vice President - Marketing
Jack E. Quinn, Office Manager
Jason D. Maurer, Communications

UNITEL AEROSPACE SUBCONTRACTORS

SmartSkin Manufacturers

Applied Sciences, Inc.

Elliot Kennel, Technical Representative (937) 766-2020 x134
Kate Monaghan, Communications Director (937) 766-2020 x134

141 W. Xenia Ave.
P.O. Box 579
Cedarville, OH 45314-0579
(937) 766-2020
fax (937) 766-5886
ekennel@apsci.com
monaghan@apsci.com
<http://www.apsci.com/asi>

Albany Metals & Alloys

Lemont B. McCracken
1150 National Way
Albany, OR 97321
(541) 928-4923

Hull & Main Frame Manufacturer

Cincinnati Machine

4701 Marburg Ave.
Cincinnati, OH 45209-1025

Helen Boerger, Corp. Rep.

Jami Leininger, Sales

(513) 841-8154

fax (513) 841-8306

jami_leininger@cinmach.com

<http://www.cinmach.com>

Lens Manufacturer

(<http://iptsg.epfl.ch/aps/BAPSMAR97/abs/s130.html>)

University of California, Berkeley

A. Paul Alivisatos, Senior Scientist

Chancellor's Professor of Chemistry and Materials Science

Department of Chemistry

B-62 Hildebrand Hall

(510) 643-7371

University of Illinois at Chicago (UIC)

Prof. Sivalingam Sivananthan

Director/Microphysics Lab.

Department of Physics

845 W.Taylor Street (room 2236 SES)

Chicago, Illinois 60607-7059

(312) 996-5092

fax (312) 996-9016

<http://www.uic.edu/depts/mplab>

siva@uic.edu

alivis@uclink4.berkeley.edu

Eagle-Picher Technologies, LLC
Gene Cantwell

Director, Technical Development
Environmental Science and Technology Department
200 BJ Tunnel Boulevard
Miami, OK 74354
(918) 542-1801
Fax 918-540-2595
gene@cantwell.com
<http://www.esat.epcorp.com>

Cleveland Crystals, Inc.

19306 Redwood Ave.
Cleveland, OH 44110-2738

Wm. R. Cook, Jr., Senior Scientist

WCook@ClevelandCrystals.com

Lee Shiozawa, Technical Representative

Shiozawa@clevelandcrystals.com

(216) 486-6100, ext. 3011

Fax: 216-486-6103

<http://www.clevelandcrystals.com>

Equipment & Hardware Components

CPI-Raytheon-Hughes

Richard J. Madore

Magnetron Engineering Manager

CPI magnetrons- CPI Beverly Microwave Div, Beverly, Ma
150 Sohier Rd.

Beverly, MA 01915-5595

(508) 922-6000 ext. 631

fax (508) 922-8914

<http://www.cpii.com/satcom/index.html>

Flight Navigation & Control System

Flight Unlimited, Inc.

H.D. Froning, Jr

Dr. Robert L. Roach

5450 Country Club Drive

Flagstaff, AZ 86004-8739

(520) 526-5916

fax (520) 286-9419

froning@flagstaff.az.us

rroach@pronetix.com

BSIE

Dr. Terence W. Barrett

1453 Beulah Rd.

Vienna, VA 22182

(703) 759-4518

fax (703) 757-5313

barrett506@aol.com

MBE Equipment Manufacturer

EPI- MBE Equipment

Michael DeBruzz

Systems Sales Engineer

4900 Constellation Rd.

Saint Paul, MN 55127

(651) 482-0800

fax (651) 482-0800

miked@epimbe.com

<http://www.epimbe.com>

Laser Design Consultant

UCLA Physics dept.

John M. Dawson (*deceased*)

Accelerator & Theoretical Plasma

Office: Knudsen 1-130M

(310) 825-7814

dawson@physics.ucla.edu

UNITEL Business Consultants

Wil F. Zarecor

9064 Myrtle Drive

Douglasville, GA 30134

(770) 489-3221

fax (770) 489-3222

wzarecor@freewwweb.com

James E. Reinmuth, PhD

(541) 346-3293

fax (541) 346-3295

JER@oregon.uoregon.edu

Cavendish Management Resources

Mike Downey, Managing Director

31 Harley Street, LONDON W1N 1DA,

UK International: 44 171 636 1744.

:0171 636 1744. UK Fax: 0171 636 5639

fax: 44 171 636 5639

cmr@cmruk.com

<http://www.cmruk.com/cmrkeele.html>

UNITEL Technical Consultants

Prof. Andreas Mandelis

Photothermal and Optoelectronic Diagnostics Laboratories (PODL)

University of Toronto
Department of Mechanical
& Industrial Engineering
5 King's road
Toronto, CA M5S 3G8
(416) 978-5106
Fax (416) 266-7867
mandelis@mie.utoronto.ca

Claudio Maccone

Colombo Center for Astrodynamics
Via Martorelli, 43
I-10155 Torino (TO) Italy
cmaccone@to.alespazio.it

Yoshinari Minami

NEC Patent Service, Ltd.
5-11, Shibaura 4-Chome
Minato-ku, Tokyo 108 Japan
81(03) 3798-6923
fax 3798-5989
NDC06286@biglobe.ne.jp

Harold E. Puthoff

Institute for Advanced Studies
University of Texas at Austin
1301 Capitol of Texas Hwy S.
Suite B 121
Austin, TX 78746
(512) 328-5751
FAX 834-9769
Puthoff@aol.com

Prof. Ernest S. Brown, MA

Director, Computer Dept.
UNITEL, Inc.

8540 Hwy. 20
Toledo, OR 97391
(541) 336-7901
fax (541) 265-3820
cell (541) 961-0583
wk (541) 265-2283 ext. 127
ebrown@teleport.com

Optical Equipment (Scanner)

Pixel Vision, Inc.

15250 NW Greebrier Parkway
Su 1250
Beaverton, OR 97006

George Williams

Pixel Vision, Inc. (formerly Imaging Technologies Inc.)
2134 Main St.
Su 160
Huntington Beach, CA 92648
<http://www.pv-inc.com>
(714) 840-9778 PV-South

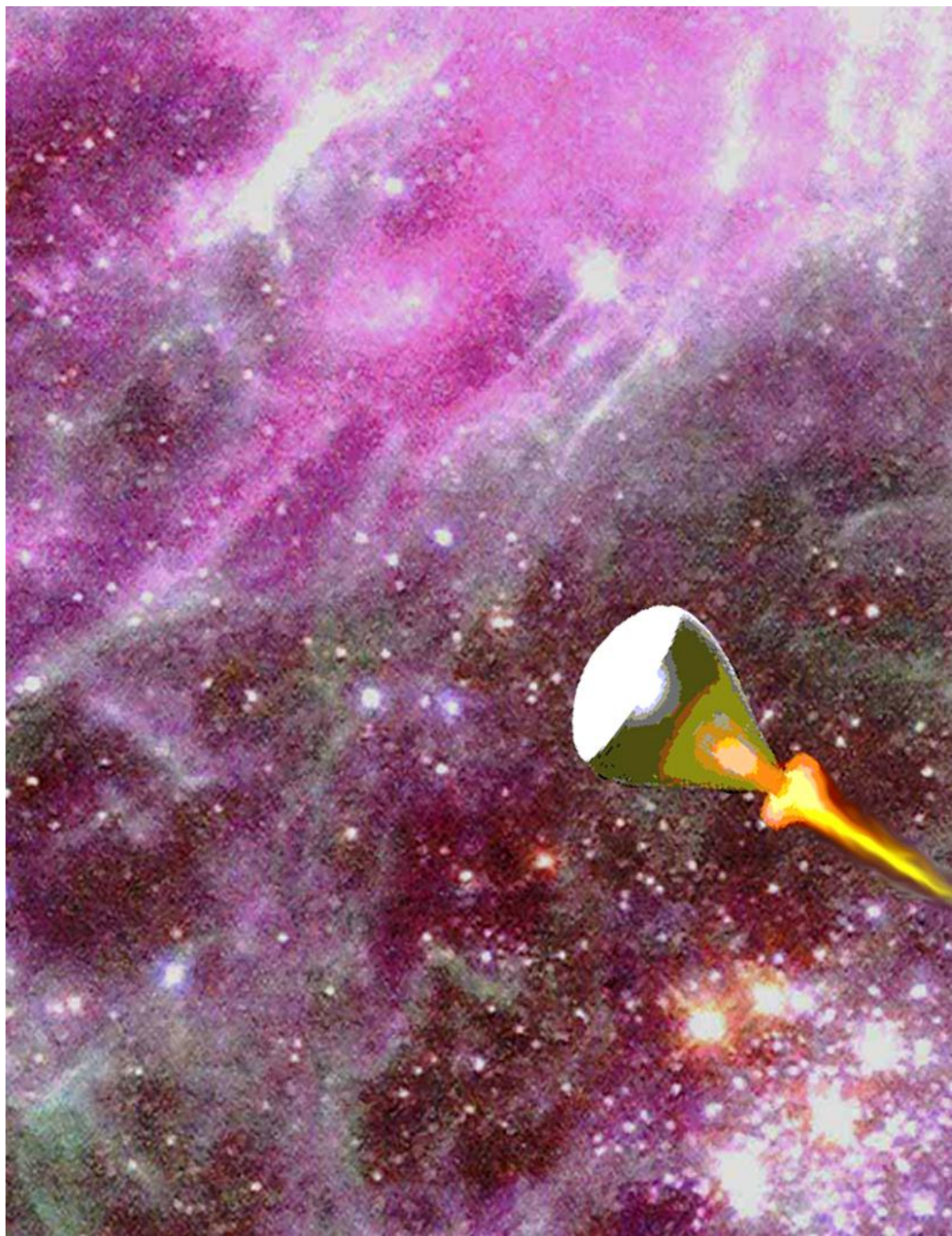
Jim Janesick

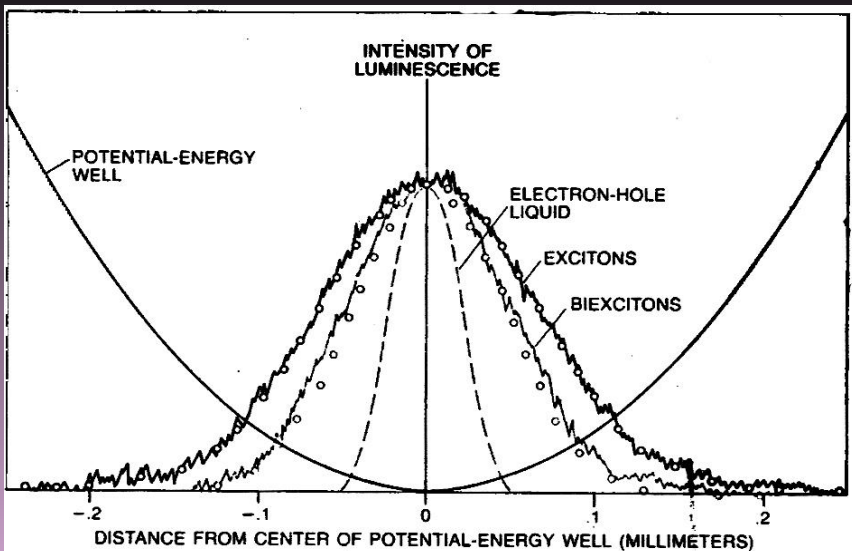
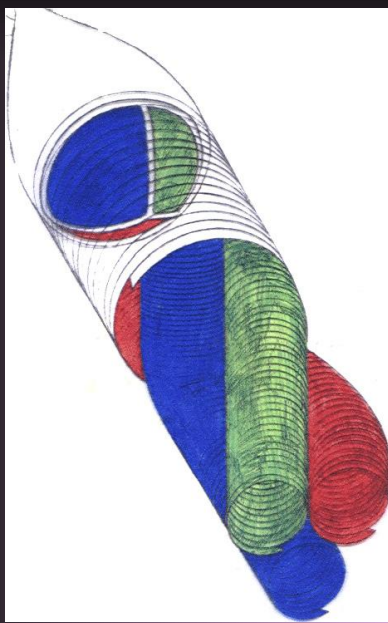
(503) 629-3210 PV-North
Mypixel@aol.com

UNITEL Corporate Attorney

Dennis F. Tripp, P.C.

1000 Oregon National Bldg.
610 SW Alder St.
Portland, OR 97205
(503) 295-2425
fax (503) 417-0174
DFTPC@aol.com





UNITE** INC.**
P.O. Box 42585 Portland, OR 97242-0585
www.unitelnw.com

